VIDEO CONTENT ANALYSIS FOR AUTOMATED DETECTION AND TRACKING OF HUMANS IN CCTV SURVEILLANCE APPLICATIONS

A thesis submitted for the degree of Doctor of Philosophy

by

Thomas Andzi-Quainoo Tawiah

School of Engineering and Design
Brunel University

August 2010

ABSTRACT

The problems of achieving high detection rate with low false alarm rate for human detection and tracking in video sequence, performance scalability, and improving response time are addressed in this thesis. The underlying causes are the effect of scene complexity, human-to-human interactions, scale changes, and scene background-human interactions. A two-stage processing solution, namely, human detection, and human tracking with two novel pattern classifiers is presented. Scale independent human detection is achieved by processing in the wavelet domain using square wavelet features. These features used to characterise human silhouettes at different scales are similar to rectangular features used in [Viola 2001]. At the detection stage two detectors are combined to improve detection rate. The first detector is based on shape-outline of humans extracted from the scene using a reduced complexity outline extraction algorithm. A Shape mismatch measure is used to differentiate between the human and the background class. The second detector uses rectangular features as primitives for silhouette description in the wavelet domain. The marginal distribution of features collocated at a particular position on a candidate human (a patch of the image) is used to describe statistically the silhouette. Two similarity measures are computed between a candidate human and the model histograms of human and non human classes. The similarity measure is used to discriminate between the human and the non human class. At the tracking stage, a tracker based on joint probabilistic data association filter (JPDAF) for data association, and motion correspondence is presented. Track clustering is used to reduce hypothesis enumeration complexity. Towards improving response time with increase in frame dimension, scene complexity, and number of channels; a scalable algorithmic architecture and operating accuracy prediction technique is presented. A scheduling strategy for improving the response time and throughput by parallel processing is also presented.

ACKNOWLEDGEMENTS

I would like to express my sincere gratitude to Professor Mike Lea, my principal supervisor, and Professor John Stonham, my second supervisor for their patience, advice, and support over the last four years. Their feedback also proved to be very good and useful.

My thanks also goes to Dr. Argy Krikelis (formerly of Brunel University) who first encouraged me to work in video processing (on video compression techniques), and Dr. Huiyu Zhou (formerly of Brunel University), for the discussions we had on the topic, which proved to be very helpful.

Finally thanks to all my anonymous friends who supported me in all diverse ways to make my research work possible.

DECLARATION

The work described in this thesis has not been previously submitted for a degree in this or any other university and unless otherwise reference it is the author's own work.

STATEMENT OF COPYRIGHT

TABLE OF CONTENTS

		Page
ABSTRACT		**i**
ACKNOWLEDGMENTS		**ii**
DECLARATION		**iii**
STATEMENT OF COPYRIGHT		**iv**
TABLE OF CONTENTS		**v**
LIST OF FIGURES		**xi**
LIST OF TABLES		**xiv**
LIST OF ABBREVIATIONS		**xvii**
DEFINITION OF TERMS		**xviii**
CHAPTER 1 INTRODUCTION		**1**
1.1	Perspective	1
	1.1.1 Surveillance for Human Survival	1
	1.1.2 Requirements of a Generic Surveillance System	3
	1.1.3 Evolution of Visual Surveillance Systems	4
	1.1.4 Challenges of Visual Scene Analysis	7
	1.1.5 Video Content Analysis	10
	1.1.6 Evaluation of Selected VCA Systems	11
	1.1.7 Algorithmic Approaches to Object Detection and Tracking	12
	1.1.8 Improving Accuracy of Feature-Based Approach in Pattern Space	14
	1.1.9 Exploiting Local Features in Two Independent Pattern Spaces	16
	1.1.10 Pattern Classification for Object Discrimination	16
	1.1.11 Bayesian Tracker for Optimal Object Tracking	17
	1.1.12 Software Functionalities Proposed for Video Surveillance Applications	17
	1.1.13 Persistent Problems of Automated Human Detection and Tracking in Space-Time Domain	20
1.2	Aim and Objectives	23
1.3	Research Strategy	24
1.4	Overview of Thesis	26

1.5 Contribution of Thesis 27

CHAPTER 2 A SURVEY ON OBJECT DETECTION AND TRACKING ALGORITHMS 28

2.1 Introduction 28
2.2 Object Detection 29
2.3 Object Tracking 33
2.4 Spatial Domain Techniques for Detection and Tracking of Humans 36
2.5 Wavelet-Domain Detection and Tracking of Humans 39
2.6 Model-Based Detection and Tracking of Humans 43
2.7 Appearance-Based Detection and Tracking of Humans 45
2.8 Shape-Based Detection and Tracking of Humans 48
2.9 Motion-Based Recognition of Humans 50
2.10 Summary 51

CHAPTER 3 REVIEW OF DATASETS, PEROFRMANCE METRICS AND STATE OF THE ART ON PEDESTRIAN DETECTION 54

3.1 Introduction 54
3.2 Review of Datasets 54
3.2.1 PETS 55
3.2.2 i-LIDS 55
3.2.3 CAVIAR 56
3.2.4 VACE 57
3.2.5 TRECVID 57
3.2.6 PASCAL VOC 2010 Challenge 58
3.2.7 Daimlerchrysler 59
3.2.8 Dataset Classification 60
3.2.9 Choice of Dataset 61
3.3 Review of Performance Metrics 61
3.3.1 Confusion Matrix Based Metrics for Detection and Tracking 62
3.3.2 F1 Measure for Detection and Tracking 64

3.3.3 Receiver Operating Characteristics (ROC) Curve for Detection and Tracking 66
3.3.4 PASCAL VOC Average Precision Measure for Classification and Detection 67
3.3.5 PETS 2005 Metrics for Tracking 67
3.3.6 Choice of Benchmark Metrics for Performance Evaluation 69
3.4 State of the Art Performance on Pedestrian Detection 71

CHAPTER 4 REFINEMENT OF RESEARCH OBJECTIVES AND STRATEGY 73
4.1 Introduction 73
4.2 Motivation for the Choice of Shape Descriptors for Human Detection and Tracking 74
4.3 Objectives 77
4.4 Strategy 77

CHAPTER 5 INVESTIGATIONS INTO FEATURE EXTRACTION TECHNIQUES FOR HUMAN DETECTION 82
5.1 Introduction 82
5.2 Feature Extraction in Scale Frequency Domain 83
5.2.1 9/7 Biorthogonal Wavelet Filter for Feature Extraction 85
5.3 Candidate Human Localization in Wavelet Domain 90
5.4 Feature Extraction in Shape Space 90
5.4.1 Reduced Complexity Boundary Extraction Algorithm 92
5.5 Candidate Human Localization in Shape Space 101
5.6 Results 101

CHAPTER 6 INVESTIGATIONS INTO PATTERN CLASSIFIERS FOR HUMAN DETECTION 102
6.1 Introduction 102
6.2 Wavelet Feature-Based Classifier Specification and Implementation 102
6.2.1 Novel Wavelet-Based Histogram Classifier Design and Training 104
6.2.2 Validation and Testing of Histogram Based Classifier 106

6.3 Shape-Outline Based Classifier Specification and Implementation 111
6.3.1 Feed Forward Neural Network Pattern Predictor Design and Training 113
6.3.2 Validation and Testing of Shape-Outline Based Human Classifier 117
6.4 Results 119
6.5 Interpretation 121

CHAPTER 7 INVESTIGATIONS INTO HUMAN DETECTION 123
7.1 Introduction 123
7.2 Wavelet Domain Search Strategies 124
7.3 Wavelet Domain Human Discrimination 125
7.4 Wavelet Domain Human Detection 125
7.5 Shape-Outline Based Search Strategies 127
7.6 Shape-Outline Based Human Discrimination 128
7.7 Shape-Outline Based Human Detection 128
7.8 Synthesised Algorithmic Architecture for Human Detection 130
7.9 Simulation 131
7.10 Results 137
7.11 Interpretation 141

CHAPTER 8 INVESTIGATIONS INTO JPDAF TRACKER 146
8.1 Introduction 146
8.2 Track Initialization 147
8.3 Silhouette and Appearance Features Extraction for Human Tracking 149
8.4 Motion Estimation 151
8.5 Measurement Validation 153
8.6 Kalman Prediction 154
8.7 Track Hypothesis Generation and Validation 155
8.8 Track Optimization 163
8.8.1 Sequential State Estimation Mode 163
8.8.2 Batch State Estimation Mode 164
8.8.3 Application to Single Motion Model 164
8.8.4 Application to Multiple Motion Models 164

8.9 Occlusion Handling 164
8.10 Computational Complexity of JPDAF Tracker 166
8.11 Synthesised JPDAF Tracker 168
8.12 Simulations 171
8.13 Results 171
8.14 Interpretation 174

CHAPTER 9 CONSOLIDATION OF RESULTS 177
9.1 Introduction 177
9.2 Determining Optimum Algorithmic Parameters for Human Detection and Tracking 178
9.3 Adaptive Monitoring and Control of Detection and Tracking Accuracy 180
9.4 Accuracy Prediction Analysis 182
9.5 Detection and Error Rates Analysis 184
9.6 Track Detection and Error Rates Analysis 194
9.7 Task Profiling and Analysis 198
9.8 Accuracy Comparisons with Other Algorithms 199
9.9 Synthesised Architecture for Human Detection and Tracking 203
9.10 Discussion 204
9.11 Review of Research Progress 207

CHAPTER 10 CONCLUSIONS 209
10.1 Conclusions 209
10.2 Future Work 210
10.2.1 Algorithmic investigations 210
10.2.2 Performance Enhancements: Parallel Processing for Optimum Execution Time and Throughput 211
10.2.3 Proposed Macro Architecture of Multiprocessor Accelerator 211
10.2.4 Task Mapping and Scheduling on Multiprocessor Accelerator 213
10.2.5 Implementation of 9/7 Wavelet Transform on Field Programmable Gate Array (FPGA) 217

REFERENCES **218**

APPENDICES

A Commercial Video Analytics Software Features **252**

B Proposed Structure of Human Detection and Tracking Algorithm **256**

C Characteristics of Human Detection and Tracking Algorithms **273**

D Classifier Accuracy Evaluation Tables **277**

D1.1 ROC Table (Hamilton2b.avi: Edge saliency) 277

D1.2 ROC Table (Hamilton2b.avi: Motion saliency) 280

D2.1 ROC Table (Stc_t1_c_3.avi: Edge saliency) 283

D2.2 ROC Table (Stc_t1_c_3.avi: Motion saliency) 287

D3.1 ROC Table (Stc-t1_c_4.avi: Edge saliency) 290

D3.2 ROC Table (Stc_t1_c_4.avi: Motion saliency) 293

E Tracker Evaluation Tables **296**

E1 ROC (Hamilton2b.avi) 296

E2 ROC (Stc_t1-c_3.avi) 297

E3 ROC (Stc_t1_4.avi) 298

F Graphs of PETS 2006 metrics for Stc_t1_c_3.avi **299**

LIST OF FIGURES

Figure 1.1	Activity flow in a surveillance system	2
Figure 1.2	A graph showing variations in detection rate in a video sequence with dynamic scene	9
Figure 1.3	Components of video content analysis system	10
Figure 1.4	Main components of VCA software components	18
Figure 2.1	General framework for visual surveillance	39
Figure 4.1	Algorithmic task pipeline for the proposed feature space based human detection	80
Figure 5.1	One-level wavelet decomposition	86
Figure 5.2	Feature detection and construction of foreground silhouette map in the wavelet domain	87
Figure 5.3	Wavelet domain primitive feature set	88
Figure 5.4	Stages in the construction of a HLLH silhouette map	88
Figure 5.5	Flowchart of shape-outline map construction in the shape space	91
Figure 5.6	Construction of shape-outline maps for frame36	96
Figure 5.7	Comparison shape outline map compared with edge maps derived from Canny and Sobel filters for frame index 300	97
Figure 5.8	Construction of Silhouette-maps (HLLH subband). Levels one and two wavelet decomposition for frame 300	98
Figure 5.9	Comparison of shape-outline map types for frame 320	99
Figure 5.10	Silhouette map types for frame 330	100
Figure 6.1	Flowchart for validation and testing of histogram-based classifier	107
Figure 6.2	Plot of cityblock measure for histogram-based classifier	110
Figure 6.3	A 3-Layer feed forward multilayer perceptron network for pattern prediction	113
Figure 6.4	Propagation of data (signals) from one layer to the next layer in the FF network	114

Figure 6.5	Flowchart for validation and testing of human outline based classifier	117
Figure 6.6	Plot of scaled (*10000) shape mismatch metric for stc_t1c_3.avi and stc_t1_c_4.avi	118
Figure 7.1	Flowchart for histogram-based human detection	126
Figure 7.2	Flowchart for shape-outline based human detection	129
Figure 7.3	Combined algorithm for human detection	130
Figure 7.4	Block diagram for HLLH histogram based classification and detection of humans (PASCAL VOC 2010 challenge)	136
Figure 7.5	Block diagram for shape-outline based classification and detection of humans (PASCAL VOC 2010 challenge)	136
Figure 7.6	Precision/recall curves for shape-outline classifier/detector and histogram classifier/detector	140
Figure 7.7	Candidate window configurations in a frame at the detection phase for test1.avi	145
Figure 8.1	Task flow in human tracking	148
Figure 8.2	Sobel filter masks for vertical edges (A) and horizontal edges (B)	150
Figure 8.3	Region of a candidate human partitioned into sub blocks of a cluster	152
Figure 8.4	Algorithmic flow for track generation and validation	160
Figure 8.5	Region of uncertainty between neighbouring clusters	162
Figure 8.6	Motion vector labels for detecting splits/merges	165
Figure 8.7	Multiple JPDAF Tracking Modules	170
Figure 8.8	Tracker output for Hamilton2b.avi: input frames 11, 20, 23, and 146	175
Figure 8.9	Tracker output for Stc_t1_c_3.avi: input frames 267, 268, 314, and 353	176
Figure 8.10	Tracker output for Stc_t1_c_4.avi: input frames 105 and 120	176
Figure 9.1	ROC curves for hamilton2b.avi sequence	189
Figure 9.2	ROC curves for stc_t1_c_3.avi sequence	191
Figure 9.3	ROC curves for stc_t1_c_4.avi sequence	193
Figure 9.4	Algorithmic architecture for human detection and tracking	203
Figure 10.1	Block diagram of the proposed accelerator	212
Figure 10.2	Execution threads for the main human detection and tracking pipeline	215

Figure 10.3 Static schedule showing main processing tasks overlapped with with frame access 216

LIST OF TABLES

Table 1.1 Evaluation of human centred visual surveillance activities against generic requirements of surveillance systems 6

Table 1.2 Required functionalities of a generic VCA system 13

Table 3.1 Publicly available benchmark for classification, detection, tracking and activity recognition 60

Table 3.2 Publicly available dataset chosen for the current investigation 61

Table 3.3 2 X 2 Confusion matrix table 62

Table 3.4 Performance metrics for image classification, object detection, event detection, and tracking 70

Table 3.5 Benchmark metrics selected for the current investigation 71

Table 3.6 Peak performance for human classification and detection 72

Table 5.1 Analysis and synthesis filters of 9/7 Biorthogonal wavelet transform 85

Table 5.2 Proposed shape-outline map construction time for a frame compared with other edge detection algorithm 95

Table 6.1 Data set for training histogram based classifier 103

Table 6.2 One way Anova for test of significance between horizontal and vertical similarity measure 109

Table 6.3 Maximum offset from the centre of the window for horizontal and vertical histogram based on principal component analysis 109

Table 6.4 One way Anova for test of significance for horizontal histogram between the human class and the non human class for stc_t1_c_3.av 111

Table 6.5 Post training evaluation of Test1.avi sequence (Level 2 decomposition) 111

Table 6.6 Video sequence used in training the object outline map pattern predictor 116

Table 6.7 One way Anova table for shape mismatch metric between the human and the non human class 119

Table 6.8 Approximate computational load given candidate human of dimension (M X N) for the shape based classifier 120

Table 6.9 Approximate number of operations for Histogram based classifier

using candidate human window of the same dimension 121
Table 7.1 Parameters of the test video sequence 131
Table 7.2 Main algorithmic parameters for histogram based detector 133
Table 7.3 Main algorithmic parameters for shape-outline based detector 134
Table 7.4 PASCAL VOC 2010 training set 135
Table 7.5 Average precision for PASCAL VOC 2010 challenge 138
Table 7.6 Task profiling of the main functions of the histogram based detector for decimated wavelet transform (level one) suband 143
Table 7.7 Task profiling of the main functions of histogram based detector function for decimated wavelet transform (level two) subband 143
Table 7.8 Task profiling of the main functions of the shape-based detector 144
Table 8.1 Relative addresses of sub blocks defining a track cluster 153
Table 8.2 Global parameter settings for JPDAF tracker 171
Table 8.3 Main task profiling of JPDAF tracker (Intensity template only) 173
Table 8.4 Main task profiling of JPDAF tracker (All templates) 173
Table 9.1 Scene complexity descriptor for human detection and tracking 179
Table 9.2 Combined shape and histogram detector for stc_t1_c_3.avi showing parameters of the third kind 183
Table 9.3 Intermediate computation for determining operating point on ROC curve during an iteration 184
Table 9.4 Baseline performance of shape-outline based detector 185
Table 9.5 Baseline performance of histogram based detector (Edge saliency) 185
Table 9.6 Baseline performance of histogram based detector (Motion saliency) 185
Table 9.7 Baseline performance of histogram based detector (Background saliency) 186
Table 9.8 Combined (shape+histogram) detector performance after tracking 194
Table 9.9 Expected false positive rate for the combined shape and histogram tracker for the test sequence 195
Table 9.10 PETS 2006 Frame based metrics 196
Table 9.11 PETS 2006 Object based metrics 197
Table 9.12 Average execution time of JPDAF tracker with frame resizing 199
Table 9.13a Peak performance of GMM detector based on classifier trained using GMM blobs 200

Table 9.13b Accuracy evaluations for proposed human detection algorithm compared with Gaussian mixture model 201
Table 9.14 Peak performance of mean shift detector /tracker. Positional accuracy expressed as a fraction of maximum distance of separation (in pixels) between human locations in two consecutive frames 202
Table 10.1 System architectural parameters for the proposed accelerator 213
Table 10.2 Macro architectural parameters of Pentium IV 214

LIST OF ABBREVIATIONS

CAD	Computer Aided Design
CCTV	Closed Circuit Television
CIF	Common Intermediate Format
CMP	Chip Multiprocessor
CWT	Continuous Wavelet Transform
CODEC	Compression Decompression
DVR	Digital Video Recorder
GMM	Gaussian Mixture Modelling
HDT	Human Detection and Tracking
JPDAF	Joint Probabilistic Data Association Filter
MHTF	Multiple Hypothesis Track Filter
MIMD	Multiple Instruction stream with Multiple Data stream
NVR	Network Video Recorder
OCWT	Over Complete Wavelet Transform
PDAF	Probabilistic Data Association Filter
PETS	Performance Evaluation of Tracking and Surveillance
POS	Point of Sale
QCIF	Quarter Common Intermediate Format
RMS	Root Mean Squared
ROC	Receiver Operating Characteristic
SIFT	Scale Invariant Feature Transform
SIMD	Single Instruction with Multiple Data Stream
SMP	Simultaneous Multiprocessor
VHS	Video Home System
VCA	Video Content Analysis
VSAM	Video Surveillance And Monitoring
WT	Wavelet Transform

DEFINITION OF TERMS

Anova: Analysis of variance. A statistical technique for evaluating whether two groups belong to the same populations.

Candidate human: A rectangular region of a frame which contains salient features and is to be probed by the classifier for the presence of human.

Candidate human localization: The processing of finding locations of candidate humans.

CIF: Common Intermediate Format defines a frame of size 352 by 288.

D1: Input video with active frame dimension 704 by 480 pixels.

MIMD: Multiple Input Multiple Data stream. Parallel processing technique which allows simultaneous input data stream to be processed in parallel.

Object Outline map: A derived frame showing the outline of all potentially interesting objects in the frame.

Object window: A rectangular region of a frame which contains salient features and is to be probed by the classifier for the presence of object of interest.

Window: A rectangular region of a frame or subband.

CHAPTER ONE

INTRODUCTION

1.1 Perspective

1.1.1 Surveillance for Human Survival

It's a paradox that humans as a species have shown remarkable ability to survive in comparison to other species, despite the fact that individually they are ill-equipped. This has been attributed to his ability to gather sensory data, communicate, analyse, and enhance information using his intellect. Indeed humans' ability to survive in life threatening situations, depends primarily on living in social communities, sharing and using sensory information gathered by individuals for the protection of the group. There are several forms of sensory information available including vision, smell, touch, and sound, although the preferred form is vision. The earliest form of surveillance, intelligence information gathering, analysis and decision making started with information gatherers, who were humans positioned at different locations in the field of operation. These were typically lookouts, spies, and ordinary observers. Information gathered was sent through intermediaries such as messengers, horses, and dogs, to their leader (centre of intelligence) for analysis and decision making. Decisions from the leader were also sent by intermediaries to action implementers who could be soldiers in battlefields or ordinary citizens. Figure 1.1 shows information flow in surveillance systems and is valid for both primitive and modern societies. This earliest approach relied predominantly on humans throughout its stages of operations. Although it has evolved over the years the basic structure has stayed the same. The next stage in the evolution process was the use of semaphores and other forms of coded messages to reduce reliance on messengers and increase reliability. Information gathered could then be sent directly to the leader. Semaphores were used extensively to communicate

positional information, and other intelligence information between sections of the army or the navy in times of war. Further, inventions such as telegraphs, Morse code, and telephones drastically improved and increased the amount of information sent from a source to the destination using copper wires. Typically messages from observers were sent first to message switching centres (essentially message exchange centres) or units for packaging and forwarding of messages. Heavy use of electro mechanical devices and less involvement of humans became apparent. Finally came the information age, characterize by heavy use of electronic devices right from the sensory data acquisition to dissemination of information. Messengers and other links were replaced by communication links such as optical fibres cables, coaxial cables and air, and other specialised communication devices. The mode of operation also changed from analogue to digital. The resulting communication links are very efficient, reliable, and carries larger amount of information.

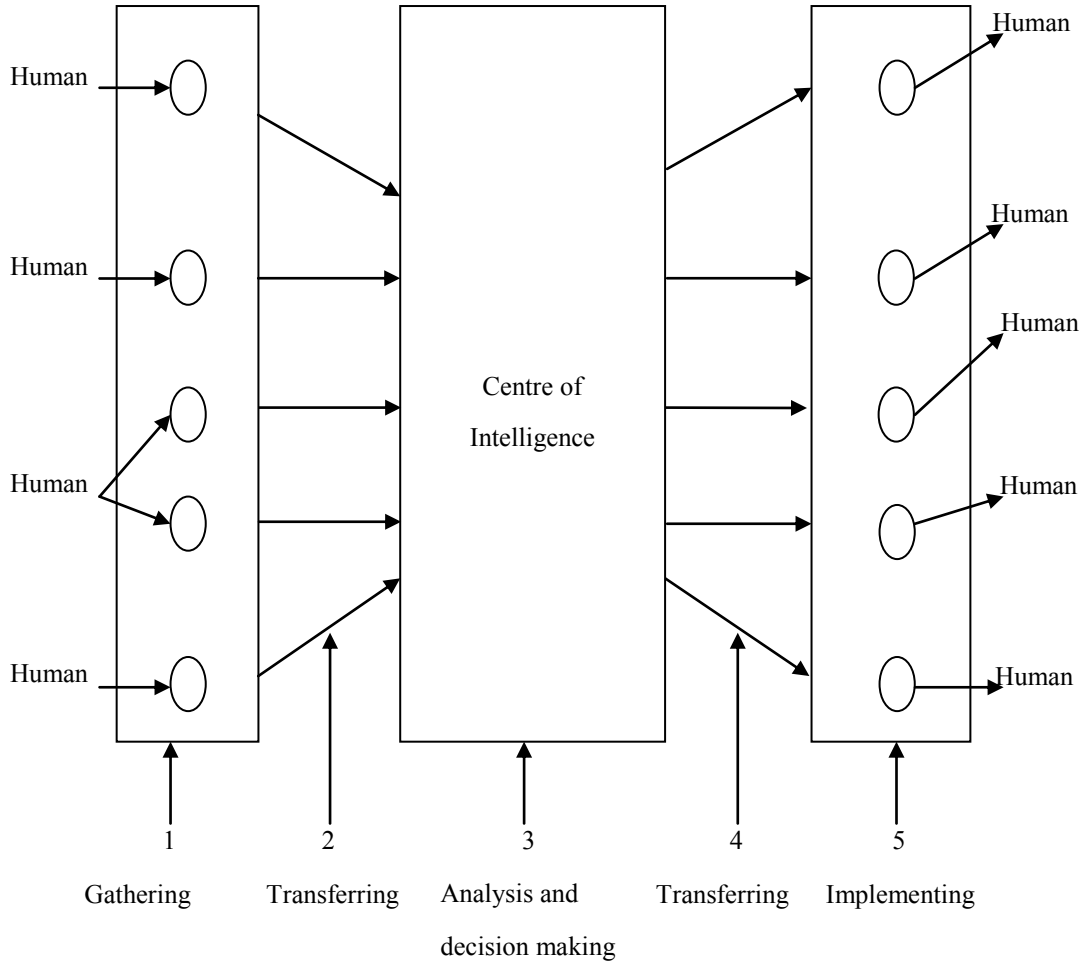

Figure 1.1: Activity flow in a surveillance system

Legend

1: Information

2: Means of transfer (birds, dogs, wires, cables, free space)

3: Centre of intelligence

4: Means of transfer (birds, dogs, wires, cables, free space)

5: Action implementers

A typical modern intelligent information processing system may still have humans and electronic sensors as data gathers. Communication links (using any of the above links) connects data sensors/humans to a central unit (message switching units) via multiplexors which is responsible for packaging, forwarding, and other housekeeping operations required to efficiently transmit data to the intelligence centre. Decisions and actions from the intelligence centre (a control room with humans monitoring and analysing information) based on the incoming data are sent first through a similar unit (message switching units) which repackages information in an efficient manner, and sends via de-multiplexors to the recipients (action implementers).

A very important class of information of interest to man is information about other humans and their activities, typically for surveillance, people monitoring in shops, real-time vehicular traffic monitoring, and perimeter protection.

1.1.2 Requirements of a Generic Surveillance System

For effectiveness the sensory information processing must be timely, accurate, reliable, and relevant to the situation on hand.

Timely: information flow from information gathers to end user must be timely and appropriate for the situation on hand. Information and action required to prevent a crime in progress must be available on the spot.

Accurate: accurate information must be provided at all stages of the system, and ideally analysis and decision making must be error free.

Reliable: information required must be available at all times independent of any external conditions. It must also be consistent and predictable.

Cost-effective: It must optimize cost, accuracy, reliability, and timeliness. The system must additionally be easy to use and flexible for widespread deployment and adoption.

The main requirements of generic surveillance systems are summarised as:

- User friendliness
  - Ease of use
  - Ease of deployment
- Operational efficiency
  - Accuracy
    - Predictable
    - Consistent
    - High
  - Timeliness
    - Real-time processing
  - Performance
    - Scalability
  - Reliability
    - Continuous operation
  - Application flexibility
  - Cost-effectiveness
    - Reliability
    - Reduce cost, high accuracy, and performance optimization

1.1.3 Evolution of Visual Surveillance Systems

Human sensory processing capabilities are limited in the domain of sound, touch, and smell but well developed in processing visual patterns. The means of human visual information capture are the eyes, and studies have shown that they have limited range of visual perception, but good at discriminating features. Man is not unique in processing sensory information since other animals such as whales have well developed sound processing capabilities, and rely on them for food and protection. For example, ants communicate using smell from pheromones deposited on the ground wherever they visit to assist the colony in search of food. Table1.1 is an evaluation of surveillance activities based predominantly on humans against requirements of performance (accuracy, timeliness and reliability), cost-effectiveness and user-friendliness. The main problems with intelligence gathering centred on humans are: the slow means of information

transfer from gatherers to centre of intelligence, slow means of transfer of decisions and commands from centre of intelligence to action implementers, and low volume of information transferred per trip. Visual communication using manual processing (rely predominantly on humans) is relatively slow, expensive and inefficient especially when visual information is to be gathered over large area of coverage.

A solution to the high cost of gathering information over large areas is the use of image acquisition devices (cameras, infra red and thermal imaging device). Closed circuit television (CCTV) cameras in particular provides a cost-effective means of acquiring images on a continuous basis, and over large areas using multiple cameras. In response to increasing volume of visual data continuously being acquired storage devices are used for archiving and playback of video streams. The first storage devices were analogue device such as charge couple device, magnetic tapes, and VHS cassettes. Later on digital storage devices such as Digital Video Recorders (DVRs, and Networked Video Recorders, NVRs) Network storage, and hard disk drives were used since they have improved reliability, and high accuracy. With increasing number of cameras being deployed, the problem of effective monitoring of cameras and analysis of visual scene by humans also came to the attention of designers. Typically operators would monitor video from several cameras deployed over wide area on display devices to make on-the-spot decisions about threats, and take appropriate action. One solution adopted is automation first by analogue storage and processing and later by electronic processing. The main reason is the higher reliability and availability of information in digital storage form and access to larger volume of digital storage devices compared to analogue storage. Electronic information processing also provides a cost-effective means of linking visual sensors to intelligent processing units using computer networks. For example several CCTV cameras could be linked remotely to intelligence centres for processing visual information. Additionally electronic computing is pervasive due to availability of cheap digital storage media and, diverse processor types (ASIC, DSP and FPGA) and communication devices. The development of international digital compression standards for removal of redundant visual information (JPEG, MPEG, H261, etc) saving on storage and transmission cost also favours digital processing at all the stages of surveillance system mentioned earlier on. However the following problems still confront most electronic visual processing systems at the analysis and decision making step:

Table 1.1: Evaluation of human centred visual surveillance activities against generic requirements of surveillance systems

Visual Surveillance activity	**Evaluation**
Information gathering	Accuracy good, but limited attention span, and coverage, poor scalability (data), poor reliability (continuous operation), low cost-effectiveness (high cost of information gathering)
Information transfer to centre of intelligence	Limited amount of information transfer, error prone, dependent on external factors (data scalability)
Analysis and decision making	Timely and accurate, but limited attention span, poor reliability (continuous operation), high scalability (independent of scale of operation)
Information transfer to implementers	Limited amount of information transfer (scalability of data), error prone (reliability), dependent on external factors
Action implementation	Good, dependent on timing and accuracy

- inadequate continuous on-the-spot analysis and simultaneous decision making capabilities. It increases with increasing number of video sources.
- analysis (processing) of large volume of archived video sequences in response to queries. It is time consuming and error prone.
- accuracy in detecting and tracking objects, events, and anomalous behaviour in image sequences with dynamic and complex scenes.

The following are possible approaches to solving these problems: the problem of continuous mode image acquisition, analysis, and instantaneous decision making capabilities on a large scale deployment scenario could be solved using, computer based systems with distributed processing, centralized/distributed monitoring and control of operations and rapid response to event in progress. The processing system must be

characterized by scalable computer processing power to match required processing power, and scalable processing techniques (parallel/distributed algorithms for robust content analysis); and real-time processing capability to meet application requirements.

1.1.4 Challenges of Visual Scene Analysis

Typical visual scene analysis algorithms involve the following sequence of tasks: pre processing, object detection, object tracking, and anomalous behaviour detection. Pre processing typically involves frame format inter conversion, noise removal, decompression, and object enhancement. Object detection typically involves scene modelling, candidate object localization, analysis/synthesis of candidate objects, classification and detection, and anomalous behaviour analysis. Object localization typically involves identifying locations of likely objects. For a given object location object analysis or synthesis technique is applied to identify its features or to model the object. When several objects are of interest in a scene then one object class must be differentiated from another object class, hence objects must be classified. Also in detecting single objects, background objects would have to be differentiated from the object of interest. Object classification may be part of an object detection task since a particular object in a class might have to be identified from among other objects not in the same class. Detection typically follows classification and involves evaluation of confidence level after classification or some validation test. The output from the detector is typically the location, and the class of the candidate object. Object tracking involves establishing correspondence between the same object in different frames. Anomalous behaviour detection involves defining atypical behaviour as a sequence of discrete events. Continuous mode visual scene analysis operating twenty-four hours a day is faced with several challenges including the following:

Analysis complexity: Increasing analysis complexity typically arises in complex scenes involving illumination changes, scene clutter, scale changes, camera motion, and low object background contrast. For instance changes in scale brought about by perspective projection due to object moving away from a stationary camera might make a feature-based detection technique fail due to difficulty in differentiating object features from noise at very low object resolution. Similarly, the choice of object models on which object analysis and synthesis depends on has direct effect on complexity. For instance 3-

D models of humans, and its associated motion models are computationally demanding, although the accuracy is better compared to 2-D models [Ju et al. 1996], [Quentin et al. 2001]. The choice of algorithms and the assumptions on which it is based also has direct effect on analysis complexity. With 2-D motion models, an assumption of smoothness of motion or changes in illumination is used in motion tracking, or optical flow to reduce analysis and computational complexity. Similarly in tracking, multiple hypotheses tracking with exponential search complexity could be avoided by excluding certain incompatible events from occurring simultaneously.

Accuracy: The accuracy of object detection and tracking measures how often the system makes correct and incorrect detection and tracking decisions and the confidence levels associated with this decision process. The accuracy of detection and tracking objects in visual scene is dependent on whether objects exist in isolation or part of a group, besides scene complexity factors. As a general observation, objects in a group tend to occlude features of each other. For example two humans moving together as a group might result in features of the person closer to the camera occluding the other person's features. Also in detection of multiple objects there are several possible outcomes depending on object configuration and interaction in the scene. The outcome could be individuals, sub groups, and the group as a whole could be detected. It also depends on the associated ground truth defined for the scene. This means that the robustness of the detection technique depends on how well the detected objects matches those of the ground truth. Thus one way of achieving flexible detection is to let the detection and tracking be algorithmic parameter driven to increase it robustness, and allow the possibility of optimizing based on algorithmic parameters. The implication of the subjective nature of ground truth labelling means that detection rates may vary with object-object interactions, and scene-object interactions.

Reliability: In general for dynamic scene, complexity may vary with time of the day, weather, scene clutter, illumination changes, and object-object interaction, and scene-object interactions. Thus assumptions valid during the daytime might not be true during the night. There is a corresponding fluctuation in detection and false alarm rates (accuracy) over time. This makes it difficult to predict performance. Figure 1.2 is a plot of detection rate versus frame index over time for stc_t1_c video sequence with multiple humans (a PETS 2006 video sequence) for frames between 33 and 500. Wide variations in the detection rate over time are clearly visible. Frame detection rate is defined as:

Frame_detect(i)=Number of humans detected in frame i by the application/Total number of humans in frame i.

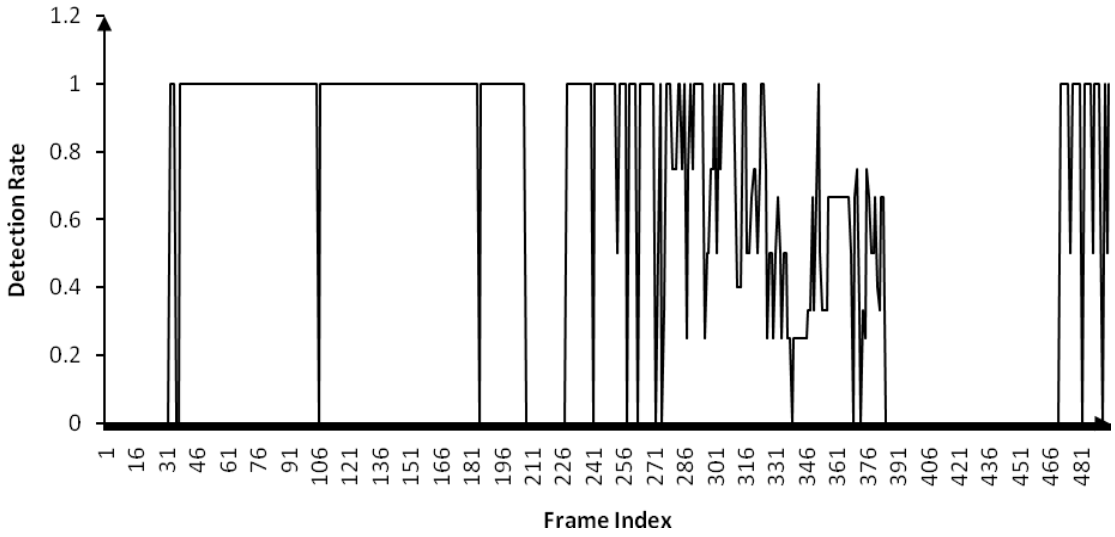

Figure 1.2 A graph showing detection rate in a video sequence with dynamic scene

Response time: The response time of the human detection and tracking application is also dependent on accuracy requirement, number of humans in the scene, and objects-scene interactions. When response time is not critical it is possible to detect most objects by applying several processing techniques and heuristics, incurring high computational cost. However by being selective in the choice of processing techniques and algorithmic parameters it is possible to achieve optimum detection with reduced processing time, and moderate computing power requirements. This typically involves investigating the influence of algorithmic parameters on accuracy, timeliness, and performance.

Cost-effectiveness: Achieving optimum accuracy requires evaluating the effect of analysis complexity, reliability, response time and performance scalability for a given algorithm.

1.1.5 Video Content Analysis

In response to the challenges of visual scene analysis has evolved video content analysis systems. VCA also known as video analytics or intelligent video, attempts to provide a computer-based acquisition and processing system, and environment for analysis of video streams.

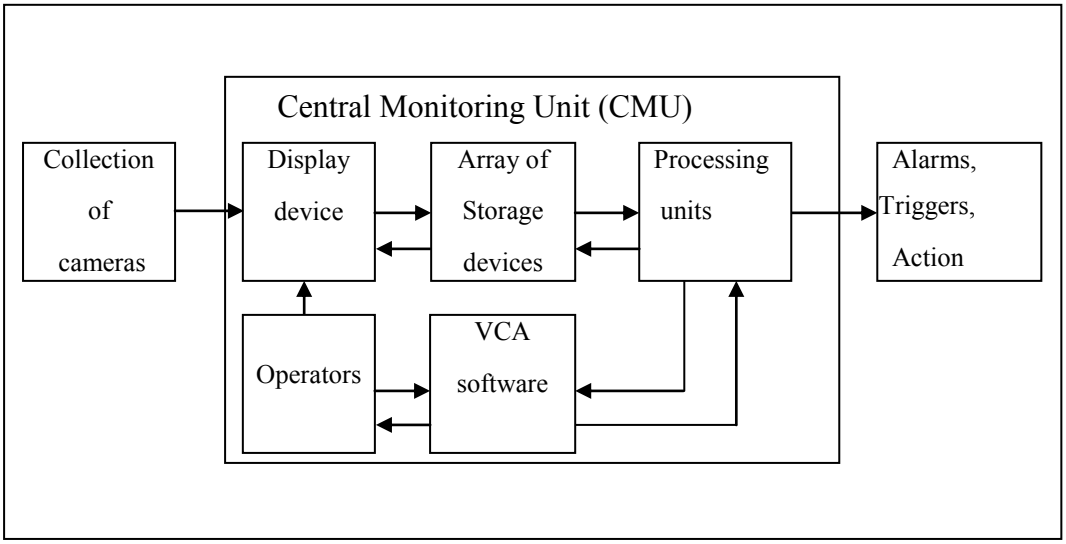

Figure 1.3 Components of video content analysis system

Intelligent video content analysis aims at understanding visual scene, with the view to learning, interpreting, and extracting meaningful information from video sequences. Applications include video retrieval, event detection, human detection and tracking, anomalous behaviour detection, real-time vehicle monitoring and traffic control, and surveillance. Typical VCA system consist of video acquisition units, video storage and display units, and network of processing units as shown in figure 1.3. A collection of cameras connected to storage device is deployed over the area of coverage for visual data acquisition via a digital communication network. The output from the cameras may be partially analysed within the camera before transmitting to the central monitoring unit, and optionally displayed on display units without any processing. The acquired video streams are also archived on storage device for later playback. Typical storage are DVRs, NVRs, and hard disks. The network of processing units provides the raw computing power for analysing the video stream by the VCA software. Typical analysis task involves detection of humans, vehicles, zone monitoring, and tripwire crossing.

The results of the analysis might also be stored on DVRs, and NVR, displayed on monitors or communicated to personnel responsible for taking actions appropriate to the situation on hand, generate alarms, or trigger other events. For example the VSAM project at Carnegie Mellon University [Collins et al. 2001] implemented a system consisting of multi-camera sub system linked by digital network which cooperatively acquire video signals, track multiple moving objects, and fuse information from multiple cameras into scene level object representation. Locations of cameras overlay the site map to enable real-time monitoring and control. It has the capabilities of setting triggers on certain events, which results in specific sequence of action taken. VCAs have put a lot of emphasis on:

Ease of deployment: End users of the system are expected to configure the application with ease. This means ability to select performance measures, and fine tune application parameters. The interface is expected to be user friendly with help facility provided. Facilities such as alarms and triggers might be required for real-time monitoring especially in situations where several video streams from different geographical locations are being monitored simultaneously.

Computational efficiency: The ability to achieve high accuracy without exceptional increase in computational work load means the system is expected to provide high reliability, and availability. This has implications on processor and scalability with increase in frame size, frame rates, and number of video streams channels.

Real-time processing: The ability to match real-time response with different application scenarios. For example in applications involving crime prevention, it might be required to prevent a crime in progress from being committed and so it would be required to set alarms to trigger events in progress for necessary action to be taken.

Cost-effectiveness: The performance of the system is expected to balance accuracy and reliability constraints, and cost on the other hand. Achieving the optimum level of performance might involve for instance scaling of algorithmic parameters, processors, and number of system components.

1.1.6 Evaluation of Selected VCA Systems

The purpose of this section is to review typical VCA software functionalities provided

by commercial vendors, and identify software functionalities which are required for robust human detection and tracking. A typical VCR system has the following hardware components: multiple cameras (analogue and digital), matrix switches for connecting cameras to storage device, monitors, video codec, DVR and NDVR for storage, and monitors for display. Installed software typically includes graphical user interface with functionalities such as video recording, playback, alarms and trigger, camera control via software interface (pan, tilt, and zoom), motion detection, human tracking, event detection, and access control management. The hardware components may be internet protocol (IP) based network. A summary of the evaluation of VCA software is presented in table 1.2 with additional information on VCA software also provided in appendix A. The following trends are observed: User interface provided is quite good since it is window-based and upgradeable with functionalities for object detection and tracking. It provided generic features and software control of cameras and its motion. Cost-effectiveness is good since it provides for both software upgrades, and hardware platform upgrades. Information on accuracy outside the controlled operating environment is not provided.

1.1.7 Algorithmic Approaches to Object Detection and Tracking

Traditionally, visual sensors capture single image or video in space-time domain and use vision and signal processing techniques also in the same domain to detect and track objects. [Dee H.M. 2008] provides a review of vision based approach to human detection. Algorithms for object detection and tracking can be classified into three main approaches, namely, feature-based detection and tracking, model-based detection and tracking, and motion-based recognition. Feature-based detection and tracking relies on detectable object features in the video stream; model-based technique relies on generated object model and its associated motion models. Typical 2-D models consist of view dependent 2-D shape models, and affine transform based motion models [Rohr 1994]. 3-D models include bone and tissues models based on finite element methods, and its associated motion and pose models, all stored in a model database. Motion based recognition uses the intrinsic motion of whole or part of the human for detection and tracking.

Table 1.2 Required functionalities of a generic VCA system

Requirements	**Functionality/Implementation**
Ease of use	Client-server based, windows-based
User functionality	Object detection and tracking, people/vehicle counting, direction, speed, object classification, triggers and alarms and controls, motion detection, abandoned object and removed object detection, directional virtual tripwire, user defined object search, and image processing functions
Generic features	Internet protocol-based, camera control, camera location overlays site map, multiple windows display, video management, links to end users, CODECS, remote live view, synchronised audio, multi camera recording and playback, remote control and configuration
Ease of deployment	Provides for multiple camera controls (1:32 cameras) both analogue and digital cameras; process CIF[1], 4CIF, D1 frames;
Accuracy	Detection rate of over 90% in controlled environment, or in a zone
Reliability	Operates continuously day and night; Special cameras (infrared + daytime) with special features well matched to application; Vandal resistant dome cameras; hardware solution for motion detection
Real-time processing	Most commercial system provides real-time processing capabilities
Scalability	Simultaneous multi-client and multi-server access
Cost-effectiveness	Provides software upgrades and support

The main processing steps for feature-based object detection are summarised as follows:

- Video acquisition and frame buffering (from IP and analogue cameras)

- Decompression and colour space conversion
- Frame enhancement
- Human detection
- Human tracking

The video acquisition and frame buffering deals with hardware-software interface for video sequence acquisition from one or more cameras. Since there are several real-time solutions available it is not covered in the thesis. Similarly the availability of Codecs (compression/decompression) solution, and the fact that it is offered as part of the camera acquisition sub system it is also not covered. Software solutions for RGB to YUV conversion routines are used where necessary. Frame enhancement functions of interest include noise removal, illumination normalization, and saturation control. Object detection involves locating instance of objects, and discriminating the object from its background or from other classes. Object could be cars, humans, and birds with emphasis mainly on object properties in the space-time domain (images) or observable in transform feature space. The outcome of the discrimination process is the assignment of the object to a class. If the object is assigned to a human class then it asserts a hypothesis on the existence of human. The output of the object detection phase is passed on to the tracking stage for mapping out the location and velocity of objects over time.

1.1.8 Improving Accuracy of Feature-Based Approach in Pattern Space

In feature space classifiable features are extracted and used for object detection or recognition. Two main types of image based features could be used for detecting objects, namely features which directly relates to observable object as a whole (global features), and primitive (local) features which do not uniquely relate to the observable object features but are used as building blocks to construct higher level object's parts. There could be combinations of local and global features for object detection [Moeslund and Granum 2001]. It could be implemented by part-based detection [Meyer et al. 1999], [Wu and Nevatia 2005] and then the object as a whole is detected by inference using the detected parts. An example is the upright human body shape, and its parts such as hands, head and shoulders, legs, and torso. On the other hand

local features such as corners, edges, lines, and circles are primitives which are used as building blocks to construct parts of the body, before assembling a complete model of the object. This closely relates to the two level object feature used in computer vision techniques, namely, local and global features [Danielsson et al. 2008]. Features which are observed in pattern spaces may have different relationship with the physical object. Typical examples include wavelet coefficients, histogram of oriented gradients, optical flow vectors, SIFT features, and shape context. Feature space based detection and tracking, has relatively smaller computational load, compared with model-based technique (an alternative approach). However a major challenge with real-world objects is that they involve concepts such as car, face, human, rather than specific objects and exhibit large class variability [Swarup 2002]. As a result there is no easy way to come up with an analytical decision boundary separating one object concepts from the other using low level image features or features in pattern spaces. The robustness of a particular solution depends on the choice of suitable feature set, and the type of application [Wikipedia]. In a typically pattern space feature extraction, the input data is first transformed into the feature space, and then good features are extracted followed by feature classification. Good local features for object recognition must be translation, rotation and scale invariants [Lowe 1999], and at the same time must be distinctive among many alternatives. [Yilmaz 2006] has provided a review of different feature types used in object detection and tracking. These include points (corners, centroids), primitive geometric shapes, object silhouette and contours. Shape as a global feature has also been used in several human detection and tracking applications [Lee 2004], [Song 200], and [Berg 2000]. The main limitations of feature based object detection or recognition [Lowe 1999] is providing enough feature points as evidence in either detection, recognition or tracking scenario, and coping with scale changes. In particular scale changes and translational invariance are requirements which are desirable in object detection. Scale refers to the level of detail at which the features of a physical object are detected. To meet scale invariance requirements designers of detectors in feature spaces like scale-frequency domain [Oren et. al 1997] use hierarchical feature analysis technique to construct wavelet templates. This ensures features are detectable across several levels of scale. Multi-scale decomposition provides a means of analysing images and video sequences across scales.

1.1.9 Exploiting Local Features in Two Independent Pattern Spaces

Clearly, a means of improving robustness of object detection is to complement space-time domain detection with scale-frequency detections: multiscale analysis of images features is part of most object detection techniques. Additionally, certain class of wavelet transform provides translation invariance which is a requirement for generic object detector. Combining detections in two independent feature space is hypothesised to improve detection rate if the feature set used in one space is orthogonal to the other feature set. This is the approach proposed to improve the accuracy of human detection and tracking. Thus by approaching the human detection and tracking as pattern analysis/recognition problem posed in two independent patterns spaces, the combined accuracy is expected to improve. The effect of the two approaches on the accuracy of human detection and tracking (in wavelet domain and space-time domain) is examined in the current study via simulation.

1.1.10 Pattern Classification for Object Discrimination

Often large number of features are extracted to represent the target concept, however many of them could be irrelevant or redundant in the sense that they appear in other categories. Essentially given a set of d features, the problem of selecting a subset of m features with the maximum discriminatory power is a classification problem. [Watanbe 1985] showed that it is possible to make two arbitrary patterns similar by encoding them with sufficiently large number of redundant features. Feature extraction aims at removing redundant and non discriminatory features not well matched to object concepts, whilst object discrimination focuses on the use of discriminatory features for object class identification. This could be achieved by classification of object features. Of the two main approaches to classification, namely, supervised and unsupervised learning, supervised learning provides a mechanism for reinforced learning since there is a desired feedback as well as inputs [Dayan 1999], whilst unsupervised learning is purely statistical technique it requires a prior assumption about the distribution of features in the scene. The difficulty in determining when adequate training has been given to a classifier however limits it's

accuracy as a universal discriminator. One class of unsupervised learning technique, histogram-based classifier (a density estimation technique), and a supervised learning technique, neural network pattern classifier, is used as a vehicle for investigating performance of classifiers in human detection in the current study.

1.1.11 Bayesian Tracker for Optimal Object Tracking

Two main issues are involved with visual object tracking, namely, object representation and localization, and filtering and data association [Commaniciu and Ramesh 2003]. Object representation and localization deals with changes in object appearance, its location and representation (by measurement estimation). It is a bottom-up process with specific assumptions about object dynamics. Filtering and data association is a top-down process dealing with dynamics of the tracked objects, learning of scene prior, and evaluation of different track hypothesis. Bayesian filters provide a probabilistic frame work for improving the accuracy of a set of parameters based on prior information and current estimate (see section 2.3). The optimal Bayesian filter for multiple object tracking suffers from high computational and memory requirements on account of its recursive nature. Sub optimal filters such as JPDAF, probabilistic data association filter, and track likelihood filter may be used provided application requirements could be met. The dynamics of objects is typically modelled using Kalman [Marcenaro et al. 2002] predictions if motion is linear, or sample based techniques such as particle filters [Zhou et al. 2004], and other Monte Carlo based techniques. The study investigated joint probabilistic data association filter for tracking of multiple humans. Its ability to reduce false detections brought forward from the detection stage was also investigated.

1.1.12 Software Functionalities Proposed for Video Surveillance Applications

Most commercial VCR software has a user interface through which user requirements defined as zones, virtual tripwire, and perimeters (region of interest), are defined as parameters to the detection and tracking module. The output from the detection and

tracking module comes out as alarms, alerts, triggers, and event login information recorded unto an event database, or to video management software. Based on VCR software evaluation and the proposed algorithm the complete software system consists of video acquisition interface, graphical user interface (GUI), detection and tracking modules, and video management module. This is shown in figure 1.4 of which the main focus of the current project is on B, C, and D (analysis and decision making stage).

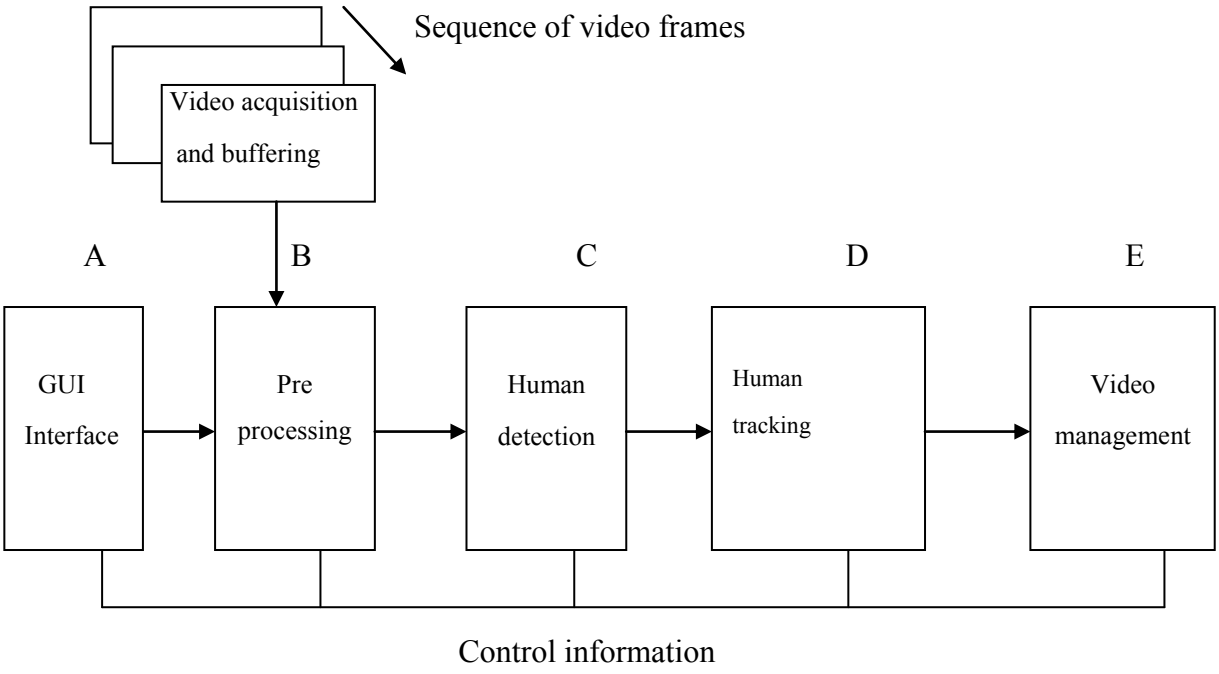

Figure 1.4 Main VCA software components

It is split into human detection and tracking pipelines. It has the following sub tasks:

- **Video acquisition and buffering interface**

- **Pre processing (frame conversion and frame enhancement)**
  - Format conversion
  - Decompression
  - Median filtering (noise removal)
  - Contrast enhancement
  - Saturation control

- Frame resizing

Human detection

- **Feature extraction**
  - Construct silhouettes map (wavelet based map construction domain)
  - Construct shape outline map (Object outline map construction)
- **Candidates localization (provides location information)**
  - Select candidate regions (from silhouette map)
  - Select candidate regions (from object outline map)
- **Human discrimination**
  - Classification and validation
    - Wavelet based classification
      - Histogram based classification
    - Shape-outline based classification
      - Pattern prediction
      - Hypothesis generation
      - Hypothesis validation
    - Validation
      - Linear discriminant test for candidate humans after classification
      - Heuristics test
  - **Update details of found humans**
    - Determine centroids of found humans
    - Database update.
      - Merge list of found humans from shape and histogram detectors

The tracking pipeline has the following sub tasks:

Human tracking

- **Track initialisation**
- **Silhouette extraction and processing**

- Silhouette extraction
  - Blur image with 5 X 5 averaging filter
  - Apply intensity-based segmentation
- Appearance template feature extraction
  - Extract gradient and chromatic colours from silhouette region
  - Determine intensity of pixels representing humans
- **Measurement computations**
- Local and global motion vector estimation;
- Location estimation;
- **Measurement validation**
- Mahalanobis based constraints;

- **Track hypothesis generation and validation**
  - Compute measurement to track cluster association;
  - Generate measurements to track association hypotheses;
  - Compute signatures of found humans in the current frame;
  - Determine best track for every candidate human using its signature;
- **Kalman prediction**
  - Next state prediction;
- **Post processing**
  - Track maintenance (Track activation, deactivation, split, merges)
  - Occlusion handling and statistics gathering;

1.1.13 Persistent Problems of Automated Human Detection and Tracking in Space-Time Domain

Most of the current approaches to human detection and tracking is object-based. It relies on segmentation techniques or indirectly figure-ground separation in the spatial domain and is based on computer vision techniques. It basically detects blobs and regions which are direct representation of the object. Vision based processing algorithms in spatial domain are faced with the problems enumerated earlier (low contrast, illumination changes, shadows, and occlusions and background motion). The main challenges are:

Scene complexity: A closer examination of the algorithmic issues mentioned in section 1.1.4 reveals that the main problems associated with feature-based approach (in spatial domain) are feature visibility, scale changes, and low contrast. The problems associated with model-based techniques are the choice and adequacy of the models, and computational complexity [Rohr 1994]. The problem associated with motion-based techniques is characterising motion, differentiating fake motion and noise from object motion, and sensitivity. Additionally, scene clutter and object-object occlusion, and object-scene occlusion, and the number interesting objects in the scene being detected or tracked affect all the three approaches, resulting in extra processing steps, and hence increase in computational complexity.

Real-time processing limitations: Computational load also increases with increasing frame rates, frame size, number of video inputs (channels), and response time constraints. Extra algorithmic steps are added to improve robustness (shadow elimination and background motion compensation, occlusion, etc). The net effect is an increase in processing workload and hence the execution time which directly affects the response time. The problem of increasing computational complexity and increasing computing power requirements can be met by parallel processing with scalable processors to match increasing computational load. Parallel processing can reduce execution time by exploiting natural and applied parallelism. Sequential processing is limited in achievable performance which worsens with increase in frame rates, number of video channels, and frame size. Issues such as processing scalability becomes a major consideration.

Accuracy: In reality there are four possible outcomes of object or event detection assuming crisp categorisation of outcomes. The first one, true negative, occurs when the algorithm does not detect the presence of a human and truly there is no human present at the location being probed. The second possibility, false positive, occurs when the system reports the presence of humans when in reality the human does not exist in the location being probed. The third outcome, false negatives occur when there is human but the system fails to detect the human. The last possibility true positive, is when there is a human and the system detects the human. This means that the detection rate (true positive divided by count of all instances of humans) is usually a fraction of the ideal detection rate. Further when multiple humans are interacting in the scene, such as coming together, and or separating other outcomes are possible. For example several

humans could be detected as an instance of a group, resulting in several false negatives for all the individuals in the group but a single detection event. Thus detection rate of multiple humans in a group may be smaller than the true positive counts of humans in the scene. This may also be due to the interactions between humans resulting in occlusion. At the detection phase another problem is the variations in detection rate and high false alarm rate when underlying assumptions about a scene are violated. In tracking the main problem to contend with are positional and tracking errors due to track data association ambiguities, sparse data resulting in tracks with no measurement association, and multiple data association with a single track. Object-object interactions, and object-background interactions also results in partial or total occlusion. This also causes data association problems, hence affects the accuracy of the system. At the tracking phase these problems results in low track detection rate, high track miss detections, track false detections, track fragmentation and merges errors.

From the end user point of view automated human detection and tracking systems are expected to provide a level of service offered by traditional CCTV cameras being monitored continuously by humans. Given the above limitations of most current system, there is the need to improve the analysis and decision making aspect, i.e, object detection and tracking. Though there have been several reported studies of success of video analytics systems deployed in indoor and outdoor environments, the majority of the deployed systems face some of these challenges [Boghossian et al. 2001]. Thus for a particular scene the analysis of the resulting video sequence using a particular algorithm might have high accuracy, whilst with another sequence the accuracy level would be very low.

However users would be comfortable working with tools whose accuracy is very high and predictable. The existence of these algorithmic accuracy limitations is the motivation for investigating human detection and tracking in scale-frequency domain, as a complement to space-time domain processing. For example [Siebel 2002] uses multiple tracking algorithms to track humans. Wavelets transform feature space provides a means of detecting both global and local features appropriate for multi-scale analysis. Several wavelet features have also been used in image analysis [Mallet 1992], [Strickland 1997], [Unser 1995]. These include wavelets coefficients, normalized wavelets coefficients, wavelets templates, and wavelets energy, wavelet packets. Combining object detection in the spatial domain with wavelet domain detection is

expected to achieve higher detection rate if multiscale processing capability is exploited such that detection is independent of scale changes. One possibility is to identify primitive features which is detectable at all scales. To what extend the increased in computational load would improve accuracy of detection and tracking of humans is the subject of the current study.

1.2 Aim and Objectives

The aim of the study is to improve operational efficiency of surveillance systems by investigating an algorithm with capabilities to improve the accuracy of human detection and tracking. The accuracy of the algorithm is expected to be independent of scene complexity, with predictable operating accuracy and performance scalability to improve timeliness. The objectives are:

Investigate novel algorithms

1. To investigate scale-frequency domain and shape space pattern classifiers for improving accuracy of detecting humans (improving detection rate, and reducing false alarm rate).
2. To investigate reduced complexity joint probabilistic data association filter for reducing false alarms and track positional errors during tracking;
3. Propose parameter driven accuracy prediction technique independent of scene complexity.

Improve response time

4. Improve performance scalability to cater for increase in frame size, frame rate, and number of video channels by deriving scalable algorithmic architecture.

Compare accuracy with other algorithms

5. Comparative accuracy evaluation of proposed detector with other competitive algorithms.

1.3 Research Strategy

Human detection and tracking is split into two main parts, namely, human detection and temporal tracking. Human detection focuses on shape-space, and wavelet template features for human discrimination via classification. However, tracking is performed in spatial-temporal domain using multiple motion models for Kalman prediction, and joint probabilistic data association filter (JPDAF) for data association. Receiver operating curve (ROC) based prediction of operating accuracy, and synthesis of scalable algorithmic architecture were also investigated. The following strategy was adopted:

(1) A review of existing algorithmic solution in the literature to the problem of human detection and tracking under background scene constraints. The effects of scene factors such as low background contrast, background clutter, scale changes, and object occlusion on accuracy were examined. The limitations and strengths of existing algorithms were evaluated.

(2) At the detection phase, proposed new algorithms for human detection by:

- Investigating discriminatory feature extraction techniques in two independent feature spaces for human detection, namely, shape-space and scale-frequency space (wavelets domain).
- Investigating three independent feature space pattern classifiers for improving human detection. This entailed design, implementation and evaluation of a shape-outline based classifiers for detecting apparent shape of humans in the spatial domain. The design, implementation and evaluation of two wavelet domain classifiers for robust movement, and scale invariant detection were also investigated.
- Specification and implementation of human detection task pipeline combining detections in the wavelet and shape domains.
- Evaluation of accuracy of proposed detection algorithm under the following scene background characteristics:
  - scene clutter
  - scale changes
  - multiple humans coming together or separating from each other

- low contrast,
- sudden illumination changes.

(3) At the tracking phase proposed a JPDAF tracker algorithm for human tracking, detailed out its specification. Evaluated the proposed tracker. Investigated low complexity tracker with the following characteristics:

- Used JPDAF and Kalman prediction with motion models for robust tracking.
- Application of linear discriminant classifier to reduce track false alarm rate.
- Use of Mahalanobis confidence limits for joint detection and tracking in batch estimation mode to reduce hypothesis enumeration complexity (reduce computational complexity).
- Matching of appearance signature of found human with candidate tracks to determine the best human-to-track association for track hypothesis validation.
- Evaluation of accuracy of proposed tracker under occlusion, scene clutter, and scale changes.

(4) Investigated use of ROC curves in predicting operating accuracy. This is based on first determining optimal algorithmic parameters for the detection and tracking phase, and then using ROC curves to predict operating performance. Synthesis of scalable algorithmic architecture for human detection and tracking deriving:

- Components (modules in software) for human detection;
- Components (modules in software) for human tracking;
- Investigated the influence of algorithmic parameters (human width, human height, aspect ratio, etc) on accuracy on the proposed architecture;
- Proposed an integrated human detection and tracking algorithmic architecture;
- Execution time profiling and analysis of the human detection and tracking algorithm, and then finally make recommendations to speed up execution based on parallel processing on multiprocessor accelerator hardware.

The end product of this work is a methodology and software modules for optimally mapping human detection and tracking application onto a MIMD (multiple Input Multiple Data) multiprocessor system.

1.4 Overview of Thesis

Chapter one introduces the rationale and main issues being addressed in human detection and tracking in the current thesis. Chapter two provides a review of published work on human detection and tracking (HDT), discusses their strength and limitations. It also reviews related work on human recognition. Chapter three provides a review of the main datasets, benchmark metrics and specify accuracy evaluation measures based on selected metrics used in the current investigation. Chapter four redefines the objectives and strategy of the current study in view of the findings of the literature review. Chapter five discusses two proposed feature extraction techniques in the shape and wavelet feature spaces. It also presents a novel object outline extraction technique for representing apparent shapes in images. Chapter six focuses on the specification and design of low complexity histogram-based classifiers in the wavelet domain, and a feed forward neural network shape-outline pattern predictor. Chapter seven synthesises architectural building blocks for human detection and evaluates its accuracy, and profiling of sub tasks. Chapter eight focuses on specification, design, implementation, and evaluation of a human tracker in space-time domain. It is based on multiple motion models and joint probabilistic data association filter. It describes a computationally efficient approach which avoids enumeration of infeasible track hypothesis, and provides sequential and batch estimation mode of operation to determine the best tracks. It also presents execution time profiling of the main sub tasks of the tracking phase. Chapter nine consolidates the results of the detection and tracking phases. It discusses a technique for determining optimal algorithmic parameters, and presents an algorithm for predicting operating accuracy. It also discusses trends in detection rate versus error rates with changing algorithmic parameters, influence of different search strategies on accuracy, execution time analysis of the combined detection and tracking, and the different configuration options for human detection and tracking. Comparative evaluation with other algorithms, and the limitations and strength of the proposed architecture is discussed. Chapter ten concludes the study and make recommendations for further investigation into algorithms, accelerator based approach to achieving real-time performance, scheduling strategies, and parallel processing to improve throughput and reduce processing time.

1.5 Contributions of Thesis

The following are the main contributions which have emerged from this work:

- Principled approach to specification and design of pattern classifiers for human detection. A reduced complexity shape-outline extraction algorithm compared to common edge detector such as Sobel and Canny edge detector has been presented.
- Specification and design of novel shape-outline based detector in the shape-space based on shape prediction, hypothesis generation, mismatch metric evaluation, similarity measure evaluation for classification and post classification validation.
- Specification and design of a reduced complexity human detector in wavelet domain based on joint statistical analysis of primitive wavelet features (histogram of features, and marginal probability of locating human given a location). The approach also provides a means of realising bank of classifiers for object detection. Each detector uses the same classifier, but operates on a different subband. Each classifier is optimized to operate on a particular scale.
- Robust JPDAF tracker with reduced computational complexity, use of multiple motion models, and use of batch estimation mode in tracking to reduce false alarms. It also incorporates an object signature based validation step for unique object-to- track assignment.
- Operating accuracy predictions based on ROC curves and linked to both detection and tracking in a closed loop fashion for algorithmic parameter estimation.

CHAPTER TWO

A SURVEY ON OBJECT DETECTION AND TRACKING ALGORITHMS

2.1 Introduction

The existence of large published works on human detection and tracking based on different techniques makes it difficult to generalise. The chapter provides a review and a classification of publications firstly on object detection and tracking in general, and then focuses on humans in both single frame and in video. It also discusses the main features of the different algorithms, applicability, and its limitations. Sections 2.2 and 2.3 provide a brief review of object detection and tracking techniques applicable to signle and multiple frames. Section 2.4 to 2.9 discus detection and tracking of humans in video. Sections 2.4 provides an overview of space-time domain techniques, whilst section 2.5 reviews wavelet domain detection and tracking of humans. Section 2.6 reviews model based techniques. Section 2.7 reviews appearance based techniques whilst section 2.8 focuses on shape-based techniques. Section 2.9 discusses motion-based recognition of humans through behaviour analysis. Section 2.10 provides a summary of the chapter. Appendix C provides details on the main approaches, and its associated problems.

2.2 Object Detection

Object detection in images deals with detecting and locating instances of interesting objects in a scene by matching features found in the image to object features, or found object model to a database of possible object models, and is essentially a classification task [Aggarwal et al. 1999]. The task of detecting and tracking all instances of object of interest in images typically occurs in computer vision, pattern recognition, autonomous

vehicle navigation, and surveillance. In general there may be more than one object in the scene, and these objects could be anywhere, hence the need for a search strategy. Another closely related activity, object recognition, is finding a particular object by discriminating among a group of objects in the same class [Weinman et al. 2006] by determining its pose. The main distinction between detection and recognition is that detection is based on inference on image features (low level and iconic), whilst recognition additionally involves higher (symbolic) level object concepts and reasoning. Both detection and recognition tasks may use object features such as motion, texture, colour and shape. Typically in a recognition task there is a database of objects from which you would have to find the closest match to the current object. Objects may be classified or categorised to differentiate from other similar objects since most features are not unique to a particular object, and may be shared by the background or other related objects. Similarly in model-based detection/recognition the pose must be determined in order to differentiate models belonging to the same objects. In the context of object detection and tracking for visual surveillance, objects are usually detected first and subsequently tracked. Objects may also be tracked for recognition. Detection provides location information, whilst tracking provides location, direction and speed of objects. Object detection task could be part of an application whose input is a single image as in image database retrieval, or image sequence as in video for automatic target detection and tracking, or human detection and tracking in visual surveillance. A survey of published work reveals there are three main classification schemes for object detection in images. The earliest object detection techniques were based on computer vision applied to single image snapshot, but there are now several other techniques from pattern recognition and statistical signal processing. There are three main techniques for object detection, namely, feature-based [Lowe 1999], motion-based recognition [Bregler 1997],[Gavrila 1996] and model-based recognition [Tan et al. 1998]. Motion-based techniques use intrinsic motion characteristics of the object for detection, for example the gait of a walking person. Model-based technique on the other hand use 2-D or 3-D models of the object for detection, together with motion model and pose constraints. For example, the VIEWS system [Tan et al. 1998] at the University of Reading is a three-dimensional (3-D) model for vehicle tracking. The Pfinder system developed by [Wren et al. 1997] is used to recover 3-D description of a person in large room. It tracks a single non occluded person in complex scenes in a video, and has been used in many applications. The first requirement of feature-based object detection in a

single snapshot image is to determine a discriminatory feature set either in the image space or in a suitable feature space. Typical feature-space include wavelets domain, eigen space (principal component analysis) [Sang 2004], multi-dimensional histogram feature space [Kang et al. 2004], [Dalai and Triggs 2005] (histogram of oriented gradients), and shape space. Typical image based features are intensity, directional intensity gradients, colour, texture and wavelet coefficients are used to describe the object in image space. Two processing approaches, namely, vision based or pattern recognition are commonly used for object detection. Vision based techniques requires analysis and extraction of object features, and detection is achieved by synthesis or discrimination of object from other classes. In pattern (transform) space criteria such as minimum variance and minimum number of discriminatory components may be used to extract features which are then passed to a learning algorithm to extract structural information.

Special techniques have evolved to exploit the temporal nature of video frames to facilitate object detection and tracking. Geometric features of objects especially shape has been used extensively for object detection [Song 2006],[Berg 2005],[Broggi 2001],[Owechko 2004] in both single images and video sequences. Motion based recognition use the intrinsic pattern of motion of objects for detection or recognition. Gait based recognition of humans [Lee and Grimson 2002] is a typical example. Model based recognition use 2-D or 3-D models of the object with some constraints on motion for recognition [Marchand et al. 1999]. Another classification in single snapshot images, is segmented versus non segmented approach. Segmented approach relies on segmentation of the scene into foreground and background objects. A common segmented approach, motion detection, aims at partitioning regions corresponding to moving objects from the rest of the image. Motion detection techniques include background subtraction [Stauffer and Grimson 1998], [Jian et al. 2006], temporal differencing [Lipton et al. 1998], and optical flow [Meyer et al. 1999]. In scene modelling a representation of the scene (background) is generated, and compared with incoming frames to compute deviations. Pixels undergoing deviations are marked for further processing. This process is known as background subtraction. The foreground is the difference between the background model and the incoming frame. Other approaches include Gaussian Mixture Modelling [Stauffer 1998], [Jian 2006], and morphological change detection algorithms [Stringa 2000]. Direct approach to segmentation include grouping of pixels in a frame independently into perceptually

similar regions and includes mean shift clustering [Comanciu 2002], and segmentation using graph cuts [Wu 1993]. [Fazli et al. 2009] presented an improved Gaussian mixture model based segmentation algorithm for detection and tracking of humans. The problem with background subtraction scheme is detection of false motion, and hence false objects. The Standard Model Features (SMF) set introduced in [Lowe 2004] also provides a non segmented approach to object detection combining texture, shape, and context. [Lowe 2004] achieved invariant detection under rotation, translation, affine, and projective transform using Scale Invariant Feature Transform (SIFT). Other detection techniques include shape-based detection [Haritaoglu 2000], [Song 2006], combine 2-D and 3-D detection models [Gavrila et al. 1996], [Bregler 1997], and point detectors [Harris 1988].

There are two main non segmented (direct) approaches to object detection, namely, statistical classifiers, and patch based classifiers. Statistical classifiers aim at establishing statistical relationship between objects and its parts (features). Patch based classifiers on the other hand detects objects by examining a patch (a window) of a frame for evidence of the object. The patch-based classifier approach applies model descriptors to an object in a single patch (window) [Gabriella 2004], [Viola and Jones 2001]. Further there are three main statistical classifiers, namely, generative, registration, and discriminative approaches. The generative approach seeks to recognize highly informative object features and their spatial relationships [Bileschi 2005],[Jordan 2004], and then recombine these features in a known way to synthesize an object model. Examples include Bayesian Networks [Schneiderman 2004], and cluster-based models. The registration approach seeks to align and match corresponding feature points between two or more images [Berg 2005] as in stereo imaging system which results in disparity maps from which objects are detected. The discriminative model seeks to categorize objects with generic descriptors by learning a discriminating function. Most of the non segmented approaches to still image classifications use some image transform such as steerable pyramid or wavelets transform, and then characterise the image in that domain using a set of filters. Patch classifier model first extract some features from the image and learn the structure of these features. The resulting structure should describe some uniquely recognizable set of features from the underlying patch.
Typical machine learning techniques used for human detection include support vector machine (SVM), Adaboost, and feed forward neural networks. Machine learning techniques such as neural networks [Kotsiatis 2007] and boosting are used to learn the

underlying structure of an object. They are typically pattern classifier which generalizes by learning object features in order to discriminate the objects from other classes. Artificial neural network on the other hand are self organising structures able to adjust itself after receiving inputs from its environment. It is a non linear network for approximating functions to any arbitrary level of accuracy. Several neural networks have been applied to classification problems and human detection [Collins et al. 2000], [Wohler et al. 1999]. In a typical classifier based human detection there is feature extraction, then human discrimination by classification. Alternatively, the classifier automatically determines the discriminating feature set and the class decision function as in Adaboost [Viola et al. 2004]. Support vector machine (a machine learning technique) seeks to maximise the margin of separation of a linear decision boundary between the classes to achieve maximum separation between the classes. Both linear and non linear SVM have been used in human detection [Paisitkriangkrai et al. 2008], [Enzweiller and Gavrila 2009]. The training of SVM involves solving a quadratic optimization problem formulated using all the training examples. It output support vectors which are the points which lie on the boundary of the separating hyper plane. The use of kernel functions enables both linear and non linear SVM classifiers to be realised. Boosting is a general technique whereby a series of weak classifiers (better than random) are combined in a voting scheme to improve classifier accuracy [Viola 2001]. An adaboost (a boosting algorithm) is a technique of constructing strong classifiers from several weak classifiers (base classifiers). It creates a sequence of base learners at each iteration where the current base learner is constructed from the previous base learner using the same training set. It assigns higher weights to misclassified example such that the weight minimizes a cost function. This approach helps the classifier ensemble focuses on the misclassified examples.

2.3 Object Tracking

Object tracking involves linking the same object in consecutive frames over time. It provides three types of information, namely, location, direction, and speed, and involves detecting and establishing correspondence between object instances across frames. It can be performed separately, or jointly. In the first case possible object locations are identified using object detection techniques. Tracking then corresponds

objects across frames. In the later case an object and its correspondence is jointly estimated by iteratively updating object location and measure object features between consecutive frames. Tracking then assigns consistent labels to tracked objects. Tracking algorithms can be classified as single object tracking or multiple object tracking. In single object tracking only interactions between object and background is considered in addition to scene complexity. In multiple objects tracking additional interactions between objects must also be considered. This makes algorithms for multiple objects tracking more complicated especially in associating measurements (observations) to model predictions. There are several published works on multiple objects tracking especially in target tracking community [Black and Popoli 1999], [Cox 1993]. Tracking can also be classified under feature-based, model based, region based and contour based tracking as discussed in [Weiming et al. 2004]. Another classification according to [Yilmaz et al. 2006] is by form of feature representation or how feature correspondence problem is solved. Under form of representation, there are three categories, namely, point tracking, kernel tracking, and silhouette tracking. Point tracking [Veenam 2001] is the correspondence of detected objects represented as point (for example centroids and SIFT) features across frames. Point trackers are suitable for tracking objects of all size. Usually multiple points are needed to track very large objects. Kernel tracking refers to correspondence of objects across frames using rectangular, elliptical templates [Berg 2005] [Bobick 1996] or density based approach. It includes geometric shape and appearance features. Motion is described in the form of parametric transformation such as affine, translation, or rotation. Silhouette tracking is performed by estimating the object regions directly in each frame [McKenna 2000]. Tracking objects can be complicated due to loss of information as a result of projection of 3-D objects unto 2-D image plane, image noise, complex object motion, partial or full occlusion, complex object shapes, scene illumination changes, and real-time processing requirements. One can simplify tracking by imposing constraints on motion and appearance of objects. For example assumption of smooth motion nearly underlies all tracking algorithms. Prior Knowledge about the number and size of objects, or object appearance can simplify the problem. Every tracking method requires an object detection mechanism in every frame or when the object first appears in a single frame. Thus object detection step is usually part of the tracking algorithm. Some object tracking methods make use of temporal information computed from a sequence of frames to reduce the number of

false detections. Given an object's region in the image, it is up to the tracker to perform object correspondence from one frame to another to generate the tracks. In tracking non rigid objects with complex shape or in high dimensional space, specific motion models and search strategies are used to reduce the complexity of the analysis.

Tracking can also be classified according to how frame-to-frame correspondence is achieved. There are two main ways of solving frame-to-frame object correspondence problem namely, deterministic and stochastic methods. Deterministic methods define the cost of associating each object in frame (t-1) to a single object in frame t using a set of motion constraints. Minimization of the correspondence cost is formulated as combinatorial optimization problem [Kuhn 1955], [Sethi 1987]. Stochastic technique on the other hand, treats each feature point as a random process. Stochastic techniques use the state-space approach to model object properties such as position, velocity and acceleration based on measurements associated with object trajectories, with some constraints on its motion. Typical measurements consist of object position in the image which is obtained by a detection mechanism. The main techniques for state estimation are Kalman filtering [Haykins 1999], [Marcenaro 2002], particle filtering [Cody 2004],[Tanizaki 1987], joint probability data association filtering [Yunqiang 2001] [RasMussen 2001], and multiple hypotheses tracking [Reid 1979], [Cox 1996]. The state space approach to object tracking within Bayesian framework requires computation of posterior state distribution, $p(X_k| Z_{1:K})$, also known as filter distribution. X_k denote the state at time step k, and $Z_{1:K}$ denotes observations obtained from k samples. Then by Bayesian inference:

$$p(X_k \mid Z_{1:k}) \propto A p(Z_k \mid X_k) p(X_k \mid Z_{1:k-1}) \tag{2.1}$$

A is a normalization constant. Particle filters provide a general framework for estimating the probability of general non linear and non Gaussian systems. They are based on Monte Carlo approach where the density is estimated by sampling. Samples are drawn from a distribution function known as proposal density or importance function. Weighted estimate of the sample density function are used cumulatively to estimate the posterior density. Sample weights are adjusted so that samples approximate the estimated density function as accurately as possible. Given adequate

number of samples arbitrary accuracy could be achieved. Several particle filter based approach has be applied to tracking of humans [Bouaynaya and Sconfeld 2005], [Wei Qu et al. 2005]. Among the search strategies are dynamic model, Taylor model, Kalman filtering, and stochastic sampling. Dynamics strategy use physical forces applied to each rigid part of the object model. These forces guide the minimization of the difference between the object pose and model [Delamarre and Faugeras 2001]. The strategy based on Taylor's model incrementally improves an existing estimation using differential of motion parameters as in [Delamarre and Faugeras 1991]. Kalman filtering is a recursive optimal linear state estimator based on the assumption that motion parameters are Gaussian [Marcenaro et al. 2002]. To handle non Gaussian, and multi modal motion parameter distributions, stochastic techniques such as Markov chain Monte Carlo, and condensation techniques [Isard et al. 1998] are used.

A major issue in multiple object tracking, data association, is how to achieve optimal mapping between observed measurements and predicted measurements. The problems of data association uncertainties generated by closely packed measurements, spurious measurements, and data association ambiguities, all contribute to track detection failures. Thus data association problems must be resolved first before state estimation (location and velocity). There are several multiple data association techniques, namely, probabilistic data association filter (PDAF) [Bar-Shalom and Jaffer 1972], joint probabilistic data association filter (JPDAF) [Chen et al. 2001], multiple hypotheses track filter [Cox and Hingorani 1996], Monte Carlo data association filter [Karlsson and Gustafson 2001], and nearest neighbour filter [Bar-Shalom and Fortmann 1988]. The optimum data association technique, multiple hypothesis filter, provides for creation of tracks (track initiation), track termination, track continuation (track updates), explicit modelling of spurious measurements, and modelling of uniqueness constraints. However it is offset by the large memory requirements, and computational complexity [Cox and Hingorani 1996]. The implication is that less optimum alternatives such as Joint probabilistic data association filter could be optimised under some constraints. The requirements of a good state-space tracker are:

- Use of robust state estimator (Kalman filter, particle filter, Monte Carlo state estimator);

- Use of robust motion model (Linear or non linear motion models) well matched to object motion;
- Detection of stopped or slowly moving objects, and detection of new objects which enters the scene;
- Detection of objects even if occlusion has occurred;
- Detection of splits and merges events.

2.4 Spatial Domain Techniques for Detection and Tracking of Humans

Human tracking algorithms are based on three main characteristics, namely, appearance, shape, and 2-D and 3-D human models together with motion models and constraints. A review of human tracking, recognition and behaviour analysis is presented in [Weiming et al. 2004]. Simple appearance based features extracted from the image include height, width, aspect ratio and moment. These vary from one frame to another, and may be view dependent. Numerous other approaches to human tracking have been proposed. These primarily differ from the form of representation, and features used in tracking. It further depends on the context/environment in which tracking is performed and the end use for which the tracking information is sought. Different features exist for tracking including: points [Serby et al. 2004], primitive geometric shapes [Commaniciu et al. 2003], object silhouette and contours [Yilmaz 2004], articulated shape models, skeletal models [Ali 2001], and appearance based representations. There are also several ways of representing object appearance features, including, probability density of object appearance [Elgammal 1990], templates [Fieguth 1997], active appearance models [Edwards 1998], and multi-view appearance models [Black 998]. Active appearance models are generated by simultaneously modelling the object shape and appearance. Multi-view appearance model represent different object views by generating a subspace from the given view. Subspaces approach such as principal component analysis and independent component analysis have been used for both shape and appearance representation [Moghadam 1997]. The selection of appropriate features to track is related to the object representation. Object features may be chosen manually or by using automatic feature selection methods, which is divided into filter methods and wrapper methods [Blum 1997]. A wrapper method selects discriminatory features for detection and tracking a particular type of object [Tieu 2003], for example the Adaboost

algorithm. Principal component analysis is an example of the filter method, and it involves transformation of possibly correlated variables into a smaller number of uncorrelated variables. The form of representation of an object's shape limits the type of motion or deformation it can undergo. For example if geometric shape representation like an ellipse is used to represent an object, parametric motion models like affine or projective transform could be used.

For non rigid object, silhouette or contour is the most descriptive representation and both parametric and non parametric models can be used to specify motion. The goal of silhouette tracker is to find the object regions in each frame by means of object model generated using the previous frame. Silhouette-based approaches provide accurate description of the shape and the interior of the object. It is useful in describing complex shape-outline than provided by simple geometric description (ellipses, rectangle, etc). The most common form of representation is in the form of binary indicator function which marks the object region by ones, and non object regions by zeros. The interior model could be colour histogram, object edges, texture, or contour. Shape matching criteria is used in establishing correspondence between frames. It may use the complete object silhouette or just the shape or contour in tracking. In [Yilmaz and Shah 2004] a contour based object tracking with appearance model described by texture and colour is presented for tracking. Tracking is presented as a two-class discriminant problem, one class being the object class, and the other class the background. The colour of the object is modelled using multivariate kernel density estimation technique based on Epanechnikov kernel. Texture is modelled using the subbands of steerable pyramids as two component Gaussian mixture model. Shape prior is defined as level sets and is used to recover object region during occlusion. Objects are tracked based on evolving contours by minimizing energy functional. During occlusion the shape of the object is recovered by evaluating a functional based on the level set.

Kernel based tracking use template matching techniques for object correspondence between frames. It treats a group of points with similar motion, colour, and texture together. The motion model is in the form of parametric model or dense flow fields. They are further divided into density-based, templates, and multi-view based models. Template matching use a brute force search to find regions in the image similar to the object template defined in the previous frame. Usually image features such as colour or intensity are used to form the template. A closely related technique, region based tracking, uses image features in the region to track. The main limitation of

region based tracking is that in absence of shape information the object model is dependent on background model used in the extraction of the region or object model [Fazi et al. 2009]. Representation such as colour histogram or mixture models can be computed as appearance model of objects. [Comaniciu et al. 2003] used a weighted histogram computed from a circular region to represent the objects. Objects are modelled based on the joint spatial and colour histogram, and Bhattacharyya metric is used to evaluate similarity between target object histogram and candidate object histogram using the mean shift procedure. Objects are modelled as ellipsoidal region in the image after applying Epanechnikov kernel [Comaniciu and Meer 2002]. Adaptation to scale changes is incorporated. It was successfully applied to human tracking and face detection in several sequences. An adaptive appearance model has also been proposed in [Jepson 2001]. He proposed three components mixture consisting of, stable, transient, and noise components. The stable component identifies the most reliable appearance for motion estimation. The transient component identifies rapidly changing part, and the noise component the random part.

A general framework for object detection and tracking in visual surveillance based on motion detection is described in [Weiming et al. 2004] is shown in figure 2.1. The environmental model aims at constructing and updating the environment. It covers modelling of camera motion, illumination changes, shadows, etc. Motion detection separates regions corresponding to moving objects from non moving part. Environmental modelling, motion segmentation, and object classification constitutes motion detection. Tracking follows motion detection.

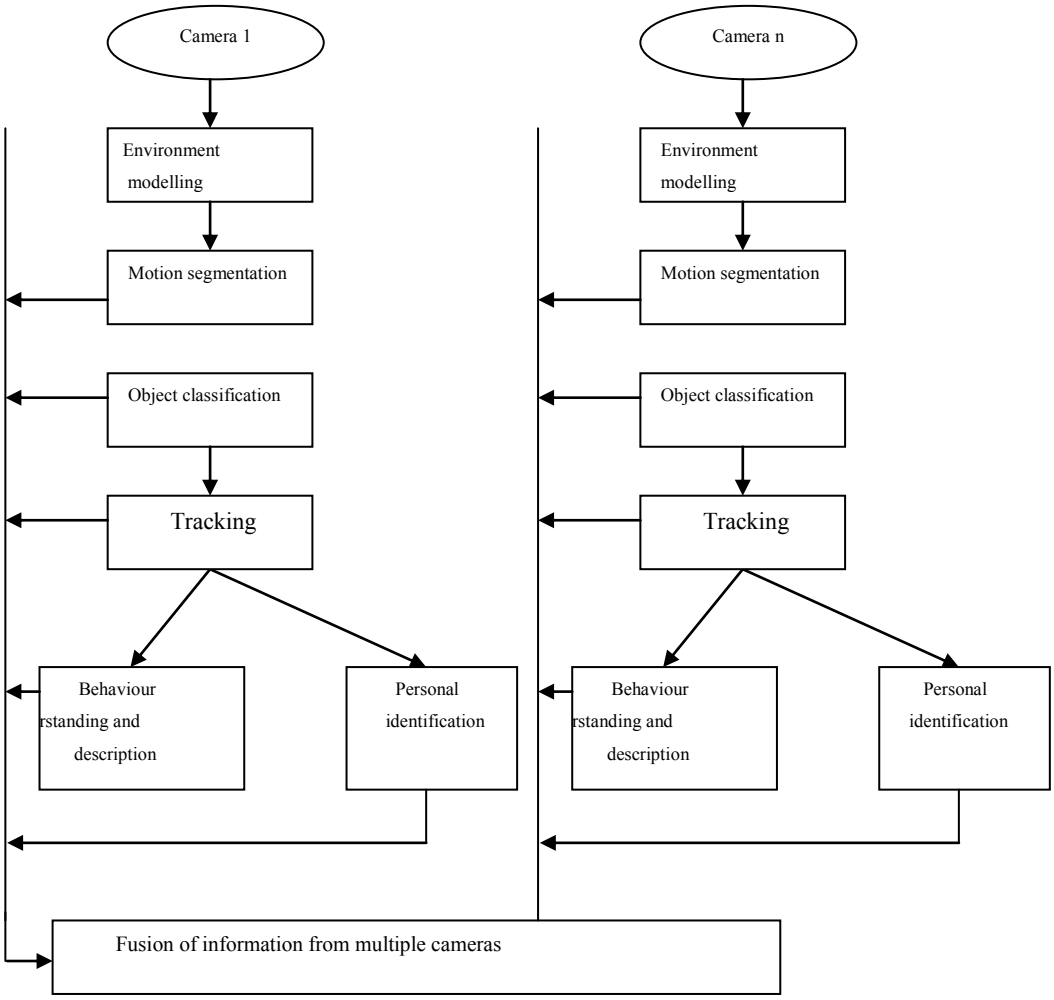

Figure 2.1 General framework for visual surveillance

Several motion detection techniques for detection of humans have been published [Haritaoglu et al. 2000], [Horprasert et al. 2003], [Ren et al. 2004]. [Moeslund and Ganum 2001] and [Weiming et 2004] present a survey on computer vision based human motion capture. The main limitation of motion based detection is that it is unable to detect very small objects under low contrast [Huang et al. 2008].

2.5 Wavelet-Domain Detection and Tracking of Humans

Wavelet analysis which originated from mathematical analysis is for both local and global analysis of signals. It is also useful in characterizing object features such as corners and edges. Wavelets and Gabor transforms have traditionally been used as hierarchical feature space for object description based on shape, edges, orientation, and

texture, and for detection of very small objects embedded in Gaussian noise [Strickland and Hee 1997]. Wavelet analysis applies wavelet filters to decompose images into subbands, providing multi-scale representation of objects features at different level of details. Certain class of wavelet transforms are invariant to affine transform, rotation, and translation and thus provides object detection under these movements. Typically extracted features are typically fed unto a classification system for object discrimination For relatively small size objects embedded in noisy background, signal detection techniques such as match filtering and correlation have been used in detecting such objects as in [Strickland and Hee 1997], [Laine and Fan 1995]. A matched filter may be viewed as a convolution kernel with a large positive centre lobe for emphasizing objects surrounded by smaller negative lobes whose purpose is to subtract the background. Peak performance occurs when the inner window completely encloses the object leaving the border window in the background region. It has been shown that the biorthogonal spline wavelet filters closely approximate the pre whitening matched filter for detecting Gaussian objects in Markov noise [Strickland and Hee 1997]. By definition a wavelet transform of an image is the correlation between the image and the scaled wavelets. Most multi-scale edge detectors smooth the signal at various scales and detect sharp variation points from their first or second derivative. The extrema of the first derivative corresponds to the zeros crossings of the second derivative and to the inflection points of the smoothed signal. There exist a class of wavelets which is constructed using Gaussian scaling functions such that the first and second derivatives are the first and second derivative of the smoothed signal respectively. These first and second derivative wavelets can be viewed edge detectors in the wavelet domain. Zero crossing detection is equivalent to Marr-Hildreth [Marr 1982] edge detection, whereas the extrema detection corresponds to edge detection [Canny 1986]. An important issue in edge detection is the scale of detection. Small-scale filters are sensitive to edge signals but prone to noise, whereas large-scale filters are robust to noise but can filter out fine details. When the scale is large enough small signal fluctuations are removed, therefore only sharp variations in sharp points are detected. Hence multiple scales are employed to synthesize various edge structures [Marr 1982]. Wavelet domain analysis preserves both the spatial and frequency domain features in images. [Liang and Fan 1995] showed that weighting by a factor greater than one across all subbands emphasis high frequencies, weighting a particular subband by a constant effectively enhances mid range of frequencies. Thus it is also possible to globally enhance the contrast between

background and foreground objects. It is shown in [Strickland 1997] that the sum of LH+HL subband approximates the output of a Gaussian convolution operator. Object detection and tracking in the scale-frequency domain (wavelet domain) has the following advantages over analysis in spatial domain; less sensitive to noise, transient motion, illumination changes, detection of objects irrespective of changes in size, ability to detect both small and large changes in motion, and reduction in computational load in object localization in the subband compared to the original frame [Cheng et al. 2006]. There have been several published studies on wavelets analysis for object detection and tracking, including face recognition, pedestrian and vehicle detection, as well as in biomedical applications [Benner 1988],[Mallet 1992],[Unser 1995]. [Oren et al. 1997] proposed wavelet domain template for pedestrian detection, having observed there is significant variability in patterns and colours within the boundaries of human body in images, as well as the lack of constraint on the image background. They proposed wavelet ratio template which defines the shape of human in terms of the subset of the wavelet coefficients. Non decimated Haar wavelet transform was applied to an image frame to define an over complete dictionary of wavelet coefficients, where the distance between the wavelets at scale n is ½* (2^n). They interpreted the wavelets coefficients as indicating an almost uniform area, i.e, 'no change', if their absolute value is relatively small, or as 'strong change' if their absolute value is relatively large. The wavelets coefficients were classified as horizontal, vertical, and diagonal (corner). Haar wavelet coefficients were used to describe the relationship between the average intensities of two neighbouring regions. Multi-scale detection was achieved by resizing an object window of 128 by 64 from 0.2 to 1.5 in steps of 0.1 based on the template matching using frontal and rear views of humans. The resulting ratio template is independent of motion or explicit segmentation. It consists of a set of regular regions of different scales that correspond to the support of subset of significant wavelet functions. Essentially the template defines a set of inequality relationships between the average intensities of different regions of the body expressed as constraints on the values of the wavelet coefficients. An input wavelet template of a candidate window is compared with the learned pedestrian template which is represented as ratio of coefficients. The matching value is the coefficient ratios in agreement with the template ratio. [Elzein et al. 2003] applied motion detection in the pixel domain to first determine time-to-collision in a pedestrian-based detection system, and followed by object classification in the wavelet domain using multiple wavelet templates similar to [Oren et al. 1997]. [Jepson et al.

2003] developed a three-part wavelet-based appearance model based on steerable pyramid and an online expectation maximization algorithm. The motivation for using wavelet filter's response is the possibility of localizing stable properties spatially, or restricted to certain scales as in optical flow estimation and stereo disparity [Fleet 1990], [Fleet and Adelson 1991]. The system successfully tracked human faces in different poses. A support vector classifier was applied independently to learn significant ratio template coefficients using bootstrap training to improve detection. Comparison was made with the wavelet ratio template matching technique. Peak performance of 81.6% detection rate with one in fifteen thousand windows turning out to be false resulted when the support vector classifier was used. The template matching scheme achieved a peak detection rate of 61%, with one in five thousand windows turning out to be false. However the method is computationally expensive since humans are searched for at multiple scales in addition to the wavelet transform computation. In another work, [Cheng et al. 2006] applied discrete wavelet transform on each frame of a video sequence resulting in four subbands (LL, LH, HL, HH) with different frequency characteristics. The high pass band (HH) extracts the detailed images which contain edges, whilst the low frequency components (LL), the average image. The LL subband of the third level decomposition was used in motion detection using frame differencing and thresholding, followed by connected component labelling. The features extracted for each object were its colours (RGB component), statistics (mean and standard deviations) and bounding box coordinates. A feature queue was created and similarity metric defined to compare objects in previous frame to the current frame. An object in the current frame is the same as in the previous frame if the similarity metrics is within a threshold. However, it had difficulties in tracking slowly moving objects. It was also observed that motion detection in wavelet domain filters out transient motion and noise. However, no explicit scheme was used in handling occlusion, although high detection rates were achieved using video sequences with multiple humans, some of them coming together. Searching, a time consuming operation was carried out on the subband rather than the original frame, resulting in reduced search time. If the computational time for the wavelet transform is less than the time spent in searching for the object then there is further justification for object detection in the wavelet domain.

2.6 Model-Based Detection and Tracking of Humans

Model-based detection and tracking algorithms represents humans using structural description and geometric constraints. Structural description describes the relationship between parts that can easily be identified spatially. Geometric constraints in the form of motion models describe permissible transformations that the structural description can undergo. Model-based tracking algorithms track objects by matching projected object models, produced a priori, from image data. The models are usually constructed based on manual measurements, CAD tools, or computer vision techniques. The general processing technique in model-based human tracking is known as, analysis-by-synthesis. First the pose of the model in the next frame is predicted according to prior knowledge and tracking history. The predicted model is synthesised and projected into the image plane for comparison with the image data. A specific pose evaluation function is required to measure the similarity between the projected and the image data. This is done recursively using a search strategy or by sampling techniques until the correct pose is finally found, and is then used to update the model. The main issues are; representation of possible motion models and constraints, and search strategies (for location and pose estimation). There are four main types of models for humans, namely, stick figure, 2-D contour, volumetric, and hierarchical models. The stick figure model consists of lines and circles representing the torso, the head, and the four limbs with links and joints. The 2-D contour essentially models the projection of 3-D human body unto the image plane. Volumetric models are 3-D models constructed to model the body movement. The hierarchical model describes the human body as hierarchy consisting of skeleton, ellipsoidal meatball, simulating tissues, and fats. More details of human body models is found in [Weiming et al. 2004]. Accompanying the human body model is the motion model with motion constraints to reduce complexity in tracking. Several motion models have been used including Hidden Markov model, multiple description length coding, and multiple principal component analysis. Search strategies include dynamics, Taylor models, Kalman filtering, and stochastic sampling. Dynamics involve application of physical force to each rigid part of the kinematic 3D model to create dynamical equations of motion. The solution provides the motion parameters [Delamarrre and Faugeras 2001]. [Bergman and Doucet 2000], [Isard and Blake 1998] applied Monte Carlo based techniques to object tracking. Particle filter, an inference

technique for estimating the unknown motion state from noisy collection of observations arriving in sequential fashion is also a Monte Carlo based technique. Two important components of this model are the state transitions and observation models. Several studies on particle filters have been reported [Zhou et al. 2004], [Peterfreund 1999]. [Karaulova et al. 2000] used a stick figure representation to build a novel hierarchical model of human dynamics encoded using hidden Markov models (HMMs) and realize view-dependent tracking of humans. In 2-D contour representation, the human body segments are modelled by 2-D ribbons or blobs. For instance [Ju et al. 1996] proposed a cardboard human body model, in which the human limbs are represented by a set of jointed planar ribbons. [Niyogi et al. 1999] used spatio-temporal pattern in XYT space to track, analyze and recognize walking figures. They examined the characteristic braided pattern produced by the lower limbs of a walking human. The projections of head movements are then located in the spatio-temporal domain, followed by the identification of the joint trajectories, allowing a more accurate gait analysis. Volumetric models include elliptical cylinders and cones [Delamarre and Faugeras 1999], [Delamarre and Faugeras 2001], spheres and superquadrics. Volumetric models requires more processing especially during the matching process. [Rohr 1994] used fourteen elliptical cylinders to model a human body. [Wachter et al. 1997] established a 3-D model using right elliptical cones. The shape of a person is modelled as a set of polygons using hidden surface algorithm. Region information such as optical flow, spatio-temporal gray values derivatives, as well as edges to fit the person's model to the human model as a search problem based on a high-dimensional figure of merit function to be optimized. Hierarchical model uses hierarchical human model to achieve higher accuracy. In [Plankers and Fua 2001] a model is presented which includes skeleton, ellipsoid meatballs for fats, polygonal surface representing skin, with shaded rendering. Compared to other tracking algorithms, model-based tracking have the following advantages: 3-D contour tracking are more robust under occlusion. Other prior knowledge about humans such as motion, and structure could be combined to improve robustness. The pose of humans is acquired naturally, after geometric correspondence between 2-D and 3-D world coordinates, and the 3-D models can be applied when objects greatly change their orientations. 3-D model-based tracking are appropriate for applications such as animation, medicine, surveillance, and man-machine interaction. Tracking and localizing human body accurately in 3-D space is a difficult problem despite progress on structure-based methods [Weiming et al. 2004]. Recovering of joint

angles from a walking human in a video is still difficult, and the computational cost is also very high.

2.7 Appearance-Based Detection and Tracking of Humans

Appearance-based systems maintain information about each pixel in an evolving model of the person. Common image appearance models include templates [Frey 2000], [Olson 2000], view-based sub space models [Black and Jepson 1998], temporally filter motion compensated images, and global statistics [Birchfield 1998]. Representation of a feature in the appearance model could be scalar or vector valued consisting of several features. Under appearance approach there are four representations, namely, active appearance, multi-view-based, template-based, density-based (multidimensional histogram), silhouette-based, and region based. SIFT [Lowe 2004] provide scale and rotation invariant features suitable for object recognition, motion tracking, and segmentation. Each feature contains 2D location, scale, and orientation. Features are robustly detected in the present of clutter and has moderate amount of computational requirements. [Edwards et al. 1998] generate active appearance models by simultaneous modelling shape and evolving image information over time. Shape is modelled by a set of landmarks defined by a contour. For each point or landmark an appearance vector representing colour, texture, intensity, gradient magnitude is stored. There is a training phase during which appearance is learned from examples. In [Balcells et al. 2003], the appearance of humans are modelled using a combination of histogram and correlogram information. A correlogram is a co-occurrence matrix $\gamma(c_x, c_y, k)$ that gives the probability that a pixel at a distance k from a given pixel of colour c_i is of colour c_j. Foreground blobs are extracted after codebook based background subtraction developed by [Horprasert et al. 2003], and likelihood based segmentation using the colour histogram and correlogram. The first time a person enters the scene a model for the individual is stored and is also assigned a label. In the subsequent frames models are updated and the most similar blobs matched using normalized first norm distance. The system is able to detect when people merge into groups and able to segment them during occlusion. Occlusion is handled by colour classification as in [Huang et al. 1999], and no assumption is made about the pose of a human. Multi-view appearance model, on the other hand models the principal views of an object using Eigen space

[Black and Jepson 1996], principal component analysis, or independent component analysis [Moghadam and Pentland 1997]. Template matching is a brute force method of tracking. It searches for a region similar to an object template defined in the previous frame [Jurie and Dhome 2001] in the current frame based on an optimizing function. Templates could be based on colour, intensity, and directional gradient image. Limitations of template matching are the high computational cost, and the need for multiple views (templates) to improve robustness. [Kang et al. 2004] used histogram of colour and edges as object models. Histograms were generated from concentric circles to achieve rotation, translation and scale invariance. A matching score was computed using distance measures such as Kullback-Leibler divergence, and Bhattacharyya distance. In shape matching a search for the object silhouette in the current frame is conducted using the previous object silhouette. A match between two silhouettes results if the matching score was below a threshold. In [Huttenlocher 1993] shape matching is performed based on Hausdorff distance. The matching score between silhouettes can be computed using several distance measure including cross correlation, Bhattacharyya distance, and Kullback-Leibler divergence. To match silhouettes in consecutive frames, [Haritaoglu et al. 2000] model human appearance using edge information. The edge model is then used to refine the translation of object using constant velocity assumption. The object model is re-initialize to handle appearance change in every frame after the object is located. In [Wu and Nevatia 2006] humans are represented by parts such as head-shoulder, torso, legs, and full body. Part based representation is used to segment blobs by considering various articulations and their appearances. First parts are detected and combined using multi-view detectors trained on Edgelet features [Wu and Nevatia 2005] using boosting technique. The combined response is the union of representation of its parts and visibility score. If visibility is less than a threshold objects are considered occluded by other humans. Humans are detected on a frame by frame basis by the combined multiview detectors (front and rear view detectors, and left/right view detectors). An affinity function is defined consisting of part type, size, spatial location, detection confidence colour, and object visibility. Multiple humans are detected using a joint likelihood function and occlusion reasoning. The appearance is described by colour histogram. Two strategies are used in tracking, namely, greedy matching with data association, and mean shift tracking. Two humans in two consecutive frames are matched if the average affinity function and the visibility function is above a threshold. Tracking is implemented in three phases, namely, track initiation, track growing, and

track termination. At the track initiation phase tracks are initialised when there is enough evidence from the detection phase to support the parts and the full-body of the human. This occurs when an initial computed confidence measure exceeds a threshold. A track hypothesis is constructed part response function, dynamic model based on Kalman prediction, and appearance model. For every found human pairs between two consecutive frames that pass the affinity test, and object visibility test a hypothesis is generated and the greedy data association technique is applied to establish track correspondence. Found humans which fail the test, the mean shift tracker is used to track the individual parts. A likelihood model is constructed from detection probability, confidence value of the parts, and constant false alarm ratio. The appearance model is constructed from the initial colour histogram of the part and principal component analysis to learn the structure of the underlying distribution. Tracks are terminated if no detection responses are found for an object after a fixed number of consecutive frames. The main limitations of the approach are that the viewpoint should not exceed 45 degrees, and the resolution not less than 24 X 58 pixels. Region based tracking techniques on the other hand model object boundary as contours and interior with suitable appearance feature such as texture, intensity, gradient, etc. Tracking could also be performed using two different approaches, namely, state-space approach, and energy minimization. Other reported works include [Isard and Blake 1998], [Terzopoulos and Szeliski 1992]. In [Bascale 1995] texture is used to represent the interior of objects which are modelled as deformable templates. The region is parameterized and tracked by applying 2-D motion model to both the contour and the texture. Matching of current region with the previous region in the previous frame the best match is obtained by optimization techniques. A major limitation with region based tracking is that it cannot handle occlusion very well, and it is also difficult to recover the pose of an object [Weiming et al. 2004]. The main limitations with appearance based approach are how to robustly handle occlusion and object splits and merges when the underlying assumptions fail [Senior et al. 2006].

2.8 Shape-Based Detection and Tracking of Humans

Although shape-based detection and tracking is part of silhouette-based techniques, it deserves a section since numerous studies on shaped based human detection and tracking, and action recognition has been published. For 2-D shapes several models exist including discrete shapes, continuous shapes (modelled by compact class conditional density learned from examples), multipart representation, and shape filters (edgelets, and shapelets assembled from low level oriented gradients), and spatiotemporal shapes[Enzweiler and Gavrila 2009]. Application of shape-based detection and tracking of humans, and their actions in video ranges from generation of ad hoc models to 3-D models specially construction for motion analysis, and action recognition. Shape-based object detection and tracking relies on the features of the perceived shape of an object of interest. Shape as a feature is sometimes used together with other appearance features such as colour, texture, and edge features, or on its own as in model based pedestrian detection and tracking. In medical imaging, sports sciences, and man-computer animation, high precision shape descriptors are required whilst in human detection for visual surveillance the main the main focus is on detecting the presence of objects, and precision requirement is secondary. In [Dalal and Triggs 2005] histogram of oriented gradients derived from normalized image orientations is used in detecting humans. The basic idea being that local object appearance and shape can be characterised rather well using local intensity gradients. Humans are characterised using this approach and a model derived using support vector classifier. The shape context [Malik and Puzicha 2001] used sampled points on object shapes described by edges, to define a distribution relative to the reference point as a global means of discriminating points along the shape. First global correspondence is established by using an aligning transform, and a shape matching similarity metric is used to measure shape similarity. Shape-based detection has been applied successfully in several studies on pedestrian detection [Owechko et al. 2004], [Conxia et al. 2007]. Typically morphological characteristics such as strong vertical symmetry of human shape is exploited to circumvent pose detection problems, and to detect stationary humans as well. This method allows detection of pedestrians in different poses, positions and clothing. In [Steffens 1998] pedestrians are detected using a layered approach and expectation maximization to separate the background from the foreground

part of the scene. Shape cue is first used to eliminate non-pedestrian moving objects and then appearance cue is used to locate the exact position of pedestrians. Templates with varying sizes are sequentially applied to detect pedestrians at multiple scales to accommodate different camera distances. A graph matching-based tracking algorithm is then applied to jointly exploit the shape, appearance and distance information. In [Song et al. 2006] a model of human shape is used in recognising and tracking humans. Shape based techniques are able to detect both static and dynamic objects in images sequences, and are typically appearance based. [Haritaoglu et al. 2000] combines global shape information and texture template in detecting and tracking multiple person in video sequence. A comparative study of shape-based retrieval techniques is also provided in [Dengsheng and Guojun 2001]. An object is typical described using shape primitives such as lines and curves, and their geometric properties. Texture, edges, points in image space, and colour may additionally be used to achieve robustness. The presence of object is then inferred by analyzing and inferring the shape of the object using shape primitives. Alternatively the whole shape may be learned using machine learning techniques. Objects are then detected by classifying instances of candidate objects in the scene. The main problems with this approach are variations in object shape, object shape visibility, camera motion, background clutter, and motion of other objects in the scene. Different type of shape descriptors such as contours, edges, feature points, corners, boxes, silhouettes and blobs are available for classifying moving objects. Contour tracking on the other hand, evolves an initial contour to its new position in the current frame by using the state space models or direct minimization of some energy functional. To track the contour evolution with time requires that the current frame overlap with the object region in the previous frame. [Chen et al. 2001] proposed a contour tracker where the contour is parameterized as an ellipse. Each contour has an associated Hidden Markov Model (HMM) and the state of each HMM is defined by the points lying on the lines normal to the contour control point. The observation likelihood of the contour depends on the background and the foreground partitions defined by the edge along the normal line on the control points. The state transition probabilities are estimated using Joint probability data association filter (PDAF). Given the observation likelihood and the state transition probabilities, the current contour state is estimated using the Viterbi algorithm. After the initial approximation, an ellipse is used to fit and enforce elliptical shape constraint. VSAM [Collins et al. 2000] takes apparent aspect ratio of bounding box, image blob area, etc, as key feature and classify moving object

blob into humans, vehicles, and clutter using neural network classifier. VSAM classify objects into single humans, group of people, and vehicles. The real-time visual surveillance system W4 [Wren et al. 1997] employs a combination of shape analysis and appearance features for tracking, and construct models of people's appearances in order to detect and track individuals, people carrying other objects, and groups of people, as well as monitor their behaviour even in the presence of occlusion in outdoor environments. The shape of a 2-D binary silhouette is represented by a projection histogram. The vertical and horizontal histograms are computed by projecting the binary foreground region unto the axis perpendicular to and along the major axis. In [Jang et al. 2000] an active template that characterizes regional and structural features of an object is built dynamically based on shape, texture, colour, and edge features of the region. Using motion estimation based on Kalman filter, the tracking of a non rigid body by minimizing the energy function.

2.9 Motion-Based Recognition of Humans

Motion-based recognition technique uses the intrinsic pattern of human motion for tracking. There are two main approaches. The first approach attempts to characterize motion itself with reference to known human motion models in order to determine location or infer behaviour. Behaviour analysis and understanding is considered as a classification of time varying feature data, i.e, matching unknown test sequence with a group of labelled reference sequence representing typical behaviour. The first technique has already been discussed in section 2.4 aims at segmenting regions corresponding to moving objects from the rest of the image for subsequent analysis, i.e, motion is used as a cue. In characterising motion itself, objects are detected over many frames and their trajectories analyzed for periodicity and other cues. By analysing periodicity of motion from image sequence it is possible to track and predict behaviour as demonstrated in [Aggarwal 1994]. Gait-based recognition techniques for humans [Takas 1988], [Boser 1992] falls under this category. There are four main ways of viewing human motion tracking and action recognition. The first one is to recognise action from among a database of human actions. The second one is to recognise different body parts like arms, legs, etc, through a sequence of motion labelling. The third defines motion as a sequence of object configurations or shapes through time (by tracking), and the last use

knowledge of shape and motion information of the human body as a guide to the interpretation of an image sequence to determine a succession of shape modifications. When transformations applied to a shape correspond with the motion constraints in the sequence tracking is achieved. In [Lipton 1999] residual flow is used to analyze rigidity and periodicity of moving objects. In [Bobick et al. 1996], a view-based action recognition is presented without reference to any feature except motion itself. It is based on the assumption that a motion model associated with an action is observed when a known movement is viewed from a given angle. The spatial distribution of motion integrated over temporal extent, is employed as a filter for associating possible action to viewing directions based on motion energy. For personal identification, human face and gait are now regarded as the main biometric identification features that can be used in video surveillance [Lee et al. 2002]. [Maybank and Tan 2000] used moment features of image regions to recognize individuals. By assuming that people walk frontal-parallel towards a fixed camera, the silhouette region is divided into seven sub regions. A set of moment-based region features is used to recognize people and to predict the gender of an unknown person by his walking pattern. In [Niyogi and Adelson 1994] the different motion pattern of head and legs under translation in time-space are used in recognising humans by fitting unto a figure-stick model. These patterns are first processed to determine the bounding box of a moving object. Gait signatures are then acquired from velocity-normalized fitted model, and used in recognition of humans. Among existing methods are dynamic time warping, finite state machine, hidden Markov model, time delay neural network, and self organizing neural network. In [Sidenbladh and Black 2000] tracking of human is achieved by projecting 3D motion of the figure in monocular sequence unto the image plane of the camera using Bayesian framework. A model is defined in terms of the shape, appearance and motion of the body, and a model of noise in the pixel intensities. Given these parameter a posterior distribution over model parameters given observation history is derived. The main difficulty is in modelling non-linear dynamics of the limbs, ambiguities in the mapping from 2D image to 3D model, and similarities singularities, among others. Approaches to recognizing human motion and action can be divided into human action recognition, and motion based recognition. The former models posture and motion together whilst the later uses motion as a cue for detection of humans. An interesting work on action recognition based on motion is presented in [Song et al. 2006].

2.10 Summary

Among the object detection and tracking techniques in video, motion detection combined with other techniques such as object segmentation, view-based classification, and background-foreground modelling have high accuracy and moderate computational complexity. The high computational complexity of 3-D model construction and model-based human detection and tracking makes it less suitable for real-time applications, whilst its 2-D counterparts with moderate complexity is frequently used in detection and tracking. In object-based approach, segmentation is applied to detect instances of interesting objects, whilst in feature-space approach low level features are use to direct a search in feature space to locate interesting regions. Discriminative features are used by object based approach to differentiate between different objects, whilst in feature space approach patch based classifiers examines salient regions, and assign a class to the hypothetical object at the given location. Verification of the object-based approach using a confidence measure is then used to confirm the existence of the object. With the feature-space based approach, similarly, heuristic tests based on the physical characteristics of the object in the spatial domain may be used to verify the existence of the object. Appearance-based features include colour distribution, oriented gradient distribution, silhouette-based features, phase information, texture, and intensity distribution. Appearance based features combined with shape or silhouette based features have high accuracy, but typically require regular update, explicit occlusion detection and object inference techniques under high clutter and low contrast. It is suitable for both part-based object detection and complete shape-based detection. Majority of the algorithms for human detection are object based, and consist of the following sequence of steps: pre processing, motion detection, candidate human definition, human discrimination (based on physical or appearance features), and human detection by validation. However there are exceptions: in [Avidan 2005] object detection and tracking is posed as binary classification problem and detection and tracking is performed jointly. The background-foreground separation schemes work well under constant lightning conditions, but unable to cope with sudden changes in lighting conditions, moving camera, moving background especially when the size of the moving background compared to the foreground region is very large.

The mean shift algorithm, a kernel-based density estimator has been used in both object detection and tracking with high accuracy in real-time. It provides moderate complexity and high accuracy when the displacement between object locations is less than the bandwidth of the kernel density estimator. It is not able to cope with fast motion which results in no overlap between the kernel locations in consecutive frames. When the underlying assumption is violated, one option is to use multiple kernels with different bandwidths, incurring extra computational steps. Statistical object segmentation techniques such as single Gaussian, multiple-Gaussian model and expectation maximization have high accuracy, and have been used to model appearance features and motion. Their main limitations are how to determine the number of components, slow convergence, high computational cost, and false motion in complex background. Four main trackers have been identified, namely, region/kernel based trackers, stochastic trackers (sample based), silhouette based trackers and model based trackers. Region based trackers use template matching techniques and achieves high accuracy at the expense of large number of computations. However, its limitation is its inability to estimate the pose of the object, and small changes in shape and motion. The main problems with trackers are how to assign measurements to multiple objects when they are very close to each other or under occlusion.

CHAPTER THREE

REVIEW OF DATASETS, PERFORMANCE METRICS AND STATE OF THE ART PERFORMANCE ON PEDESTRIAN DETECTION

3.1 Introduction

Performance evaluation in algorithm development is necessary to provide feedback on quantifiable progress towards automated human detection and tracking, and event recognition. The main problem with ad hoc approach is exaggerated performance using dataset which is not representative of the application, and the lack common performance metrics without which there is no basis for comparison. Thus the first requirement is availability of standard dataset and performance metrics. The next requirement is to provide a common site where algorithms can be tested and evaluated. Since the year 2000, there has been several efforts towards providing standardised dataset and performance metrics appropriate to specific application domain. Section 3.1 presents a survey of currently available datasets, whilst section 3.2 presents a review of associated performance metrics for object detection and tracking.

Sections 3.2.1 to 3.2.7 describe the individual dataset from PETS to Daimlerchrysler. Section 3.2.8 provides a classification of the dataset. In section 3.2.9 the dataset used in the current investigation is also described. Section 3.3 discuses metrics for detection and tracking, and publicly available dataset. Section 3.3.1 to 3.3.5 discusses confusion matrix, ROC curves, and metrics associated with the dataset. Section 3.3.6 defines the metrics chosen for the current investigation. Section 3.4 reviews state of the art performance in pedestrian detection and tracking.

3.2 Review of Datasets

The dataset covers single and multiple humans, cars, and other objects. The following is a brief description of the main datasets available in the public domain:

3.2.1 PETS

The Performance Evaluation of Tracking and Surveillance (PETS) series of workshops [PETS 2006] was originally sponsored under EPSRC REASON (UK) project in conjunction with IEEE computer Vision conference with the goal of evaluating visual tracking and surveillance algorithms in 2000. It was in response to meet the scientific challenge of devising and implementing automatic systems for obtaining detailed information about activities and behaviour of people. To date a total of ten workshops have been held. At every workshop a video dataset is made public to researchers in order to tackle problems in tracking quantitatively, and submit results to the workshop. Over the years several dataset has been accumulated and available for research. Currently performance metrics for motion-based segmentation has been defined [Aguilera et. al 2005] in the PETS website. The metrics are negative error rate, misclassification penalty, rate of misclassification, and weighted quality measure. All the metrics are the sum of two parts: a false positive and false negative scores. PETS 2006 workshop published several approaches to performance evaluations on object tracking. PETS 2007 was devoted to activity and behaviour analysis of people and vehicles (loitering, attended/unattended luggage) in train stations using multiple camera system. PETS 2009 was devoted to crowd image analysis (crowd density estimation, tracking of individuals, detection of separate flows in a crowded scene, and detection of specific crowd events).

3.2.2 i-LIDS

i-LIDs (Imagery Library for Intelligent Detection Systems) is a UK government initiative to facilitate development of vision based detection systems (VBDS) which

meet Government requirements. It was launched in 2006 and deals with events detection and human tracking. The dataset covers the following scenarios:

Event detection:

- Parked vehicle detection
- abandoned baggage detection
- sterile zone monitoring
- doorway surveillance

Object tracking:

- multiple camera tracking

Within each event detection scenario certain alarm events are defined. For example in a parked vehicle scenario if a vehicle is parked in a predefined area for more than one minute it triggers an alarm event. Video based detection system (VBDS) are required to report an alarm when any of these events occur in the footage, with minimal false alarm reports. In object tracking scenarios, individuals or targets identified in the CCTV imagery are presented to the tracking system. Five CCTV cameras are used to capture multiple views of the object or target. Object tracking systems are required to track the target through a network of cameras until the target is either no longer present or a new target is specified. Tracking systems may be evaluated by HOSDB for either an overlapping camera or mixed camera role. The overlapping role comprises cameras 2, 3, and 4, with the mixed role including all the five cameras. Each dataset scenario is split into three parts; one part is kept by HOSDB (Home office Scientific Development Branch) for evaluation. The remaining two set is available to system designers to use to train and evaluate their system. The dataset is also available for academic research. i-LIDS benchmark data set is based on the F1 measure (see section 3.3.2). The F1 values which must be obtained in order to qualify for system certification are not made public (i-LIDS user guide 2009). However, i-LIDS consider events with overall F1 score of 0.75 as meeting evaluation commissioning acceptance criteria. More information on the evaluation procedure is available in the i-LIDS user Guide, and the website.

3.2.3 CAVIAR

Caviar (Context Aware Vision using Image-based Active Recognition) is an European Commission (EC) funded research project (IST-2001-37540) to address the challenge: Can rich local image descriptions from foveal and other image sensors, selected by a hierarchical visual attention process, guided and processed using task, scene, function and object contextual knowledge improve image based recognition process? It was launched in 2002 with the focus of the project on city centre surveillance, and monitoring of shopping habits of people in order to improve management of shops. The output of this project has resulted in large dataset which is available to the public for surveillance algorithm evaluations. However there are no recommended evaluation metrics (see http://homepages.inf.ed.ac.uk/rbf/CAVIAR/caviar.htm).

3.2.4 VACE

VACE (Video Analysis and Content Extraction) aims to develop innovative technologies to perform autonomous analysis on large volumes of video, multimodal fusion, and event understanding. It was launched in 2000 and sponsored by Advanced Research and Development Activity (ARDA) in United State of America. It focuses on detection and tracking of mobile objects such as pedestrians and vehicles from video sources such as television news broadcasting and Un-manned air vehicles. Surveillance is one of the application domain. Surveillance events are classified as person walking, running, or jumping. Action is recognised using multiple agents. Tracking, events detection and surveillance applications use video sequences for evaluation.

3.2.5 TRECVID

TRECVID TRECvid (Text REtrieval Video Retrieval Evaluation) is a text-retrieval conference (TREC)-style video analysis and retrieval. It was launched in 2001 and sponsored by Intelligence Advanced Research Project Activity (IARPA), and US

department of Homeland Security. It consists of several tasks classified under video summarisation, feature-based searches/retrieval, and surveillance event detection. It uses a subset of the i-LIDS dataset for surveillance event evaluation. The surveillance task is meant to track a specified person or multiple people in an airport scenario using both single and multiple cameras. TRECvid 2009 was co-sponsored by Home Office Scientific Development Branch (HOSDB) and centre for the protection of national infrastructure (CPNI). Events such as detection of direction of flow of people in airport scenario (OpposingFlow), people splitting up from a group (PeopleSplitUp), people meeting to form a group (PeopleMeet) were tracked. Gestures such as pointing, embracing, running were also monitored. Data was collected from major airports in the UK by HOSDB. It is split into development and evaluation sets. The main performance measure used in the evaluation is the Normalized Detection Cost Rate (NDCR). NDCR is a weighted linear combination of the miss detection probability, and the false alarm rate (measured per unit time).

3.2.6 PASCAL Visual Object Classes (VOC) Challenge

Pattern Analysis, Statistical modelling, and Computational Learning (PASCAL) Video Object Class (VOC) Challenge is a yearly contest which started in 2005. PASCAL VOC 2010 contest is sponsored by network of excellence on PASCAL, and the European Union (EU). The dataset is part of a benchmark whose objective is to investigate methods of object recognition in a wide spectrum of natural images. It consists of the following tasks: object classification, detection, segmentation, person layout description, and action classification (Everingham and Gool 2008). Since it shares common tasks with video surveillance (classification, detection, and segmentation) it is relevant to video content analysis. The 2010 object class covers twenty objects including person, horse, bicycles, cars, and cat. Any of listed object classes, for example a person, could be selected for both classification and detection. The classification task requires that for each test image the class of any of the objects of interest is indicated, as well as the classifier confidence value. For the detection task the bounding box and the confidence value of the detected object is required for evaluation. The evaluation is based on average precision computed from precision-recall curves by ranking of the confidence value. The average precision is computed

by evaluating the area under the curve by numerical integration. The detection task is based on an area overlap between the ground truth and the found object. It is required that the overlap must be more than 0.5, otherwise it is a miss detection. The segmentation task follows detection, and assigns pixels to the object or the background within the bounding box of the found object.

3.2.7 Daimlerchrysler

The dataset is meant for generic pedestrian detection in outdoor environment. It was recorded at various (day) times and locations with no particular constraints on pedestrian pose or clothing except that pedestrians are standing in an upright position and are fully visible. The training and test set consist of four thousand and eight hundred (4800) pedestrian samples each. The dataset is further split into five fully disjoint sets, three for training and two for testing during experiments. There are five hundred non pedestrian samples each for training and testing. There are additional one thousand and two hundred images of non pedestrians for more training if required. Classifier performance is evaluated by ROC (receiver operating characteristic) curves which quantify the trade-off between detection rate and false positive rate (see section 3.3.1). Cross validation is used over the training set to determine optimal setting for algorithmic parameters. The stopping criteria used during training in the original benchmark was fifty percent false positive rate at detection rate of ninety-nine and half percent (99.5%). Three detection and false positive rates for a given classifier algorithm is realised by selecting two out of the three training set to design a classifier, realising three different classifiers. The three classifiers are then tested on each of the two training set. Performance of classifier algorithms are evaluated by computing the mean detection rate at 95 percent confidence interval as given by equation 2.1.

$$\bar{y} \pm_{\alpha/2,\,N-1} {}^{S}\!/_{\sqrt{N}} \approx \bar{y} \pm 1.05 * S \qquad 2.1.$$

N=6, and t denotes student t-distribution at 1-α=0.95. $\bar{y}$ and S denote the estimated detection rate and the standard deviation respectively. Hence the estimated standard deviation S of the detection rate represents 95% confidence interval.

Table 3.1 shows the main publicly available benchmark for image and video content analysis. It is ordered by its relative importance to human detection and tracking. The first six is geared towards tracking applications, whilst the last one is towards classification, retrieval and recognition.

Table 3.1 Publicly available benchmark for classification, detection, tracking and activity recognition

Benchmark	People	Vehicle	Animals	Objects
PETS	√			√
i-LIDS	√	√	√	√
CAVIAR	√			√
VACE	√	√		√
TRECvid	√			√
Daimlerchrysler	√	√		
PASCAL challenge	√	√	√	√

3.2.8 Dataset classification

The dataset could further classified as single-frame or multi-frame based, computer vision based or surveillance based, and academia-based or industry-based as follows:

- Single Frame (computer vision based/retrieval/object recognition)

  PASCAL VOC Challenge, Daimlerchrysler data set

- Multi frame (People and event related)

  PETS -- Tracking and event detection
  i-LIDS-- object detection (cars, humans, aircraft and associated monitoring
  TRECVid--People monitoring (individuals, groups), and associated events in offices. Evaluation is based on F4DE by NIST

(National Institute of Standards and Technology)

- Academia

  PETS, Daimlerchrysler, i-LIDS,PASCAL challenge

- Industry

  i-LIDS, TRECVid

3.2.9 Choice of Dataset

The algorithmic approach proposed in the current investigation splits the human detection and tracking in two sub tasks, namely detection, and tracking. Thus taking two datasets one from single frame category (PASCAL VOC challenge), and the other from the multi-frame category (PETS 2006) would allow accuracy of the human detection to be evaluated separately from human tracking. Table 3.2 shows the main dataset chosen for the current investigation.

Table 3.2 Dataset chosen for the current investigation

Task	**Dataset**
Detection	PASCAL2 VOC 2010 challenge dataset
Detection and Tracking	Selected PETS 2005 and in-house videos

3.3 Review of Performance Metrics

In the literature, several measures have been defined for measuring accuracy of object classification, such as misclassification rate, error rate based on posterior probability expressed graphically as ROC (Receiver Operating Characteristics) curves, and confusion matrix based metrics (based on class label or rank). It is generally difficult to obtain analytic expression for the misclassification rate and it is estimated from the available dataset. Misclassification error metrics include, true error rate, apparent error rate, Bayes error rate, and expected error rate. There are two main approaches to estimating the accuracy of object detection algorithms, namely, object-based and pixel-based metrics. Pixel-based metrics assign pixels within a region enclosing the

detected object either as part of the object or the background. There are two main approaches to object-based approach, namely, area-based metrics for bounding box, and distance-based metrics for point based annotations. Area-based metric is based on spatial overlap between ground truth objects and system output objects to generate a score. [Manohar et. al 2006] use the metric (Sequence Frame Detection Accuracy, SFDA) to capture both the detection precision (misses and false alarms) and the detection precision (spatial alignment). Similarly for tracking, both the tracking accuracy (number of correctly tracked objects) and the tracking precision (spatial and temporal accuracy) are measured in a single score (Average Tracking Accuracy). Miss detection rate versus false positive rate per window is use to evaluate the accuracy of human detection [Dalai and Triggs 2005]. Miss rate (see equation 2.6) is plotted against false positives per window plotted on log-log scale. Another measure is the F1 measure which is the harmonic mean between the Precision and Recall (see section 3.2.2). Thus it takes into consideration the ideal detection rate and that realised by an algorithm. The accuracy of these measures is determined by evaluating the area under the precision-recall curve.

3.3.1 Confusion Matrix Based Metrics for Detection and Tracking

A confusion matrix [Gunther and Benz 2000] contains information about actual and predicted classes assigned by a classification system. In pattern recognition, a confusion matrix is used to represent beliefs in assigning classes to observed patterns in which the *i,j*th element represents the number of samples from class *i* which were classified as class *j*. Performance of such systems is commonly evaluated using the data in the matrix. Its reliability is measured by kappa statistics [Byrt et al. 1988]. The simplest way of measuring object detection and tracking accuracy is to assign detected objects into crisp categories, resulting in categorical classification if detailed accuracy assessment is not important, as is the case with confusion matrix based metrics. Table 3.3 shows a two by two confusion matrix with categorised labels for a binary classifier.

Table 3.3 2 X 2 Confusion matrix table

		Predicted (Observed)	
		Negative	Positive
Actual	Negative	TN	FP
	Positive	FN	TP

The entries in the confusion matrix have the following meaning:

--TN is the number of correct predictions that an instance is negative.
--FN is the number of incorrect predictions that an instance is positive;
--FP is the number of incorrect predictions that an instance is negative;
--TP is the number of correct predictions that an instance is positive.

The following are the basic standard terms defined for the two class matrix:

--The true positive rate (TPR) or recall is the proportion of positive cases that were correctly identified, as calculated using the equation 2.2.

$$TPR=TP/(FN+TP) \quad 2.2.$$

--The false positive rate (FPR) is the proportion of negatives cases that were incorrectly classified as positive, as calculated using the equation 2.3.

$$FPR=FP/(TN+FP) \quad 2.3.$$

--The true negative rate (TNR) or specificity, is defined as the proportion of negatives cases that were classified correctly, as calculated using the equation 2.4.

$$TNR=TN/(TN+FP) \quad 2.4.$$

--The false negative rate (FNR) is the proportion of positives cases that were incorrectly classified as negative, as calculated using the equation 2.5.

FNR=FN/(FN+TP) 2.5.

The following complementary relations hold:

TPR+FNR=1 2.6.

TNR+FPR=1 2.7.

Other measures are:

-- Accuracy (AC) is the proportion of the total number of predictions that were correct. It is determined using the equation 2.8.

AC=(TN+TP)/(TN+TP+FP+FN) 2.8.

-- False discovery rate (FDR) is defined as:

FDR=FP/(FP+TP) 2.9.

--Negative predictive value (NPV) is defined by equation 2.10.

NPV=TN/(TN+FN) 2.10.

--Positive predictive value (PPV) or precision is defined as:

PPV=TP/(TP+FP) 2.11.

The following additional complimentary relation hold:

FDR+PPV=1 2.12.

3.3.2 F1 Measure for Detection and Tracking

In information retrieval the influence of recall on precision is evaluated by computing the harmonic mean of precision and recall. The F1 measure is used in information

retrieval [Van Rijsbergen 1979] and it is defined by equation 3.13.

$$F_{ß} = (1+ ß^2)\ (precision * recall)\ /(ß * precision + recall) \quad 3.13.$$

ß is the weight associated with precision. The F1 measure is defined for the special case where ß=1. Typically in event retrieval in VCA higher detection rate (TPR) is achieved at the expense of higher probability of false detection (FPR). To achieve a balance between TPR, which evaluates the performance of the system without taking into consideration any error, and FPR, which measures the false detection probabilty in using the system the F measure is used.

i-LIDS uses a combination of F1 and area overlap test to evaluate event detection and object tracking performance. The defintion for F1 for event detection is given by equation 3.14. The recall bias (α) which is equivalent to ß, selectively weighs recall relative to precision is user defined. α takes on values between zero and one.

$$F1=[(\alpha+1)Precision*recall]/[recall+\alpha*precision] \quad 3.14.$$

On substituting the basic definitions above into equation 3.14 and simplifying gives equation 3.15.

$$F1=(\alpha+1)*TP/(TP+ \alpha TP+FP+ \alpha FN) \quad 3.15.$$

From equation 3.15 higher values of FP and FN reduces the value of F1, i.e, negatively influences the measure.

An object based approach is adopted in i-LIDS for object tracking with α set to one. The following are the criteria for the basic categories used for object tracking:

Let GTP: Total number of ground truth pixels;

TTP: Total number of tracker pixels;

OP: Total number of overlapping pixels;

True positive (TP) event occurs if there is an area overlap between the ground truth

and found object, and additionally

if F1>=0.25 and TTP<3 * GTP 3.16.

False negative (FN) event occurs:

if F1<0.25 and/ or TTP> 3* GTTP 3.17.

False positive (FP) event occurs

if F1< 0.25 and precision< 1 3.18.

Further a system output that produce a very small bounding box (less than 10% of the ground truth is classified as FP. An overall F1 metric is aslo computed for each object over the duration of its existence. The average precision is also computed and expressed in percentage as given by equation 3.19.

Average recall (express in percentage)=Recall *100 3.19.

In object tracking F1 thus evaluates the accuracy of an object on a fame-to-frame basis, and the average for the existence of the object.

3.3.3 ROC (Receiver Operating Characteristics) Curve for Detection and Tracking

An alternative to confusion matrix based metrics is the ROC curve (Erkel et al. 1998), (Centor et al. 1985). It is generated by paired values (P_d, P_f) where P_d is the probability of correct signal detection, and P_f is the probability of false alarm, i.e, false detection. Both parameters depend on the values of the parameters regulating behaviour of the decision module. It was introduced into decision theory as a tool for signal-processing applications [Trees 1968], and now used to measure accuracy of classifiers and detectors. The area under the curve gives the probability of correct detection given that the priori probability of detection is 50%. Global performance is obtained by plotting

$P_e=(1-P_d+P_f)/2$ against different values of detection rate, P_d, under a set of operating constraints. In object detection task true positive rate may be plotted against the false alarm rate on the x-axis, or the logarithm of a metric which evaluates the detection rate versus the false alarm rate. The ideal curve for a binary detector is concave. ROC points are typically interpolated between measured values if it parametric curve is known.

3.3.4 PASCAL VOC Average Precision Measure for Classification and Detection

The basic measure use in computing average precision is the confidence value associated with the object classification and detection. Firstly a ranking (percentiles) in ascending order based on the confidence value is produced. Precision is defined as the proportion of all examples whose ranking exceed a given percentile, and are from the positive class (humans). In the case of object detection, an area overlap ratio between the ground truth object and the predicted object (see equation 3.27) of more than 0.5 to be a true positive, otherwise it is treated as false positive. The precision-recall curve is produced by computing the precision at a set of eleven equally spaced recall levels [0, 0.0, 0.2, 0.3, 0.4, ... 1]. The precision at each level is interpolated by taking the maximum precision measured for a method for which the corresponding recall exceeds r as defined by equation 3.20. The average precision is defined by equation 3.20.

$$\text{Average precision (AP)}=(1/11)*\sum P_{interp}(r) \qquad 3.20.$$

R takes on the values listed above.

3.3.5 PETS 2005 Metrics for Tracking

Tracking involves complex interactions between object-background, and object-to-object resulting in splits merges and occlusion. Towards evaluating these complex interactions the PETS (Performance Evaluation of tracking and Surveillance)

workshops was set up. Papers submitted by several groups have proposed different metrics to capture object interactions and evaluate object tracking performance for surveillance. Two main types of metrics have been proposed, namely, frame-based and object based metrics. Frame-based metric applies to objects in individual frames. Each frame is evaluated individually in terms of the number of objects, their sizes, and locations. Performance is then evaluated by averaging over all the test frames. On the other hand object-based approach considers the trajectory of object in the frame sequence (both spatially and temporally) where individual objects are detected and tracked over their lifespan as separate entities. Temporal overlap is defined as the ratio of the number of frames where the spatial overlap is met to the number of frames where the object is observed. Both object-based and frame-based metrics are used in evaluating video surveillance applications in PETS 2006 (Devijver and Kittler 1982). Objects are described using either a rectangular bounding box or the actual shape of the object. Two bounding boxes are said to be coincident if the centroid of one of the boxes lie inside the other. The PETS metrics in the current investigation is based on definitions provided in [Bashir and Porikli 2006]. The Frame based metrics are slightly different from confusion matrix measures (defined above) since multiple detection events and single detection events occurring within a particular frame are not differentiated. In frame-based approach a TP event occurs if at least a human is detected in the frame, otherwise it is classed as FN. An area ratio (spatial) overlap criteria is used in defining a TP event in object-based approach. In object-based approach the average overlap over the definition of a track is used in defining TP event. The averages of the metrics are also computed over the duration of tracking. It uses both spatial overlap and temporal overlap criteria to detect a track associate with an object. The following metrics are also defined for tracking: Track detection rate, track false alarm rate, and average area overlap.

The average area overlap is defined by equation 3.21.

$$Overlap(k)=area(B_p \cap B_{gt}) / area(B_p \cup B_{gt}) \quad 3.21.$$

B_p and B_{gt} denotes bounding box for human predicted by the algorithm (application) and labelled by the ground truth respectively. $\cap$ and $\cup$ denotes the intersection and

union operations respectively. The average positional error is defined by equation 3.22.

$$APE = \left(\sum (B(k) * (G(X_{f,k}) - X_{f,k})^2 + B(k) * (G(Y_{f,k}) - Y_{f,k})^2\right) / N_{rg} \quad 3.22.$$

where, subscript f denotes the frame index, $G(X_{f,k})$ denotes the X-coordinate of the ground truth frame object with index k, similarly $G(Y_{f,k})$ denotes the y-coordinate of ground truth object with index k, and N_{rg} denotes the number of objects in the current ground truth frame. The summation is over all the objects in the current frame with no multiple object matching allowed. The average merge error is defined such that for every one ground truth object there is a possibility of multiple predicted object matches, i.e, one-to-many relations. Similarly the average fragmentation error is defined to allow one–to-many matches for predicted to ground truth matches. Detailed discussion of tracking metrics, is provided in [Brown et al. 2005], [Bashir and Porikli 2006]. Table 3.4 is a summary of the main performance metrics associated with the publicly available dataset.

3.3.6 Choice of Benchmark Metrics for Performance Evaluation

The following criteria were used for human detection:

- A minimum area overlap (see equation 3.21) criteria of 0.5 is used to define true positive instance, otherwise it is treated as false negative instance in both detection and tracking scenarios (PASCAL VOC 2010 challenge).

- Euclidean distance constraint: The maximum Euclidean distance between the centroid of the ground truth (X_g, Y_g) and the system found human (X_s, Y_s) half the width and height of the bounding box (Generic requirement for overlap).

Table 3.4 Performance metrics for image classification, object detection, event detection, and tracking

Benckmark/Conference	**Performance measure**
i-LIDS	F1
PETS	Confusion matrix based measures for object segmentation and tracking
TRECvid	NDCR
Advanced Video and Signal based Surveillance (AVSS)	F1,NDCR, Tracking precision
PASCAL (Patten Analysis, Statistical Modelling and Computational Learning Visual Object Classes Challenge (VOC2010)	Classification (Precision/Recall curve, and Average precision) (area overlap ratio between ground truth and object> 0.5)
Daimlerchrysler	ROC curve at 95% confidence interval

$$|X_g - X_s| < 0.5*\text{Width1} \quad (3.23)$$

$$|Y_g - Y_s| < 0.5*\text{Height1} \quad (3.24)$$

TP must meet all the above criteria: area overlap (equation 3.21) and Euclidean distance constraint (equations 3.23 and 3.24). TN is estimated as total number of windows examined less the sum of TP and FP. TP, FP, and FN is based on the definition provided by i-LIDS. TPR (average precision), FPR, FNR, and F1 are computed over all frames for human detection.

For tracking the following metrics would be used:

- PETS 2005 based metrics for human tracking TPR, FPR, and FNR are computed. The following metrics are also computed: TDR, TFAR, and APE.

- F1 measure for human tracking.

Selected video from PETS 2005 and in-house datasets were used in evaluating human detection algorithm based on precision-recall curve. F1 measure and performance metrics discussed above and proposed in [Bashir and Porikli 2006] were used for human tracking on account of the fact that it measures occlusion, and overlap between objects. It also captures some interactions between object-object interactions (merges and splits) in tracking scenarios. Table 3.5 shows the benchmark metrics chosen for the current investigation.

Figure 3.5 Benchmark metrics selected for the current investigation

Task	**Performance metrics**
Detection	Average precision (PASCAL VOC definition) (Area overlap ratio >0.5); F1 measure
Tracking	PETS 2005 metrics (see PETS metrics above) and F1 measure (F1>0.75)

3.4 State of the Art Performance on Pedestrian Detection

A recent study [Enzweiler and Gavrila 2009] on detection of pedestrians where the human body covers a small part of an image has highlighted performance constraints in human detection and tracking in outdoor environments. Three state of the art human detectors (Haar wavelet with Adaboost cascade detector, Histogram of oriented gradients (HOG) features combined with linear support vector machine (HOG/linSVM), and Neural network using local receptive fields (NN/LRF)) were used in generic and application specific scenario. The generic scenario is pedestrian detection in outdoor environment, whilst application specific scenario focused on pedestrian detection from a moving vehicle. The training set used was extended Daimlerchrysler data consisting of 16,600 examples, and a test set of 21,790 images

(640X480) with 56,492 manual labels, and 259 trajectories of fully visible pedestrians. Temporal integration of detection results via tracking was used to suppress spurious false positives. Performance was evaluated at the frame and track level using sensitivity, precision, and false positives per frame, and reduction in false positives per frame after tracking. An area overlap ratio (see 3.27) is used in defining true positives. Frame level performance was visualised using ROC curves. Peak detection rates of more than ninety-five percent for all three detectors are observed from the ROC curve for the generic scenario. However, the problem of high false positives remains. For example at a detection rate of 70 percent, false positives per frames for HOG/linSVM detector was 0.045, compared to 0.38 and 0.86 for the wavelet-based cascade and NN/LRF. Thus higher false positives are expected as they approach the peak detection rate. In the case of application specific scenario the best performance of six false trajectories per minute at a detection rate of sixty percent was achieved by the wavelet-based cascade. However the required target performance is eighty percent trajectory level detection, and a false alarm per ten hours of driving in urban traffic. Table 3.6 provides a summary of peak performance for person classification and detection task based on PASCAL2 VOC challenge 2010 and the above study.

Table 3.6 Peak performance of human classification and detection

Task	**Dataset**	**Peak performance**
Classification	PASCAL2 VOC 2010	89.5% (Average precision)
Detection	PASCAL2 VOC 2010	47.9% (Average precision)
Detection	Extended Daimlerchrysler dataset	95% (detection rate)

CHAPTER FOUR

REFINEMENT OF RESEARCH OBJECTIVES AND STRATEGY

4.1 Introduction

Human detection is investigated as pattern recognition problem based on classifiers trained to discriminate humans from non human class in pattern spaces. It combines motion detection and object detection techniques in video. Tracking on the other hand is posed as optimum temporal linking of found humans in consecutive frames based on probabilistic data association, with investigations centred on reduced complexity implementation. In order to assess the robustness of feature-space based detection, two features spaces are investigated via pattern classifiers, namely, shape and wavelet spaces without any assumptions about scene complexity. Most spatial domain detection techniques on the other hand are based on computer vision and statistical techniques with assumptions about scene background. Thus comparative study of the effect of scene background factors with object based detection algorithms in the space-time domain, and proposed detection algorithm is evaluated. However, the tracking phase is implemented in the space-time domain, focusing on point-based feature tracking of humans using the centroid of the bounding box. The centroids are initially obtained from the output of the detector, and is based on two frames (previous, and the current frame). It is refined in course of tracking to reduce positional errors. A pattern space human detector is expected to: detect by parts such as head, upper body, lower body, arms, and legs, as well as detecting under full human appearance.

The tracking phase primarily provides trajectory information for found humans over several frames. Since some of the centroids found by the detector are false positives, and additionally higher detection rate is usually achieved with higher false detection rate, there is a need to reduce the false positives. In order to reduce false

detections it is proposed to use the tracking phase to investigate whether there could be a reduction in false alarms during tracking. It is supported by fact that if tracking decisions are made based on more than one frame in the past, it results in improved detections compared to those based on the previous frame only.

The investigations are aimed at detecting the presence of humans in upright posture, and no assumptions are made about the camera motion. The input video sequences are monocular with only one channel of input video. The viewing angle between the ground plane and the top of the human should be less than 60 degrees. Extension to multiple video bit streams is provided by considering processing scalability. Achieving real-time performance and anomalous behaviour detection are not considered in the current project but relevant research issues are highlighted in the conclusion chapter. Section 4.2 provides the motivation leading to the investigation into shape-based descriptors for human detection. Section 4.3 refines the objectives, whilst section 4.4 the strategy in the light of the findings in chapter two.

4.2 Motivation for the Choice of Shape Features for Human Detection and Tracking

Geometric features of humans are nearly always observable in image space, thus they provide a reliable means of human detection. This is due to its insensitivity to colour and texture, and invariance to scaling and translation. Typical shape descriptors are silhouettes and shape-outlines. These in turn may be described by intermediate feature primitives such as lines, corner points, and curves. They in turn may be described by low level features such as edges. Features of humans in spatial and image-transform domain for detection, albeit, sharing some of the features with the background are investigated to synthesise classifiers to discriminate humans from its background. The background class thus refers to any object in the scene which is not human but might be significant in the scene. Two proposals, namely, the use of frequency distribution of co-occurring primitive wavelet features, and low complexity shape-outline descriptor to model the human and the background classes are investigated. A discriminant function based on similarity or mismatch measure is used for differentiating the human from the background class. The alternative approach of looking for unique features between the human and background class is not

investigated since shape based features are robust. Histogram techniques in wavelet domains have also been applied in related studies in image retrieval [Mandal and Aboulnasr 1999], object detection [Schneiderman and Kanade 2000], and object tracking [Huwe and Niemann 1998]. Histogram techniques further, on account of its low complexity for low dimensional vectors (up to two), makes it a good choice for human detection. It estimates the underlying probability density function describing an object category.

The filter bank implementation of wavelet transform acts as a hierarchy of detectors at discrete object scale [Strickland and Hee 1997]. Wavelet template was applied to object detection by [Papageorgiou and Poggio 1999]. Over complete Haar wavelet transform was applied to images with no feature selection. The resulting subbands were trained using support vector machine. Peak detection rate of more than 90% with false alarm rate of one per ten thousand windows examined was achieved. The system was later deployed in DaimlerChrysler S class demonstration vehicle for pedestrian detection. However in (Oren et. al 1997) the shape of an object is described be a subset of wavelet coefficients. Wavelet template defines the average intensity of a region with respect to its neighbours using three types of Haar wavelet supports. Feature selection was achieved by statistical analysis of wavelet coefficients. The system achieved a pedestrian detection rate of 52.7% with false positive rate of one in every five thousand windows examined. The effect of wavelet space in filtering out false motion has also been demonstrated [Yunqiang et al. 2001]. The histogram of oriented-gradient [Dalai and Triggs 2005] uses a dense grid of uniformly spaced cells with overlapped local contrast normalization cells for improved performance. The large number of oriented gradient magnitudes uses block normalization technique to improve invariance (against illumination and shadows), incurring additional computations. Finally support vector machine is use to train the classifier using examples for the human and background class. The histogram captures the normalized gradient magnitude over orientations between zero and one hundred and eighty degrees. Very high detection rate with low false positive rate in pedestrian-based applications [Munder and Gavrila 2006] has been reported. Most shape-based detectors search for objects at multiple scales by sliding object window (a rectangular patch of the image) across the image. This also incurs high computational cost in object localization. Object detection/ recognition is still a challenge in arbitrary image

context. Another challenge involves low resolution video surveillance involving multiple human tracking. For example, the maximum average precision reported in PASCAL challenge [Mark and Luc 2010] is 48% for human detection. It is 16% in Caltech 101 dataset [Fei-Fei et al. 2004]. The general conclusion is that higher detection rate and low false positive rate could be achieved by taking the background context into consideration as in video where typically higher detection rate has been reported. It is clear that accuracy varies from one dataset to another, and also depends on the evaluation modality.

While SIFT features [Lowe 200] provide a general technique for identifying salient features points invariant to scale and rotation, computationally large number of operations are required per feature point, as well as large number of feature points. A good feature space additionally is required to be able to provide unique features which characterises the object of interest, although in practice features may be shared by the background class. In absence of unique features co-occurrence of a set of features in the object regions, and density estimation techniques may be to model an object class if the underlying distribution of these features is different from the background class.

The shape context [Belongie et. al. 2001] at a reference point captures the distribution of other feature points relative to it. It offers a globally discriminative characterization of shapes. It provides a means of comparing two shapes for point-to-point correspondence: corresponding points have similar shape context. Dissimilarity between two shapes is computed as the sum of matching errors between correspondence pair. Finding correspondence between two shapes means finding points that have the same shape context. However shape matching is posed as tripartite graph matching introducing algorithmic complexity

On the other hand silhouette descriptors for object boundaries require less number of primitive to adequately describe the contour. For example a 2-D silhouette of objects requires sixteen possible blocks of two by two binary shape primitives. The only requirement is that most of the object boundary must be visible. Contour-based shape descriptors also suffer from the problem of noise and scale changes although level set and snake minimization algorithms have achieved high tracking accuracy in human tracking. Investigation into suitable low complexity shape-outline extraction and matching in the shape-space is via shape prediction by feed forward neural network is motivated by the above observations.

4.3 Objectives

The main research themes are summarised as: on improving accuracy independent of scene content; Improving reliability by predicting operating accuracy; improving performance scalability, and improve timeliness by predicting real-time performance. Additionally the following objectives have emerged:

1. Investigate salient feature localization techniques to reduce search time in feature space. The output is the creation of salient (foreground) feature maps and extraction of candidate humans. This relates to objective one.
2. Investigate the use of tracking phase to reduce false alarms. This objective is related to objective two.
3. Use of PETS and iLIDS based metrics for accuracy evaluation. This is in addition to the use of confusion matrix based measures and ROC curves, and it is related to objective five.
4. Evaluate accuracy of propose detectors on single shot images using PASCAL2 VOC challenge benchmark (objective five).
5. Comparative accuracy evaluation human detection stage with Gaussian mixture based segmentation and the proposed human detection algorithm. This is related to original objective five.
6. Comparative accuracy evaluation of proposed JPDAF tracker with mean shift tracker. This is related to the original objective five.
7. Investigate scheduling strategies to improve application performance scalability. This involves scheduling for frame based processing sub tasks, and for window (patch) based processing sub tasks. This is related to objective four.
8. Theoretical investigation on meeting timeliness and throughput requirements. This is related to objectives four.

4.4 Strategy

The main focus is on feature extraction, optimal classifier design for human detection, optimal JPDAF tracker design, operating accuracy prediction, synthesis of scalable algorithmic architecture, and scheduling strategies to improve scalability. At the

feature extraction phase suitable shape-space and wavelet domain representation are investigated. Optimal search strategies are also investigated to enable rapid localization of salient feature regions as candidate windows. At the salient feature localization stage the number of features in the feature space is reduced such that only the most important cues likely to contain humans are retained. A search is conducted using the salient feature map to determined candidate humans. Thus it aims to retain minimum number of features required to locate humans. A patch classifier is subsequently used to discriminate between the human and the background class given an object window. It returns a hypothesis assigning the window to a human or non human class. It additionally returns the centroid of the found human relative to the patch. Linear discriminant test is applied to newly found human windows in addition to pixel count, and size thresholds to further validate humans found by the classifier. The detection phase has the following processing steps: pre processing, feature extraction, salient feature localization, human discrimination, and validation. The shape-outline and the wavelet domain classifiers are only used at the discrimination stage. The detection stage thus entails the following four steps:

(1) Pre processing

- **Frame enhancement**
  - Median filtering to remove impulse noise
  - Saturation control for brightness adjustment
  - Histogram Equalization for contrast enhancement
  - Illumination normalization to compensate for non uniform illumination

(2) Identify candidates

- **Feature extraction**
  - Shape-outline map construction
  - Wavelet based feature map construction
- **Candidates localization**
  - Foreground (salient) shape-outline map construction (by feature rejection and filtering)
  - Foreground (salient) silhouette map construction to be used (by feature rection and filtering)
- **Define candidates**

        - Rectangular regions in the frame

(3) Human discrimination (from background class)

- Classification
    - Shape-outline based classifier
        - Hypothesis generation
        - Hypothesis validation
        - Validation
            - Linear discriminant test for verification of found humans
            - Heuristics test (size and pixel count test).
    - Wavelet based histogram classifier
        - LL subband classifier
        - HLLH subband classifier
        - Validation
            - Heuristics test (size and pixel count test).

(4) Update details of found objects

- Determine centroids of found humans
- Update global database of found humans

The detection task is realised with the processing pipeline shown in figure 4.1.
It consists of two processing pipelines, one for shape-outline based detection (A), and the other wavelet based detection (B). The output of each pipeline is stored on a frame by frame basis in the common database. The two detectors complement each other, thus candidate already probed by one detector is not probed again by the other detector. Two classifiers are trained offline, one for each classifier. Input frames are processed by passing through the pipeline stages. EOF denotes end of file test condition. Salient feature localization starts with a dense feature map as input, and applies feature rejection (by threshold) filtering to reduce the number of features, and a search strategy to identify candidate human windows. The output is the candidate human window which is passed to the classifier for discrimination.

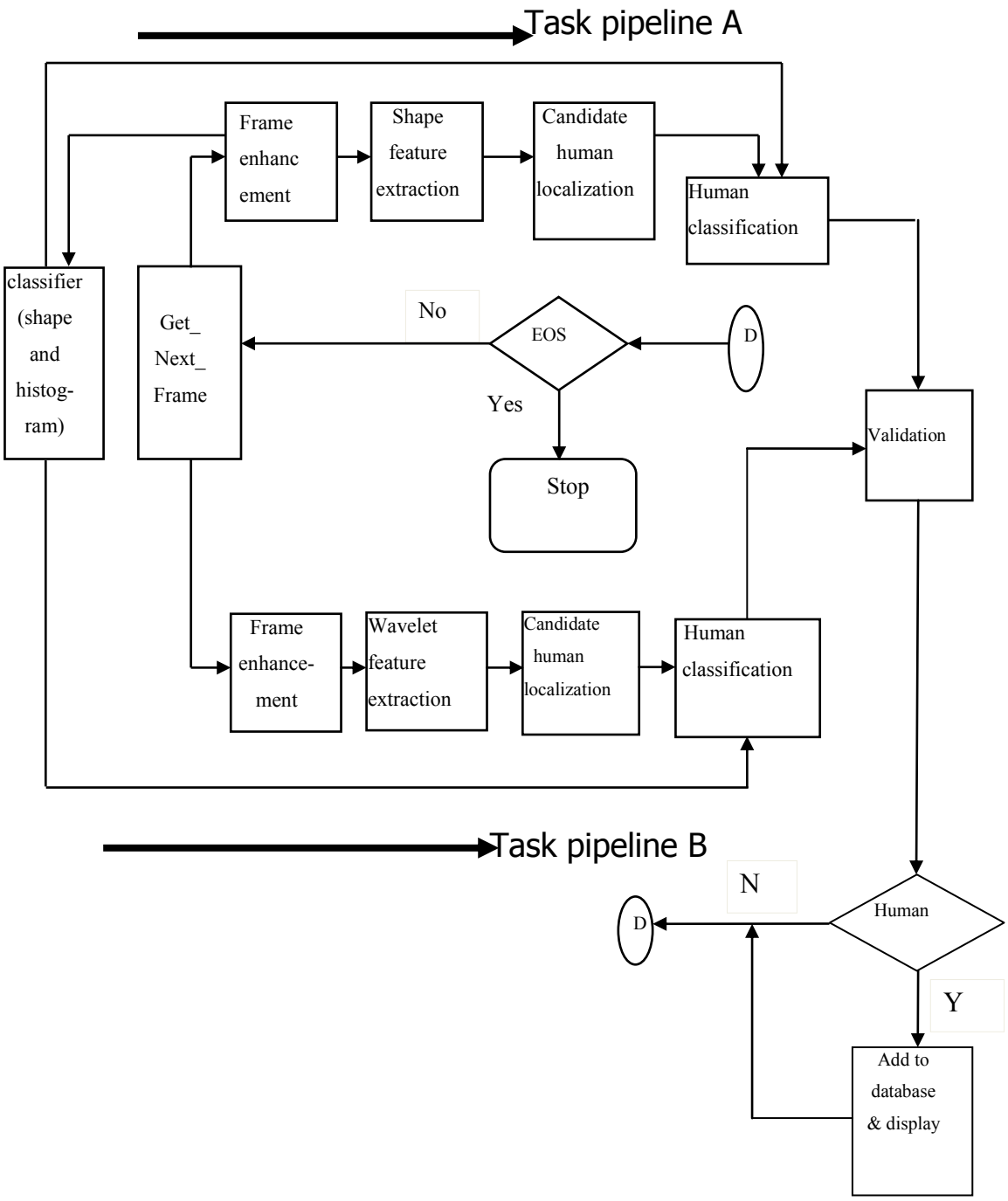

Figure 4.1 Algorithmic task pipeline for the proposed feature space based human detection. EOS denotes end of sequence

The following computational steps are applied iteratively at the tracking stage to each frame: track initialization, feature measurements, measurements clusters are validated and assigned to existing tracks as hypothesis, JPDAF (joint probabilistic data association) is applied spatially to determine valid measurement–to–track association, and temporally tracks are propagated based on maximum track likelihood. Tracking

decisions are made within a group of overlapping frame processing window (a frame window of ten frames was used in the evaluation phase). Accuracy predications are made to generate expected detection rate and false alarm rates for the next frame. The output of the tracker after every track processing window is used to update the achievable accuracy on a frame-by-frame basis. The processing steps for the tracker are as follows:

Track initialization

- State vector initialization using centroids of found humans

Silhouette and appearance feature extraction (segmentation and outline extraction)

- Appearance templates extraction (intensity, chromatic colours, gradient magnitude)
- **Measurements computations** (Local and global motion vector estimation)
- **Measurement validation**

Track hypothesis generation and validation

- Determine measurement to cluster association (between previous track state and current measurements based on Kalman prediction)
- Update measurement to track cluster association (JPDAF) probabilities
- Validate measurements to track hypotheses
- Compute signatures of all found humans in the current frame
- Determine the best associated track for every candidate human using its signature
- **Kalman filtering and prediction**
  - Next state prediction

Post processing

- Track maintenance (track activation, deactivation, splits, merges);
- Occlusion handling;

Appendix B is hierarchical block diagram of the proposed structure for human detection and tracking algorithm.

CHAPTER FIVE

INVESTIGATION INTO FEATURE EXTRACTION TECHNIQUES FOR HUMAN DETECTION

5.1 Introduction

This chapter presents the investigation carried out to determine suitable feature space transformation and representation for humans based on apparent shape-outline in shape space, and scale-frequency domain feature descriptors for human silhouettes. As will be shown later on, the two forms of representation complements each other in detecting humans independent of scale changes. Scale changes are brought about whenever the size of an object and its features change significantly relative to its local neighbourhood. Section 5.2 justifies the use of wavelet transform to determine discriminatory and orthogonal feature set. An implementation of 9/7 biorthogonal spline wavelets used in search of orthogonal and discriminatory features is described in section 5.2.1. A feature map consisting of the silhouettes of all interesting objects in a frame is proposed as the basis for human detection in wavelet space. From the feature map are extracted binary silhouettes of objects using two by two (2X2) binary patterns of the wavelet coefficients as features. Frequency analysis of the pattern of binary silhouette of humans leads to the choice of density estimation technique (a projected histogram) as a model for the human class. Section 5.3 discusses the need to reduce the number of interesting features in order to probe the wavelet feature space during candidate human localization. A sparse feature map is also proposed for probing feature locations for candidate human identification. Section 5.4 on the other hand takes the geometric representation of humans based on shape-outline, and describes a suitable form of representation similar to edges in shape space. It is shown that by a suitable choice of threshold, this form of representation is very similar to edge based representation but with reduced computational cost, and with

less spurious points. A boundary extraction algorithm based on this approach is presented in section 5.4.1. Section 5.5 discusses salient feature map generation in shape space similar to that discussed on section 5.3. In section 5.6 the main findings and computational characteristics are discussed.

5.2 Feature Extraction in Scale-Frequency Domain

Two main types of features spaces are available for object detection and tracking, namely, spatial domain and non spatial domains. Non spatial domain includes eigen space, principal components feature space, wavelet and Gabor transform feature spaces, and SIFT (scale invariant feature transform) feature space. Features space transform techniques aim at reducing the dimensionality and correlation between object features to facilitate object detection. An image is transformed into wavelet feature space on applying a wavelet transform. A wavelet filter is any function which has finite energy and is square integrable, satisfies wavelets regularity and admissible conditions [Daubechies 1990]. It decomposes signals (functions) into multiresolution components, enabling space-time domain signals to be represented in scale-time, and frequency-time domains. The basis function of wavelets transform (defined in equation 5.1), the wavelets, is generated from the mother wavelet by dilation and translation. The variables s and τ denotes respectively scale and translation parameters. The wavelet transform (WT) of a one-dimensional signal is two dimensional, and that of two-dimensional signal is four-dimensional. WT applies high frequency analysis of signal using small windows and low frequency analysis using large windows. There are two main types of wavelet transform, namely continuous and discrete wavelet transform. Continuous wavelet transform results when both the function and the wavelet are continuous. The continuous wavelet transform of a function f(t), belongs to the vector space of square integrable function defined by equation 5.2. $H_{s,t}(t)$ denotes the discrete wavelet basis function defined in equation 5.1, and * denotes the complex conjugate operation.

$$H_{s,\tau}(t) = \frac{1}{\sqrt{s}} h\left(\frac{t-\tau}{s}\right) \qquad 5.1$$

$$W_f(s,\tau) = \int f(t) h^*_{s,\tau}(t)\, \partial t \qquad 5.2$$

Wavelet transform (WT) can also be considered as a bank of filters consisting of low pass (scaling function) and band-pass filter (Wavelets). It could be also interpreted as the correlation between the signal (function) and the scaled wavelets. The Fourier transform of wavelets are referred to as wavelet transform filters. The discrete wavelet transform uses discrete wavelet basis function $h_{s,k}(t)$ (discrete values of s and τ) to decompose f(t) into a sequence of coefficients known as wavelet series decomposition defined as:

$$W_f(i,k) = \int f(t) h^*_{s,k}(t) dt = < f, h_{s,k} > \qquad 5.3$$

The angle brackets denote inner product (scalar product). Wavelet decomposition applied to the analysis stage of signals is referred to as forward wavelet transform. It results in wavelet series decomposition of the signal and in the reverse case, the inverse wavelet transform, is used to recover the original signal. Two forms of representation of wavelet transform exist, namely, the critical sub sampled (dyadic decomposition), and the over complete wavelet representations. The critical sub sampled version provides minimum redundancy for perfect reconstruction of signals. Over complete wavelet analysis is essentially a frequency domain based wavelet representation with redundant sampling [Teolis 1998]. Translation invariance property of wavelet transform has also been demonstrated in several studies on wavelet based classifiers for human detection and tracking [Oren et al. 1997], [Papageorgiou 1999]. Features which are typically extracted in the wavelet domain include edges, motion vectors, texture, corners, and contours. Several wavelets filters have been designed and applied to signal and image processing problems, including, Haar, Morlet, Mexican-hat, B-spline wavelets, and non orthonormal wavelets. [Rioul and Vetterli 1991] provides a survey on wavelet applications in signal processing. Wavelet filter analysis can be viewed as a bank of filters for hierarchical analysis of image features. Certain class of wavelets such as orthonormal wavelets, and biorthogonal wavelet transform analyse image features into orthogonal feature set which facilitate object classification and tracking. In object detection only the forward transform is required. The computational complexity of the analysis filter is essentially multiply-add operations using the recursive pyramid algorithm. The fact that it provides scale invariant detection of objects is a very important consideration since in video sequences,

changes in scale may be brought about by perspective projection due to humans moving away or towards the camera or changes in object resolution. Wavelet domain motion analysis is also less sensitive to noise and transient background motion than in pure spatial domain [Yunqiang et al. 2001]. The wavelet filters chosen for the analysis of video frames in the current investigation is 9/7 biorthogonal spline wavelets filter The use of this filter (an orthogonal wavelet) is justified since the resulting subband provides orthogonal feature set representation across scale, has near perfect reconstruction properties, and edge preserving across scales. Since all its (n-1) derivatives exist the 9/7 biorthogonal wavelet filter also meets the requirements of a good edge detector.

5.2.1 9/7 Biorthogonal Wavelet Filter for Feature Extraction

The wavelet filter coefficients of 9/7 biorthogonal wavelet transform is listed in table 5.1. The 2-D implementation of the pyramid algorithm applies 1-D transform along the rows followed by applying along the columns using different filters. The input sequence is also symmetrically extended before applying the filters H(z) (high pass), and G(z) (low pass) to ensure perfect reconstruction. In image and video analysis only the analysis filter is used. Figure 5.1 shows one stage (one level) decomposition of an image frame into four subbands using the recursive pyramid algorithm [Vishwanath 1994].

Table 5.1 Analysis and synthesis filters of 9/7 biorthogonal wavelet transform

Analysis filter		**Synthesis filter**	
H[z]	**G[z]**	**Bar_H[z]**	**Bar_G[z]**
-0.0645	0.0378	0.0645	-0.0378
0.0407	-0.0238	-0.0407	-0.0238
0.4181	-0.1106	0.4181	0.11060
-0.7885	0.3774	0.7885	0.3774
0.4181	0.8527	0.4181	-0.8527
0.0407	0.3774	-0.0407	0.3774
0.0645	0.1106	-0.0645	0.1106
	0.0238		-0.0238
	0.0378		0.0378

The computation cost of each wavelet coefficient is seven multiplications, six additions, and nine multiplications and eight additions respectively for the high pass ($Cost(N_H)$) low pass ($Cost(N_G)$) filters.

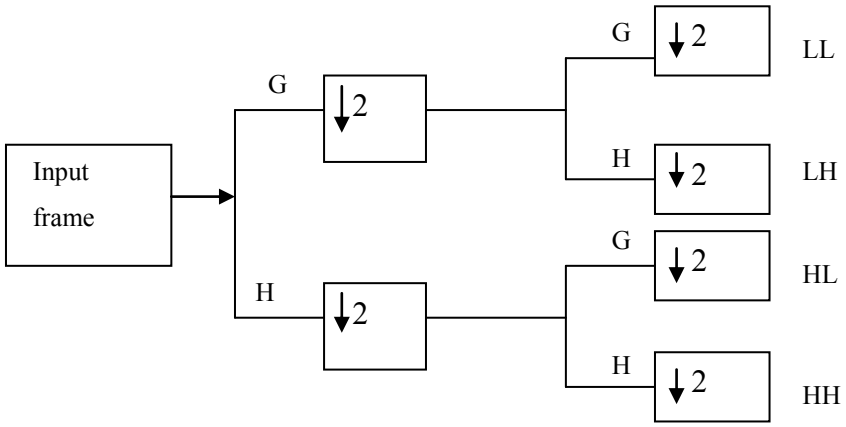

Figure 5.1 One-level wavelet decomposition: G denotes low-pass filter, and H denotes high-pass filter

Given an NXM input frame (samples) the number of computations points required at level j is given by equation 5.4 in the case of the biorthogonal non decimated wavelet transform. j takes on the values between 1 and J.

$$(NM/2^{(j)}+2)*Cost(N_G) + (NM/2^{(j)}+2) * Cost(N_H)+(NM/2^{(j)}+4)) *Cost(N_G) + (NM/2^{(j)}+4)* Cost(N_H). \quad (5.4)$$

The addition of extra computation steps of two for each of H and G filters due to symmetric extension along the ends of the input sequence is to ensure perfect frame reconstruction. With the decimated approach the sub sampling operation drops every other sample, and results $(2NM/2^{(j)})+6)$ points for each of the two filters. Thus the intermediate points need not be computed. The total number of computation points at level j is given as 6*NM+6*2 of which 3*NM +6 is due to filter G, and 3*NM+6 due to filter H for the non decimated approach. Every one level decomposition (analysis) of a 2-D frame results in four subbands, namely, HH, LH, HL, and LL subbands. The LL subband is then used in the next level (octave) computation. The number of memory access and intermediate computation points are given as: $(1+1/4+1/16 \ldots +(1/4)^{J-1})*NM$

for the decimated transform and JNM for the non decimated transform. Direct implementation of the pyramid algorithm is not optimum in terms of number of operations and memory access. Alternative implementations to meet real-time requirements is discussed in section 10.2.5. The algorithmic flow of wavelet domain feature extraction step is shown in figure 5.2.

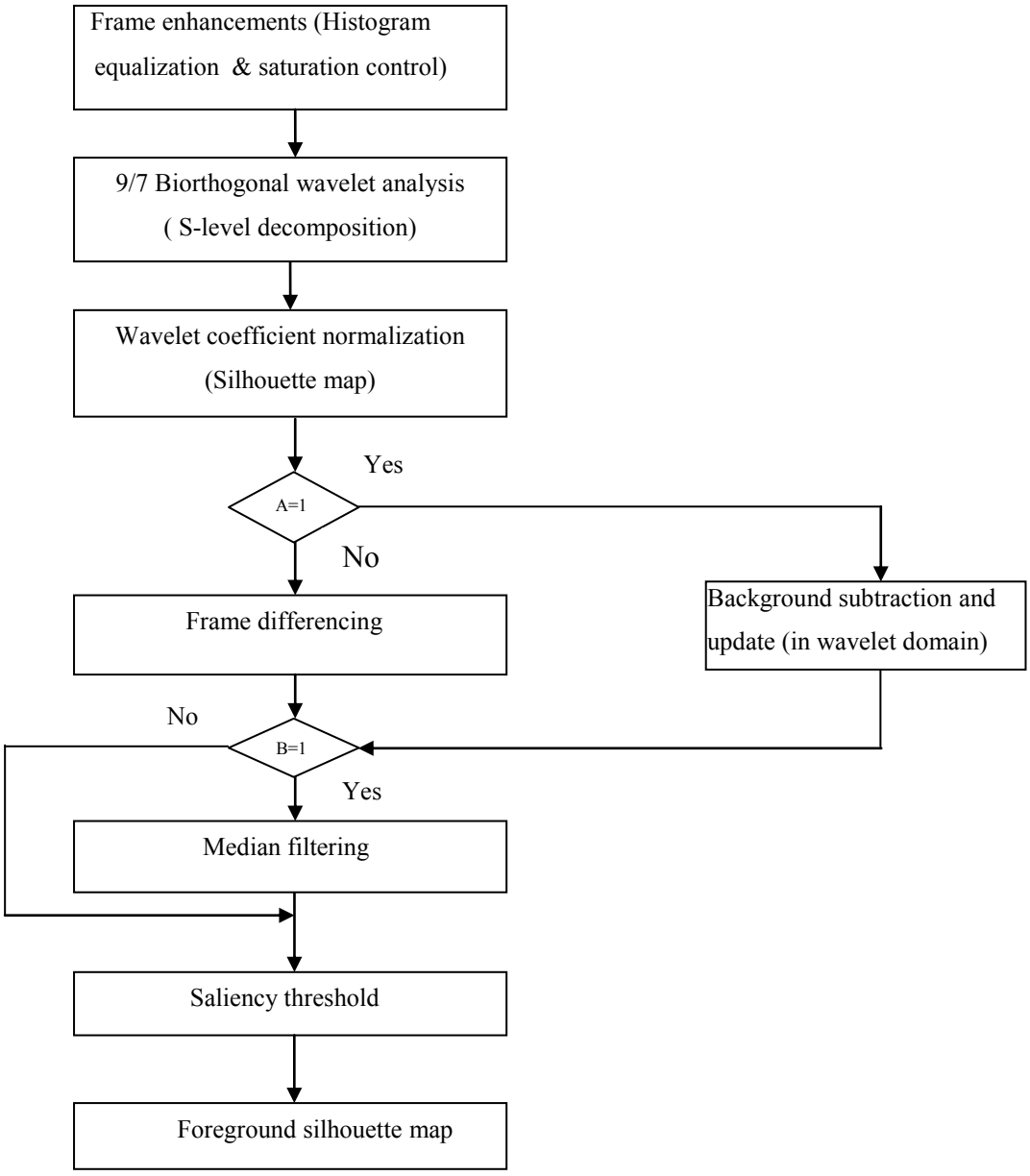

Figure 5.2 Feature extraction and construction of foreground silhouette map in the wavelet domain.

The pre processing step starts with YUV/RGB conversion, histogram equalization and saturation control optionally being applied to the input frame. Then wavelet analysis is applied to the enhanced frames and optionally coefficient normalization to construct a silhouette map. The initial silhouette map is a gray scale image of the frame. A binary silhouette map may also be obtained on applying a threshold (usually a fraction of the maximum wavelet coefficient in a frame) to the initial silhouette map. Flag A in the figure denotes background subtraction flag. If it is set to one the wavelet feature map is obtained using background subtraction scheme, otherwise it is computed using frame difference. Median filtering is applied if flag B is set to one. After median filtering, saliency based threshold is applied to the original wavelet coefficient map, resulting in the foreground silhouette map. By a suitable choice of threshold the silhouette of humans are enhanced. The foreground silhouette map represents silhouettes of changed regions.

Frequency analysis of the occurrence of the two by two block features in ten thousand frames and visual inspection of the silhouettes suggested ten initial feature primitives. The selected primitives are shown in figure 5.3. Features C and D have probability distribution which is different for the human and non human class. Features A and B have the same distribution but the magnitudes are different. The other features are either indistinguishable from the non human class or may not appear at all. Features I and J were chosen on visual inspection of the interior of the silhouettes. Thus for boundary description the four diagonal features (A, B, C, D) are the minimum set required. Single patterns E to H might not appear on its own, and hence are not independent. The patterns appearing with two or three binary patterns have the same binary value appear in most of the samples used. Features E to H were rejected since they either not independent or the frequency distribution are indistinguishable. [Viola and Jones 2001] proposed rectangular filter masks for constructing candidate regions by linear combination of pixels in a region. However, the proposed features are binary silhouette descriptors obtained by thresholding, and are different from rectangular features. Figure 5.4 illustrates the stages in the construction of a silhouette map. The input image is shown in a, the HLLH subband (gray scale image: after wavelet transform) is shown in b, and c, shows the silhouette map (binary image) on applying a threshold. The completeness of a human silhouette depends on the choice of the threshold. Two types of subbands were investigated, namely, the combination of low-high and high-low subbands, and low-low subband.

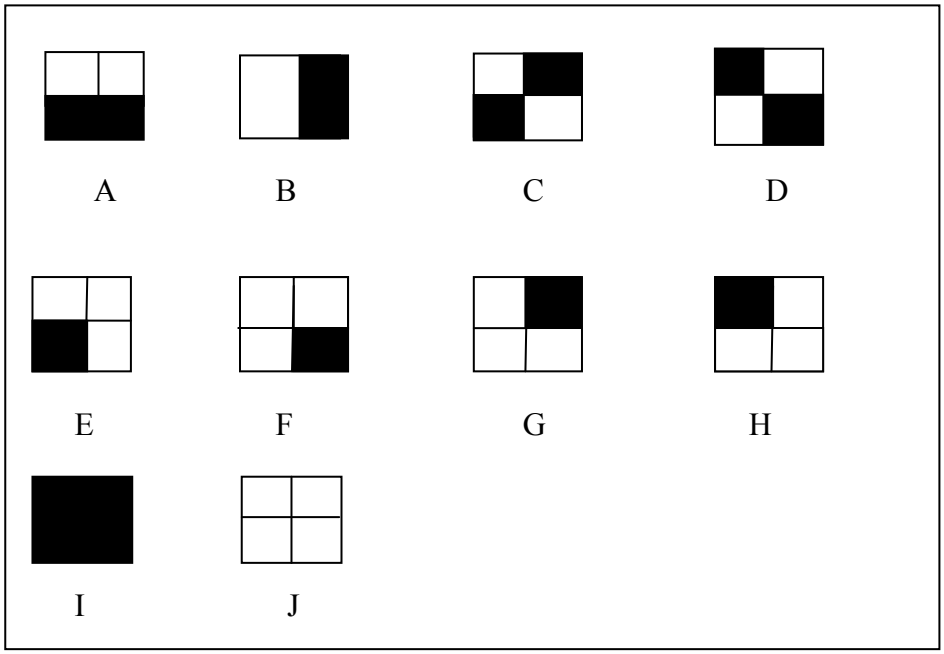

Figure 5.3 Wavelet domain primitive feature set

a

b

c

Figure 5.4 Stages in the construction of a HLLH silhouette map

5.3 Candidate Human Localization in Wavelet Domain

For efficiency reason exhaustive search is not applied to the original feature map to find candidate humans, since this is very costly. Instead, an intermediate map, salient feature maps are first created through feature rejection. This reduces the relatively large number of features locations which would have to be probed to determine the presence of humans by applying a threshold. The results is a foreground silhouette map. The filtered version typically has reduced (sparse) feature points and hence reduces the computational effort spent in searching. Salient blocks are then identified using a search strategy. The centroids of the salient blocks are used to define candidate humans (rectangular regions). Other criteria such as strong vertical symmetry [Owechko et al. 2004], [Broggi et al. 2000] have been used for human localization. Three saliency techniques for locating salient feature regions were investigated, namely, edge saliency, motion saliency, and background saliency. The result of this investigation is presented in chapter six as part of the human detection task.

5.4 Feature Extraction in Shape Space

In the shape-space the main geometric feature used in object detection is the shape-outline which for 2-D shape is required to be view independent. For a complete representation of 3-D shape several views might have to be stored in a database. Given a particular view of an object the best matching view is selected to represent the current view. The main requirement of multi-view object representation is that it must be invariant to rotation, translation and affine transform. The approach adopted here is to represent the outline of the human shape with points defined by edges, i.e, edge-based representation of shape. Shapes of interesting objects are extracted from a frame based on local neighbourhood analysis and a global threshold. The output of this analysis is the shape-outline map which describes the outlines of all the objects in the frame. Although there are several techniques for shape extraction including computationally proposed approach requires fewer operations, and contains less spurious patterns than traditional edge detectors. Shape-outlines generated using this approach are independent of the size of objects and depends only on the choice of the threshold and local neighbourhood size. The shape-outline map may also be subtracted from the previous shape-outline map or a

fixed shape-outline map may be used to derive foreground shape-outline map (similar to fixed background subtraction scheme). The principles are similar to that used in the wavelet domain. The detailed processing steps for constructing shape-outline map are shown in figure 5.5. The pre processing step optionally involves YUV/RGB conversion, histogram equalization, and saturation control.

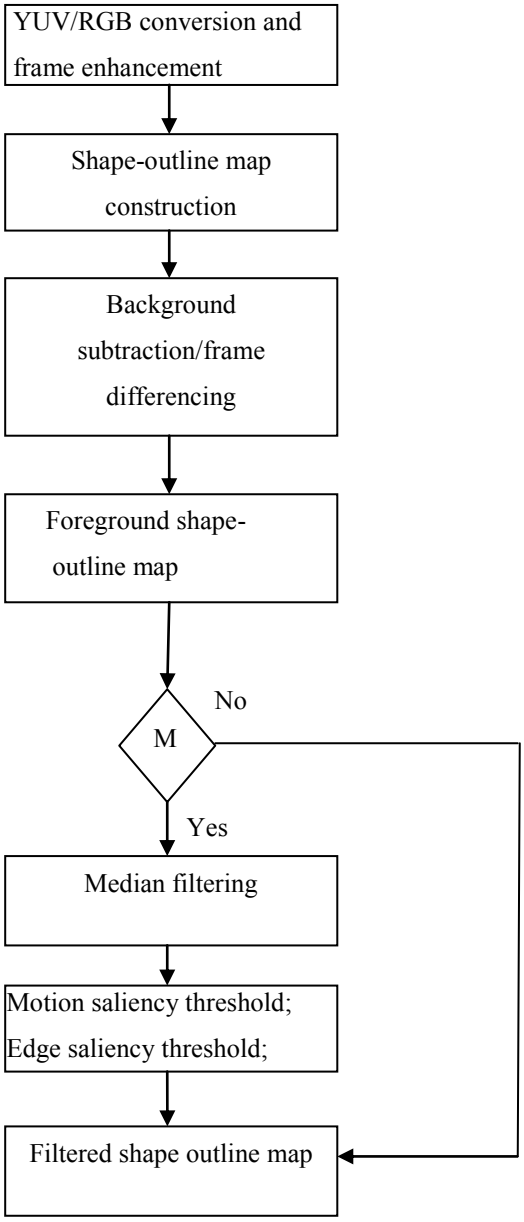

Figure 5.5 Flowchart of shape-outline map construction in the shape space. M denotes

It is dependent on the setup information provided. The initial shape-outline map (after boundary extraction algorithm) is typically noisy hence background subtraction or frame differencing is applied to extract foreground shapes. Additionally median filtering may be applied to remove impulse noise and small regions depending on the size of the median filter applied.

5.4.1 Boundary Extraction Algorithm

The boundary extraction algorithm is based on 8-local neighbourhood comparison for 2-D arrays. It compares each of the eight neighbours based on intensity. The pseudo code for the proposed shape-outline map construction given an input frame P(x,y) is as follows:

Let Nrows, and Ncols be height and width of a frame respectively. Let Threshold, be the global threshold value for comparing two pixels. Let Map(x, y) be the intermediate binary image after local neighbourhood pixel comparison. Let Shape_outline_Map be the final output.

```
    Initialise Map to zeros.
    For index1 from 2 to Nrows-1
        For index2 from 2 to Ncols-1
            Map(x+1,y+1)=(absolute| P(x+1,y+1)-P(x,y)| < Threshold);
            Map(x,y+1)=(absolute| P(x,y+1)-P(x,y)| < Threshold);
            Map(x,y-1)=(absolute| P(x,y-1)-P(x,y)| < Threshold);
            Map(x-1,y)=(absolute| P(x-1,y)-P(x,y)| < Threshold);
            Map(x+1,y)=(absolute| P(x+1,y)-P(x,y)| < Threshold);
            Map(x+1,y-1)=(absolute| P(x+1,y-1)-P(x,y)| < Threshold);
            Map(x-1,y+1)=(absolute| P(x-1,y+1)-P(x,y)| < Threshold);
            Map(x-1,y-1)=(absolute| P(x-1,y-1)-P(x,y)| < Threshold);
        end
    end
%Invert map. This is a comment
Shape_outline_Map=1-map;
```

The number of operations per pixel are nine subtractions (eight plus one), eight absolute value, eight comparisons, and eight assignments. Compared this with traditional edge detectors (Canny and Sobel detectors) which are either based on first or second local derivative operation it becomes obvious the saving in computation times. The algorithm for Sobel and Canny edge detection in pseudo code are also listed below for comparison. The pseudo code for Sobel edge map construction is as follows:

Let G_x and G_y denote Sobel filters for vertical and horizontal edge detection.

$$G_x = \begin{bmatrix} -1 & 0 & 1 \\ -2 & 0 & 2 \\ -1 & 0 & 1 \end{bmatrix}$$

$$G_y = \begin{bmatrix} 1 & 2 & 1 \\ 0 & 0 & 0 \\ -1 & -2 & -1 \end{bmatrix}$$

Let P(x,y) denote pixel intensity at point (x,y) in the image space. Let Ncols and Nrows denote the width and height respectively of the image.

For all x=1:Ncols

For all y=1: Nrows

$G=\sqrt{(G_x*P(x,y))^2+(G_y*(Px,y))^2}$

$\theta=\arctan (G_y*P(x,y))/(G_x*(P(x,y))$

end

end

The number of operations per point is twenty multiplications, seventeen additions, one division, and one square root operation. The output image G is the magnitude image and θ is the directional image of the input image. The pseudo code for Canny edge map construction:

1. Let the image function be described by P(x,y) and δG the partial derivative of G.

2. Choose a value for standard deviation (σ=K) of a Gaussian smoothing filter

And substitute into statement 3.

3. $G(x,y)=e^{(x2+y2)/2\sigma2}$

4. $G_n=\delta G/\delta n=n\nabla G$

5. $\delta^2/\delta n^2(G*P)=0$

6. $\nabla(G*P)=|G_n*P|$

Initialise σ to K;

Repeat until (σ=0)

a. Convolve image g(x,y) with a Gaussian smoothing filter G(x,y) defined above at scale σ.

b. Estimate the local edge normal direction using (4).

c. Find locations of edges using equation (5).

d. Compute magnitude of edges using (6).

e. Apply hysteresis threshold to output from d.

f. Decrease the value of σ by 1 (σ=σ-1)

end

7. Aggregate the final information about edges at multiple scales (1 to σ).

Clearly the operations involve more complex operations (derivative operation is approximately equivalent to one sobel-point computation), and threshold is applied iteratively. Table 5.2 shows execution times for Canny edge map, Sobel edge map, and proposed shape-outline map applied to the same frame. Matlab functions for Canny and Sobel edge maps were used. It is based on 2.6 GHz Pentium personal computer with two Gigabytes RAM, and running on Windows professional XP. From the table the minimum

execution time corresponds to the proposed shape-outline map. Thus it is preferred to other approaches if real-time requirement is to be met.

Table 5.2 Execution times for proposed shape-outline map construction for a frame compared with other edge map algorithm. The frame size is 240 X 320.

Algorithm	**Execution Time/Frame(seconds)**
Canny	0.13
Sobel	0.13
Object Outline Map	0.097

Figures 5.6 illustrates the different ways of constructing shape-outline map for input frame thirty-six of PETS 2005 video sequence (stc_t1_c_3.avi). The first approach shown in figure 5.6b involves comparing neighbouring pixels only. Figure 5.6c involves frame differencing of output from 5.6b. The third, approach shown in figure 5.6d, involves applying median filter to 5.6c. Figures 5.7 compares the output from the filtered shape-outline map and the edge map constructed from Sobel and Canny edge detectors using Matlab functions. The unfiltered shape-outline maps are usually noisy, whilst filtered maps might have eliminated some humans if the threshold is not carefully chosen. Figures 5.8 shows the output of level one and two HLLH subband, and the resulting silhouette map after applying median filtering. Figures 5.9 and 5.10 provide more examples to illustrates different shape-outline and silhouette maps.

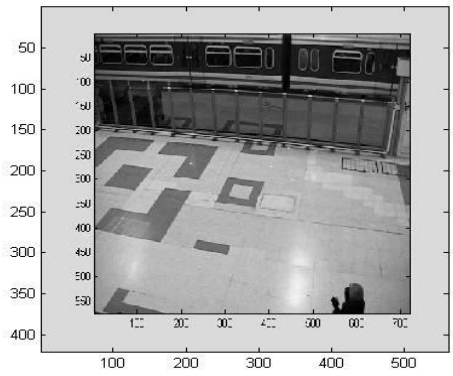

a

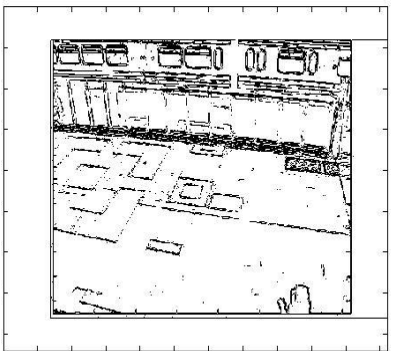

b

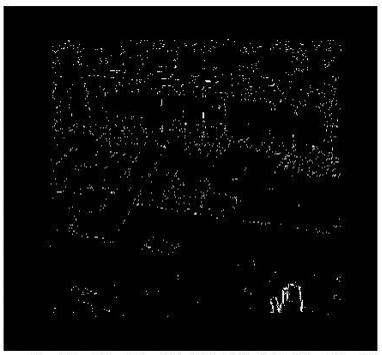

c

d

Figure 5.6 Construction of shape-outline maps from frame 36. (a) Input image (b) After neighbourhood pixel comparisons (c) frame differencing of b (d) after applying median filter.

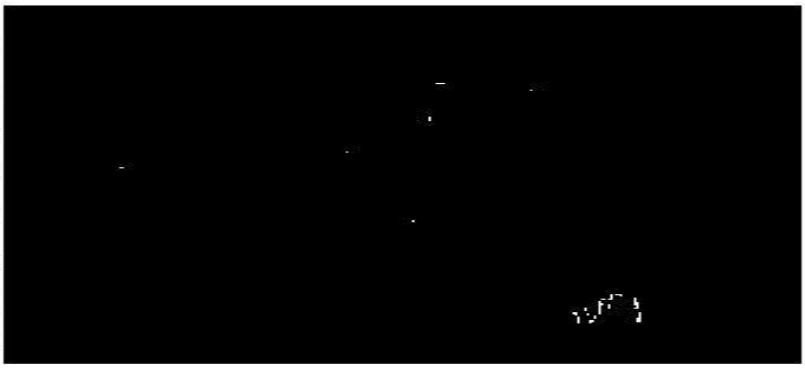

a

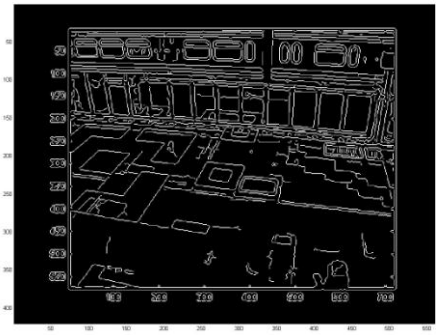

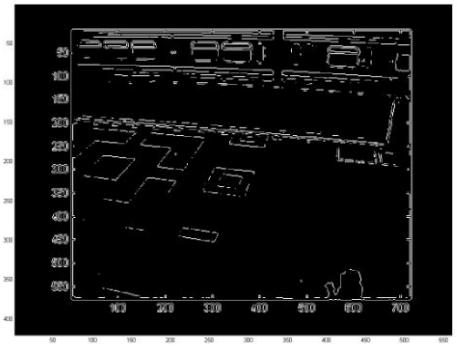

b c

Figure 5.7 Comparison of shape outline map with edge maps derived from canny and Sobel filters. From top, left and right (a) Foreground shape-outline map (b) Canny edge map, (c) Sobel edge map of the same input image (frame index 36)

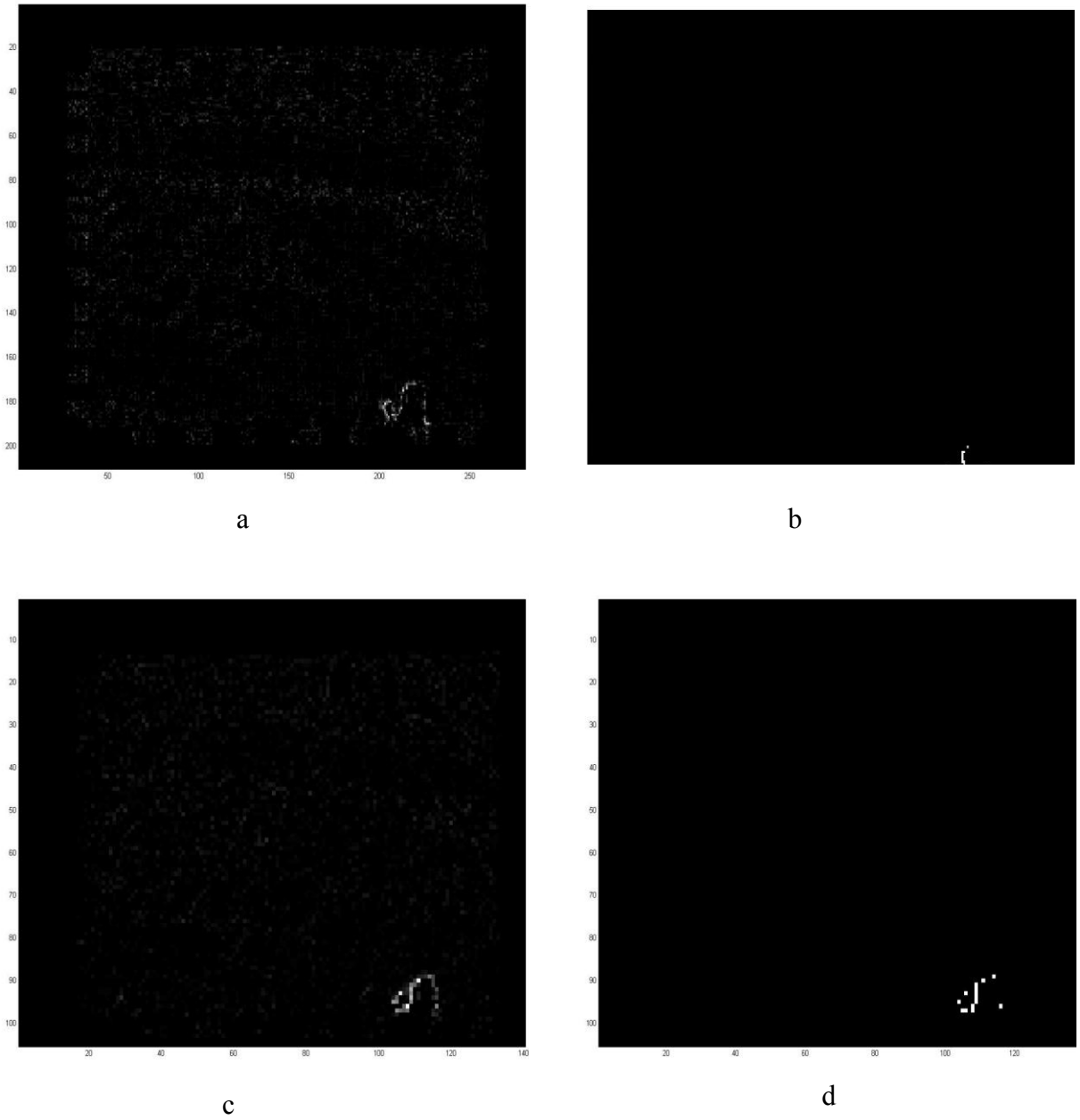

Figure 5.8 Construction of Silhouette-maps (HLLH subband) for frame 300. (a) level 1 unfiltered wavelet feature map (b) filtered level 1 wavelet feature map (c) unfiltered level 2 feature map

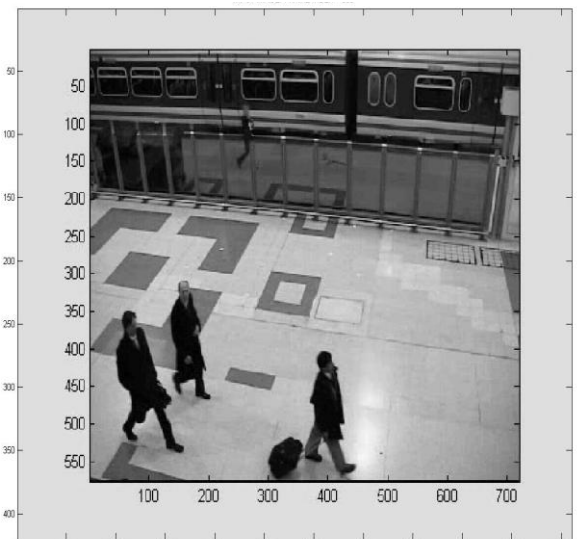

a

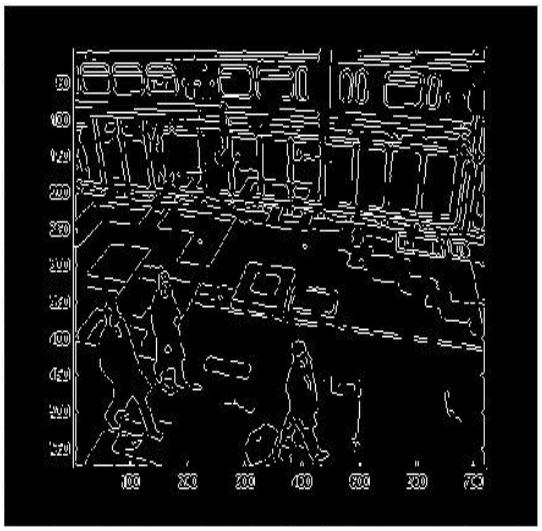

b

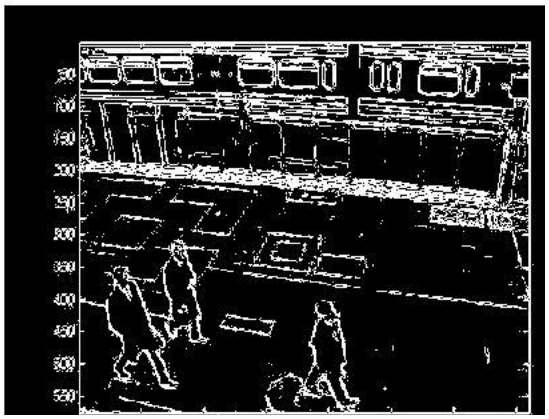

c

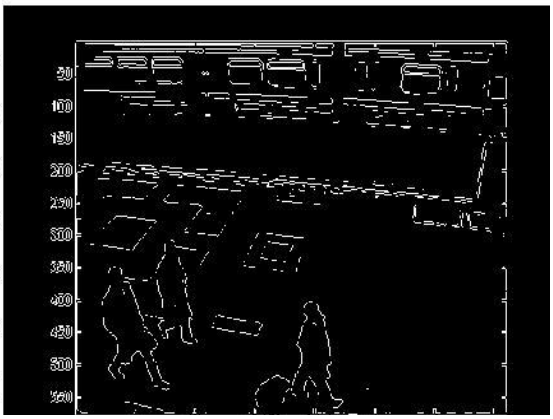

d

Figure 5.9 Comparison of shape-outline map types for frame 320 (a) input frame (frame 320) b) Canny edge map (c) unfiltered shape-outline map (d) filtered shape-outline map

a

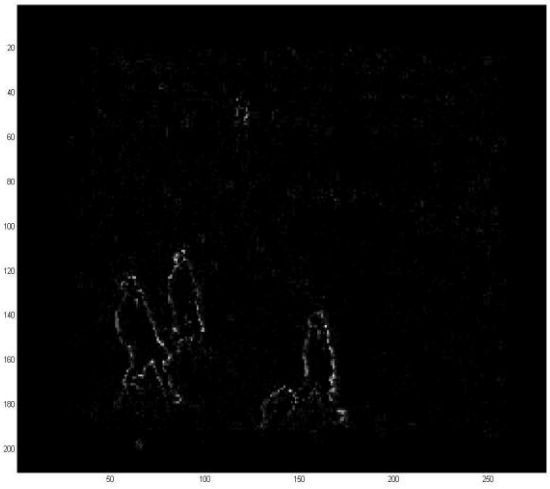

b

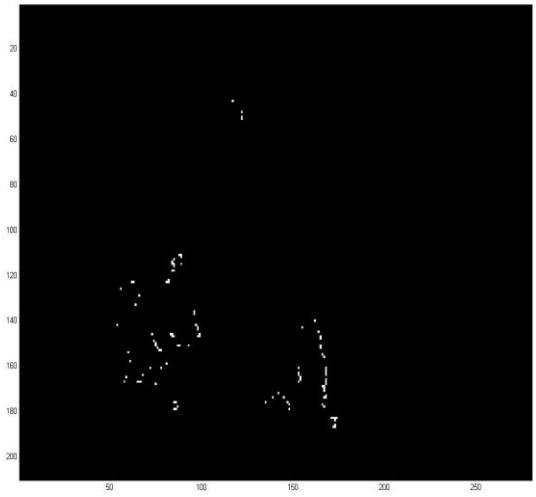

c

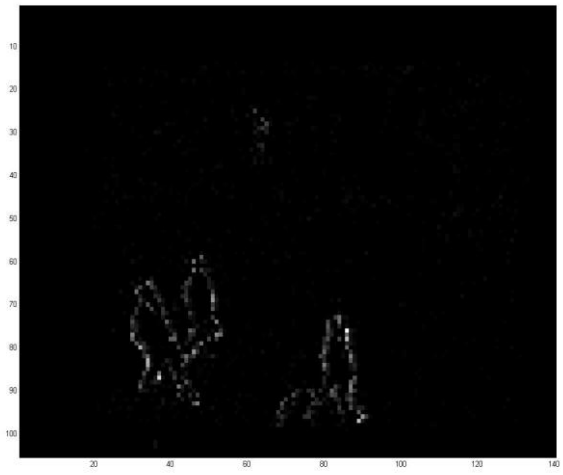

d

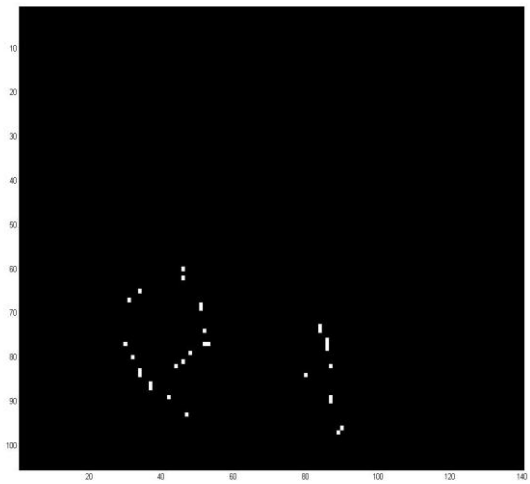

e

Figure 5.10 Silhouette map types (a) Foreground silhouette map (b) level 1 unfiltered wavelet feature map (c) filtered level 1 wavelet feature map (d) unfiltered level 2 wavelet (e) filtered level 2 wavelet subband for frame 330

5.5 Candidate Human Localization in Shape Space

The steps for candidate human localization is similar to that in wavelet domain as discussed in section 5.3. The only difference is that it is based on shape-outline map in shape space. Details of investigations into this aspect of processing are also presented in chapter seven.

5.6 Results

In scale-frequency space investigation revealed that ten normalized wavelet template features are adequate to describe the silhouette of humans in the wavelet domain. Simulation of the full sixteen features using PASCAL VOC 2010 sequence revealed marginal increase in accuracy compared with the computational effort The spatial distribution of these patterns for human class varies from that of the background. In shape space a reduced complexity shape-outline map extraction algorithm has been proposed. The alogrihm is dependent only on the choice of feature threshold and the size of the local neighbourhood. It was observed that complete shape-outlines resulted if the threshold is a fraction of the standard deviation of a subband. The continuity of shape-outlines of real-objects in the scene implies that some background noise can be removed by applying median filtering.

It is proposed to use the silhouette and shape-outline maps to investigate pattern classifiers for human discrimination and detection. The computational complexity of the proposed shape-outline map extraction is lower than that of the traditional edge detectors. One of the conclusions from visual inspection of the maps is that global threshold approach sometimes fails to detect humans if its dimension is smaller than neighbouring objects in the scene. The wavelet domain approach provides discriminatory descriptors for silhouettes of humans. Thus the two representations complement each other in detecting shapes of humans.

Scene background appear as random noise when the size of the background objects is smaller than humans, and by applying suitable median filter of a particular dimension most of the background noise is removed. For background objects larger than humans, the application of background subtraction techniques is able to remove most of the stationary objects. Simulations results are presented in the chapter six.

CHAPTER SIX

INVESTIGATIONS INTO PATTERN CLASSIFIERS FOR HUMAN DISCRIMINATION

6.1 Introduction

The chapter discusses issues related to the wavelet based histogram and shape based classifiers for human discrimination. It first provides the specification, design, testing and validation of the proposed classifiers. Sections 6.2, 6.2.1, 6.2.2 discuss wavelet based classifier design, validation and testing. Section 6.3, 6.3.1, 6.3.2 discuss shape-outline based classifier design starting from the feed forward pattern predictor, hypothesis generation, validation and testing. Section 6.4 discusses the results of the validation of the two classifiers. Section 6.5 provides an interpretation of the results.

6.2 Wavelet Feature-Based Classifier Specification and Implementation

An investigation into the use of density based appearance representation using the wavelet feature primitives (see section 5.2.1) was undertaken. These features are observable in all the silhouette of humans irrespective of the subband. Projection histogram of each of the primitive features along the X and Y-axis were generated as a model of human and background. For each feature, the occurrence frequencies along the axes are used in constructing the histogram. To ensure a fixed computational cost the dimension of the histogram is fixed. Two classifiers were designed using silhouette of humans from LL, and HLLH (sum of LH and HL) subbands. Preliminary classifier design revealed that of the ten initial primitive features (see page 89), six were selected as sufficient to discriminate human from the non human class for the

HLLH subband classifier (features A, B, C, D, I, J). With the LL subband classifier four features (A, B, C, D) were selected to discriminate between the human from the non human class. The selection was made by removing a particular feature during classification and observing the classification and misclassification rates. Matching of candidate histogram to model histogram is implemented by matching all the bin values (frequency count) along the span of the histogram given the centroid of the candidate location of the human. Since this location is not known in advance, the matching process starts from one end of the candidate window (naive search) or an offset from the assumed centroid of the candidate. The position corresponding to the best match after local neighbourhood search is then selected as the centroid of the candidate window (see section 6.2.1). To facilitate the search for the centroid of the human, the following assumptions are made:

(1) The joint distribution of a feature at a location is independent of other features.

(2) The joint distribution at the best matching location of a candidate occurs at the position with minimum distortion.

Compared to template based representation which typically requires large number of templates coefficients across scales, the number of features is fixed and the same at every scale. The simplicity in constructing 2-D histogram model histogram compared to automatic feature extraction classifier design means that alternative techniques such as Adaboost was also not considered. Further, the advantage of low complexity in computing 2-D histogram enables more effort to be focussed on the training of the classifier.

Three data sets were extracted from three video sequences with humans centered in a window of dimension 64 pixels high by 32 pixels wide as defined in table 6.1.

Table 6.1 Data set for training histogram based classifier

Video Sequence	**Number of Windows Extracted**
Combinetrainsequence.avi	1248
Hamilton.avi	2690
Testdata.avi	966

6.2.1 Novel Wavelet-Based Histogram Classifier Design and Training

The two practical difficulties in the use of histogram in object detection are (1) both the background and the object may have in common some features, and (2) how to align the object in the candidate window to the captured histogram of the object model. To solve the first problem several rectangular windows centred around an upright humans were used as human class examples for training, whilst a second group without any human were used for the non human class. A candidate is defined as a rectangular region enclosing a candidate. Rectangular region is used to describe a human since it is assumed to be in upright position, hence it is only the limbs which moves a small distance away from the body most of the time. One advantage with histogram based approach is that it does not require any assumption about the motion of the object: it is applicable to both still and moving objects. In contrast, the meanshift clustering for object detection, considers only locations along the principal modes of the kernel function. When the displacement falls outside the kernel bandwidth tracking or detection failure results. [Porikli and Tuzel 2006] use multiple kernels to overcome this limitation. A 2-D histogram could aslo be scaled to any dimension without distorting the distribution, and is also translation invariant.

Two histogram classifiers, namely, the vertical histogram and the horizontal histograms based on human silhouette projected horizontally and vertically were investigated. The joint frequency distribution of features along the horizontal and vertical span of several candidate windows were analysed. The histogram classifiers proposed takes into account the joint spatial distribution of features to predict the approximate location of the centroid of the human in the window. To combine multiple feature histograms, the class conditional probability is modelled as the product of histogram of features occurring at a given location within the candidate window. The human and the non human class models are obtained through supervised learning approach via histogram density estimation. The probability mass function of a class (human or non human) feature is defined by equation 6.1.

$$\text{Model\_PDF}(F_i, X0) = \left(\sum_{j=1}^{\text{NoObjects}} \sum_{i=1}^{\text{Length1}} \Delta F_{j,i}\right) / (\text{Length1} * \text{NoObjects}) \qquad 6.1.$$

$\Delta F_{j,i}$ denotes frequency of occurrence of feature F_i in candidate window j. X0 denotes the distance from the left hand corner (top left corner) of a candidate human. X0 takes on the values between one and the span (width) of the histogram. NoObjects denotes number of training samples, i.e, samples of windows with humans or non human used. Length1 denotes the length of the candidate human window and is the same as the span of the histogram (vertical or horizontal). F_i takes on a patterns [A,B,C,D,I,J] or [A,B,C,D] (from figure 5.3) depending on whether the subband is HLLH or LL subband respectively. The model is derived by training several candidate windows with humans centred, and examples without humans respectively for the positive and negative histogram. Given any window centred at position (x,y) in the feature map the human and non humans features are modelled by equation 6.1. The distribution of all the features occurring at a particular location in a candidate human is modelled as the vector of probability mass functions defined by equation 6.2 assuming feature independence. It is described in vector notation as $[V_0,V_1,V_2, \ldots V_{length1-1}]$, where V_i is k-element column vector where k is either 4 or 6 depending on the subband being used.

$$PDF(*, X_c) = \bigcup_{i=1}^{4(6)} [\sum_{X0=1}^{Length1} PDF(F_i, X0)] \qquad 6.2.$$

$\bigcup$ denotes the union, X_c denotes the centre of the candidate human window, and * denotes all the primitive features. Thus four or six projected histograms are constructed as a representation for a human depending on whether four or six features are used. Equation 6.2 captures the distribution of all features occurring in a candidate window. It is used to model the maximum likelihood of the candidate human turning out to be a human or non human using the similarity measure (defined below). Finding the best match between a candidate human and one of the two models (human and non human class) is interpreted as a sliding window comparisons based on the model histograms captured using equation 6.2 along the candidate human window region. The position of maximum similarity between the model histogram and the candidate histogram (which corresponds to minimum similarity measure as defined below) corresponds to the centroid of candidate human. The similarity measure proposed is

based on city block metric and related to histogram intersection method [Swain and Ballard 1991]. It is defined as:

$$Sim(model\_class)=\prod(Model\_Class(x)-Candidate\_Class(x))^2/(2*Width) \quad 6.3.$$

X takes on the values between 1 and length1. It is computed for both the human and non human model. The square operation magnifies the differences. The $\prod$ operation takes on values between one and four or six depending on whether the subband is LL or HLLH. The similarity measure is computed per feature and can be interpreted as the difference between a model histogram Equation 6.3 essentially computes on a bin by bin basis the distortion between the model histogram and the candidate histogram for every feature, and evaluates the element wise product for all the features. The result is a vector of joint feature probabilties. A decision is made to assign the candidate human to the human class if equation 6.4 is true. It sums up the contribution from each of the features.

$$\sum Sim(NonHuman\_Mark)>=\sum Sim(Human\_class) \quad 6.4.$$

The summation is over all the feature set (four or six depending on the subband in use). The closer the candidate histogram is to the model histogram the smaller is the city block metric (equation 6.3).

Training: The two classifiers were trained using the holdout approach with bootstrapping. The training set consisted of 4904 samples (1248+2690+966). During training any sample which was misclassified was added to the new training set, and the classifier retrained. This was repeated for until the detection rate is more than 80%.

6.2.2 Validation and Testing of Histogram Based Classifier

The algorithmic steps for the validation and testing of the histogram based classifiers is outlined in figure 6.1. First the data set is split into validation set and the evaluation set.

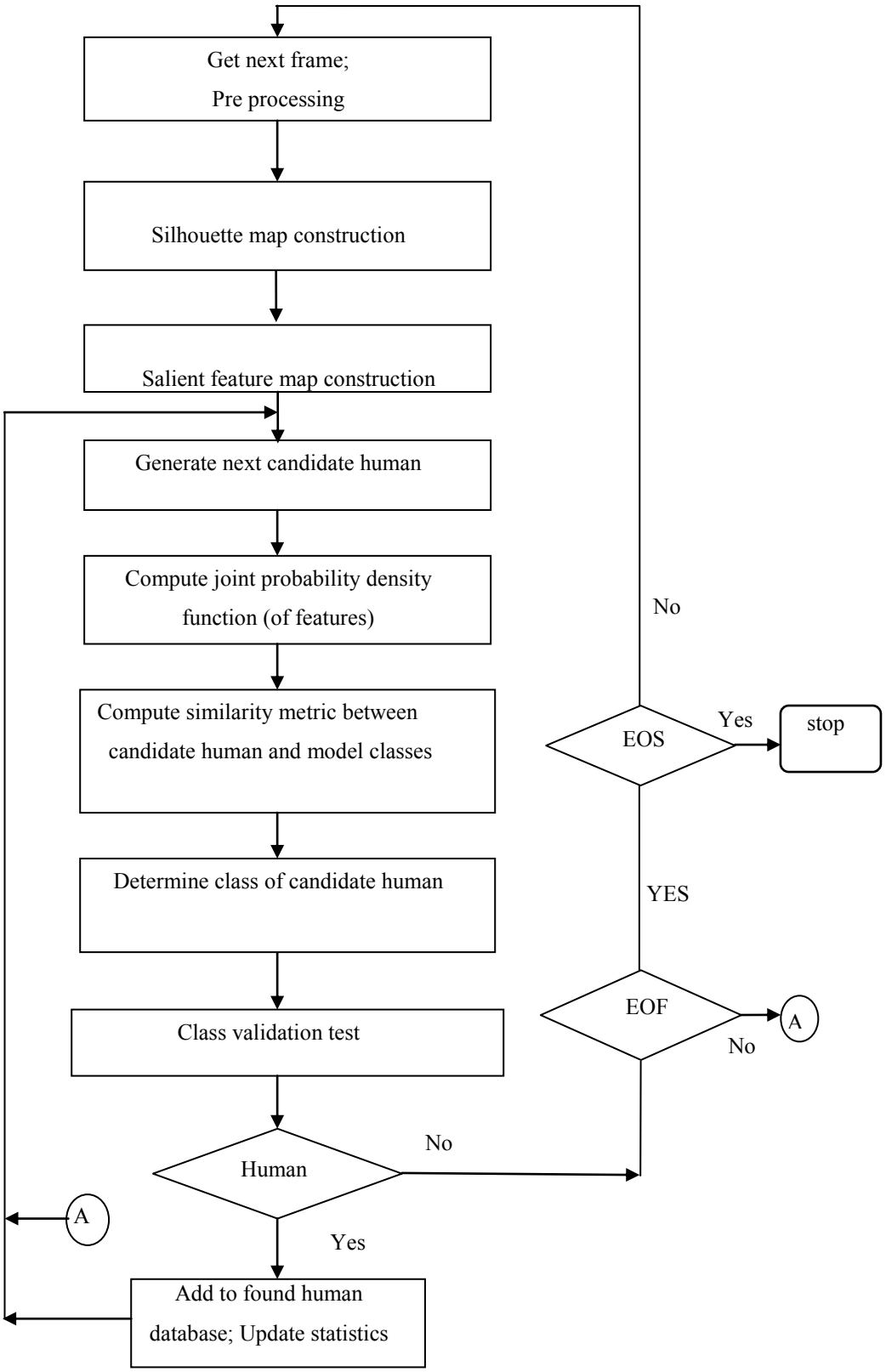

Figure 6.1 Flowchart for validation and testing of histogram based human classifier. EOF and EOS denotes end of frame and end of sequence processing

The pre processing step applies median filtering, and illumination normalization to the incoming frames. The next step applies either level one or level two wavelet transform depending on whether there is significant scale changes in the scene. Square wavelet features are constructed from the displaced frame difference of the LL subband or the HLLH subband. Saliency based thresholding are applied to the resulting feature map (foreground object map) to reject non salient features. The resulting salient feature map is used to locate salient regions as candidate humans. Candidate human localization starts with the construction of salient feature map and ends with the generation of candidate humans (candidate window). Following candidate human construction, frequency analysis of the wavelet feature histogram is generated as described in section 6.2.1. Similarity measures are computed between the histogram of the candidate human and the model histograms. Due to the fact that the classifier is not linearly separable, validation of class assignment is confirmed by area and size test. This entailed evaluating the area occupied by the human, and its dimension. Only candidate humans which additionally pass the two tests were confirmed as containing humans, otherwise rejected.

Next, the two underlying assumptions of the classifiers are verified. The first assumption is verified by one way Anova test on the probability mass function and the similarity measures, assuming independence of horizontal and vertical features. This is shown in table 6.2. The low probability of F (0) at 95% confidence level validates this assumption. The high mean squared error for horizontal histogram classifier (5.34432e+009) and the vertical histogram classifier (8.65613e+007) indeed confirms that the positive and negative classes indeed belong to a different population. The second modelling assumption is verified by principal component analysis. The output from the wavelet classifier includes the location of the centre (centroid) of the found human in the candidate human window based on this assumption. The centre of the found human in the candidate human window (32*64 dimension) relative to the frame is obtained by adding an address offset. The result of the analysis is shown in table 6.3 which analysis the location output by the classifier by principal component analysis (PCA) separately, and similarly to the approximate centroid defined manually in the ground truth based. The table list only the first component which accounts for the smallest variance. It is noted from the table that least variation occurs in the centroid location (X,Y), in the following order: vertical features, diagonal plus, and white

features, and so no with the least being horizontal features. Vertical features are used in the horizontal histogram, whilst horizontal features are used in the vertical histogram.

Table 6.2 One way Anova for test of significance between horizontal and vertical similarity measures

Function	**Degree of Freedom**	**Mean Square Error**	**F Statistic**	**Probability of F**
Probability mass function	4154 (H)	1.20712e-009	4.07	0
	4764(V)	0.002	125.5	0
Similarity measure	4764 (H)	5.34432e+009	31.65	0
	4154 (V)	8.65613e+007	3.35	0

Table 6.3 Maximum offset from the centre of the window for (X) horizontal histogram and (Y) vertical histogram based on based on principal component analysis

Feature	**Ground Truth (First PCA component of location)**		**Classifier (First PCA component of location)**	
	X	Y	X	Y
Vertical	15.5	20.30	16.5	21.02
Horizontal	16.5	32.50	21.65	22.07
Diagonal Plus	18.78	32.50	18.78	28.30
Diagonal Minus	17.38	32.11	22.09	22.97
Black	16.5	20.65	16.5	17.28
White	16.5	20.67	16.5	21.28

Note the assumption implies that you would expect half the histogram span to be the approximate centroid, namely 16 (span is 32) for horizontal histogram, and 32 (span is

64) for the vertical histogram assuming the human is located at the centre. This is not exact since the centre is manually labelled in the ground truth, and in practice the constructed candidate human may not have the human aligned exactly to the centre. Thus using the horizontal histogram (vertical features) gives the average position of the centroid based on the ground truth label along the x-and y-axes as (15.5, 20.3) compared to (16.5, 21.02) predicted by the classifier. Similarly, using the vertical histogram (use horizontal features) gives the average position of the centroid based on the ground truth label along the x-and y-axes as (16.5, 32.5) compared to (21.65, 22.07) predicted by the classifier. Additionally it was observed that the classifier responds more to vertical features (use in the horizontal histogram) than horizontal features.

The histogram model is further verified by a stacked plot of the similarity measures for human class and non human class as shown in figure 6.2 based on the horizontal histogram classifier. The similarity measure is based on city block (Manhattan distance) [Fabri et al. 2008] measure. The similarity block measure from the graph appears to be constant. This is attributed to the fact that only one person is in the video segment for which the measurements were taken. One way Anova result of the city block distance is shown in table 6.4.

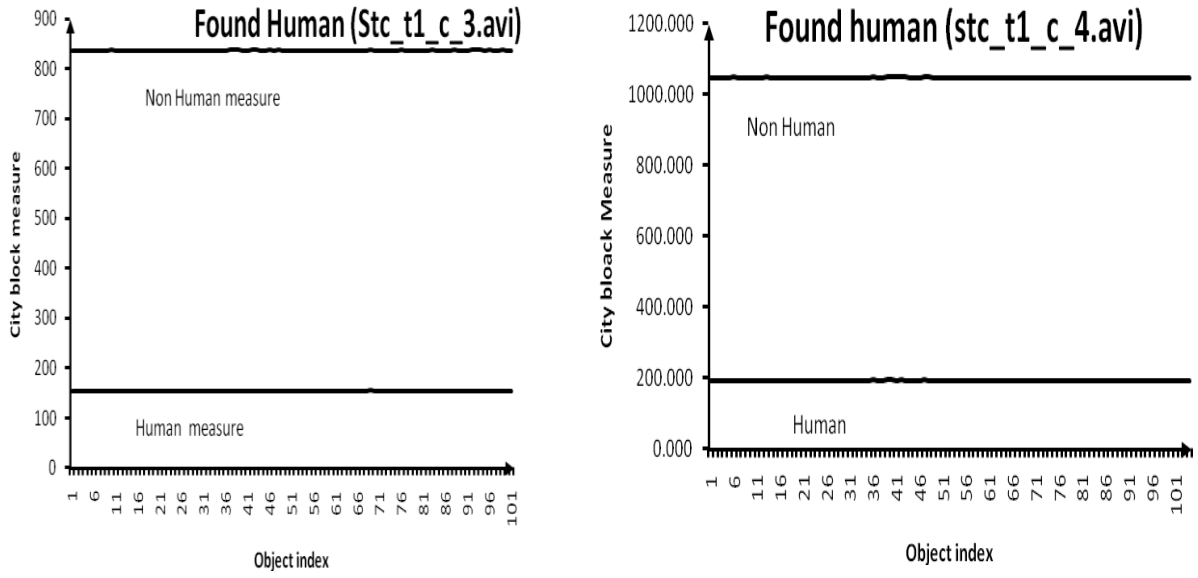

Figure 6.2 Plot of city block measure for histogram-based classifier (a) video sequence Stc_t1_c_3.avi (b) sequence Stc_t1_c_4.avi

The label H denotes features extracted from the horizontal histogram, whilst V indicates features extracted from the vertical histogram. The high mean squared error (3.3942e+21) between the similarity measures for the vertical and horizontal similarity measure suggest that the horizontal and the vertical measure can not belong to the same population. The Low value of the Probability of F at 95% confidence level also confirms that there is a significant difference between the human class and the non human class. Finally, table 6.5 shows the confusion matrix for one of the test sequence.

Table 6.4 One way Anova table for similarity metric for horizontal histogram between the human and non human class for stc_t1_c_3.avi sequence

Source	**Mean Squared Error**	**Degree of Freedom**	**F Statistics**	**Prob> F**
Human/Non Human	3.3942e+21	1	15.72	8.397e-05
Error	1.101e+23	510	-	-

Table 6.5 Post training evaluation of Test1.avi sequence (Level 2 decomposition)

Category		**Predicted**	
Actual		Human	Non Human
Human	192	177	15
Non human	170	24	146

6.3 Shape-Outline Based Classifier Specification and Implementation

Whereas the basic primitive features in wavelet-based histogram is a square block of dimension two by two pixels, the basic feature of the shape based classifier is an edge since the shape-outline map is binary. Two main problems confronts this approach, namely, noise, and changes in human outline. To be able to detect humans in more

complex poses, detection by parts such as the head, upper body, lower body, and then synthesis into whole human outline may be required. Another approach is view based supervised learning approach provides a solution at the expense of increased algorithmic complexity. Apparent shape derived from a shape-outline map is used as a shape descriptor on account of its reduced computational cost and simplicity. Other shape-based representation investigated included polynomial, Fourier transform based representation, and continuous shape descriptors. They were not pursued further since the performance gain in terms of accuracy and computational time compared to the shape-outline based approach was smaller and higher respectively. Shape based representation in Fourier space has been studied in [Dengsheng and Lu 2001], in wavelet space in [Shen and Ip 1999], [Oren et al. 1997], and in spatial domain in [Berg and Malik 2005], [Lakshmiratan et al. 2000]. Silhouette-based detection has been studied in wavelet domain and in spatial domain however with noisy inputs the detector may suffer degradation in performance and this led to a search for a technique which is tolerant to noise, and led to neural network based pattern predictor for human shape description. The approach is similar to shape-based detectors which use matching metric such as Hausdorf distance [Huttenlocher et al. 1993].

Thus instead of using the shapes of candidate humans directly, a feed forward neural network is trained to learn the complete or partial shapes of humans in upright posture in order to predict a human shape. The input to the classifier (candidate human), typically contain noise in the form of spurious edges and shapes. The shape prediction approach avoids other problems in the spatial domains such as variation in prototype shape, shadows, illumination and changes. In fact no prior assumption is made about the scene complexity and composition. It thus provides a means of removing spurious edges and shapes. From the noisy out of the predictor, two candidate human windows are generated, one for the human class and the other for the non human class. Correspondingly, two hypotheses are generated from the predictor's output, one for the human class and the other from the non human class. A mismatch measure is used to assign the output of the predictor to the most likely class. It penalises mismatched points on predicted output. The measure validates one of the hypotheses, namely, that the current candidate human window belongs to the human class or non human class. The sequence of steps which constitutes human detection are pre processing, foreground shape-outline map creation, candidate human

localization, candidate human window prediction, hypothesis generation, hypothesis validation, class label assignment, and post processing.

6.3.1 Feed Forward Neural Network Pattern Predictor Design and Training

The feed forward neural network classifier is shown in figure 6.3. Given an input pattern it predicts an output pattern. A feed forward (FF) network has four main properties, namely, the network connections, network transfer function, weights, and bias. The network connection describes how the input to a layer is connected to the neurons of the next layer. The network transfer function defines the how the network signals are propagated from one layer to another.

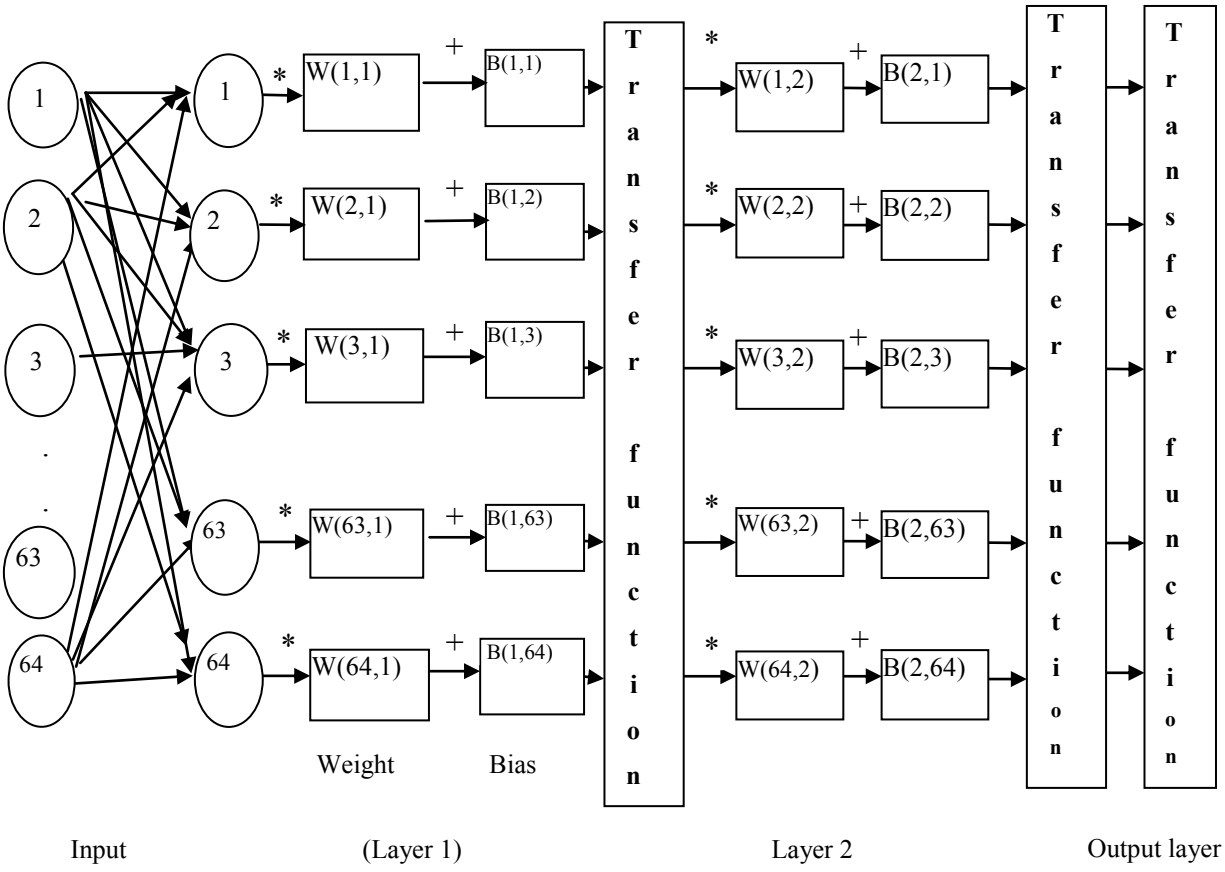

Figure 6.3 A 3-Layer feed forward multilayer perceptron network for pattern prediction

The weight determines the effects of the inputs on the signal propagated, and the bias is added to the weighted inputs to determine the net amount of signal available for propagation into the next layer. The proposed FF network is a 64-element input layer with a fully interconnected 3-layer neural network. It has one hidden layer and a 64-element output layer. The input to the network is a 2-D binary pattern. Figure 6.4 illustrates the propagation of a binary column vector of 64 elements which is feed to the network at one time step. The net weight of a neuron (k) at the layer (L) is made up of contributions from all the inputs to the layer (defined by $I_{m,L-1}$), and is given by the expression 6.5.

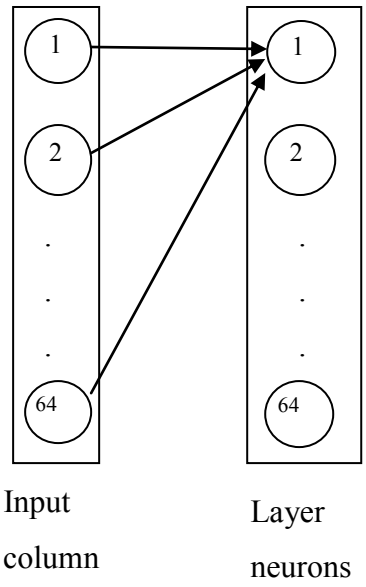

Figure 6.4 Propagation of data (signals) from one layer to the next layer in a FF network.

$$W_{k,L} = W_{1,L,k} + W_{2,L,k} + + W_{3,L,k} \ldots + W_{M,L,k} \qquad 6.5.$$

k takes on the value between one and sixty-four (M) in the current network (there are sixty-four neurons in each layer). Thus the net weight for a neuron in a layer can be expressed as a row vector, and for all the neurons in the layer as a weight matrix. The current network has a 64 by 64 weight matrix, with neuron k's signals given as the scalar product of the input and the weight vector for k (row k) of the matrix. $B_{k,L}$ is

the bias element which is added to neuron k's signal. The signals for all the neurons I the layer is given by equation 6.6.

$$Y = \begin{bmatrix} W_{1,1,1} & W_{1,2,1} & W_{1,3,1} & \cdots W_{1,64,1} \\ W_{2,1,2} & W_{2,2,2} & W_{2,3,2} \cdots & \cdots W_{2,64,2} \\ W_{3,1,3} & W_{3,2,3} & W_{3,3,3} & \cdots W_{3,64,3} \\ \cdots & \cdots & \cdots & \cdots \\ W_{64,1,64} & W_{64,2,64} & W_{64,3,64} & \cdots W_{64,64,64} \end{bmatrix} * \begin{bmatrix} I_{1,L-1} \\ I_{2,L-1} \\ I_{3,L-1} \\ \vdots \\ I_{64,L-1} \end{bmatrix} + \begin{bmatrix} B_{1,L} \\ B_{2,L} \\ B_{3,L} \\ \vdots \\ B_{64,L} \end{bmatrix} \quad 6.6.$$

Finally the transfer function is applied to Y to propagate the signal to the next layer as expressed in equation 6.7.

Signal_out(L)= Transfer function(Y) 6.7.

Signal_out is a column vector with 64 elements. Signal_out (L) becomes the input to layer L+1, and the procedure is repeated at the subsequent layers until it comes out as output. In the current network layer one implements the logsig (logarithm to base two of the sigmoid function), layer two (hidden layer) implements tansig (tangent of sigmoid function) transfer function, and the layer three (output layer) a linear transfer function respectively. During one training period, 32 input vectors (each consist of 64-element input) are fed to the network. The training is performed in batch mode with the training epoch defined as multiples of 64 X 32. Additionally a target vector defining the desired output for the input vector is input as one of the parameters. For positive examples candidate window pixels with binary value of has a desired (target) value of one, whilst with the negative examples binary value it has a desired value minus one. This ensures that an output pattern of less than zero is assigned to the negative class, whilst values greater than zero is assigned to the human class. Output values of zero are ignored. The predictor is designed with the expectation that if the desired output pattern is the same as the input pattern then the prediction is optimum. Each time the output of the predictor (either positive or negative) becomes available, two intermediate patterns are derived from this output. A mismatch measure is computed using equation 6.8 is for each class assignment. The mismatch metric seeks to assign more scores to matched input-output bit pair, and penalize mismatch points.

Penalty(Class)=ExactMatch_Class(Class)/Miss_Match_Class(Class)) 6.8.

ExactMatch_Class(class) denotes sum of locations with exact match, following comparisons between the input pattern and the two derived patterns. The comparison is between the output pattern from the neural network and the intermediate pattern. The comparison returns a binary value where both patterns have binary value of one, otherwise zero. The Miss_Match_Class (class) thus scores the mismatch between the input pattern and the derived pattern. The class of the candidate is determined as the class with the smallest mismatch measure. With equation 5.9, a similarity measure is computed between the input candidate human and the intermediate human class and the non human class.

Similarity (class)= Penalty_Class(class)/
[Penalty_Class(Human class)+Penalty_Class (Non human class)] 6.9.

With the similarity measure approach, a human is detected if similarity (Human class)>Similarity (Non human class).

Training: The training strategy adopted was hold one out estimate with bootstrapping using the data set of shown in table 6.6. Two training regimes were carried out using Matlab neural network toolbox, one for the human class, and the other for the non human class. Candidate humans were extracted from foreground shape_outline maps of the three video sequences with humans approximately located at the centre of the window. At each run, the training period was increased whilst reducing the mean square error criteria until it gets to 10^{-7}.

Table 6.6 Video sequence used in training the shape-outline map pattern predictor

Extracted candidate human sequence	**Positive set**	**Negative set**
Combinetrainsequence1.avi	620	180
Hamilton.avi	630	170
Testdata.avi	480	200

6.3.2 Validation and Testing of Shape-Outline Based Human Classifier

The task flow for the validation and testing of the shape-outline classifier is shown in figure 6.5. The input to the pre processing step is the current frame. Applied pre processing functions include histogram equalization and median filtering. There are

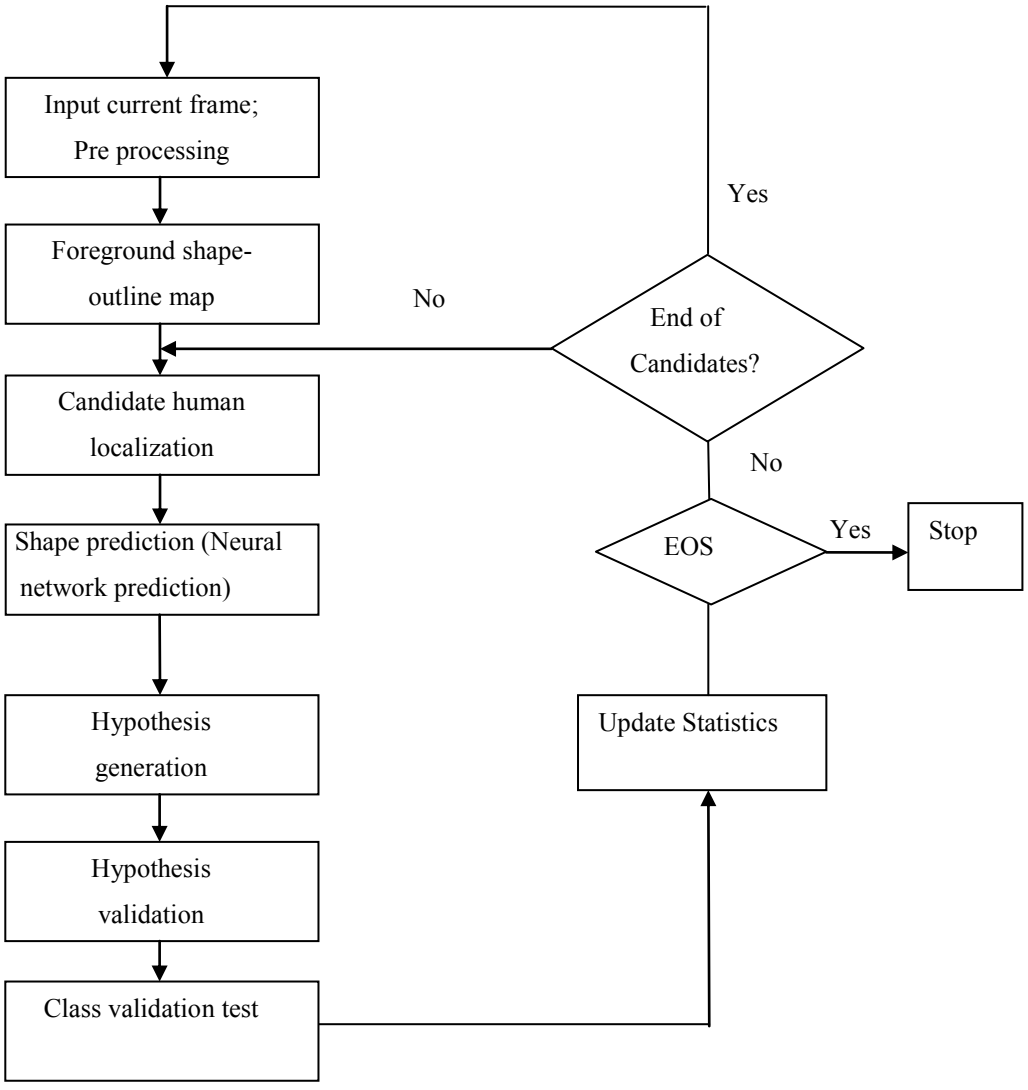

Figure 6.5 Flowchart for validation and testing of human outline based classifier. EOS denotes end of sequence.

several approaches to creating foreground shape-outline map, including subtraction of two consecutive outline maps (absolute frame differencing), with background memory

(uses outline map memory with background update). From the foreground shape-outline map salient candidate human locations were identified for the construction of candidate human. Edge saliency (frame activity) measure was used locating salient regions. Candidate human localization thus starts with the construction of the salient foreground shape-outline map and ends with the construction of candidate humans. They were then fed unto the feed forward pattern predictor. From the output pattern predicted the two hypotheses are generated. Validation step then assigns the candidate human to either the human class or the non human class. Two validation tests were used, one based on linear discriminant test using the similarity measures, and the other test, the area and size test are similar to that used in the wavelet based classifier to improve classification accuracy. This was repeated whenever there was a misclassification until the detection rate was above 80%. Figure 6.6 is a graph of mismatch metric for human (positive) class and non human (negative) class for the first two hundred frames. Clearly the two classes are separable using the magnitude of the metric. The result of the one way Anova test between the human class and the non human class is shown in table 6.7.

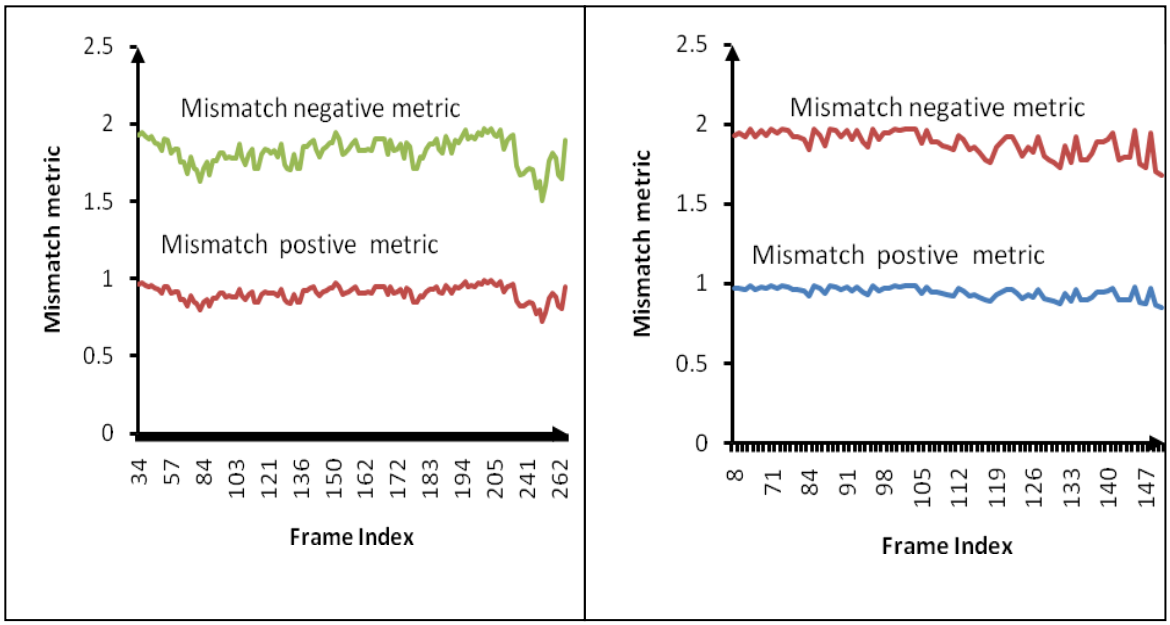

1 2

Figure 6.6 Plot of scaled (*10000) shape mismatch metric: (1) Stc_t1_c3.avi and (2) Stc_t1_c_4.avi

The Anova tests were evaluated at 95% confidence interval. The high mean squared error value (5.54776e+009) invalidates the null hypothesis which considers both the human and non human class as from the same population, suggesting strongly that it cannot be true. The value of the F statistics is zero hence the hypothesis that they are from the same population is rejected. Clearly there is a significant difference between the human class and the non human class.

Table 6.7 One way Anova table for shape mismatch metric between the human and non human class

Source	**Mean squared error**	**Degree of freedom**	**F statistics**	**Prob> F**
Human/Non Human	5.54776e+009	1	10.3.56	0
Error	2.7348e+009	510	-	-

6.4 Results

The two proposed classifier types have been specified, designed and validated, and tested. Of the ten initial candidate primitive wavelet features set investigated, the HLLH subband use only six features, whilst the LL subband use four features to discriminate the human from the non human class. Features that were eliminated showed the same characteristics between the human class and non human class or were not present in most of the training samples. It was also observed that the sensitivity of primitive features responds mostly to diagonal edges, followed by vertical edges and finally horizontal edges. The problem of high false detections was also observed. One reason was due to the high number of candidate windows which were examined. The problem of high human density in the scene was also observed to limit detection rate of hamilton2b.avi, despite the fact that the scene was well lit. It is thus clear that scene clutter, poor illumination, and human density still affect detection capabilities of the proposed classifier. A validation set incorporating heuristics was thus added to the discrimination stage to improve classification accuracy. The shape-outline based classifier adequately detects humans when it has dimension comparable

to most objects in its surroundings. With the histogram classifier an important parameter which determines the accuracy is the choice of level for wavelet decomposition which would result in subbands with humans appearing significant in its surroundings. The choice of the level is between one and three. The current implementation used a detection threshold of 80% during training as adequate. This proved a limiting factor in accuracy evaluations in stc_t1_c_4.avi sequence with multiple humans and pixel saturation. To improve detection rate and reduce false positive rate more training is required until the detection rate exceeds 90%, and false alarms falls to less than 40% of the number of windows examined by the classifier. The computational loads of the two classifiers are detailed out in table 6.8 and 6.9 assuming floating point operations requires 2 units of basic operations.

Table 6.8 Approximate computational load given candidate human of dimension (M X N) for the shape-outline based classifier

Function	**Number of operations**
Pattern prediction	(Matrix-Matrix multiply+Matrix-Matrix add)* 3
Pattern generation	(Matrix-Scalar subtraction) *2
Mismatch measure	[Sum(Matrix-Matrix subtraction)+sum(Matrix-Matrix subtraction + (divide)]*2
Comparison	1

Table 6.9 Approximate number of operations for histogram based classifier using candidate human window of the same dimension

Function	**Number of operations**
Candidate human model	(Vector-Vector Subtraction) Scalar division (Normalization and scaling product) +Vector-Vector multiply (square operation)
Similarity measure	2*(Sum (absolute value operation |Vector-Vector subtraction)|))
Comparison	2

6.5 Interpretation

This chapter has presented three pattern classifiers, one in the shape space, and two in the scale-frequency space. Each pattern classifier has been implemented and evaluated. The wavelet domain classifiers model the silhouette of a human as multiple feature histograms. The joint distribution of the features is modelled as product of histogram similarity. The similarity measure is based on city block like function. Detailed statistical analysis validating the modelling assumptions and predicted centre of the candidate human window has also been presented. When only horizontal histogram (uses only vertical features) classifier is used in background and edge saliency localization scheme, the accuracy level was higher than motion and edge saliency mode. This suggest that vertical features are more important in human detection. The shape space classifier first predicts an output pattern given an input pattern. From the output pattern two intermediate patterns are generated in support of a hypothesis for existence of human, and the null hypothesis, i.e, the existence of non human class. A shape mismatch measure is defined which penalises for unmatched points on the shape-outline map window. The shape based classifier predicts fairly very well with both complete and partial object outline whenever the candidate human outline map has dense number of points in the window than when it has sparse number

of points. For video sequence with large scale changes (changes in resolution of object), level one or two wavelet (histogram) classifier achieves higher detection rate, and low false positives. For sequence with little scale changes, shape-outline based classifier achieve high detection rate and relatively low false positives at moderate computational cost. Combining the two classifiers result in both an increase in detection and false positive rates at a higher computational cost.

The computational complexity of the classifier could be improved if candidate human window resizing is avoided. One approach is to design multiple classifiers to detect body parts such as the head, upper body and lower body. The current implementation is trained on the global shape and does not detect by part. Although the proposed classifiers achieve high detection rate it also has high false detections which is a problem in most visual surveillance application.

CHAPTER SEVEN

INVESTIGATIONS INTO HUMAN DETECTION

7.1 Introduction

Whereas the outputs of the previous two chapters relate to objectives one, two and four in human detection, namely feature extraction, candidate human localization, and classification. The focus of the current chapter is on proposed algorithmic task for human detection, accuracy evaluation, task profiling, and algorithmic configuration options for human detection. The task flow for human detection is a synthesis of sub tasks involving pre processing, feature extraction, candidate human localization, discrimination (classification), and update of found human database. Detailed block diagram of the algorithm is shown in appendix B. From the extracted features in the pattern space an efficient search mechanism is required to generate candidate humans before discrimination. This functionality is provided by the search strategies in the pattern spaces using salient feature maps. Section 7.2 discusses wavelet domain search strategies for candidate human localization. Section 7.3 discusses human discrimination in the wavelet domain whilst section 7.4 describes the overall task flow for wavelet based detection of humans. Section 7.5 discusses shape-outline based search strategies for candidate human localization, whilst section 7.6 describes shape-outline based human discrimination. Section 7.7 describes the overall task flow for shape-outline based human detection. Section 7.8 presents the synthesised algorithmic architecture for human detection, whilst section 7.9 discuses simulations, accuracy evaluations, and profiling of human detection tasks. Section 7.10 presents the results. Section 7.11 discusses the results, trends on accuracy, and task profiling analysis.

7.2 Wavelet Domain Search Strategies

The computational load of human detection depends on the effort required in locating candidate regions for subsequent processing. An efficient search strategy is required to reduce the number of locations required to identify all candidate humans. For example if the expected size of the candidate window is 64 pixels high by 32 pixels wide given an input frame of 480 pixels high by 640 pixels wide then an exhaustive search requires 52928 (416*608) blocks to locate all instances of human assuming there is overlap. Inefficient search strategy adds extra processing time, and hence increases response time. The three search strategies investigated in the current study are essentially attention drawing mechanisms in feature space, namely, motion saliency, edge saliency, and background saliency. Motion saliency applies threshold to frame difference or foreground frames to remove insignificant motion. It is essentially a feature rejection step. Edge saliency estimates significance of a region based on edge count after eliminating spurious edges. Background saliency applies threshold to the difference between LL subband and an accumulated background memory. The assumption is that foreground objects becomes part of the background frame after some time. Hence the need to examine background blobs. Saliency is estimated by applying a global threshold to a subband frame, and grouping residual pixels (binary) into rectangular blocks, and estimating the pixel activity in these blocks. It is parameterised as a threshold expressed as a fraction of the brightest pixel in the frame. In the case of edge and motion saliency it is followed by grouping the residual frame into blocks and estimating the pixel density in the blocks. With background saliency connected components (blobs) are located in the background memory as candidates instead. It is justified since on visual inspection of wavelet subbands of humans and other moving objects' in a frame have silhouettes which appear brighter than the background. The threshold fraction is typically between 0.1 and 0.9. It defines the fraction of the maximum pixel intensity which is due to salient motion or edges of significant objects in the scene. The use of candidate human localization techniques is justified since edges or high frequency components of images are found in HH, HL and LH subbands, whilst the LL subband contains low frequency component (low pass image) at a given level of wavelet decomposition or the low pass version of the frame. Low pass version is appropriate for describing global motion. In the saliency

based scheme candidate humans are generated by defining rectangular regions centred around salient feature locations. The three search strategies optionally use median filter to remove noise. Edge saliency approach provides good candidate humans with less computational effort than other saliency based searches. By defining the dimension of the blocks used in saliency searches to be the same as the candidate human, high activity blocks could be used directly as candidates.

7.3 Wavelet Domain Human Discrimination

Human discrimination involves candidate human classification using wavelet domain histogram classifier, and validation of the class. Two wavelet domain histograms (probability density estimator) are used to model the human and the non human class. The joint probability density function of the wavelet features has properties similar to the density functions of the individual feature primitives, in particular it is invariant to scale changes and translation. The property of the global probability histogram that resizing does not affect the distribution function is also invoked to arbitrarily compare an input window of any dimension. However to ensure a fixed number of computations the size of the global histogram is fixed at thirty-two pixels (span) for the horizontal histogram and sixty-four for the vertical histogram or sixteen and thirty-two respectively for the horizontal and vertical histograms. An input candidate window is resized to the dimension of the histogram. The dimension of candidate object windows is determined by the mean of the largest and smallest human dimension measured in pixels estimated directly from the video sequence. The validation step performs a threshold test based on the pixel count and area of the human silhouette in the candidate human. Validated candidate humans have pixel count and area above the count and area thresholds respectively.

7.4 Wavelet Domain Human Detection

Human detection tasks pipeline in the wavelet domain consists of five main parts, pre processing, feature extraction, salient feature localization (search strategy), human discrimination and post processing. The complete algorithm is shown in figure 7.1.

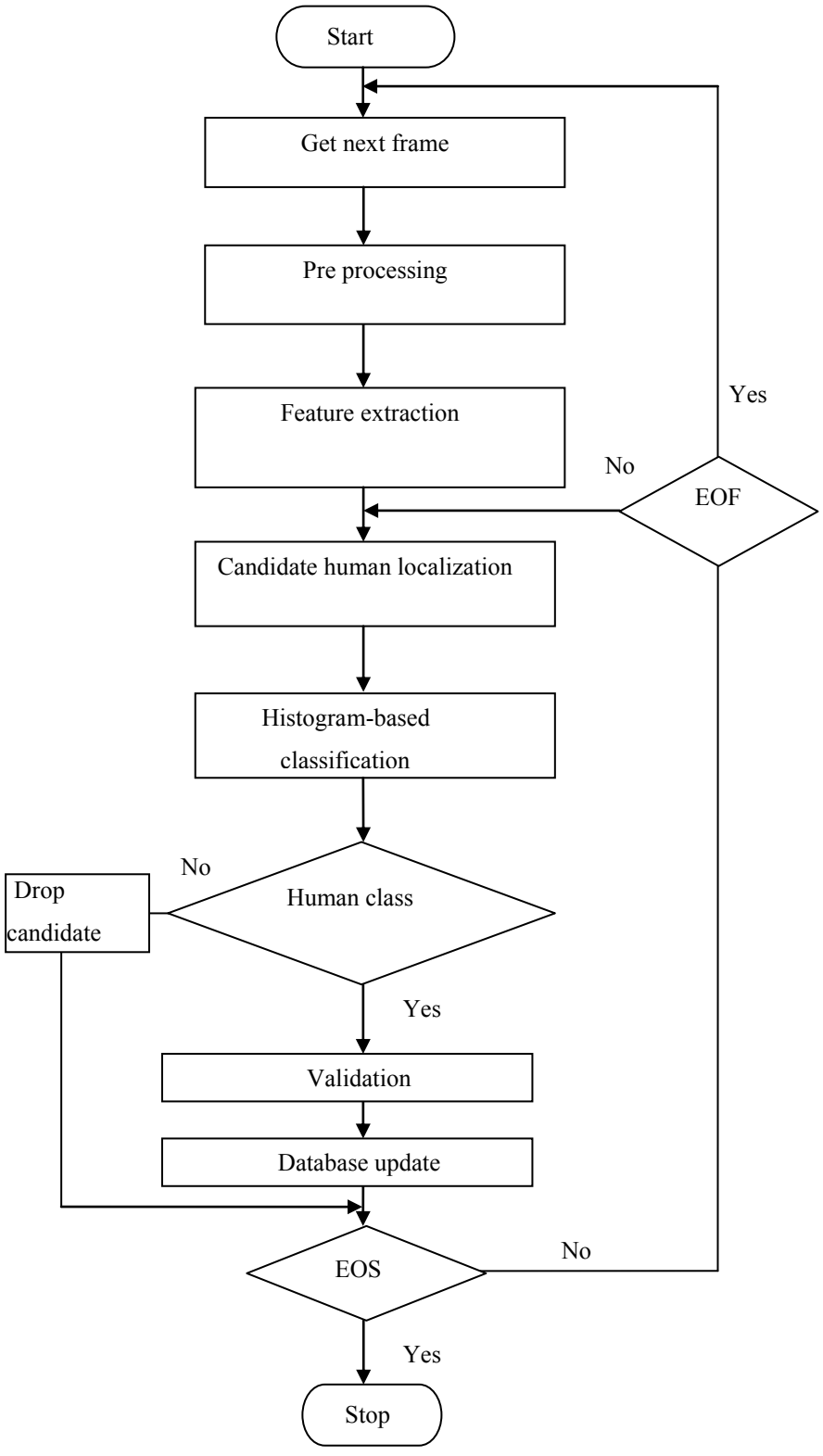

Figure 7.1 Flowchart for histogram-based human detection. EOS and EOF denote end of sequence and end of frame processing

The processing starts with the current frame being wavelet transformed into wavelet subbands (see section 5.2.1). The resulting subband is searched for candidate humans using saliency directed search mechanism (see section 5.3). Selected humans candidates are then passed on to the histogram based classifier. A similarity metric (city block like measure) is computed for the human class using the histogram model corresponding to the human class, whilst that of the non human class is computed using the non human histogram model. A decision is made using equation 6.8. Finally the validation step involves heuristics (pixel count and size test). It is only when the validation test is satisfied is the candidate human assigned to the human class.

7.5 Shape-Outline Based Search Strategy

Two salient feature localization techniques were investigated to reduce the number of salient features in order to efficiently locate candidate humans. The first one is based on edge saliency (using block activity measure). Given a shape-outline map the edge saliency approach partitions the frame into non overlapping blocks and computes the number of edges within each block. It then selects the centroids of blocks whose edge count exceeds a user defined threshold as candidates. This is described by a pseudo code below. Another edge saliency scheme selects candidate windows after suppressing multiple feature points and very small shape outlines within the block by applying median filtering. Morphological filters could also be applied alternatively. Motion saliency is similar to the edge saliency, the difference lies in how the map is obtained. Motion saliency is based on subtracting a previous shape-outline map or a fixed background map from the current shape-outline map. The main parameters of the edge saliency based searches are the minimum human separation distance along the X and Y-axis. The centroid is computed based on the first moment of the candidate window.

1. Construct shape-outline map for the current frame.
2. Find maximum pixel intensity of the current frame (Max).
3. Select saliency threshold ($0<\alpha<1$) as a fraction of the maximum intensity value.
4. Threshold current shape-outline map:

   For all pixels

Salient_shape_outline_map=Find (shape_outline map> (α *Max))

End

5. Output Salient_shape_outline_map.

7.6 Shape-Outline Based Human Discrimination

The processing steps for shape-outline based discrimination are similar to that of wavelet domain human discrimination in section 7.3. The difference is that it is based on the shape-outline classifier using shape mismatch measure instead of similarity measure to assign a class label (see section 6.3, and 6.3.1). Secondly, the validation step involves two tests. The first test involves using a linear discriminant function. The discriminant function (Discr) is given by equation 7.1, where Neg, and Pos denotes shape mismatch due to assigning to non human and human class respectively. It is only when the discriminant function returns the same class label as that of the histogram classifier is the next validation step executed. The last validation step essentially performs a threshold test on the pixel count and area of the human silhouette in the object window.

Discr (Neg,Pos)=4.014*Pos-5.54*Neg-1 7.1.

7.7 Shape-Outline Based Human Detection

Figure 7.2 shows the task flow for human detection. Detection task involves pre processing, feature extraction (foreground shape-outline map extraction), candidate human localization (via block activity measure), shape-outline prediction, generate hypotheses patterns, shape mismatch measure computations, human classification (assigns a class label to the current object window). Finally validation is based on either confidence measure, heuristics (pixel count threshold test, size test), or linear discriminant function evaluation. In the current implementation heuristics and linear discriminant function are used to validate the class assignment. It is only when the validation step is consistent with the human class is the candidate human detected. The bounding box is then used to describe the detected human.

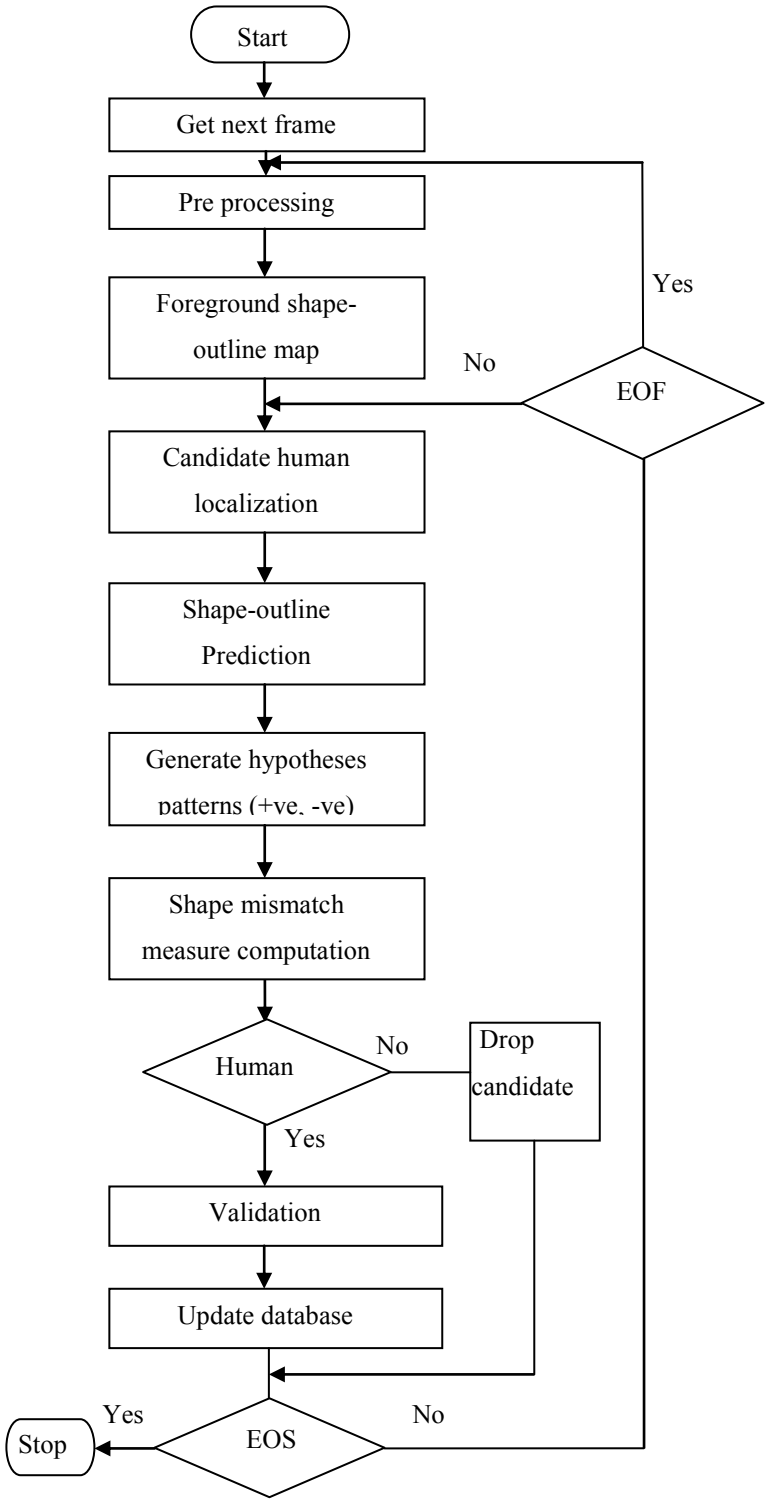

Figure 7.2 Flowchart of shape-outline map based human detection. EOF denotes end of frame processing, and EOS denotes end of sequence processing.

7.8 Synthesised Algorithmic Architecture for Human Detection

The proposed architecture seeks to combine the two approaches to complement each other in improving the detection rate. Figure 7.3 shows the architecture for the combined detector. The algorithm operates in three modes, namely, shape classifier only, histogram classifier only, and combined shape-histogram classifier. Shape and histogram classifier mode involves executing pipeline A and B respectively. The combined mode involves running pipelines A and B in parallel. When an object window is found by one of the classifiers, the other classifier does not probe candidate regions within a fixed distance from the found human.

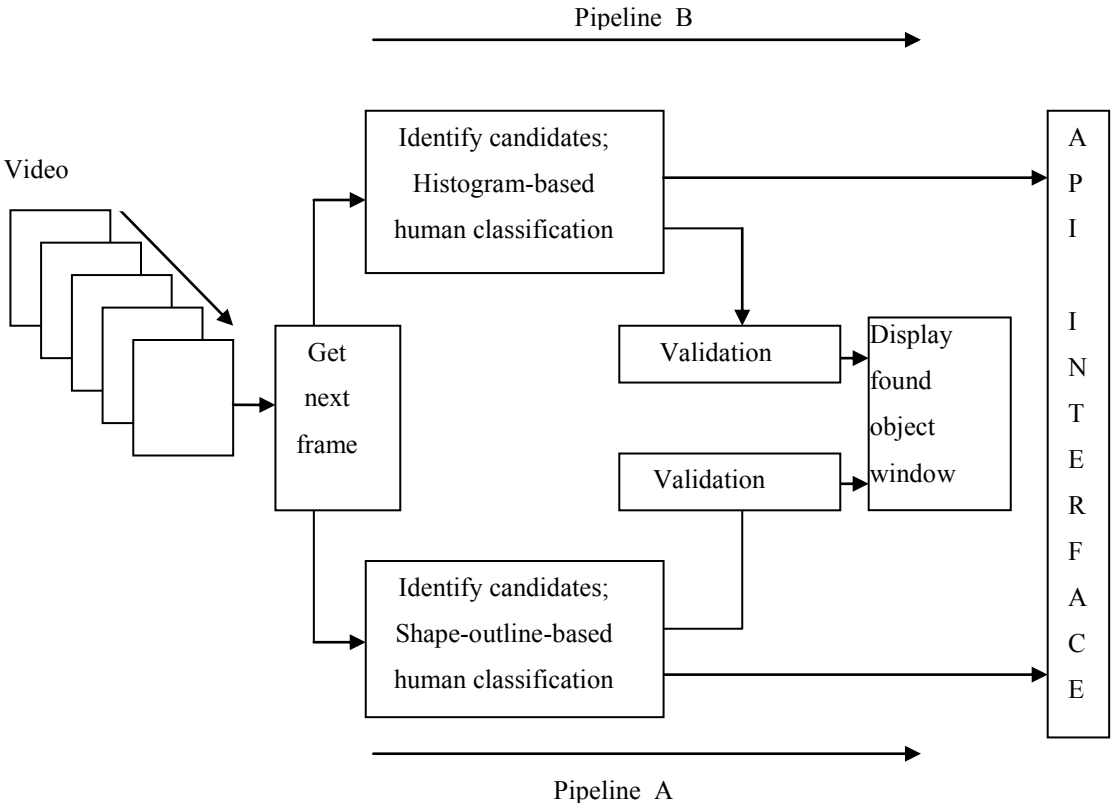

Figure 7.3 Combined algorithm for human detection

The net effect is that the overall detection rate is the contribution from the two distinct detectors.

7.9 Simulations

The proposed detection algorithms were implemented and evaluated in MATLAB running on 2.6 GHz Pentium IV dual-core processor with one gigabyte memory on Windows XP operating system. The evaluation of the algorithm is in two parts, namely, accuracy evaluations, and execution time analysis. Four dataset, three of which are video sequences were used in the evaluation. The fourth is PASCAL VOC 2010 challenge dataset. With PASCAL VOC 2010 the evaluation criteria is based on the prescribed procedure (see PASCAL VOC 2010 website). PASCAL VOC 2010 allows classifiers to be designed using in-house dataset, and PASCAL VOC 2010 provide data set. Simulations carried out under accuracy are classified into three main types, namely, a study of the effect of the main algorithmic parameters on accuracy of individual classifiers, combined classifiers, and the accuracy of the different search strategies. Three search strategies were used in evaluating the accuracy of the video sequences based on saliency mechanism, namely, edge saliency, motion saliency, and background saliency (LL subband).

In addition to the three video sequences (trainingsequence1.avi, hamilton.avi, and campus1.avi) used in training the classifiers, three video sequences were used in testing the classifier. Table 7.1 specify the parameters of the video sequences used for the evaluation of the proposed architecture. Two of the video sequences are part of PETS 2006 data, whilst the third was taken on Brunel university campus. Hamilton2_avi sequence frames were resized to half its original dimension, whilst the other two used the original frame dimension for accuracy evaluation.

Table 7.1 Parameters of the test video sequence

Test Sequence	**Width**	**Height**	**Number of Frames**
Hamilton2_avi	640	480	1000
STC_T1_C_3.avi	560	420	3012
STC_T1_C_4.avi	560	420	3012

For the wavelet domain histogram classifier, the accuracy of vertical and horizontal histogram were studied separately, and then in combination. The threshold values used in the saliency searches are all expressed as fraction based on the maximum wavelet coefficient in a frame. Nominal threshold used are [0.1, 0.2, 0.3, 0.4, 0.5, 0.6, 0.7, 0.8, 0.9, 0.95] of the maximum wavelet coefficient in a frame. Background memory flag enables two background modes to be tested, namely, frame differencing, and fixed background with update. Use_subband_Flag (see table 7.2) is set when decimated wavelet transform function is invoked, and was set off when non decimated wavelet transform is invoked. Tables 7.2 and 7.3 show the main parameters of the histogram classifier and shape based detector respectively. Discussions on the effect of algorithmic parameters are based on these tables. In studying the effects of algorithmic parameters on accuracy for the histogram based detector, maximum distance of separation in X and Y (from parameters 8 and 9 from table 7.2) were kept constant at half the candidate object window in X and Y (parameters 2 and 3 from table 7.2) respectively, i.e, found humans within half the dimension of object search window is classified as the same object to avoid duplication. The rest of the parameters were kept constant for a given sequence. As a guide the candidate human dimension was determined by estimating the width and height of human in the sequence. This required since the ground truth label only marks the approximate centroid of the candidate human, and the size of the humans varies from one frame to another. Thus candidate human dimension is required in order to bound a candidate to a region. Similar criteria were used in evaluating the shape-based detector. A classification scheme was also derived to characterise the sequence in terms of scene complexity and hence a measure of analysis complexity. Video scene complexity were classified as: slow motion, fast motion, significant scene changes, no scale changes, highly cluttered, and low contrast for the purpose of setting the algorithmic parameters for optimal operating accuracy. Profiling of the sub tasks and the proposed architecture were also evaluated to identify critical sub tasks in the task execution pipelines, throughput, and scalability of the proposed algorithm.

Table 7.2 Main algorithmic parameters for histogram based detector

Parameter	**Description**	**Maximum**	**Minimum**
Saliency_Type_Flag	Edge saliency, motion saliency, background saliency	1	3
Search_Window_Width	-	Variable	Variable
Search_Window_Height	-	Variable	Variable
Feature-Detection_Threshold	Edge saliency threshold	1	0
Motion_Detection _Threshold	Motion saliency threshold	1	0
Wavelet_Decomposition _Level	Decomposition level	3	1
Magnification factor	Magnification factor	3	0.125
Max_Separation_ distanceX	Distance between two humans(X) in database	variable	Variable
Max_Separation_ distanceY	Distance between two humans(Y) in database	Variable	Variable
Median Filter Flag	Median filtering	1	0
Use_subband_Flag	Decimated/ Undecimated	1	0
Background Memory Flag	Background memory /Frame difference	1	0
Dbase_SpacingX	Human width in pixels	Variable	-
Dbase_SpacingY	Human height in pixels		
MaxNoObjects	Maximum number of humans in a frame	Variable	-
Histogram_Equalization _Flag	Histogram equalization	Variable	-

Table 7.3 Main algorithmic parameters for shape-outline based detector

Parameter	**Description**	**Maximum**	**Minimum**
MaxNoObjects	Maximum number humans in a frame	Variable	-
Frame_Activity_Flag	Measure edge density in a region	1	0
Window_Width	Human search window width	Variable	-
Window_Height	Human search window height	Variable	-
Threshold1	Threshold for outline extraction	variable	variable
Maximum_Separation _distanceX	Distance between humans in database (X)	variable	variable
Maximum_Separation _distanceY	Distance between humans in database (Y)	variable	variable
Background Memory Flag	Background memory/Frame difference	1	0
Median Filter Flag	Median filtering	1	0
Background Memory Flag	Background memory/Frame difference	1	0
Dbase_SpacingX	Human width in pixels	Variable	-
Dbase_SpacingY	Human height in Pixels	Variable	-
Fixed_Background_Flag	Set to one if fixed background scheme is used in object outline map	1	0
Magnification factor	magnification factor searching for multiple humans in X	1	0.125

Table 7.4 is a summary of PASCAL VOC 2010 dataset used in training for human classification and detection tasks. The dataset is split into fifty percent for training and and fifty percent for testing. The other object class covers non humans (dogs, cat, TV, bicycle). The dataset for training is further split into two non overlapping set, one for training, and the other (validation set) for algorithmic parameter optimization. The total for training set is ten thousand and one hundred and three single shot images. A sliding window of dimension a factor of the frame (1, 0.5, 0.25, 0.125) were used in searching for candidates. The shape-outline based and the HLLH subband histogram classifiers were evaluated. Since the annotation for the test set has not been released, the result of the evaluation based on the validation set is presented. The validation set has five thousand and one hundred and three images.

Table 7.4 PASCAL VOC 2010 training set

Category	**Count**
Humans	3559
Other objects	8018

The sequence of processing steps are shown in figure 7.4 for HLLH subband based histogram classifier and detection system. Figure 7.5 shows the processing steps for the shape-outline based classifier and detection system. The silhouette and shape-outline map is constructed in the same manner as explained in chapter six. A mandatory median filtering step is applied before searching for candidates. The computation of similarity and mismatch measure remains unchanged. A new discriminant function had to be incorporated to separate the human for the background class since the existing discriminant rule for classification was not effective. The detection task start with blob analysis and classify each blob. The outcome is either a human is detected or not.

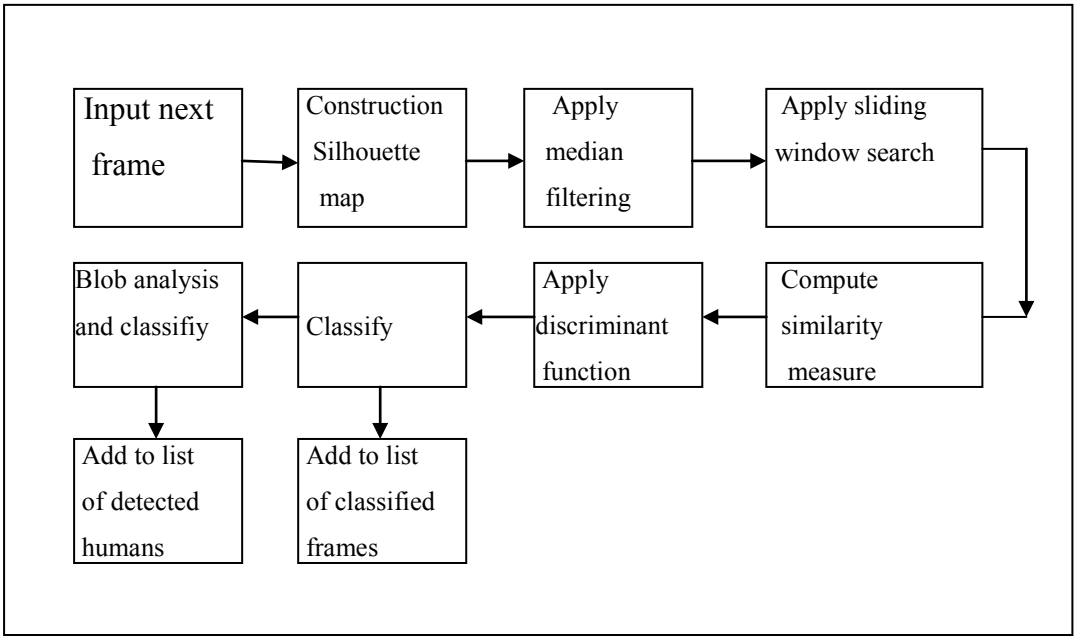

Figure 7.4 Block diagram for HLLH histogram based classification and detection of humans (PASCAL VOC 2010 challenge)

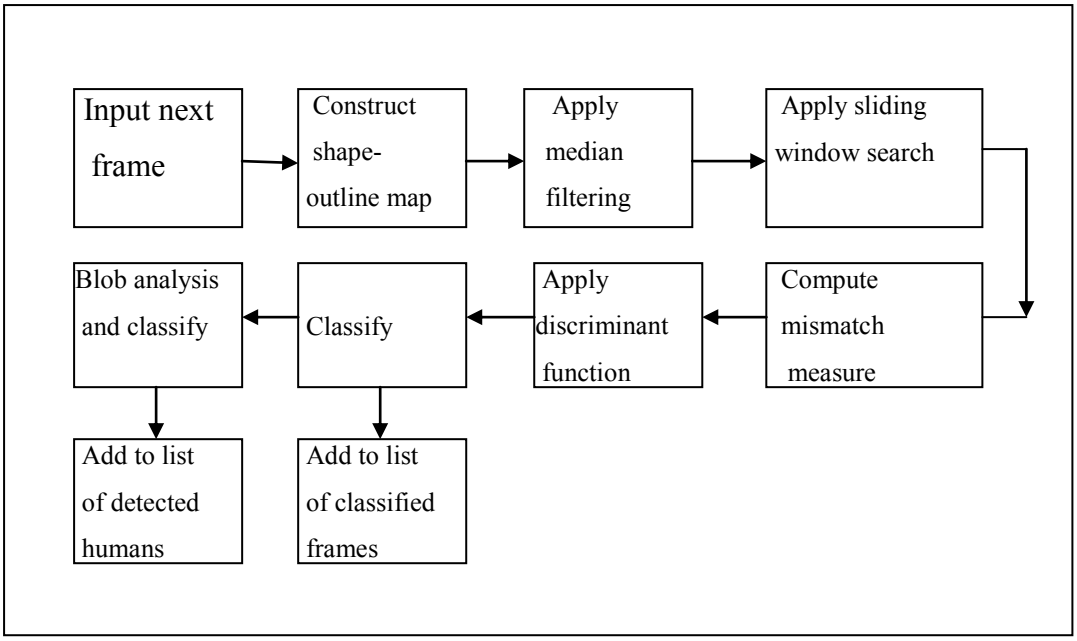

Figure 7.5 Block diagram for shape-outline based classification and detection of humans (PASCAL VOC 2010 challenge)

7.10 Results

Of the three search mechanisms in wavelet domain the background saliency provided the best performance in accuracy for all the three video sequences. This can be observed from the baseline tables (see tables 9.4, 9.5, 9.6). Background saliency strategy provided accuracy level above that of motion saliency with higher computational work load. Motion saliency and edge saliency provided approximately the same level of accuracy, with motion saliency incurring higher computational cost. Pre processing functions which have significant effect on the accuracy is the median filtering. Increase in threshold of the shape-outline map incrementally enhances the outline of human candidates in well illuminated environment (stc_t1_c_3.avi). However as the dimension of the human candidates becomes smaller, smaller threshold is required to extract the foreground objects whilst the shape-outline map becomes noisy.

With PASCAL VOC 2010 several modifications had to be made to the proposed detection algorithm. When the LL subband was used in training the histogram classifier the detection rate was very low and did not improve. Thus it was not used in the evaluation. The HLLH subband provided higher detection rate during post training analysis. However the similarity metric for the human and the background class appeared very similar. To solve this problem, a linear discriminant classifier was designed to separate the human class from the non human class using the similarity metric as input. The linear discriminant classifier is based on the feed forward neural network with three layers. Table 7.5 shows the average precision for the detection and classification tasks using PASCAL VOC 2010 training set. Figure 7.6 shows the precision/recall curves for the two tasks. With PASCAL VOC 2010 challenge the sliding window approach is a search mechanism was used to determine candidates. The shape-outline map and the silhouette maps were very noisy even after applying median filtering. The presence of noise in the feature maps (shape-outline and silhouette maps) make the discriminant rules derived for image sequence inapplicable. Hence new discriminant functions (for both shape-outline and histogram classifiers) had to be developed to separate the human class from the non human class. The average precision/recall of the detection task was less than one. The main reason for the low performance is that the area overlap constraint is not met by most of the

detected humans. It is attributed to the feature map produced in using the test sequence for candidate localization, which is noisy. In the case of video frames, application of frame differencing or background subtraction followed by median filtering removes move of the features shared by the background class. The peak detection rate of the histogram detection is less than 0.003 on account of the high detections which fails to meet the area overlap test. The actual number of detections (candidates) passed on to the classifier is 470,520,200 out of which 20,000,540 met the area overlap constraint. The number of test frame used is 5105. Thus clearly the low average precision is attributed to the large number of candidates.

Table 7.5 Average precision for PASCAL VOC 2010 challenge

Algorithm	**Average precision**	
Classifier/Detector	**Classification (%)**	**Detection (%)**
Shape-outline based classifier/detector (In-house training set)	54	-
Shape-outline based classifier/detector (PASCAL training set)	40	0.003
HLLH subband classifier/ detector(PASCAL training set)	54	0.003

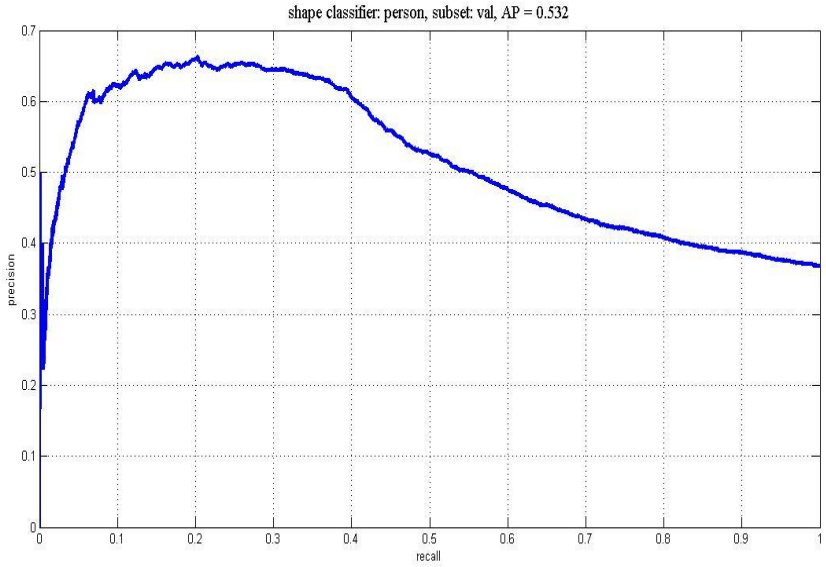
shape classifier: person, subset: val, AP = 0.532
precision
recall
0
0.1
0.2
0.3
0.4
0.5
0.6
0.7
0.8
0.9
1

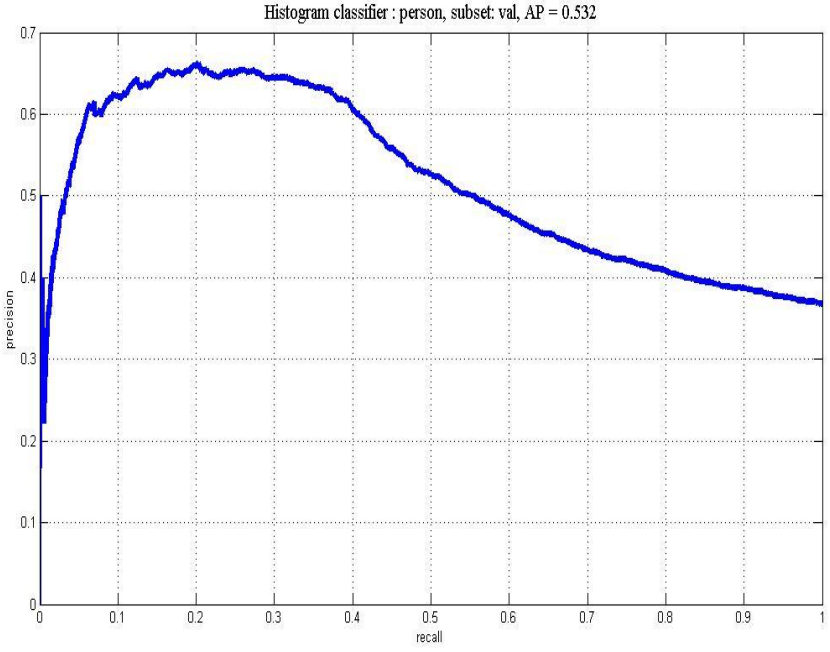
Histogram classifier : person, subset: val, AP = 0.532
precision
recall
0
0.1
0.2
0.3
0.4
0.5
0.6
0.7
0.8
0.9
1

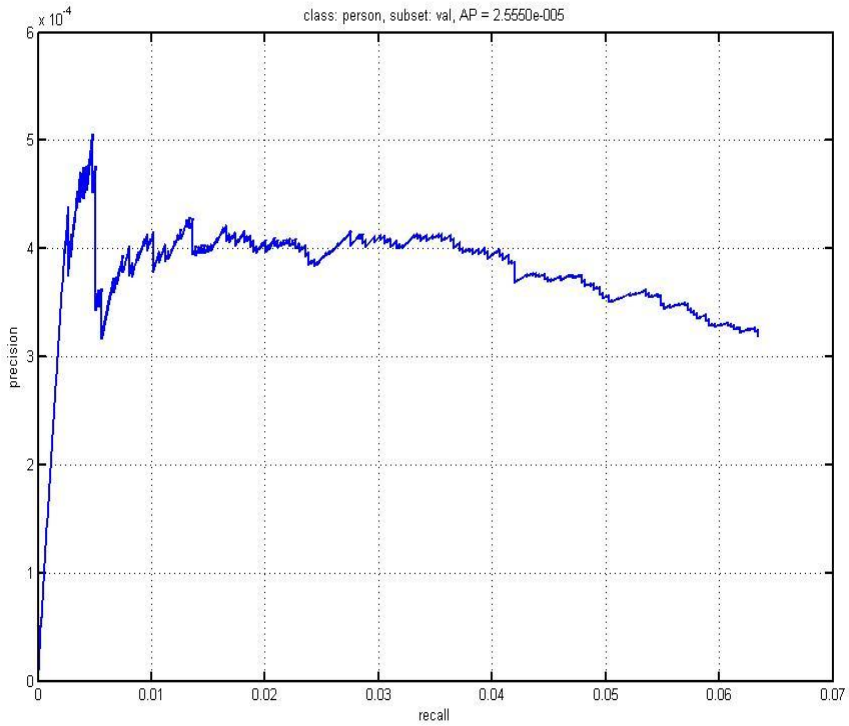

Figure 7.6 Precision/recall curves (Top to bottom) (a) shape-outline classifier (b) HLLH subband histogram classifier (c) Histogram-outline detector

observed that the response of the vertical features (horizontal histogram) is the main distinct feature in classifying and detecting humans. As a result the horizontal feature histogram was not used in the evaluation step.

Chapter eight provides more details on accuracy of the combined detector. Tables 7.6, 7.7 and 7.8 provide execution time profiling by function using MATLAB profiler. The tables exclude initialization (classifier tables and parameter file), frame access, overheads unique to MATLAB, and post processing. Initialization and post processing task are executed only once during a run. It was noted that the execution time in MATLAB varies but the relative execution time expressed as a percentage is stable hence it is used to measure the relative computational effort required. Since the execution time depends on the frame dimensions and the number of frames, the figures quoted are based on assuming a standard frame size of 320 wide by 240 pixels high. Overheads includes functions such as displaying of graphical objects, colour

space conversion, intrinsic functions called when generating outputs, and other functions not directly related to the main task.

7.11 Interpretation

This chapter has investigated three search strategies for candidate human identification and the rest of the building blocks which forms the two detectors for video content analysis. These are edge and motion saliency, and background saliency. Edge saliency estimates the edge density within a block of a candidate search region. Motion saliency estimates the amount of motion present in a candidate region, and background saliency estimates the dimension of blobs in the background image and hence its importance as candidates when background memory scheme is active. Edge density based measure was used in locating the candidate human. It was noted that although the candidate human localization strategy is effective, it sometimes filters out some discriminatory features and limits the ability of the classifier to discriminate humans from non humans. As an alternative, the original feature map is used by the classifier in discriminating. The same conclusion is applicable to the wavelet domain features. Wavelet domain detectors are less sensitive to transient changes due motion and have more stable detection and false alarm rates. It is supported by higher detection and lower false positive rates in the background saliency mode of the wavelet detector

The ROC curves of all the test sequences are a plot of the measured detection and false alarm rates, and non parametric; thus no attempt was made to fit the points unto to a curve. This enables the sensitivity of the algorithmic parameters to be studied. The influence of the following parameters were evaluated during the simulation run: median filtering, candidate human width, candidate human height, background modelling scheme, and window scaling factor. In general an increase in candidate window dimension results in increase in detection rate and false alarm rate until beyond certain dimension the detection rate falls with increase in window dimension. Median filtering tends to reduce the detection rate for less cluttered scene but increases the detection rate for cluttered scene with humans coming together to form groups frequently. The following observations were made: the difficulty in differentiating the human class from the background becomes more severe as the

scene clutter increases with increasing number of humans to detect. The size of the median filter chosen must match the background noise characteristics to avoid removing discriminatory features. The main problem with the proposed detectors is the high false positive rates. This is observed in the high values of FPR and low values in PPV and F1 measures. This problem is addressed in chapter seven.

From the result of PASCAL VOC 2010 challenge dataset it is clear that the proposed technique is not suitable for detection of humans in single frame but suitable for classification of images. Further work needs to be done to improve the localization of humans in single frames in order to be suitable for human detection in single frame.

The computational effort spent on the wavelet transform is offset by a reduction to a quarter the input frame size of the output subband for every unit increase in wavelet decomposition level. The execution time of wavelet transform is similarly halved for every level increase in decomposition. From tables 7.6 it is noted that the most demanding task, the edge saliency tasks operates on candidate windows (images patches), and are independent of each other. From table 7.7 which uses level-two wavelet transform the bottleneck lies with the wavelet transform and not the edge saliency sub task. This is due to the reduced subband frame size (a sixteenth of the original frame size) compared to table 7.8. From the execution profiling it is also noted that the level two wavelet detector has the fastest execution times of the three detection modes. The smaller subband of level two requires correspondingly less amount of search time, and reduction in execution time of resizing operations (a major source of computation) on the subband windows. With level one decomposition on the other hand, the reduction in processing time of salient object feature localization and frame resizing at level one wavelet transform (giving a reduction of frame size of 0.25) was not enough to offset the execution time of level one wavelet decomposition. From table 7.8 (shape-outline based detector), the dominating task is object localization. It is also obvious that approximately equal amount of time is spent executing the classifier as is spent in object window analysis (Shap_Pre_Window, Shape_Window_Analysis and Shape_find_ROI_Centroid). Each takes about 14.5% of the executing time. On the other hand the shape search strategy (Improved_Shape_Search_Strategy) takes about 38.4%. Most of the sub tasks also operate on patches of the frame which are independent of each other.

Table 7.6 Task profiling of the main functions of histogram based detector for decimated wavelet transform (level one) subband

Function	**Normalized Execution Time(Sec)**	**Percentage of Execution Time**
Improve_Histogram_Analysis	0.027	1.41
Resizing (Frames and windows)	0.24	12.55
Level_One_Wavelet_Transform	0.14	7.32
Improved_Wavelet_Object_Search	0.12	6.28
Histogram_Window_Analysis	0.005	0.26
Edge_Saliency	1.38	72.18
Total	1.91	100

Table 7.7 Task profiling of the main functions of the histogram based detector for decimated wavelet transform (level two) subband

Function	**Normalized Execution Time(Sec)**	**Percentage of Execution Time**
Improve_Histogram_Analysis	0.021	4.07
Resizing (Frames and windows)	0.032	6.23
Level_Two-Wavelet_Transform	0.257	49.9
Improved_Wavelet_Object_Search	0.104	20.19
Histogram_Window_Analysis	0.001	0.19
Edge_Saliency	0.10	19.42
Total	0.52	100

Table 7.8 Task profiling of the main functions of the shape-based detector

Function	**Normalized Execution Time(Sec)**	**Percentage of Execution Time**
Improved_Shape_Search_Strategy_ Object_Window	0.088	38.40
Partial_Human_Shape_Classifier_New	0.034	14.84
Resizing (Frames and object windows)	0.0054	2.36
Object_Outline Map	0.065	28.37
Compute_Frame_Activity	0.003	1.32
Shape_Pre_Window	0.0008	0.35
Shape_Window_Analysis	0.028	12.21
Shape_Find_ROI_Centroid	0.004	1.74
Shape_FoundObjectdatabase	0.00085	0.37
Verify_FoundObject_Objectdatabase	0.0001	0.04
Total	0.23	100

From the above profiling data it is obvious that the application would benefit from applying parallel processing techniques. Figure 7.7 illustrates the difficulty in assigning evaluating accuracy of detection task. It includes over using sized windows, humans appearing with variable dimension, and multiple humans being enclosed in a bounding box. This makes the evaluation task highly variable. The use of proportion-based threshold (fraction of maximum wavelet coefficient value) in the pattern spaces (shape and wavelet space) also allows rapid detection of features.

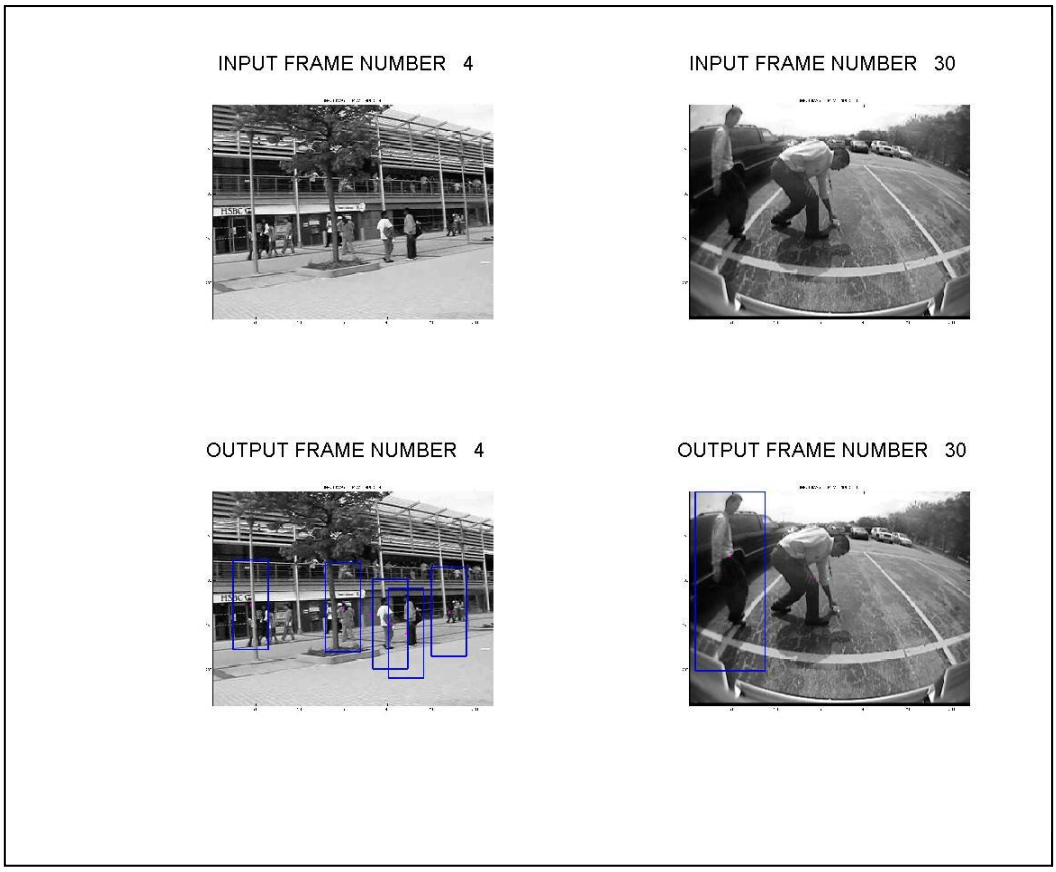

Figure 7.7: Object window configurations in a frame at the detection phase for test1.avi sequence

Chapters six and seven together have presented two reduced complexity, and a novel human detection techniques in video. The algorithms operate on both gray scale and colour images, and no make any assumptions about the scene. The use of motion information enables noise to be removed from the maps (shape-outline and silhouette maps). This improves both the detection rate compared with PASCAL2 VOC where there is no motion. Individually the detectors achieve moderate accuracy (high detection and false alarm rates), but when combined achieve high detection rate is expected. The algorithm presented for detection of humans in wavelet domain provides the possibility of synthesizing variable accuracy detectors using bank of classifiers. Each classifier operates on a subband of an input frame at a given scale, and shares a common database of found humans.

CHAPTER EIGHT

INVESTIGATION INTO JPDAF TRACKER

8.1 Introduction

This chapter presents a reduced complexity silhouette based JPDAF (Joint probabilistic data association filter) tracker for human tracking based on state-space approach, and evaluates its accuracy and real-time performance. Firstly, four appearance features (intensity, directional gradient, chromatic red and green colours) are extracted using the binary silhouette of candidate humans in the frame. JPDAF is used for data association spatially within a frame, and track likelihood filter to resolve measurements conflicts between frames. Additionally the signatures of found humans are used to uniquely assign humans to track.

Measurements are assumed to be normally distributed, and Kalman prediction is used to determine the next state vector of the tracks. Section 8.2 describes track initialization and measurement validation based on Mahalanobis distance. Section 8.3 describes the algorithm for extracting appearance features. Section 8.4 details out the cluster based motion vector estimation technique which allows motion vectors to be determined as a look up table. Partition of measurements into clusters is also discussed. Section 8.5 discusses measurement (location and motion vector estimation) validation constraints. Kalman prediction for evaluating trajectory of humans undergoing linear motion is discussed in section 8.6. Section 8.7 discusses measurement-to-track hypotheses generation and validation. The computation of similarity measure between the signature of found human and that of a candidate track to determine the best track for association is also discussed. The use of JPDAF and measurement cluster to update the state of a track

is also discussed. Section 8.8 describes the different track optimisation techniques implemented including multiple motion models, sequential and batch state estimation mode for improving the accuracy of the tracker. Section 8.9 deals with detecting occlusion and how it is handled. Section 8.10 analyses the computational complexity of the tracker. Section 8.11 presents a scalable algorithmic architecture for the tracker. Simulations and accuracy evaluations are described in section 8.12. Section 8.13 discusses the results whilst 8.14 interprets the results.

8.2 Track Initialization

One of the parameters required for the tracker, Mahalanobis distance, is derived from the confidence level associated the measurement process as defined by the user. For an M-dimension measurement vector, Mahalanobis distance is chi-squared distributed with M degrees of freedom. The locus of points given Mahalanobis distance K, is an M-dimension ellipse where M is the dimension of the measurement matrix. Thus every measurement vector has associated with it a validation volume defined by M. It is used in validating measurements assigned to tracks. A new track is initialized if there is no evidence between the previous frame and the current frame linking a candidate human to a track. New tracks are initialized with the x and y coordinates of the centroid. This occurs at the start of track processing window when the first frame with humans is passed to the tracker. A track processing window denotes a sequence of frames upon which track decisions (assignments, expiration, splits, and merges) are made during tracking. All known tracks are initialised at the start of track processing window. It operates as a sliding window of the frame sequence. At the end of every track processing period, for all found humans not associated with any track, the tracker automatically assigns them to a new track. Global parameters of JPDAF tracker used for the simulation are shown in table 8.2. The algorithmic task flow for tracking is shown in figure 8.1. The first sub task, pre processing involves associating centroids in the current frame to existing tracks from the previous frame provided that the measurement is within its validating volume, otherwise it is a new track.

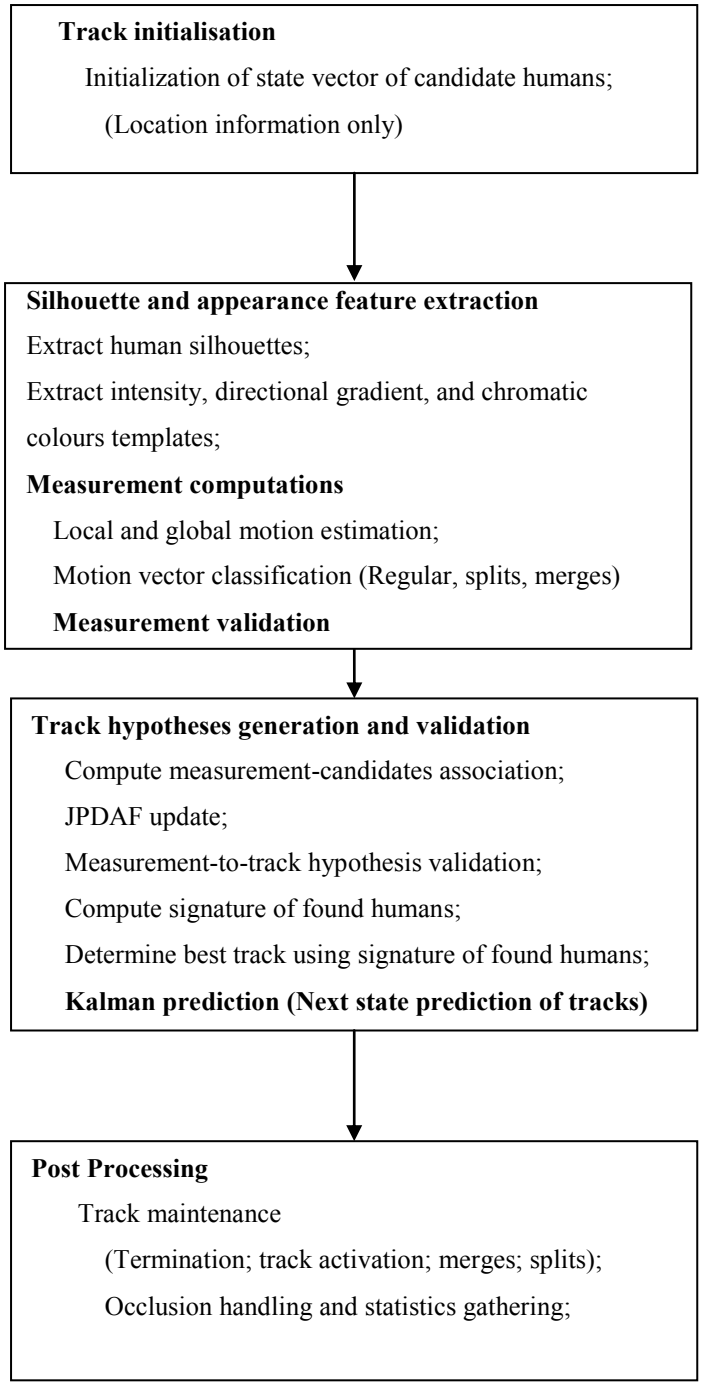

Figure 8.1 Task flow in human tracking

8.3 Silhouette and Appearance Feature Extraction for Human Tracking

The appearance feature extraction starts with silhouette extraction and then appearance template modelling based on found humans in the current frame. It is based on the assumption that there are no significant view point changes between consecutive frames. Appearance feature extraction based on the silhouettes computed on every frame avoids the need to update a global template on a frame-by-frame basis. Accumulation of small changes over several frames would introduce significantly deviations if fixed templates were used. In [Jephson et al. 2003] an online appearance model consisting of three components is modelled as Gaussian mixture to reduce the effect of dynamic changes between frames. The approach adopted is to use the associated appearance descriptor of the silhouette as the best representation of the candidate human in the window when comparisons are made between humans in the previous frame. Human silhouettes are extracted by blurring with an averaging filter (5 by 5 averaging filter) to obtain a low pass version of the candidate window. Spatial domain segmentation based on intensity pixel threshold is applied to obtain the silhouette. The resulting silhouette is a binary representation of the human. They are intensity, directional gradient, and two chromatic colours (red and green). Chromatic colour space is used since it is less sensitive to illumination changes [Yeasin et al. 2004]. Any of the four templates could be used alone or in combination with others for motion tracking. From the appearance templates are extracted two measurements, namely, motion vector, and spatial location. The decision on the number of appearance templates to use is dependent on the computational load and the expected improvement in accuracy required. The directional gradient image is extracted by applying Sobel filter masks for detecting vertical and horizontal edges as shown in figure 8.2 and defined by equation 8.1.

1	2	1
0	0	0
-1	-2	-1

A

-1	0	1
-2	0	2
-1	0	1

B

Figure 8.2 Sobel filter masks for vertical edges(A) and horizontal edges (B)

$$GradImage(x,y)= \sqrt{(GradImageY^2 + GradImageX^2)} \quad 8.1.$$

X and Y refers to the X and Y cartesian coordinates of a point in the silhouette of the candidate human. GradImageY refers to the intensity gradient image computed using vertical mask A, whilst, GradImageX refers to the intensity gradient image computed using the horizontal mask B. The chromatic colours are computed from the red, green and blue component colour as defined in equation 8.2 and 8.3 for red and green components. The blue component is not used since the three components are complementary and adds up to unity. The colour model is appropriate for skin colour and is perceptually discriminative.

$$Chrom\_Red\ (x,y)= r/(r+g+b) \quad 8.2$$

$$Chrom\_Green\ (x,y)=g/(r+g+b) \quad 8.3$$

R,g,b are the red, green, and blue components respectively. An appearance feature template is further sub divided into nine neighbourhood blocks during motion estimation. The median displacement is used as the motion vector for a candidate human when multiple appearance features are used. The use of motion vector from multiple features is used in resolving ambiguities and improving the accuracy of motion vector. A motion vector is assigned to the sub blocks of a candidate human and together with the location

information define the state vector of the current object window, i.e, the vector (X, Y, Xbar, Ybar), where X, Xbar, Y, Ybar are the x coordinate, velocity along x-direction, y-coordinate, and the velocity along the y-direction respectively.

8.4 Motion Estimation

For every human known in the previous frame and associated with a track motion estimation is used to find its correspondence in the current frame. Two types of motion vectors are computed, namely local motion vector, and global motion vector. The global motion vector is computed for every candidate human, whilst the local motion vector is computed for sub blocks of the candidate human. In every motion estimation, nine neighbour blocks (sub blocks) defined as shown figure 8.3 (numbered 1 to 9) are used. The assumption is that there can be a maximum measurement overlap of up to WX and WY in the x and y direction respectively (WX=floor($SizeX_d$/3), WY=floor($SizeY_d$/3)), where $SizeX_d$ and $SizeY_d$ refers to the dimension of the human window, and floor is the floor function. To improve robustness measurement are grouped into clusters. A cluster is defined as an n-dimensional (n=2) space within which measurements are normally partitoned and innovation (predicted measurement error) is chi square distributed. All measurements associated with a candidate human define a cluster. A cluster is partitioned into non overlapping regions. The dimension of the cluster depends on the confidence level required in the measurement process. Block based motion estimation is applied to each sub block of a cluster using maximum absolute difference as the criteria for best match. To reduce search complexity only eight nearest neighbours are examined as defined spatially in figure 8.3. The matching block is defined by equation 8.4 assuming the current block is number five.

$$MV(x,y)= \min \sum |Image_j (x+diffx,y+diffy)–Image_{j-1} (x+diffx,y+diffy)| \quad 8.4.$$

for every sub block, diffx and diffy takes on values between +WX and –WX, and +WY and –WY along the x and y axis respectively, and $Image_j$ denotes an appearance template

extracted from a frame at time j, and whose centre coordinates are x and y, and the top left corner is used as the reference coordinate. All motion vectors are approximated to the centre of the nearest sub block. Motion vectors are defined either by an index assuming the top left block has index number one with the motion index increasing in row major order, or using the relative address. Thus the relative addresses are pre computed in a table, and could be referenced optionally by its label as shown in figure 8.3 or its relative address.

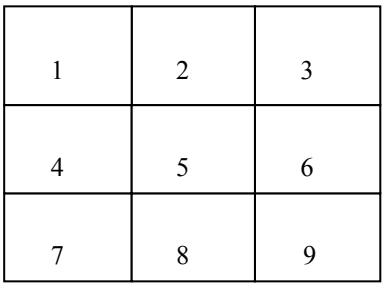

Figure 8.3 Region of a candidate human partitioned into sub blocks of a cluster

For each appearance template (intensity, chromatic red, chromatic green and intensity gradient magnitude frame) ten motion vectors are determined and assigned to every cluster. There are nine motion vectors from the sub blocks (follows the above labels) and one for the main block. In case multiple motion vectors result from the motion estimation phase, motion vector is assigned to the sub block with the smallest label. This applies to both the local and global motion vector. Table 8.1 lists the top left corner (starting coordinates) of the sub blocks of a candidate human. The state vector for a cluster has one vector for the whole block, and one each for the nine sub blocks. Following motion vector computations, motion vectors are used to classify candidate humans into regular, splits, and merge type. Multiple motion vectors associated with a candidate human signifies the possibility of occlusion (see section 8.9). Motion vectors are validated for the current cluster using next predictions of the associated track state vectors. In case two neighbouring cluster share some common sub blocks, the motion vector of the sub blocks are assigned to one cluster depending on track maximum likelihood (see section 8.7). A

motion vector from the sub blocks of a cluster must pass measurement validation test, whilst the motion vector for the whole block must pass both the validation test based and motion constraint test (based on Kalman prediction) of the associated track.

8.5 Measurement Validation

Measurements estimated are the motion vectors and approximate centroids of human locations from the four appearance templates, namely, directional gradient, chromatic red and green components. The expected centroid of human is determined by computing the median of all centroids of feature template measurements associated with a candidate human. Measurements are associated with tracks based on the following:

- Euclidean distance between a track's location and the feature template's location (along x and y directions);
- Euclidean distance between current track's motion vector and motion vector of the feature template (along x and y directions);
- Constraints on separation along the x and y axes between a track's location and the feature template's location;
- Constraints on separation along the x and y axes between a track's motion vector and the feature template's motion vector;

These constraints are typically determined by the dimension of the candidate human region. The result of applying the criteria above is to assign measurements into partitions associated with tracks, represented as track association matrix. The element of the matrix $R_{j,i}$ has a value of one if i and object j belong the same object, otherwise it has a value of zero.

8.6 Kalman Prediction

Kalman filter is an optimum linear detector when measurements and noise distributions are Gaussian [Haykins 1999]. Kalman prediction is defined by equations 8.5 and 8.6.

$$Y(n)=C(n)X(n)+Q_2(n) \quad 8.5.$$

$$X(n+1)=F(n+1)*X(n)+Q_1(n) \quad 8.6.$$

Table 8.1 Relative addresses of sub blocks defining a track cluster

Sub block Index	**X**	**Y**
1	1	1
2	WX+1	1
3	2WX+1	1
4	1	WY+1
5	WX	WY
6	2WX+1	WY+1
7	1	2WY+1
8	WX+1	2WY+1
9	2WX+1	2WY+1
10	WX+1	WY+1

Y(n) defines the observation (measurement) vector, C(n) defines the measurement matrix, X(n+1) defines the next state vector given the current state, and F(n+1) defines the state transition matrix from state n to n+1, $Q_1(n)$ defines the measurement noise, and $Q_2(n)$ defines the process noise (noise from the state estimation process). Equation 8.6 describes the state model whilst the vector Y describes relationship between the measurement and state vectors (describes the measurement process).

$$R(n)=C(n)*K(n)*C^{H}(n)+Q_2(n) \quad 8.7$$

$$G(n)=F(n+1)*K(n)C^{H}(n)*R^{-1}(n) \quad 8.8$$

$$Est\_X(n)=X(n-1)+G(n)\ *(Y(n)-C(n)*X(n-1)) \quad 8.9.$$

Where n denotes time step, R(n) is innovation vector error correlation matrix, G(n) is Kalman gain matrix, K(n) is the predicted state error correlation matrix, Est_X(n) denotes the estimated state at time step n, and $R^{-1}(n)$ denotes the inverse of matrix R. The superscript H denotes the transpose as in $C^{H}(n)$, which is the transpose of the measurement matrix. The superscript -1, denotes the inverse operation. F(n+1), and K(n) are assumed constant.

The search for the best correspondence between a candidate human in the current frame and an existing track is determined by validating the state vector of the candidate human against Kalman prediction (next state) of a candidate track. The inputs to the next state of a track are the current state (based on current measurements) parameters defined as a table of association, i.e, track association matrix. The Kalman filtering is defined by equations 8.7 and 8.8. Equation 8.9 are used to predict the next state. The advantage of using Kalman prediction is that the next state is dependent on the current measurements, state, and Kalman gain vector, and the system parameters either evolves with time (one-step Kalman prediction). Sudden changes in state vector then signifies deviation from its expected behaviour. Should this happen then the measurement would fall outside the validation region of the track. Such measurements could be false alarms, object splits, or merges. The use of Kalman filtering enables multiple motion models to efficiently handle motion dynamics of humans such that the best model is selected for the particular scene. The output from the Kalman prediction stage is the innovation matrix, and next state prediction matrix. An innovation vector is associated with a track if the corresponding track association matrix element has a value of one, otherwise it is not associated with the track.

8.7 Track Hypothesis Generation and Validation

The next step track, hypothesis generation and validation requires the following: the estimated state vector defined for every track, measurement association matrix describing associations between valid measurements, and innovation matrix, relating computed innovations associated with valid tracks. Since several closely packed measurement vectors may occur for multiple humans close to each other, a suitable data association filter is required. Candidate filters include multiple hypotheses track filter, JPDAF, and the maximum likelihood filter. Multiple hypotheses track filter (MHTF) is the optimum data association filter. The complexity in enumerating all possible tracks using track trees (as in multiple hypotheses track filter) for the whole sequence is avoided by redefining the tracking problem, using JPDAF within a frame and maximum likelihood filter between consecutive frames. JPDAF however requires a fixed number of objects to track at any time.

Measurements Y are validated normalized to give Z (normal variable), and linked to previous hypotheses to create a new hypothesis. When a measurment is assigned to a track a measurement assignment event is said to have occurred. The new hypothesis at time k for each track, Θ^k, is made of current measurement assignment (event) θ_k, and previous hypothesis based on measurements up to and including time k-1 ($\{\Theta^{k-1}, \theta_k\}$). Event-to-track association probability is computed using Bayes rule by equation 8.10, where C is a normalizing constant.

$$P\{\Theta^{\kappa} \mid Z^k\} = P\{\theta(k), \Theta^{k-1} \mid Z(k), Z^{k-1}\} = \tfrac{1}{C} P(Z(k) \mid \theta(k), \Theta^{k-1}, Z^{k-1}) P(\theta(k), \Theta^{k-1}, Z^{k-1}) * P\{\Theta^{\kappa-1} \mid Z^{k-1}\} \quad 8.10.$$

It defines the current hypothesis probability in terms of its previous hypothesis and is the approach used in multiple hypothesis track filter (MHTF). In MHTF, to determine the optimum track filter, N best tracks are selected based on the maximum track association probability defined by equation 8.10. Two approaches are combined in the current investigation to compute optimal tracks, namely, the weighted innovation approach based

on JPDAF, and the likelihood filter based on minimization of Mahalanobis distance. The probability of all joint events assignment to all tracks is given by equation 8.11 based on Bayesian framework for JPDAF filter.

$$P(\theta_l^k \mid Z^k) = \frac{1}{C}\frac{\Phi!}{m_k!} * \mu_f(\Phi) V^{-\Phi} * \Pi_{i=1}^{m_k} (N_t[Z_i(k)])^{\tau} * \prod_1^T * P_D{}^o * (1 - P_D{}^t)^{1-o} \qquad 8.11.$$

T denotes the total number known humans in the scene, Φ denotes number of false measurements, $\mu_f(\Phi)$ denotes priori probability of false measurements, m_k denotes total number of measurements at time k (assume $m_k >= 2T$), θ_l^k denotes an assignment event at time k, and V denotes measurement validation volume. τ is an indicator function and has a value of one if measurement is validated to the current track, and zero otherwise. Similarly o is an indicator function which has a value of one if a particular track is detected, and zero otherwise. N_t [Z_i (k)]) denotes the normal distribution function. It models measurement $Y_i(k)$ (see equation 8.16) as a normal distribution. Alternatively equation 8.12 models the probability of valid measurements under clutter conditions assuming clutter is Poisson distributed with spatial density γ, Y_Φ denoting the actual measurement of a feature, λ_Φ denoting the expected feature measurement, q denoting prior probability of detection, σ_z standard deviation of measurements assuming normally distributed, and S_Φ the innovation covariance (predicted error covariance). The measurement process under clutter is modelled temporally by equation 8.12.

$$\max(P(Y_\Phi \mid S_\Phi) \propto 1 + \frac{1}{\sqrt{2 * pi} * |S| q\gamma} \sum_{m=1}^{T} \exp^{(z_\Phi - \lambda_\Phi)^2 / 2|S|} \qquad 8.12.$$

With JPDAF, the joint probability of occurrence of all tracks of found humans in the scene are computed using equation 8.11. Tracks which are close enough to each other (there is an overlap in measurement validation regions) may be grouped and updated together or individually. The corresponding innovation vector update is defined by equation 8.13 which could be applied spatially or temporally. The current investigation applies JPDAF

spatially within a video frame assuming a fixed number of tracks (T) which could be very close to each other. To manage complexity and processing regularity, every candidate human region is partitioned into nine spatial sub tracks corresponding to the ten measurements as discussed in section 8.4. Within the framework of Kalman prediction, track innovation is computed using equation 8.13.

$$\alpha_{new}(i) = \sum_{l=1}^{mk} B_l(i) * \alpha(i) \qquad 8.13.$$

The weights $B_l(i)$ are the probabilities of detection of event i occurring jointly with other event in the sub blocks of the candidate human (equation 8.11). Thus two track filters are maintained spatially. One filter is jointly defined for a track and its sub tracks, and the other jointly for all the T tracks in the current frame. Track likelihood defined by equation 8.12 is used to select tracks sequentially for update. All tracks in the current frame whose track likelihood exceeds the threshold is updated. This approach allows parallel updates of tracks. The threshold is normally multiples of $\left(\frac{1}{\sqrt{(2*\pi)^d} * |S|}\right)$. Track log likelihood approach [Morefield 1977], [Cox 1993] is used to select tracks temporally. Track log likelihood ($\lambda^l(k)$) models measurement likelihood temporally by equation 8.14, assuming target measurements and conditions remain unchanged.

$$\lambda^l(k) = 2 * \log[\Gamma(\theta^{k,l}) / (\sum_{j=1}^{k} \| 2 * \pi * S(j) \|^{-1/2})] = \lambda^l(k-1) + v_{ik,l}(k)^H * S_{i,l}(k)^{-1} * v_{ik,l}(k) \qquad 8.14.$$

Equation 8.14 is the summation of Mahalanobis distance for a track. $V_{ik,,l}$, is the innovation (error) for measurement i at time step k, and for track l. It is defined by equation 8.15.

$$V_{ik,,l} = (Y(k) - Y\_Est(k|k-1) \qquad 8.15.$$

Mahalanobis distance is the second term of right hand side of equation 8.14. $S_{i,j}(k)^{-1}$ is the inverse of the covariance of the innovation at time step k, and Y_Est(k|k-1) is the predicted

value. Equation 8.14 essentially states that the sequence of measurements that minimizes Mahalanobis distance (second term) over some interval is selected, assuming track likelihood is normally distributed. With track log likelihood equation 8.14 is used in selecting and updating different tracks. The log likelihood track filter is used between frames to resolve measurement uncertainties. Alternatively, the best N tracks may be chosen at any time to propagate the tracks to the current frame. Clustering and gating techniques are typically used to reduce enumeration complexity.

$\Gamma(\theta^{k,l})$, the likelihood of an event occurring (track likelihood) is then defined by equation 8.16.

$$\Gamma(\theta^{k,l}) = \prod_{j=1}^{k} (2\pi)^{-d/2} |S(j)|^{-1/2} \exp[\frac{1}{2}(v_{ik,l}(j)^{H} * S_{i,l}(j)^{-1} * v_{ik,l}(j)] \qquad 8.16.$$

$N_t[Zi(k)]$, the is normal distribution and is defined by equation 8.17.

$$N_t[Z_i(k)] = (2\pi)^{-d/2} * |S(k)|^{(-1/2)} * \exp((1/2)*(v_{ik,,l})) \qquad 8.17.$$

D is the dimension of measurement. The model based on weighted innovation (equation 8.13) assuming false alarms are uniformly distributed in the observation volume V is discussed in [Bar-Shalom 1992]. The task flow for the tracker is shown in figure 8.4 for track generation and validation steps. In the current implementation JPDAF tracker starts with current measurements being partitioned into clusters (represented as measurement indicator matrix) based on Mahalanobis distance constraints described in section 8.5 after validation, and with subsequent construction of track association matrix. The forty cluster measurements (four for feature type and ten measurement for candidate human) are used to construct a state vector by computing the median of all the measurements. Next the determination of track events (i.e, assignment of measurements to tracks) probabilities given the frequency count, and construction of track association matrix. The track

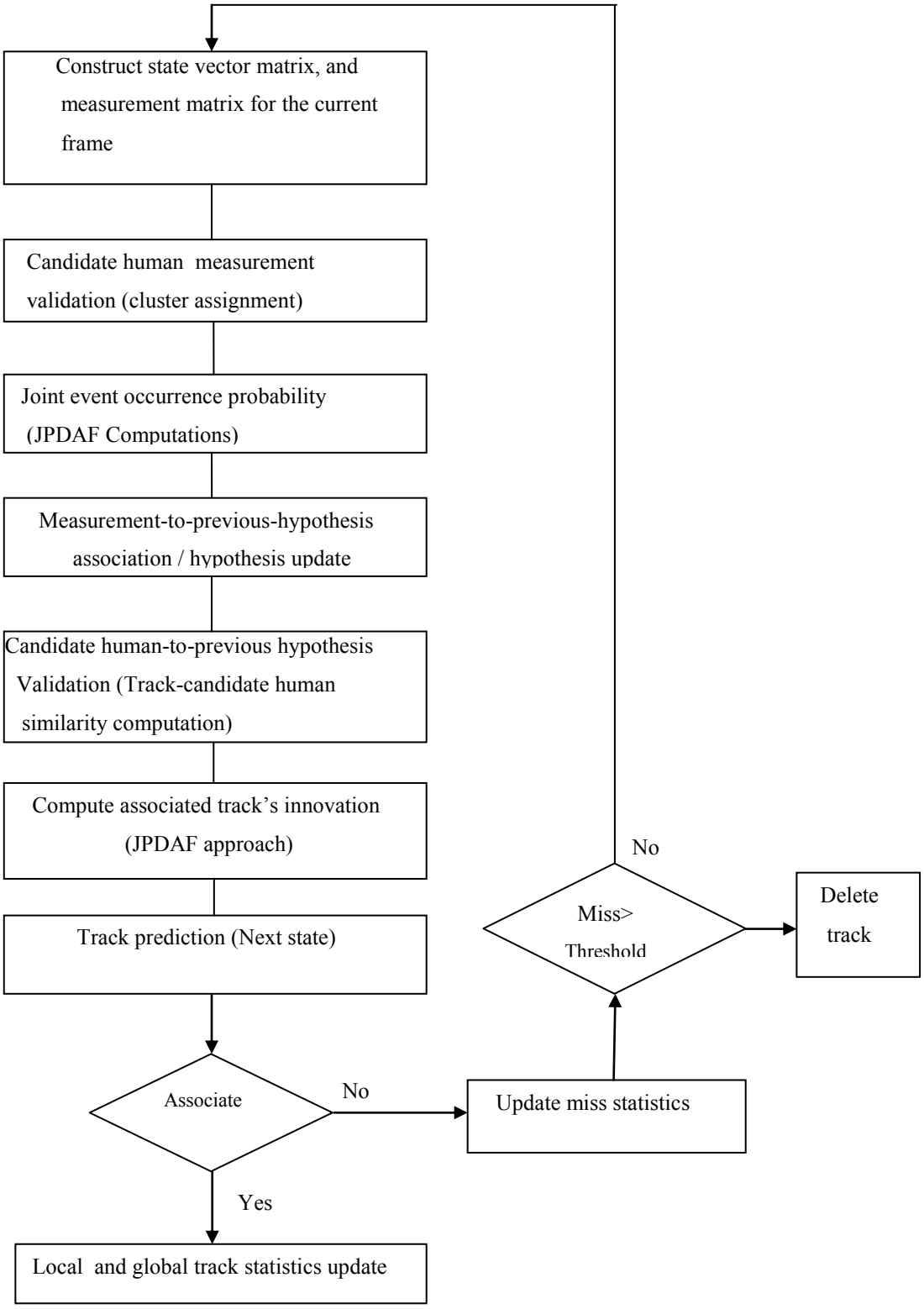

Figure 8.4 Algorithmic flow for track generation and validation

association matrix enumerates all possible cluster associations. Then the probability of joint occurrence of all assignment events occurring within a cluster and between different clusters (defines the spatial occurrence of track-measurement events) are computed. JPDAF probabilities are computed for every sub block of a track, given that N humans appear in the scene at any time by examining measurement association matrix. The joint probability of assignment to the different tracks are computed, and tracks whose probability threshold are above the value set by the applications are selected for update. The signature of all candidate humans in the current frame is computed and compared against the signature of the tracks. The signature used in the current investigation consists of the mean and the standard deviation of the intensity image corresponding to the candidate human. For every track a measure is defined which evaluates how closely a candidate human matches a given track. The measure is defined in equation 8.18.

M1= abs(Track_Mean(i)-Cand_Human_Mean) + abs(Track_Std(i)-Cand_Human_Std) 8.18.

I denotes the track index, Track_Mean denotes the mean of the candidate human associated with track i, Track_Std(i) denotes the corresponding standard deviation, Cand_Human_Mean denotes the mean of the current candidate human, and Cand_Human_Std denotes the corresponding standard deviation. The track which best associates with the current candidate human is the track which gives the minimum value of M1. The validated state becomes the next current state vector. The innovation matrix generated for every candidate human cluster is used in computing the innovation of the valid tracks as defined in equation 8.13. The innovations are computed by using the predicted state vector (from the previous Kalman next state prediction) of the track. The innovation update equation (8.13) is used to compute the innovation for tracks. Track statistics, and local and global track information are also updated. Tracks with no valid measurement associations are declared as miss tracks, and track miss statistic is updated. The old track signature is replaced by the new track signature. When the miss count of a track exceeds a threshold it is declared as inactive. For non valid tracks whose miss count

is less than the threshold an offset is added to the state vector. The update procedure is repeated for all candidate humans in the current frame. Two lists of tracking information are maintained, namely, local track information which is applicable to the current frame being processed, and global tracking information which is applicable to the frames in the track window already processed. After every temporal track window processing, local track information is used to update global track information. Tracks are also moved from active status to inactive status when track misses exceed a certain count usually less than temporal track window size. JPDAF tracking could be implemented sequentially or in parallel on a candidate human basis depending on memory constraints. Since valid hypothesis enumeration is predefined according to track cluster (defined using ten sub blocks of candidate human), Mahalanobis distance criteria is used to select the best representation for each cluster and in the computation of joint probability of occurrence based on minimum innovation vector. The posterior probability of occurrence of a human and false alarm probability density function are modelled individually and then jointly. In figure 8.5 the region between the thick square region and the outer square defines the region of maximum overlap between neighbouring object windows, and also the region of uncertainty in measurement-to-track association. There is a maximum overlap of half the dimension of a sub block between two clusters (candidate human).

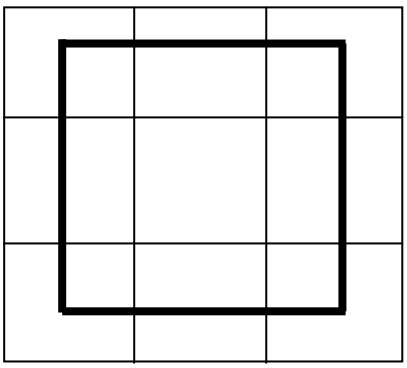

Figure 8.5 Region of uncertainty between neighbouring clusters

8.8 Track Optimization

The objective of track optimization is to reduce false alarms which occurred at the detection stage by applying temporal continuity of motion constraints to improve positional accuracy, filter out false detections, and optimally link found humans temporally. This is provided through the following means: multiple motion models are used to describe motion in two contra directions along the x-axis, and two contra directions along the y-axis. The justification is that motion along the 2-D image plane is described as consisting of translation along the x and y-axis assuming in-plane rotation is negligible between consecutive frames, and different motion model might suit different human motion in the scene. It provides the capability to quickly evaluate different track motion patterns to determine the most appropriate model based on estimates of detection rate, positional error, and false alarm rate. Changing the confidence levels associated with tracks from 95% down to 10% in steps of 10% for measurements-to-track validation, also results in varying number of measurements associated to tracks. The constraint essentially filters out unlikely tracks. Further the ability to apply the tracking module in sequential or in batch processing model enable either reduction in execution time or to jointly to optimize execution time and tracking accuracy. The influence tracking parameters are discussed in chapter eight.

8.8.1 Sequential State Estimation Mode

Online implementation of JPDAF tracking is sequential since tracks are updated per candidate human after measurement-to-track event association probability computation. The main parameters are the Mahalanobis confidence interval, candidate human dimension, and Kalman motion parameters. Temporal consistency is verified using two consecutive frames within which motion is assumed to be Gaussian with clutter modelled as either Poisson or uniform distribution. The limitation of this approach is that decisions are made based on the previous and current frames. Instances of track merges cannot be determined with higher certainty and this may affect the overall accuracy. Since the list

of found humans over all the frames in the past is available and could be used to improve temporal consistency, this approach may not be optimal and inflexible.

8.8.2 Batch State Estimation Mode

In batch processing mode a sequence of N consecutive frames are defined for temporal optimization (Track window). During track window processing temporal coherency is used to eliminate false detections. Similarly track merges and occlusion events detected. This approach provides a more flexible way of optimizing the accuracy of the tracker. Different track processing window could be investigated to determine the best setting.

8.8.3 Application to Single Motion Model

There are six motion models describing different pattern of motion in the Kalman predictor. The accuracy of tracker is dependent on the how close the motion model is to the actual motion of the human in the scene. Different motion models could be combined with varying Mahalanobis distance to determine optimality of a given set of algorithmic parameters. This enables fine tuning of parameters.

8.8.4 Application to Multiple Motion Models

Multiple motion models for a fixed set of algorithmic parameters could also be studied to derive optimum algorithmic parameters. The result of the simulations into the influence of algorithmic parameters is presented in the result section.

8.9 Occlusion Handling

To be able to detect occlusion, merging of multiple candidate humans must first be detected and then if it persists over more than one frame occlusion event is assumed to

have occurred. To detect merging and splitting of candidate human regions, the motion vector labels are partitioned as shown in figure 8.6, and used in classifying neighbouring motion vectors. Let L denotes the left side labels, C the centre labels, R the right hand labels, T the top labels, and B the bottom labels. For a merge to occur neighbouring candidate humans must be separated by less than the width or height of the candidate human from each other, and must have motion vectors label corresponding to the central label (2,5,8), or the middle label (4,5,6). If more than two neighbouring candidate humans have any of these labels, merging of candidate humans is said to have occurred. In the case of splitting the distance between the centroid of neighbouring candidate humans must be more than the corresponding dimension of a candidate human. The neighbouring sub blocks must also have motion vector labels belonging to the outer labels (1,3,7,9), Left labels (1,7) or right labels (3,9), or top labels (1,3), or bottom labels (7,9). If more than three have any of these labels occur within a candidate human region then a split has occurred.

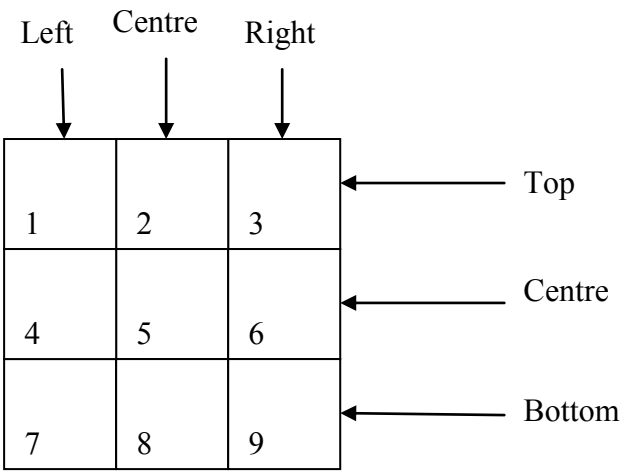

Figure 8.6 Motion vector label for detecting split/merge

In the event of splits or merges occlusion event is also tested. An occlusion event is detected by comparing the candidate human in the previous frame with the corresponding window in the current frame. Sub blocks with common motion vectors are labelled as a

sub region of the candidate human. The Hausdorff[1] distance between the previous silhouette and the new partitions in the current object window's silhouette is computed. When the resulting distance is less than half of the original size occlusion is confirmed, otherwise object splitting has occurred. On detecting occlusion candidate humans the centroid of the human is updated by adding the Hausdorff distance, and setting the motion vector to zero. The algorithm was verified by comparison of the output of the motion vector classifier prediction's for occlusion event with several visual observations of instances of occlusion due to humans coming. However more studies are required to formalize this approach. Also by comparing the new partition with the matching silhouette in the previous frame it is possible to detect events such as abandoned and moved objects based on merge and split events. However the current investigation has not implemented detection of these events.

8.10 Computational Complexity of JPDAF Tracker

The computational complexity of the critical sections of the tracking task are examined here. These are the measurement to cluster (hypotheses) association, and computation of innovation vector based on JPDAF. One-step Kalman prediction is used for both measurement-to-hypothesis association validation, and in track prediction update step. Most of the parameters are pre computed offline, however the joint data association probabilities are updated globally on a frame basis making the calculation sequential up to that point. Beyond that point the computations could proceed in parallel. Every update involves pre multiplication by a constant term (update of transition probabilities), and re-computation of step using equation 8.11. This is due to the fact that the computation is recursively defined as an update on the previous joint probabilities. Assuming that there T objects (total number of known objects) with N objects currently present (validated from current measurements), and assuming there are m measurements (total

[1] Hausdorff distance measures how far tow subsets of a metric space are from each other. It turns the set of non-empty compact subsets of a metric space into a metric space in its own right.

measurements) have been taken, the number of possible measurement-to-object association is given by equation 8.19. Equation 8.20 also gives the total number of track hypotheses possible, assuming m measurements (includes clutter, i.e, false alarms).

$$V_{\lambda}(N,T) = \frac{m!T!}{N!((m-N)!((T-N)!} \qquad 8.19.$$

$$\text{Hypth} = \sum_{k=1}^{T} V_{\lambda}(K,T) \qquad 8.20.$$

To reduce this combinatorial enumeration clustering approach is adopted where within each cluster the best hypothesis is used to represent the track and is propagated to the next frame unless splits and merges are detected. Since the size of a cluster is fixed (ten) it essentially involves (Mahalanobis distance validation using the predicted state of the track, JPDAF probability update, track prediction, and track statistics update). This results in generating T (maximum number of objects per frame) best hypotheses for every frame. The hypothesis validation takes approximately T*10*10 multiplications (from hypothesis matrix assuming innovations have been computed and JPDAF weights have been pre computed). Computation of normal function (Gaussian) requires one subtraction, one multiplication, and one division for calculating the exponent of the e function. Since there are m_k measurements the number of operations is multiplied by m_k. In addition there is pre multiplication by a constant. Since the outcome of the measurement assignment is either detection or no detection event, only one of P_d or (P_d-1) is applicable at any time (refer to equation 8.11). The total number of computations is T, is independent on the number of measurements. V, $\mu_f(\Phi)$, and $1/Cm_k$ are treated as a constants. Φ however varies from one frame to the other. It is assumed not to vary by more than a quarter of T (T/4), then the number of computations are (T/4-1) for the factorial operation. At the end of the computation of JPDAF update the output is a matrix of weights corresponding to the T tracks such that the sum is unity. The One-step Kalman prediction involves matrix multiplication and inversion and is detailed as: 4 X 4 matrix-matrix multiplications cost (16 operations), 4 X 4 matrix-matrix addition (15 operation), 4 X 4 matrix inversion (32 operations) assuming all values are in floating

point units. Clearly the computations are linear with the product of the number of measurements and number of humans to track. It is independent of any enumeration complexity. The memory requirement is also linear.

8.11 Synthesized JPDAF Tracker

Figure 8.7 shows the proposed tracking architecture. It consists of a fixed number of clusters (N). On every cluster there are six stages, namely, track initialisation, silhouette and feature extraction, and measurements computations (estimation). Clusters are defined based on measurement computations and validation. Additionally the previous track hypothesis (known tracks) are used to define new hypothesis through measurement event assignment to tracks. It is followed by JPDAF update, and hypothesis validation. The input to the JPDAF step are the validated measurements expressed as measurement matrix. Clusters are defined based on spatial proximity of humans and they run concurrently, however they share the first three stages. Silhouette and the appearance template. Motion vectors (local and global) are estimated for the human corresponding to the current frame. Measurements (motion vectors and location information) are validated, and assigned to a cluster. A cluster is associated with a sub set of the tracks to reduce track enumeration complexity. Measurements are associated with tracks on passing validation test. JPDAF probabilities are computed for the current frame, and tracks are updated by associating with a human in the current frame. The outputs from the JPDAF stage are the updated tracks. Among the valid tracks the best track is selected using the signature of the associated found human. The signature is defined as the mean, and the standard deviation of the bounded region enclosing the found human. The best match is defined by computing the sum of the absolute differences between the means, and the standard deviation. The track with the minimum value is selected as the matching track. This completes the hypothesis generation and validation step. At the post processing step predictions are made for the next states of the tracks. Track maintenance is implemented as the last step. The architecture operates in both frame and mixed mode. In frame processing mode only clusters related to the current frame are used, whilst in mixed

mode previous and current frame clusters could coexist. The computational load depends on the configuration for the detector. If the detectors run in the combined mode, then there will be more centroids to track. It also depends of algorithmic parameters such as human window height, and width and other parameters listed in table 7.4. Thus different configuration schedule would result in different level of concurrency.

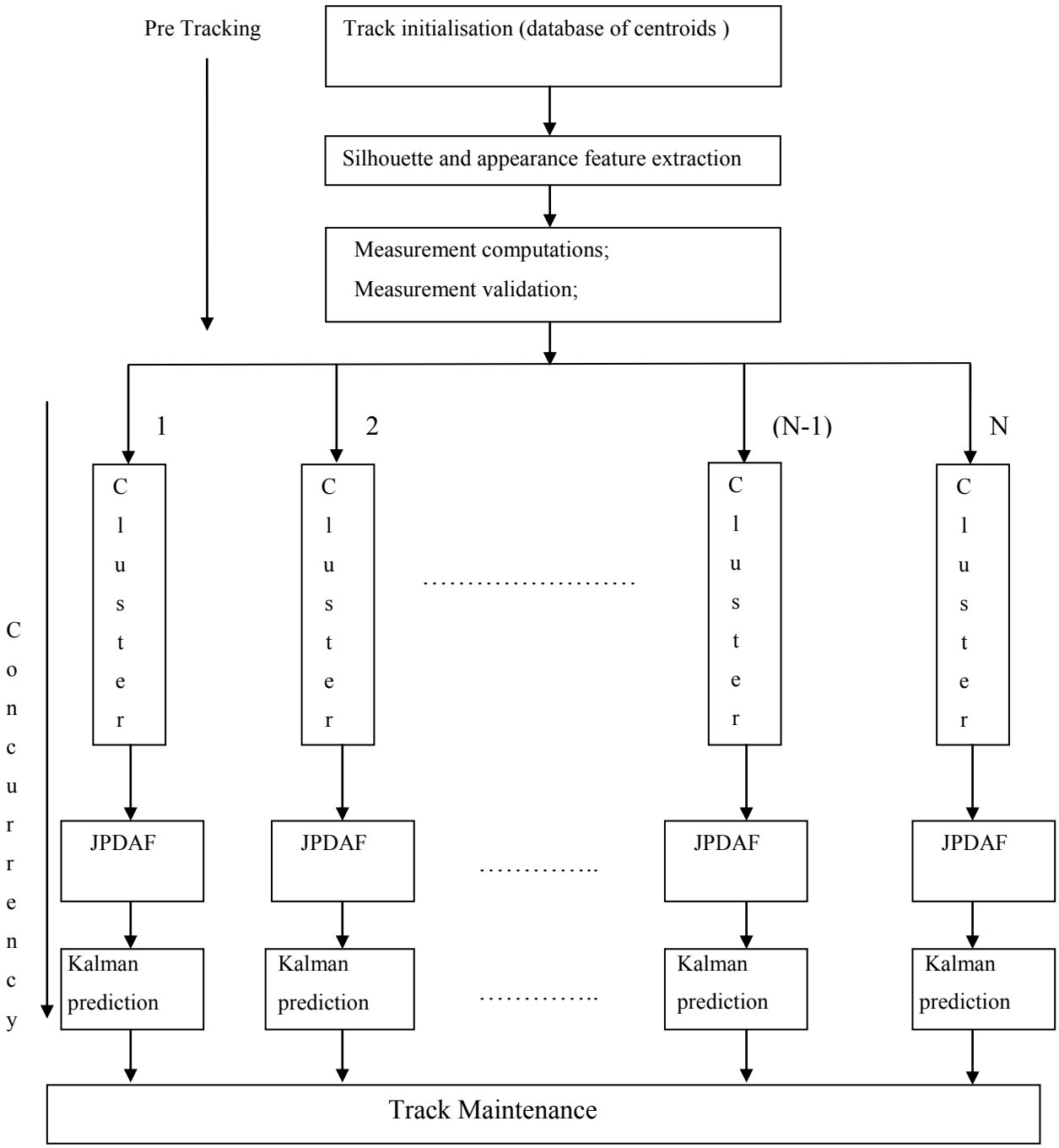

Figure 8.7 Multiple JPDAF tracking modules

8.12 Simulations

Simulations were carried out to evaluate the accuracy of the proposed tracker and to verify if there is indeed a reduction in false alarm rate compared to the output from the detector. First the proposed tracker algorithm was simulated in Matlab and execution time profiling of the sub tasks evaluated. Table 8.2 lists the global parameter settings for JPDAF tracker.

Table 8.2 Global parameter settings for JPDAF tracker

JPDAF parameter	**Value**
Track probability constant	20
PMF of false measurements	0.25
Prior Probability of detection	0.1
Observation volume	MaxNoObjects *(1+10)
Mahalanobis distance for measurement validation	{1.06, 1.64, 2.19, 2.75, 3.35, 4.04, 4.87,5.98, 9.48}
Mahalanobis confidence limit	{10%,20%,305,40%,50%,60%,70%, 80%, 95%}

It was assumed that a track cluster the maximum number of false alarms is fixed. This simplifies the computation of JPDAF probability given by equation 7.11 to have a constant term $(\frac{1}{c}\frac{\Phi!}{m_k} * \mu_f(\Phi)V^{-\Phi})$, multiplied by the event likelihood $(\Pi_{i=1}^{m_k}(N_t[Z_i(k)])^{\tau} * \prod_1^T * P_D{}^o * (1 - P_D{}^t)^{1-o}$).

8.13 Results

Peak accuracy performance is shown in table 9.8. The values are expressed in percentages. The relatively lower false detection rate compared to the detector table as shown in table 9.13b for the combined detector is due to three main reasons.

Comparison with the false positive rates reveals that the false positive rates for hamilton2b.avi, stc_t1_c_3.av, and stc_t1_c_4.avi is lower at the tracking stage than at the detection stage. Table 8.3 shows the execution time profiling of the non optimized JPDAF tracker and the percentage of time spent on the main sub tasks using intensity template only. Table 8.4 is the execution time profiling of the tracker based on using all the appearance templates. These are the intensity, directional gradient, and chromatic red and chromatic green templates used for motion correspondence. It excludes Matlab function calls which are not directly relevant to the tracker such as image display, colour map conversion, and function calls to graphic handlers. Other functions excluded include pre processing and post processing function calls specific to the tracker but are called only once during the execution of the application. The accuracy of the tracker measured by detection rate, and false positive rate was unchanged for both tables 8.3 and 8.4, however whilst the execution time was significantly reduced. It is seen that from table 8.4 that about one half of its time is spent running motion estimation and the main control function. A critical analysis of the code reveals that most of the main module is related to track management. Since all these critical steps are window based choice of human window size directly impacts on the computational load. The current implementation of motion estimation is sequential, although motion estimation exhibit large amount of data parallelism. Track initialization and parameter file upload which constitutes the pre processing task has not been included in determining the computational effort since these functions are executed once for the run of the tracker. In sequential mode, given an operating confidence level and a motion model, optimal tracks are determined using only the past and the current frame. In batch mode on the other hand, given an operating confidence level required of the tracker, the best fitting motion model with the highest accuracy is searched for from among the six motion models. From table 8.3, by applying frame resizing factor of four, frame processing rate of twenty-nine frames per second is achieved on 2.6 GHZ Pentium IV dual core processor. The frame resizing operation only increases the initial latency of the processing pipeline. Processing option two, defined by table 8.4 achieves a frame processing rate of ten. More details on reducing the processing time is presented in section 9.7.

Table 8.3 Main task profiling of JPDAF tracker (intensity template only). Frame size is 320 X 240.

Task	**Exec_Time/Frame (milliseconds)**	**Percentage**
Main_Tracker_V8(Main module)	22	14.87
Classifier_Functions	5	3.38
Motion_Estimation_Functions	13	8.78
Object_Window_Based Processing	8	5.40
JPDAF Tracking	100	67.57
Total	148	100

Table 8.4 Main task profiling of JPDAF tracker (all templates). Frame size is 320 X 240

Task	**Exec_Time/Frame (Milliseconds)**	**Percentage**
Main_Tracker_V8(Secondary module)	180	13.34
Classifier_Functions	10	0.74
Motion_Estimation_Functions	940	69.62
Object_Window_Based Processing	30	2.23
JPDAF Tracking (Main module)	190	14.07
Total	1350	100

8.14 Interpretation

Investigation into use of tracking to reduce false positives has been validated by simulation and the result is discussed in section 9.6. It is shown that a better estimate of the expected false alarm rate is given by the average of the false alarm rates for the shape and histogram classifier. It is further shown that with this approach the tracker also reduces the false alarm rates at the tracking stage compared with the detection stage. By exploiting different motion models offline the best model setting for tracking can be determined.

The tracker runs in both sequential and batch estimation mode. By using different settings for Mahalanobis confidence metric it is possible to quickly select the best track hypothesis. In sequential mode decisions are made based on the previous frame only, whilst in batch estimation mode decisions are based on a group of past frames up to the current frame. In batch estimation mode tracking accuracy is improved compared to sequential estimation mode. The computational complexity is linear in the number of humans to track, and is also dependent on the number of feature measurements. There are four algorithmic configuration options available for tracking based on the number of feature templates used. It has also been shown that the tracker achieves real-time processing more than thirty (30) frames per second based on an input frame size of 240 X 320. Figures 8.8 to 8.10 shows typical output of the JPDAF tracker based o the three test sequence. An ellipse is used to indicate found human. Comparative study with mean shift tracking is also presented in chapter nine which demonstrates that it achieves higher detection rate compared to mean shift tracking, but the false positive rate for the mean shift tracker is relatively low. By carefully adjusting algorithmic parameters is possible to optimized to track both individuals in a group as well as the group itself. Appendix E is a table showing accuracy of the proposed JPDAF tracker under changing algorithmic parameters.

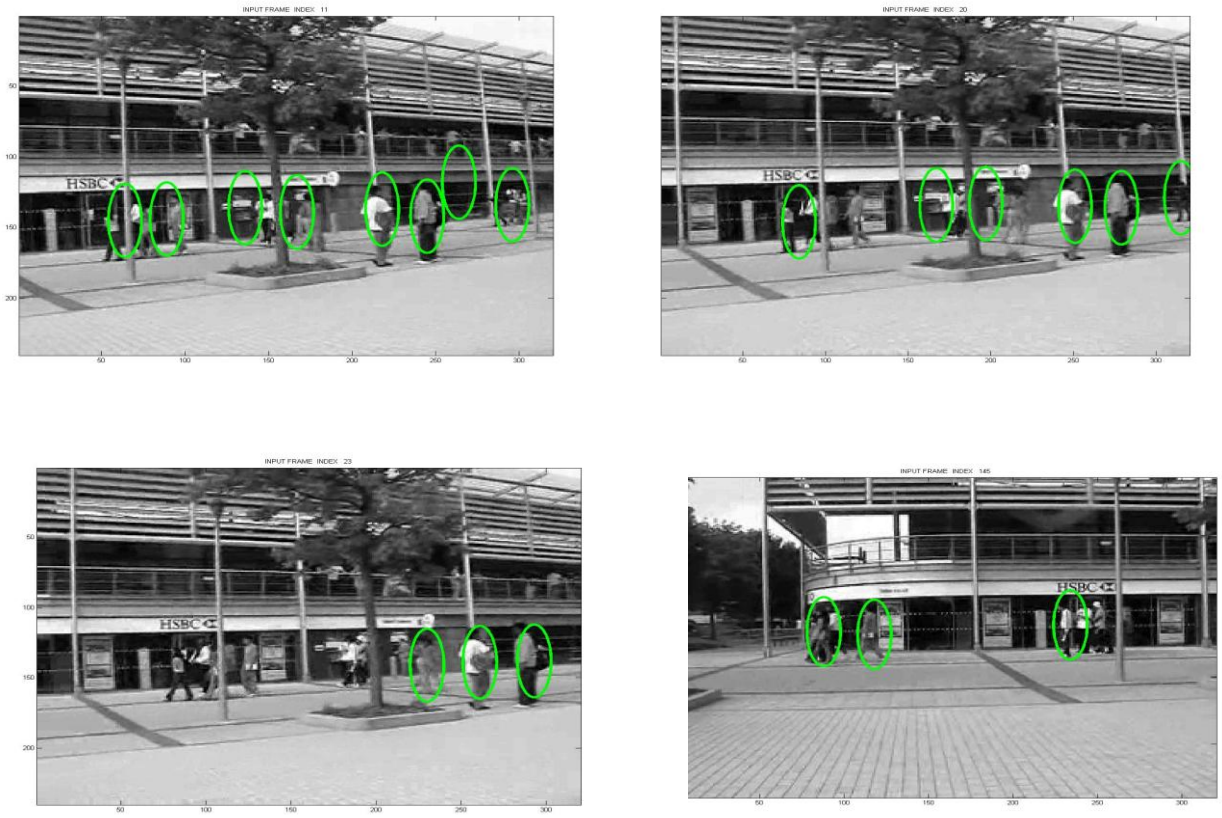

Figure 8.8 Tracker output (from top left to bottom right) for Hamilton2b.avi : input frames 11, 20, 23, and 146

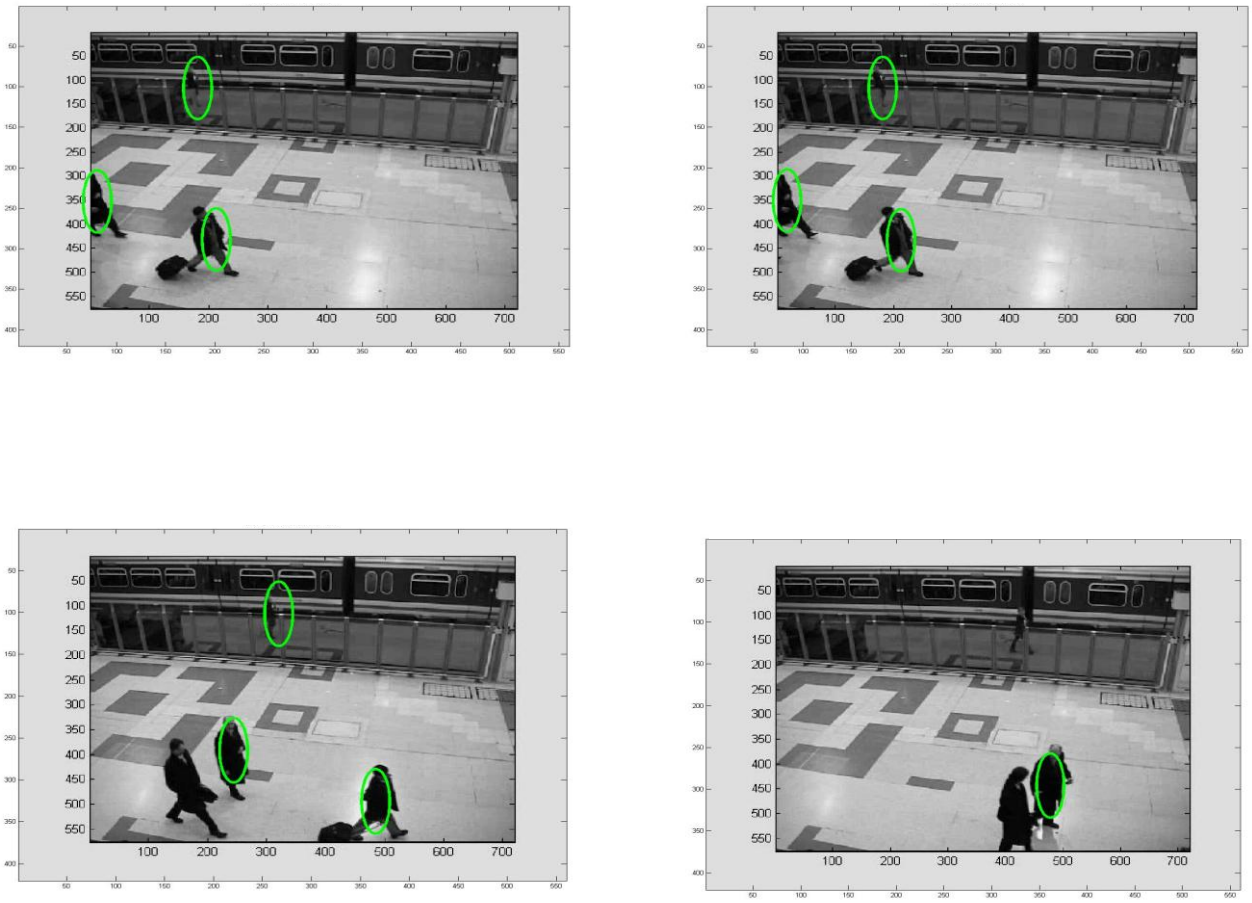

Figure 8.9 Tracker output (from top left to bottom right) for Stc_t1_c_3.avi : input frames 267, 268, 314, and 353

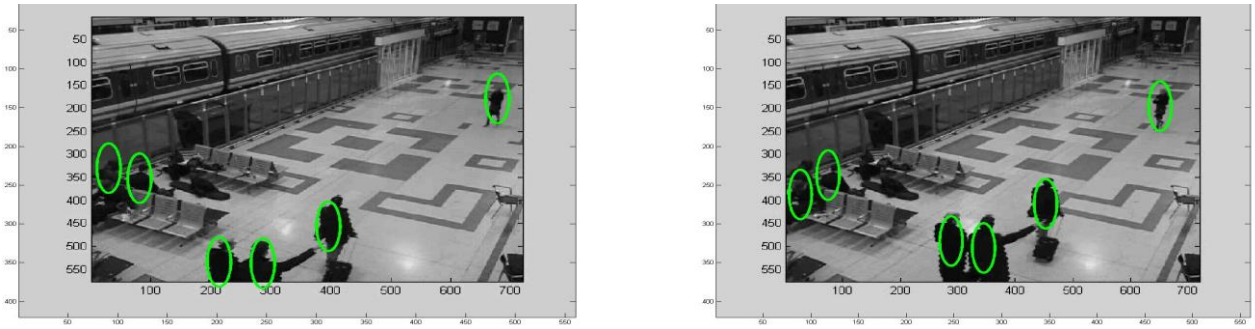

Figure 8.10 Tracker output (from left to right) for Stc-t1_c_4.avi: input frames 105 and 120

CHAPTER NINE

CONSOLIDATION OF RESULTS

9.1 Introduction

The results of the combined human detection and tracking stages (chapters six and seven) are presented in this chapter. Section 9.2 starts with an approach for online estimation of optimum algorithmic parameters, whilst section 9.3 introduces an algorithm for adaptive monitoring and control of detection and tracking accuracy. Section 9.4 by way of analysis illustrates the algorithm implemented as part of accuracy control in human detection. Section 9.5 discusses trends on detection, miss detections and false alarm rates, and their sensitivity, whilst section 9.6 discusses accuracy at the tracking stage. Section 9.7 provides analysis of execution times of sub tasks of histogram detectors, shape-outline detector, combined shape and histogram detector, and JPDAF tracker, as well as the different algorithmic configurations options. Section 9.8 compares the accuracy of the proposed detection and tracking algorithm with other competitive algorithms using the same video sequences: Gaussian mixture modelling based human detection technique is compared with the proposed human detection technique, whilst that of mean shift tracker is compared with the proposed JPDAF tracker. Additionally the accuracy of the system based on PETS 2006 evaluation metrics proposed in [Bashir and Porikli 2006] is also presented. In section 9.9 a scalable algorithmic architecture is synthesised for combined human detection and tracking. Section 9.10 discusses the results detailing out problems and progress made at different stages of development of human detection and tracking algorithm. Section 9.11 provides a review of the research findings.

The three video sequences used in the evaluation stage are classified into three scenarios: Scenario one is a scene with high clutter, high human density, with humans

appearing in groups and as individuals at different times on Brunel university campus with no scale changes (Hamilton2b.avi sequence). Scenario two is a scene outside a train station with travellers moving about. It has low scene clutter with moderate background contrast and poor illumination. Several humans appear in groups of three or more, as individuals moving towards different directions at different times, and sometimes partially visible (Stc_t1_c_3.avi). Scenario three is a train station with low illumination, low contrast with humans appearing darker than the background, and with low scene clutter. Several individuals come together at different times, and sometimes with significant scale changes (Stc_t1_c_4.avi). Ground truth labelling was done such that it included selected individuals in a group, whilst all isolated individuals in a frame were also labelled. The capability of the proposed algorithm to detect individuals appearing alone, and within groups were evaluated in the presence of scene clutter, low contrast, and scale changes. The criteria for detecting matching candidate humans were discussed in section 2.10.3. The problems of insufficient overlap, and oversized candidate windows being matched to a ground truth objects are avoided by specifying minimum area overlap and maximum distance of separation between system found humans (found by the algorithm) and the ground truth. These requirements were specified as part of the metrics in section 2.10.2.

9.2 Determining Optimum Algorithmic Parameters for Human Detection and Tracking

There are three main parameter types used in controlling the accuracy of the human detection and tracking application. They are constants, flags, and non constants. Constants remains fixed throughout the execution time of the application. These include region of interest definition, average dimension of human window, thresholds for shape-outline map, and minimum pixel count threshold for found human. Flags (the second category) are used to determine the type of intermediate processing required. These include flags for median filtering, histogram equalization, pixel saturation control, classifier type, wavelet decomposition level, and sub sample flag. The third category includes variable parameters whose values fall within a range of values. These include threshold for motion detection, threshold for salient feature localization, number of regions to segment, and minimum pixel count threshold for

silhouette of human. Constants and flags are determined by examining few seconds of the video sequence. Optimum values for parameters of the third class (variables with dynamic range) are determined by running the application and changing the parameter values (in steps of 0.1 till 0.9) for motion and feature detection thresholds, and threshold for shape-outline map (in steps of 5) independently. The final set of optimised parameters is used as input to the algorithm after classifying the sequence according to scene content category defined in table 9.1.

Table 9.1 Scene complexity descriptor for human detection and tracking

Scene descriptor	**Parameter value**
Slow motion	Flag (MOTION_TYPE=SLOW)
Fast motion	Flag (MOTION_TYPE=FAST)
Scale changes	Flag (Level_Index)
Clutter	Flag (Background_Memory, MedianFlag)
Shadows	--
Low contrast	Flag(HISTOGRAM_EQUALIZATION)
Multiple humans	Maximum human count (MaxNoObjects)
Object brightness control	SATURATION_CONTROL_FLAG

The following are the main algorithmic parameters: region of interest, human window width, and human window height. Human window width and height are obtained by direct measurement from the image frame. For example the average height and width of a human is measured in units of pixels directly from the image. The remaining parameters are determined by systematically varying their initial values. The selection of the optimum parameter set is based on statistical characterisation of detection rate and false alarm rates using a 2X2 confusion matrix. The resulting set of parameters is used in generating ROC curves for the shape-based detector, histogram based detector, and the combined shape and histogram detectors (either by assuming a parametric curve or otherwise). The following empirical observations were made during earlier accuracy evaluations:

- When there is significant change in average dimension of humans in part of the video sequence, higher level wavelet decomposition (level 2 or 3) may be used to reliably detect reduced size (low resolution) humans;
- Region of interest should be defined such that it covers areas where most of the humans are located to reduce candidate localization time.

9.3 Adaptive Monitoring and Control of Detection and Tracking Accuracy

There are three main stages in adaptive monitoring and control of accuracy of human detection and tracking applications, namely, parameter tuning (calibration) phase, accuracy adjustment, and accuracy prediction. An initial parameter set is chosen for simulation and the parameters are adjusted over several iterations until an acceptable accuracy level is achieved. The user selects humans by examples in some frames and defines them as ground truth. Ground truth frames are labelled by marking the approximate location of the centroid of humans and passing a table file containing the centroids and the corresponding frame labels during training. Algorithmic parameters are determined as discussed in section 9.2, and ROC curves are plotted according to motion type (table 9.1). The approach adopted in providing operating detection and false alarm rates is based on using the best and the worst case scenario. It is also similar to the work of [Oberti et al. 2001] in the use of ROC curves and mean squared error criteria. ROC curves are generated for different motion type and desired detection rate estimated initially from the stable section of the combined shape and histogram detector curves. The stable section corresponds to the part of the ROC curve where change in one parameter does not change the detection rate significantly (less than 5%). Instead of evaluating the area under the curve, the minimum root mean squared error is used in determining the stability of the operating point assuming that each of the points on the curve is a candidate operating point. The error term is defined by equation 9.1. Equation 9.2 also defines the average distortion.

$$\text{term(i)} = \sqrt{(\text{D\_Pdetect(i)} - \text{O\_Pdetect(i)})^2 + (\text{D\_FA(i)} - \text{O\_FA(i)})^2} \qquad 9.1$$

$$f(P_d(i), P_f(i)) = [\sum_{\substack{j=1 \\ j \neq i}}^{NoPoints} term(j)) / NoPoints] \quad 9.2$$

Terms D_Pdetect(i) and D_FA(i) defines the desired detection and false alarm rate, whilst O_Pdetect(i) and O_FA(i) defines operating detection and false alarm rates respectively. Equation 9.1 computes the root square error for every point on the ROC curve. The justification for this approach is that the detection rate and false alarm rate is determined by varying several algorithmic parameters simultaneously from the initial operating point on the ROC curve. Under this condition the shape of the curve does not follow the ideal ROC curve. Equation 9.2 computes the error (using equation 9.1), and then the root mean squared error is computed (equation 9.2) as the average deviation. It is used in adjusting the detection and false alarm rates. The point on the ROC curve with the minimum root mean squared error is selected as the operating point. The probability of correct detection is still given by the area under the curve. Different operating points on the ROC curve could hence be defined based on the desired operating accuracy defined by detection rate and false alarm rate. Assuming there are only seven algorithmic parameters, let the shape-outline (histogram detector) threshold during iteration i be denoted as OT(i), FA_i, and D_i the false alarm and detection rate respectively. Let the corresponding candidate human width be W1(i), candidate human height H1(i), feature detection threshold F1(i) and motion detection threshold M1(i). The following steps are applied recursively to dynamically determine operating parameters on a frame by frame basis:

1 Initially generate ROC curves for the combined classifier based on the detection and false alarm rate pair, (D_0, FA_0), during the training step. Assuming there are N sample points on the resulting ROC curve.

2. Select the maximum of D_k(1:N) on the ROC curve with minimum FA_k(i) as the initial operating point (k denotes the index on the ROC curve). In case there are multiple points, select one at random. Let X(k)=[D_k, FA_k, OT(k), W1(k), H1(k), F1(k), M1(k)] be the parameters for the ROC point, (D_k, FA_k). Use the algorithm below to determine an operating point on the feasible part of the ROC curve whilst a point on the curve is dropped, a new point is added to the curve. This ensures that at anytime only N points are on the ROC curve.

   r=1;

   Set distort (r, i)=0 for each of the initial N points.

Repeat

3. Vary either one or more of the five parameters, and run the application using the new parameter set. Let the new parameter set be X(k+r)=[$D_{(i+r)}$, $FA_{(i+r)}$, OT(k+r), W1(k+r), H1(k+r), F1(k+r), M1(k+r)];
4. Determine the new operating point using equations 9.1 and 9.2.
   a. r=r+1;
   b. Compute Distort(r, i) for point i based on equation 9.1 for each of the N points.
   c. Compute Min= $f(P_d(i), P_f(i))$ (equation 9.2).
5. Determine Operat(i) = argmin [Min- Distort(r, i)] of all N points on the ROC curve. The point on the curve to be dropped is the point closest to the Min(i): X(o)=[D_o, FA_o, OT(o), W1(o), H1(o), F1(o), M1(o)]. Add the new point (D_k,FA_k) to the ROC curve, and use [D_k, FA_k, OT(k), W1(k), H1(k), F1(k), M1(k)] as the new algorithmic operating parameter set.
6. Repeat steps 4 and 5 until an operating point as close to the desired operating point is achieved.

   The point on the ROC curve which leaves the ROC curve is the one with the largest Distort (r, i) term. Section 9.4 applies this accuracy prediction algorithm to evaluate the optimum accuracy level for stc-t1-c_3.avi. The proposed accuracy level prediction algorithm is applicable to both the detection and the tracking phase. The adjustment is performed in steps five and six.

9.4 Accuracy Prediction Analysis

The algorithm defined in section 9.2 is applied to the detection stage of video sequence stc_t1_c_3.avi as follows: The initial set of points extracted from the combined shape-outline and histogram detector accuracy table (values as a percentages) is shown in table 9.2 with the following parameters:

TPR: True positive rate

FPR: False positive rate

C: Candidate human width

D: Candidate human height

A: Feature detection threshold proportion

B: Motion detection threshold proportion

OT: Outline threshold

Assuming the desired operating point is (90.9, 0.66) on the ROC curve, then row 1 is chosen as the initial operating point since it has the highest detection rate. Row 11 is not chosen as the operating because of its higher false positive rate. Parameters OT, C, D, A, B are used in setting the parameters for the next iteration. The root mean squared error term is computed for all other points. Deviation from root mean squared error term is shown in table 9.3 from which the parameters corresponding to the smallest deviation is chosen as the next operation point for the next iteration. The row 4 is hence chosen as the parameter setting for the next iteration.

Table 9.2 Combined shape and histogram detector for stc_t1_c_3.avi showing parameters of the third kind

Run	TPR	FPR	OT	C	D	A	B
1	90.9	0.66	15	48	128	0.6	0.7
2	78.66	0.8	15	32	128	0.2	0.7
3	83.27	2.36	15	32	128	0.2	0.7
4	90.59	2.5	15	48	128	0.4	0.7
5	89.61	7.19	15	56	128	0.2	0.7
6	89.98	7.51	15	48	128	0.2	0.7
7	89.67	9.41	15	64	128	0.1	0.7
8	87.95	9.81	15	48	128	0.2	0.7
9	88.03	10.65	15	56	128	0.2	0.7
10	70.93	42.15	15	48	128	0.2	0.7
11	94.51	79.3	15	48	128	0.2	0.7

By repeating the above procedure for row 4 and subsequently iterating the algorithm, optimal operating accuracy as close as possible to the desired operating accuracy is achieved. Accuracy prediction is made by interpolation on the derived ROC curves for histogram, shape, or combined shape and histogram detector. The ROC curve is derived by fitting a parabola to the set of derived operating points described in the algorithm above. The ninety-five percent confidence interval probability (for detection and false alarm rates) could also be estimated and use as the basis for comparison (as in Daimlerchrysler benchmark).

Table 9.3 Intermediate computation for determining operating point on ROC curve during an iteration

Run	TPR	FPR	Term	Deviation (from average)
1	90.9	0.66	89.9511762	0.2711762
2	78.66	0.8	77.7123163	-11.967684
3	83.27	2.36	82.3483333	-7.3316667
4	90.59	2.5	89.6695021	-0.0104979
5	89.61	7.19	88.9351207	-0.7448793
6	89.98	7.51	89.3295976	-0.3504024
7	89.67	9.41	89.1967628	-0.4832372
8	87.95	9.81	87.52915	-2.15085
9	88.03	10.65	87.7047827	-1.9752173
10	70.93	42.15	81.5904584	-8.0895416
11	94.51	79.3	122.516463	32.8364626
Average			89.680333	0.000333

9.5 Detection and Error Rates Analysis

The baseline performance for shape-outline based and histogram based detectors are shown in tables 9.4 and 9.5, 9.6, and 9.7. The baseline performance was evaluated by computing the average detection rate and false alarm rates over several runs, and choosing the run closest to the average TPR. The column labelled std, refers to the standard deviation of the TPR. Only one algorithmic parameter was changed at anytime with the other parameters fixed. The ideal ROC curve is concave when one parameter is varied, exhibiting increasing detection rate with increase in false alarm rate, and vice versa. The underlying assumption is that at detection rate of zero the false alarm rate is zeros, i.e, it passes through the origin. However when several parameters are varied as in a typical deployment scenario the curve deviates from the ideal one due to the influence of several parameters each with its own associated

operating point. The shape of the graph is generally non linear and unpredictable. It is best described as piecewise continuous.

Table 9.4 Baseline performance of shape-outline based detector

Video sequence	**TPR**	**FPR**	**FNR**	**PPV**	**F1**	**Std**
Hamilton2b.avi	63	45	37	0.36	0.46	0.04
Stc_t1_c_3.avi	75	5	27	0.82	0.78	0.12
Stc_t1_c_4.avi	62	20	38	0.46	0.53	0.09

Table 9.5 Baseline performance of Histogram based detector (Edge saliency)

Video sequence	**TPR**	**FPR**	**FNR**	**PPV**	**F1**	**Std**
Hamilton2b.avi	49	35	51	0.29	0.36	0.29
Stc_t1_c_3.avi	53	5	47	0.83	0.65	0.08
Stc_t1_c_4.avi	47	34	53	0.90	0.15	0.20

Table 9.6 Baseline performance of Histogram based detector (Motion saliency)

Video sequence	**TPR**	**FPR**	**FNR**	**PPV**	**F1**	**Std**
Hamilton2b.avi	46	25	54	0.22	0.30	0.09
Stc_t1_c_3.avi	43	7	57	0.59	0.50	0.12
Stc_t1_c_4.avi	47	26	53	0.31	0.26	0.18

Table 9.7 Baseline performance of Histogram based detector (Background saliency)

Video sequence	TPR	FPR	FNR	PPV	F1	Std
Hamilton2b.avi	82	39	18	0.27	0.36	0.19
Stc_t1_c_3.avi	80	6	19	0.78	0.80	0.03
Stc_t1_c_4.avi	81	31	19	0.41	0.54	0.12

At a confidence level of ninety-five percent the following peak detection rates would be realised 66%, 80%, and 65% respectively for the hamilton2b.avi, stc_t1_c_3.avi, and stc_t1_c_4.avi for the shape based detector.

Figures 9.1 to 9.3 is a plot of detection rate versus false alarm rate by varying several algorithmic parameters to evaluate sensitivity in detection and error rates with changes in parameters. For each of the figures the first three curves refers to the case when the shape, histogram levels 1 and 2 detectors are running alone, whilst the last two curves refers to when the combined shape and histogram are running in parallel. It was noted that the quoted values varies by as much as 5% . This is attributed to uncertainty in manually labelling the centroid of the candidate human, and in locating candidate humans. Additionally, selected human locations from the salient feature map may vary from one run to another to changes in algorithmic parameters. It is observed that the detection rate falls off rapidly for changes in false alarm rate of more than five in hundred. With increasing candidate human window dimension there is also an increase in detection rate and false alarm rate until a threshold point is reached at which the detection rate starts falling with the false alarm rate remaining relatively unchanged. It can be seen that the peak detection rates of the combined shape and histogram based detectors is consistently higher for all the three test sequences over small changes in false alarm rate. Hamilton2b.avi sequence has no change in the dimension of humans, since everyone is moving along the pavement with the camera moving horizontally. With this sequence, it is observed that the shape-outline detector achieves relatively high detection rate with small range in false alarm rate. The histogram detectors (levels 1 and 2 achieve relatively low detection rate over the same false alarm rate. The combined shape-outline and histogram detector achieves high detector at the cost of higher false positive rate (false alarm rate) following the trend

of false alarm rate of the histogram detectors. Clearly using level 2 histogram detector has not resulted in a significant increase in detection rate. The relatively low detection rate compared to the other sequence is due to the fact that most of people being detected are in groups, thus a group might have been detected but a particular individual may not have been detected. The ground truth labelling was done for individuals and not for groups as a whole. The main challenge with this sequence is the high scene clutter, and high human density. The effect of scale changes are noticeable in Stc_t1_c_3.avi and Stc_t1_c_4.avi, two sequences with multiple humans appearing with scale changes. Applying level two wavelet analysis results in higher detection rate compared to level one histogram detector over relatively large changes in false positive rate. Stc_t1_c_3.avi however has higher detection rate compared to Stc_t1-c_4.avi where illumination was not quite good, with humans appearing darker than the background. In sequence stc_t1_c_3.avi, there are several instances where travellers come to the scene and exit from the scene in different directions, as well as obvious instances where the classifier fails to detect humans because they were wearing hats, overcoats, or in a posture exposing minimal features to the classifier. Histogram equalization technique was applied to the frames but the improvement was marginal. With the shape based detector the relative sensitivity of detection rate with false alarm rate, candidate human width and height, and shape-outline threshold were investigated. Peak detection rate varies between 50- 85% for the shape-outline based detector. The detection rate also increases with the scale factor parameter for candidate human window size up to a factor of two after which there is no more increase. Similarly with histogram detector candidate human window dimension, saliency thresholds, separation distance between candidates when classifying multiple humans, and scale factor when searching for multiple humans are the most important parameters. The general observation is that the histogram detector is relatively less sensitive to most algorithmic parameter changes. However it is sensitive to changes in separation distance between humans. It is also observed that the RO curve for the combined detector can be partitioned into two sections, a stable section and non stable section. The stable section is less sensitive to changes in false alarm rate (corresponding to less than 5%), whilst the non stable section is sensitive to algorithmic parameters changes.

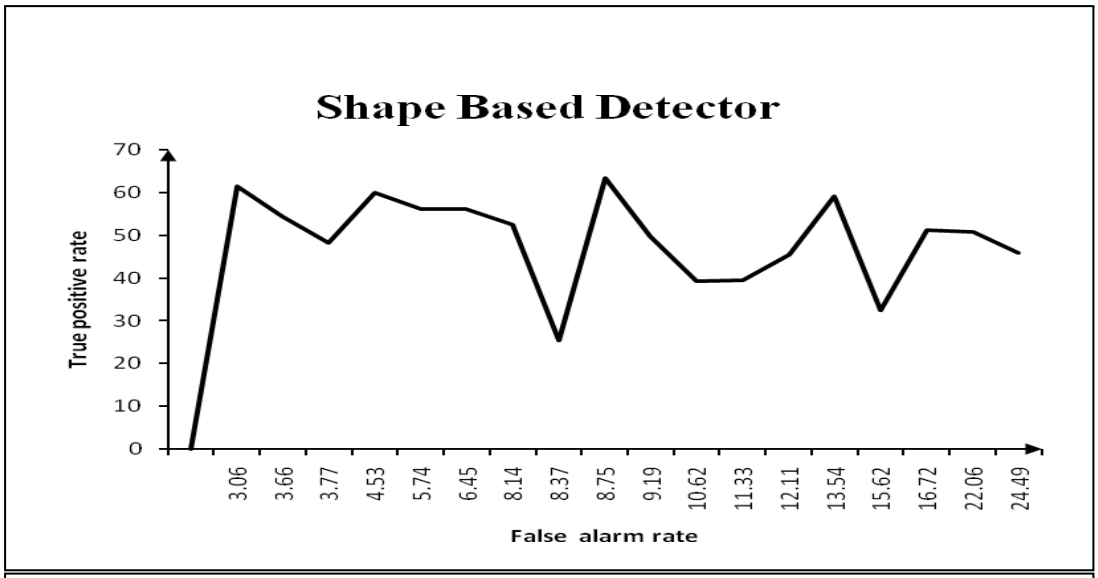
Shape Based Detector
True positive rate
70
60
50
40
30
20
10
0
3.06
3.66
3.77
4.53
5.74
6.45
8.14
8.37
8.75
9.19
10.62
11.33
12.11
13.54
15.62
16.72
22.06
24.49
False alarm rate

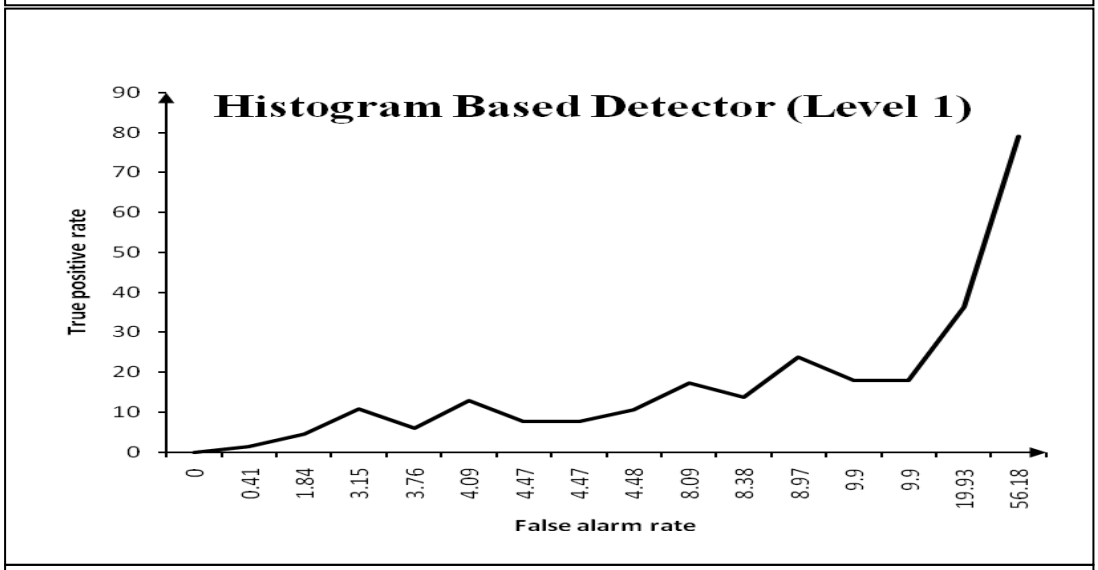
Histogram Based Detector (Level 1)
True positive rate
90
80
70
60
50
40
30
20
10
0
0
0.41
1.84
3.15
3.76
4.09
4.47
4.47
4.48
8.09
8.38
8.97
9.9
9.9
19.93
56.18
False alarm rate

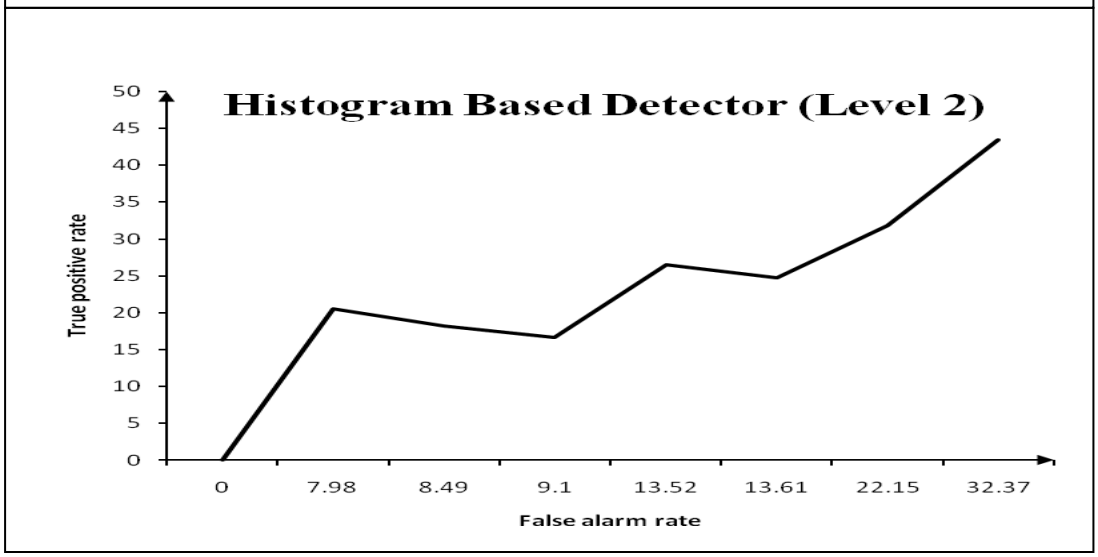
Histogram Based Detector (Level 2)
True positive rate
50
45
40
35
30
25
20
15
10
5
0
0
7.98
8.49
9.1
13.52
13.61
22.15
32.37
False alarm rate

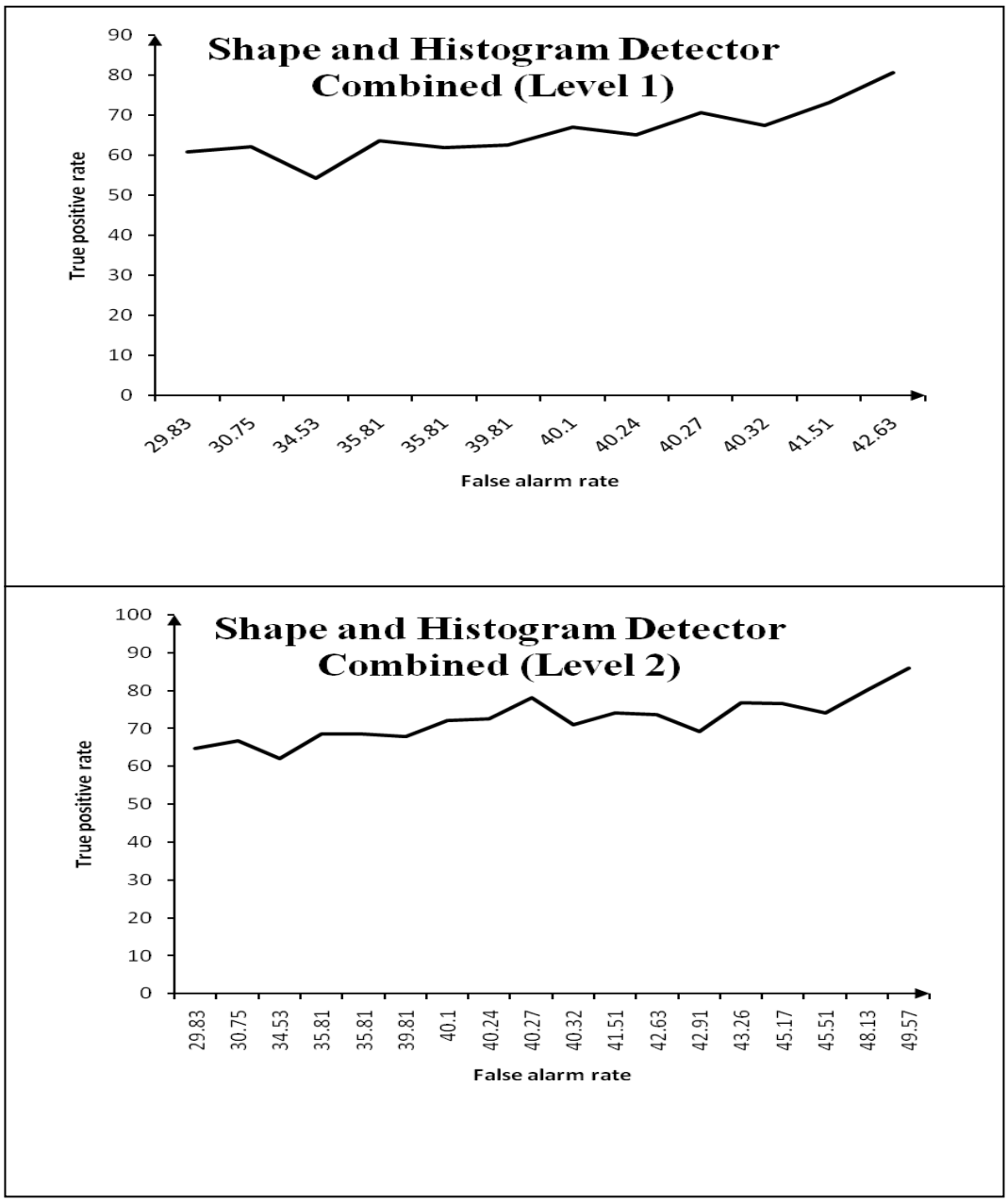

Figure 9.1 ROC curves for Hamilton2b.avi showing accuracy trends for different detectors

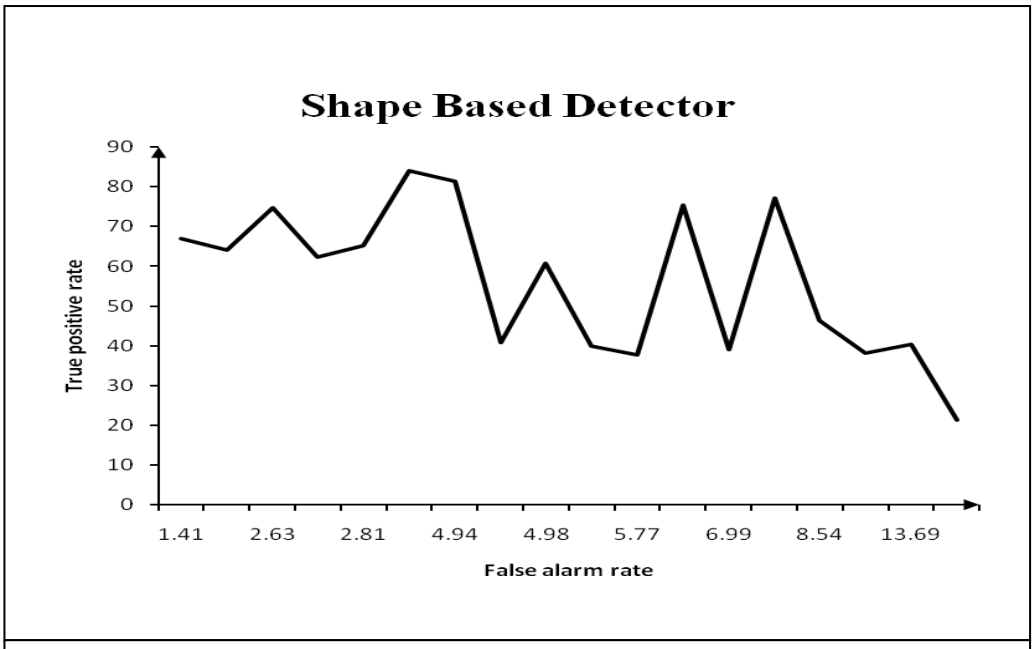
Shape Based Detector
True positive rate
90
80
70
60
50
40
30
20
10
0
1.41
2.63
2.81
4.94
4.98
5.77
6.99
8.54
13.69
False alarm rate

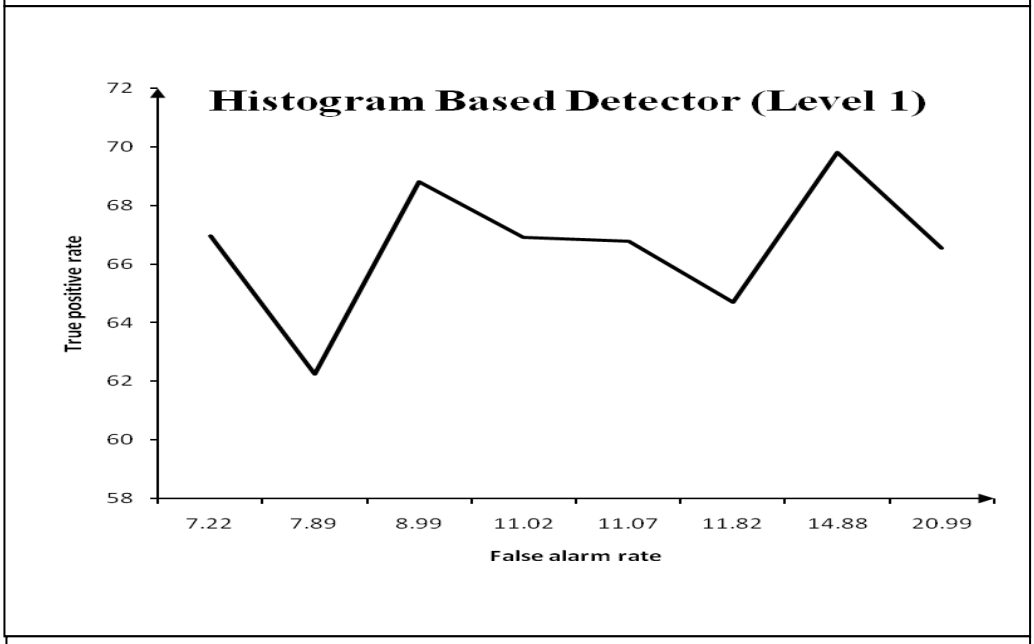
Histogram Based Detector (Level 1)
True positive rate
72
70
68
66
64
62
60
58
7.22
7.89
8.99
11.02
11.07
11.82
14.88
20.99
False alarm rate

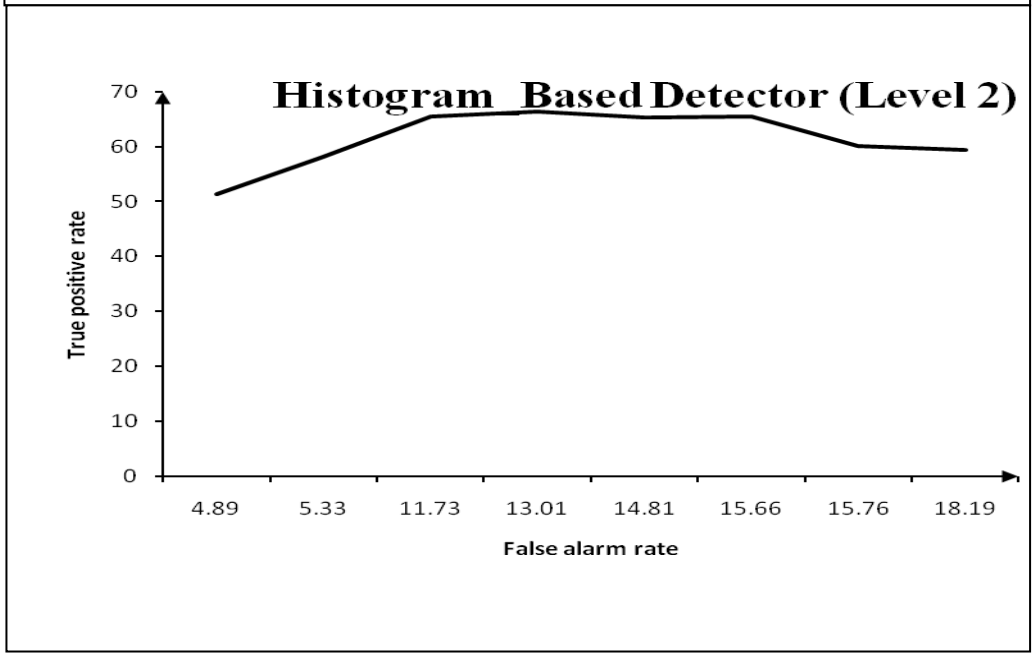
Histogram_Based Detector (Level 2)
True positive rate
70
60
50
40
30
20
10
0
4.89
5.33
11.73
13.01
14.81
15.66
15.76
18.19
False alarm rate

When these parameters are changed the detection rate increase with increase in false alarm rate until it gets to the threshold point thereafter accuracy trend is reversed. The general observation is that:

- each curve can be partitioned into two sections, namely, the stable section (low variation in detection rate versus false positive rate) and the unstable section (high variation in detection rate versus false positive rate).

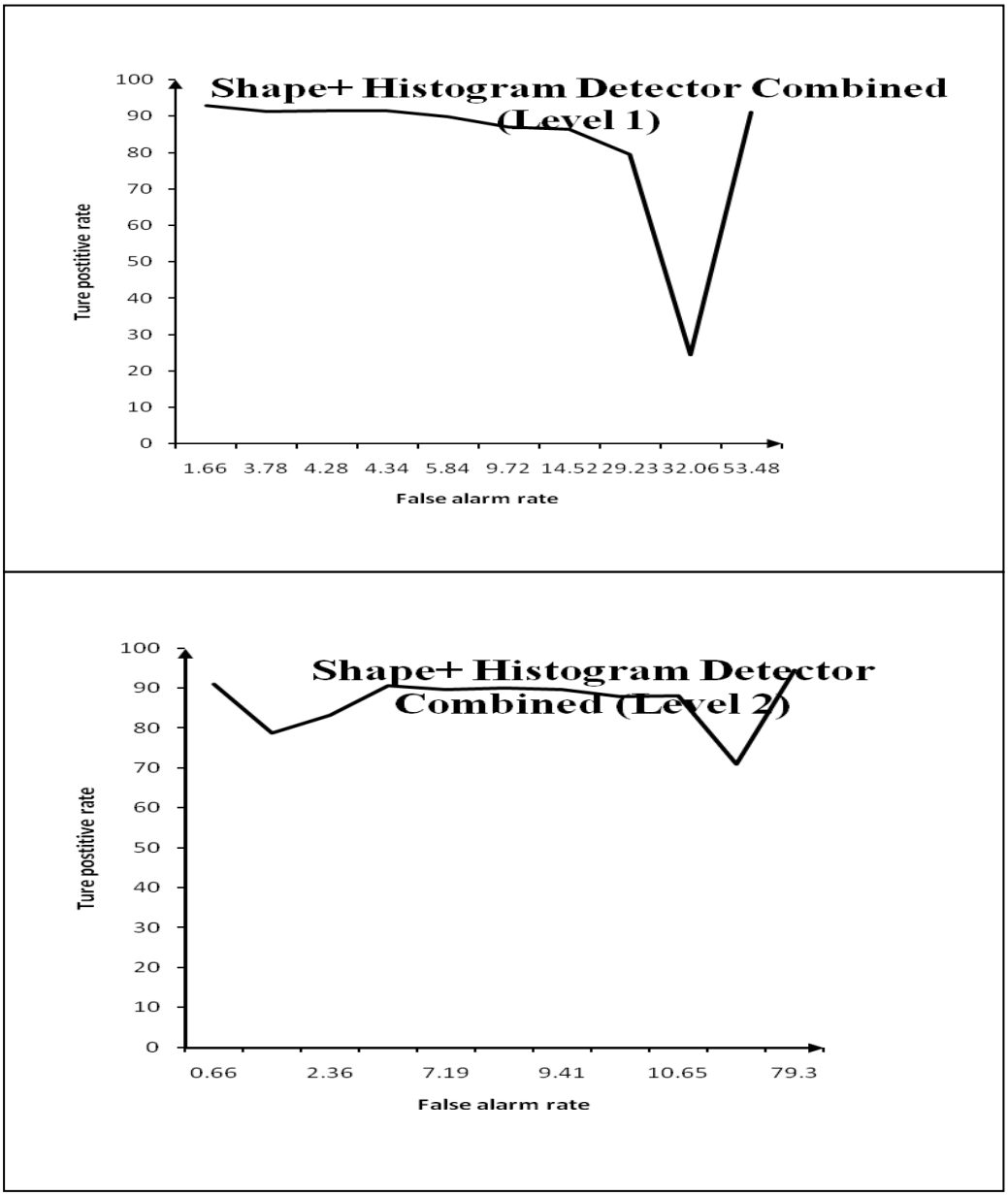

Figure 9.2 ROC curves for stc_t1_c_3.avi sequence showing accuracy trends for different detectors

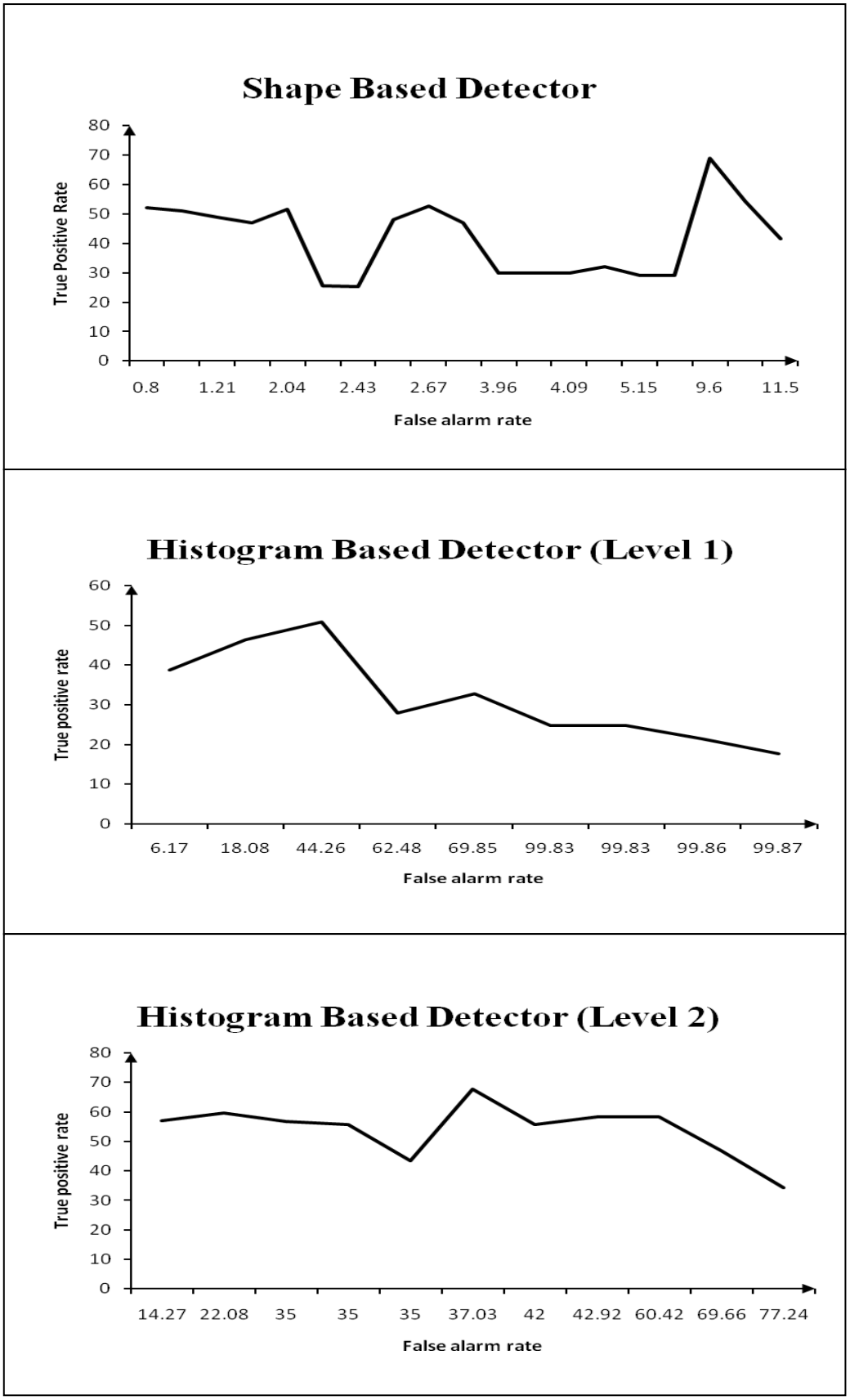
Shape Based Detector
True Positive Rate
80
70
60
50
40
30
20
10
0
0.8
1.21
2.04
2.43
2.67
3.96
4.09
5.15
9.6
11.5
False alarm rate
Histogram Based Detector (Level 1)
True positive rate
60
50
40
30
20
10
0
6.17
18.08
44.26
62.48
69.85
99.83
99.83
99.86
99.87
False alarm rate
Histogram Based Detector (Level 2)
True positive rate
80
70
60
50
40
30
20
10
0
14.27
22.08
35
35
35
37.03
42
42.92
60.42
69.66
77.24
False alarm rate

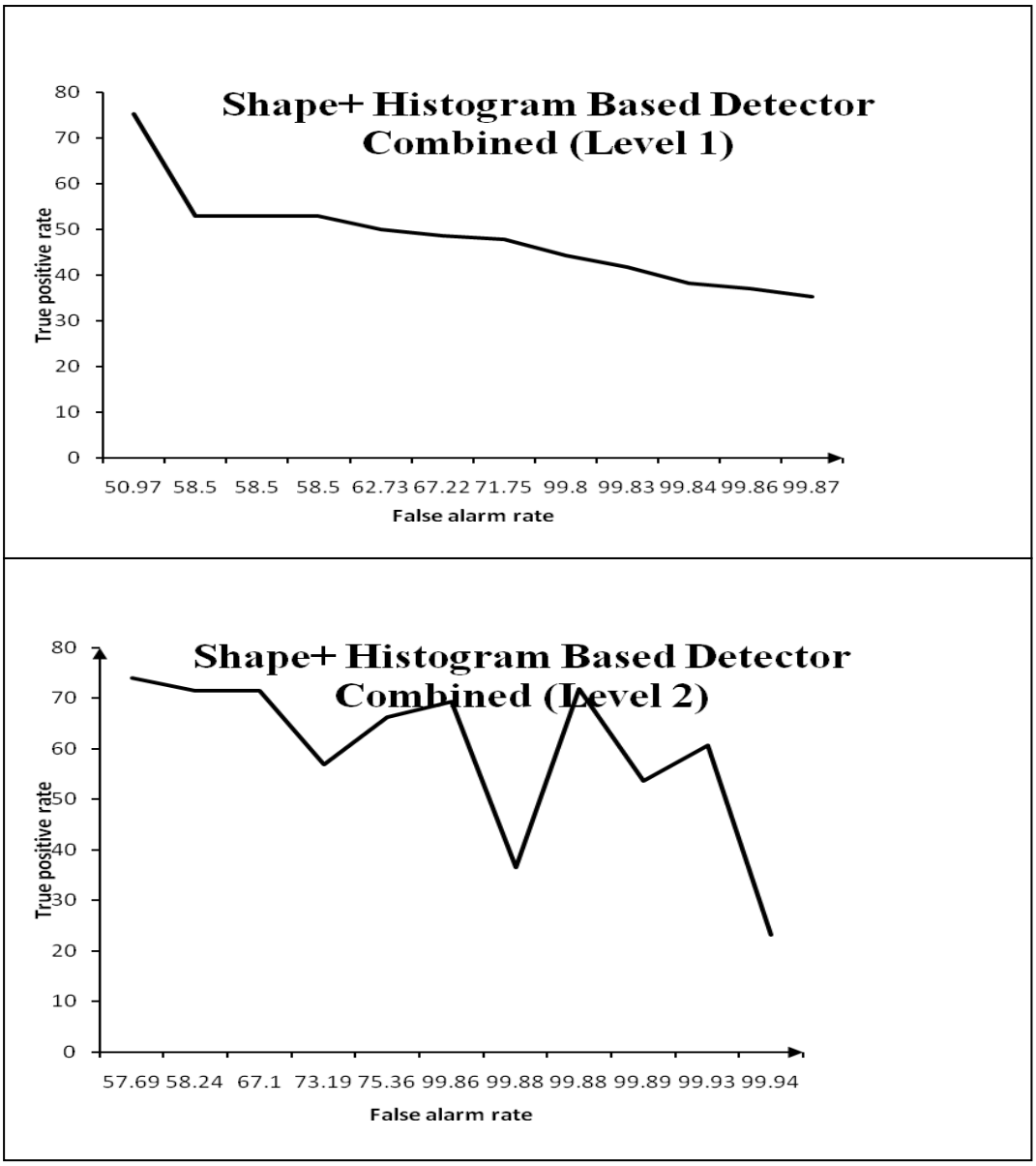

Figure 9.3 ROC curves for stc_t1_c_4.avi showing accuracy trends for different detectors

Thus using the stable section of the combined detector to predict operating accuracy level would ensure minimum fluctuation in accuracy level. Further accuracy fluctuations in the combined shape-outline based and wavelet histogram based detectors were more than that of any of the individual detectors, in the stable section, however, the highest detection rate is obtained when the output of the two detectors are added up.

9.6 Track Detection and Error Rates Analysis

The objectives of the tracking stage are to provide tracking information (location and velocity information) by linking found humans over several frames, and to investigate the use of tracking phase to reduce the high false detections incurred at the detection stage. The tracker optionally has a human detection module which automatically detects any humans missed at the detection stage (e.g, when a group splits into multiple people). New tracks could then be initiated by the tracker. The minimum area overlap between the ground truth and the found human (system found human) is set to fifty percent of the area of the human defined by the ground truth. Similarly the maximum error in the centroid of the system found human (humans found by the algorithm) and the ground truth is set at fifty percent the dimension of the width and height of the ground truth. Other parameter settings for the tracker are as follows: the maximum number of humans to track in a frame are 8, 10 and 10 for hamilton2b.avi, stc_t1_c_3.avi, and stc_t1_c_4.avi respectively. By considering that the detection output as noisy, the tracking phase is able to reduce the high false positive rate. The performance of the detectors after tracking is shown in table 9.8. Clearly the tracker has reduced the high false alarm rate compared to the baseline performance before tracking (see table 9.13b).

Figure 9.8 Combined (shape+histogram) detector performance after JPDAF tracking

Sequence	**TPR**	**FPR**	**FNR**
Hamilton2b.avi	94	29	6
Stc_t1_c_3.avi	89	5	11
Stc_T1_C_4.avi	90	28	10

With the optional detection module running during tracking more spurious candidate humans are found and passed to the tracker. This accounts for the higher track detection rate for hamilton2b.avi at the tracking stage compared to before tracking. Tracking thus acts as a temporal filter able to match consistently labelled human over its duration, and rejecting spurious detections. It accounts for the higher detection rate after tracking

compared to the detection rate before tracking. The analysis of the average false alarm rate for the combined detectors and tracker is summarised in table 9.9 for the three test sequence. The aggregate false alarm rate for the combined shape and histogram detector may be estimated as weighted combination of the false positive rates of the two detectors since they run in parallel with each other. Further the combined false positive rate cannot be less than the maximum of the two detector. It is justified since this measure depends on the number of windows examined. Thus the expected combined false detection rate for hamilton2b.avi sequence is 84 (maximum {68, 84}), for stc_t1_c_3.avi is 84 (maximum{81, 84}), and for stc_t1_c_4.avi is 86 (maximum {71, 86}). Comparing 82, 53, and 67 respectively obtained by simulation (column 3 of table 8.4) with the false positive rate of the JPDAF tracker which are respectively 6, 11, and 10 (column 4), it is obvious that the proposed JPDAF tracker has significantly reduced the false positive rate (false alarm rate).

Further analysis of the true positive and false positive rates for the detector and the tracker reveals that there is a decrease in both metrics after tracking. This further confirms that the tracker has removed spurious humans found by the detector.

Table 9.9 Expected false positive rate for the combined shape and histogram tracker for the test sequence

Video	**False positive rate shape, histogram detector)**	**False positive rate (combined detector)**	**Expected false positive rate (for tracker)**	**JPDAF Tracker False positive rate**
Hamilton2b.avi	{68,84}	82	84	6
Stc_t1_c_3.avi	{81,84}	53	84	11
Stc_t1_c_4.avi	{71,86}	67	86	10

The decrease in true positive rate compared with the tracker suggests more of the candidate humans classified at the detection stage were false positives. Spurious candidate humans were eliminated by the tracker.

Towards automated evaluation of tracking, PETS 2006 metrics proposed in [Bashir and Porikli 2006] for the three test sequence is presented in tables 9.10 and 9.11 (refer

to section 2.10.2 for definitions of metrics). Each table presents one of the two main approaches, namely, frame-based, and object based. The frame based metrics treats each frame's outcome independently. On the other hand the object based approach uses the average area overlap given a particular human (track) as a threshold to determine valid humans and is essentially centroid in rectangle approach to tracking. In the object based metric an object overlap of fifty per cent of the ground truth labelled area of the human was also used.

Table 9.10 PETS 2006 Frame based metrics

PETS metrics	**Hamilton2b.avi**	**Stc_t1_c_3.avi**	**Stc_t1_c_4.avi**
TRDR	83	90	99
False alarm rate	0.03	0.08	0.04
Detection rate (Sensitivity)	0.98	0.99	0.99
Specificity	0	0	0
Accuracy	0.84	0.9	0.99
Positive prediction (Precision)	0.98	0.97	0.96
Negative prediction	0	0	0
False positive rate	1	1	1
False negative rate	0.02	0.01	0.01
Mean positional error	4.10	2.90	3.20
Mean Positional error variance	2.10	3.60	4.70

The main difference lies in how the frame based approach enumerate countable events true positive, true negative, false positive, and false negatives. For example, in frame based approach a frame is counted as TP if a least a human is detected in the frame. Thus events at the frame level are counted. In object based approach individual human (object) events are averaged over the duration of the event. Countable events depends on the extent of overlap between ground truth humans and those detected by the application (system) reported smaller values for the same statistics. From table 9.10

higher track detection rate compared to table 9.11 is due to area overlap threshold chosen. The mean values presented in the table is based on a tracking window of ten, and using the average track overlap of 0.5 as threshold. The average area overlap of 0.35. 0.47, 0.41 for hamilton2b.avi, stc_t1_c_3.avi, and stc_t1_c_4.avi respectively, implies lower area overlap was obtained on the average. The mean positional error measures the relative error in using the ground truth as the reference coordinates along the x and y axis. It is measured in units of pixel spacing. The values for the three sequences are: 2.10, 3.60, and 4.70 (in pixels) for the three sequences.

Table 9.11 PETS 2006 Object based metrics

PETS metrics	**Hamilton2b.avi**	**Stc_t1_c_3.avi**	**Stc_t1_c_4.avi**
TRDR	21	73	34
False alarm rate	0	0	0
Detection rate (Sensitivity)	0.50	0.50	0.5
Specificity	0	1	0
Accuracy	0.21	0.63	0.34
Positive prediction (Precision)	1	1	1
Negative prediction	0	0.50	0
False positive rate	0	0	0
False negative rate	0.50	0.50	0.5
Mean overlap	0.35	0.47	0.41
Track fragmentation error	0.02	0.06	0.03
Track merge error	0.02	0.06	0.03

Track detection rate (TDR) metric measures the extent to which a track links the appearance of a particular human continuously over time. The low TDR for hamilton2b.avi sequence compared with the other sequence is partly due to the high occurrence of humans in groups making it difficult for unique track to be associated to a particular human. The zero values for the negative prediction and false positive rate is due to exclusion of frames with no humans in the ground truth. Compared with object

based approach where candidates in a frame are counted when the area overlap threshold is exceeded. TDR for stc_t1_c_3.avi, and stc-t1_c_4.avi are higher since it has less groupings. The frame based metric however is comparatively high since it reports a hit if at least one of the track in the current frame is successfully updated, thus accounting for the higher values than, whilst that of the object based metric is applicable to tracks with both spatial and temporal area overlap above 0.5 threshold. Similar explanation holds for the detection rate. The accuracy metric shown above, closely follows that of TDR) for both approaches. All reported false positive rates are based on number of windows examined. Appendix F shows several graphs of PETS 2006 accuracy metrics trends for various parts of stc_t1_c_3.avi sequence. The discontinuities in the graphs are due to the fact that ground truths were not defined for those frames.

9.7 Task Profiling and Analysis

All profiling analysis was carried out on 2.6 GHz Pentium processor with two gigabytes RAM memory, and running on Windows XP platform. From the profiling analysis average time for the shape-outline based detector given that up to ten humans are expected to be detected in a frame is 0.23 seconds (table 7.8) for an input frame of 240 X 320, whilst that for the level 1 histogram based detector is 1.91 (table 7.6), and 0.52 seconds (table 7.7) for level 2 histogram based detector. The corresponding peak performance for the JPDAF tracking based on only the intensity template is 0.15 seconds. By applying frame resizing to reduce the input frame size to half the original dimension, the execution time for the different task categories listed in the tables is reduced to one quarter their values. Table 9.12 shows the execution time for the different modules of the detector assuming frame resizing is added to the processing pipeline incurring a fixed amount of processing latency. All quoted processing time excludes processing latency for frame input and management of database of found humans, overheads specific to Matlab, and pre and post processing sub tasks. From the profiling result, the base module (shape outline detector plus JPDAF tracker running on one template would achieve a peak processing of twelve frames per second based on input frame size of 120 X 160, and using shape detector and JPDAF tracker running sequentially in a processing pipeline.

Table 9.12 Average execution time of JPDAF tracker with frame resizing

Module	Execution time (seconds)
Shape detector	0.05
Histogram detector(Level1)	0.476
Histogram detector (Level 2)	0.13
JPDAF Tracker	0.037 (One appearance template)

The different algorithmic configuration options for detection are shape-based outline, histogram (level 1), histogram (level 2), Combined (level 1), and combined (level 2) detectors, whilst that of the tracking are one feature, two feature, three features, four features options. When the detector and tracker are running in parallel, it should be possible to improve throughput by re-organising the pipeline. To what extent the processing pipeline could be improved requires investigating scheduling strategies and code optimization techniques.

9.8 Accuracy Comparisons With Other Algorithms

The proposed detection algorithm has been compared with Gaussian mixture modelling (GMM) foreground/background separation (a segmentation technique) in detecting humans. Three out of ten Gaussian mixture components were used to model a pixel, with the most varied components used in creating the foreground pixel as described by equations 8.3 and 8.4 using a temporal window of ten frames.

$$P(X) = \Sigma \; W_{i,j} * N(X_t, \mu, \sigma^2) \qquad 9.3$$

where $N(X_t,\mu,\sigma^2)$ is a multi normal distribution defined as:

$$N(X_{t,}\mu,\sigma^2) = \frac{1}{(2\pi)^{n/2}\sigma} * e^{\ 1/2(x_t - \mu_{tt})^T (x_t - \mu_t)/\sigma} \qquad 9.4$$

where n denotes the number of components used in defining the foreground regions, and $W_{i,j}$ are the weights of the components. μ and σ^2 are the mean and the covariance of the components. The algorithm first determines the foreground regions which appear as blobs. GMM blobs consist of a group of blobs (accumulated blobs) displaced over one frame period, and appears to be together. Thus the first blob of the group is the silhouette of the object at frame instance (frame index-T/2), where frame index denotes the current frame index, and T denotes the number of components of the mixture. Thus blobs seen in the current frame refers to objects in the corresponding past frame. Two detectors were realised, namely, one based on the shape-outline map, and the other based on classifier trained on the GMM blobs. Table 9.13a shows the peak performance when the classifier is based on the shape-outline map using an area overlap threshold of 25%. Table 9.13b shows the peak performance when GMM blobs were used in training, and an area overlap threshold of 50% were used. In all instances the peak performance of the proposed detector (shape+histogram detectors) out performs the Gaussian mixture modelling human detector.

The low performance of GMM may be attributed to the fact GMM is unable to detect individuals in a group. This is obvious by comparing the performance of stc_t1_c_3.avi with that of hamilton2b.avi and stc_t1_c_4.avi where there are several instances of human groupings.

Table 9.13a Peak performance of GMM detector based on classifier trained using GMM blobs

Video	**TPR**	**FPR**	**FNR**	**F1**
Hamilton2b.avi	43.4	0.5	57	0.6
Stc_t1_c_3.avi	50	0.5	50	0.6
Stc_t1_c_4.avi	27.2	1.6	72.8	0.3

Table 9.13b Accuracy evaluations for proposed human detection algorithm compared with Gaussian mixture model (total number of components is five). Values are in percentages.

Video	Detection Algorithm	True positive rate	False positive rate	False negative rate	F1
Hamilton2b.avi	GMM	39	34	61	--
	Shape	68	37	32	0.52
	Histogram	84	31	16	0.36
	Shape+Histogram	93	82	7	0.66
STC_T1_C_3.avi	GMM	59	44	41	--
	Shape	81	5	19	0.50
	Histogram	84	7	16	0.81
	Shape+Histogram	93	53	7	0.51
STC_T1_C_4.avi	GMM	36	40	64	--
	Shape	71	12	29	0.63
	Histogram	86	33	13	0.38
	Shape+Histogram	95	67	5	0.85

The peak detection rate of 93%, 93%, and 955 achieved by the proposed detectors is comparable to the reported performance in Daimlerchysler experiment conducted recently [Enzweiler and Gavrila 2009]. However the false alarm rate is comparatively very high. Compared with i-LIDS benchmark only stc_t1_c_3.avi achieves performance acceptable to i-LIDs benchmark(F1>0.75). It can also be observed that the F1 values do not scale linearly when the two classifiers are combined. Compared with the histogram of oriented gradients [Dalal and Triggs 2005] which uses dense feature space consisting of normalized oriented gradients to classify and detect object, the proposed approach works with very small features which are essentially edges, and its derivates making it also error prone. The other advantage is less computational load. The lack of details on how the false the false positive rate is estimated makes it difficult to compare the false alarm rates.

Table 9.14 Peak accuracy of mean shift detector/tracker. Positional accuracy is expressed as a fraction of maximum distance of separation (in pixels) between humans. MaxPosX and MaxPosY denotes maximum errors in x and y

Video	TPR	FPR	FNR	MaxPosX	MaxPosY
Hamilton2b.avi	52	10	48	3	3
Stc_t1_c_3.avi	62	9	38	3	3
Stc_t1_c_4.avi	65	46	35	3	3

The JPDAF tracker algorithm has also been compared with Mean shift detector /tracker as shown in table 9.14. The version of mean shift developed use Battacharyya measure to determine similarity between a candidate human from the previous known location to the current location, and links consecutive locations as a track if the mean shift distance between corresponding humans in consecutive frames is less than three pixels wide or high. At every iterative shift along the X and Y directions by a unit pixel distance, the corresponding mean shift vector is computed. Alternatively if the number of iterations exceeds half the width and height of the object windows the candidate human is deemed not to have been found. The mean shift tracker does not use any discriminatory mechanism except that provided by the histogram classifier. The results shows that the true positive and false positive rate are lower than the proposed JPDAF tracker even when the illumination conditions and object background contrast is high as shown by Stc-t1_c_3.avi. The low performance is similarly attributed to grouping and other interactions between humans in the scene. It was also noted for scenes with multiple humans interacting with each other in groups, the accuracy is not high due to frequent interactions. One possible explanation is that detecting multiple individuals in a group is difficult for the mean shift tracker. It is attributed to the fact that the degree of overlap between the kernel and the blob remains the same once the group has been detected with either one, two or more humans uniquely detected. It persists over several frames.

9.9 Synthesised Architecture for Human Detection and Tracking

The synthesised architecture for combined human detection and tracking is shown in figure 9.4. It consist of human detection module which operates on two consecutive frames at a time, and outputs to a database of found humans described by the centroid of bounding rectangle. The next stage is the Pre Tracking Module. It initialises the state vector from silhouette features: intensity, intensity gradient, chromatic red and green colour components. It also associates valid measurements (location and motion vector) to known tracks. Multiple JPDAF tracker modules compute JPDAF probabilities and validate track hypothesis. Kalman filter, the last part of the JPDAF module predicts next state. There could be several JPDAF tracking module operating in parallel. The adaptive monitoring and control module update algorithmic parameters, and predicts achievable detection and false alarm rates in a closed loop fashion.

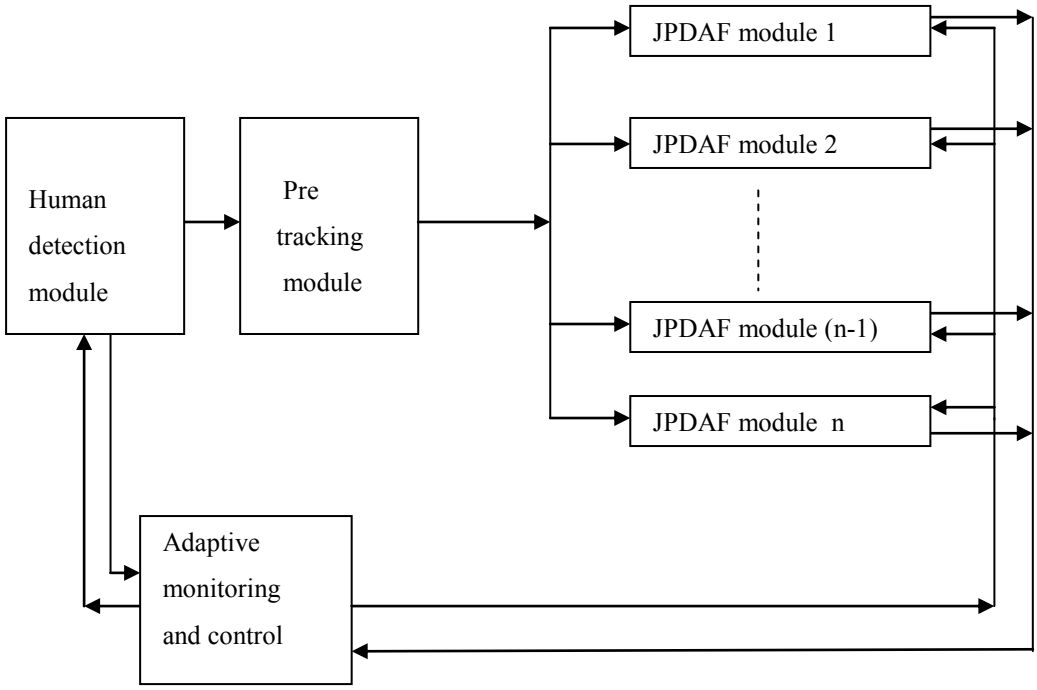

Figure 9.4 Algorithmic architecture for human detection and tracking

9.10 Discussion

If VCA applications target at human detection and tracking is to be widely accepted, it has to be proven to be as good as the human operators who monitor scenes through visual display devices. To robustly detect humans as (i) individuals, as (ii) a group or part of a group, (iii) recognise events such as someone entering protected premises, (iv) abandoning an object, (v) picking up an object, (vi) or running towards a particular facility. The application must consistently achieve high detection rate with low false alarm. It must also be supported by event statistics captured continuously for effective monitoring and control. Other requirements for generic surveillance system were discussed in section 1.1.2. Requirements such as user friendliness, application flexibility, and cost-effectiveness were excluded from the current study since most existing VCA system meets these requirements. The study has focussed on improving the accuracy of both detection and tracking of humans. One way of comparing the accuracy of existing system is to use standard data set and evaluation metrics. PETS (Performance Evaluation of Tracking system) databases and accuracy measures based on confusion matrix, i-LIDs metrics, and ROC were used in the current investigation.

Towards achieving high accuracy independent of scene complexity new techniques have been developed which has proven to be robust in human localization and discrimination. The first proposed detection technique, a novel shape-outline based detector based on a feed forward neural network designed to predict an output pattern given an input pattern. The discrimination of the human class from the non human class is based on a shape mismatch measure expressed as a similarity measure (used as a discriminant function). The proposed shape mismatch metric is defined such that there is a penalty whenever there are mismatch points on the predicted pattern generated compared with the input pattern. The number of such points appear as a factor in the denominator of equation 6.6. The problem of variable human dimension in the frames are avoided by resizing the pattern predictor to height and width of 16 by 32 pixels respectively. This approach copes well when there are no significant scale changes. Localization of humans in the shape space is based on edge density and motion saliency measure in a candidate human window. Higher edge density corresponds to salient feature locations which are further probed by the classifier. Detection is validated after passing linear discriminant and heuristic tests

(threshold and area tests). The main reason for introducing this step is to reduce further classifier errors. Edge saliency based localization thresholds were chosen as a fraction of the maximum edge density in the shape-outline map. The offset used is typically a multiple of the standard deviation of the edge density.

The second detector, a novel wavelet domain based histogram detector is designed to cope with large scale changes. The detector is based on six square wavelet templates as primitives wavelet features. These features describe humans irrespective of the subband in which the candidate is found. Thus it is independent of scale Wavelet representation such as over complete wavelet transform which is translation invariant, was used to design two histogram classifiers based on two different subband types. Saliency based localization thresholds were chosen as a fraction of the maximum of the normalized wavelet coefficient in a frame deemed significant for efficient determination of salient locations in the wavelet domain.

The proposed detectors have also been evaluated using single frames from PASCAL VOC 2010 challenge. It was observed that the detector is acceptable for single frame classification, but not suitable for human detection in single frame.

Pattern classifier based approach for human detection has been demonstrated as highly accurate with reduced computational cost despite the need to provide adequate samples during training to capture as much variability as possible. Detection capability is however dependent on the spatial distribution of the primitive features. By providing large number of training examples from different views of humans high detection of individuals in isolation has been achieved. However there are problems in detecting groups with classifiers trained on individuals, suggesting the need to develop separate classifiers for detection of humans in groups. In the test runs it was observed that when several humans come together to form a group there were high miss detections and false alarms due to the difficulty of separating the group into individuals by the search technique. Validation of the centroid of the location of the human in the candidate human during training was achieved by statistical analysis of the X and Y values of the estimated centroid. Principal component analysis was used to determine the principal location along the horizontal and vertical histogram which accounts for the smallest variation. This corresponds to the centroid of the found humans. Comparison with the manually extracted values agreed with the observation. Further one way ANOVA test for F statistics with significance (see section 7.2.2) at 95% confidence level also validated the derived model. It was observed that classifier

responded very well to vertical edges but not so well to horizontal edges. The classifier designed using motion or edge saliency based localization and vertical edges (horizontal histogram) based on LL subband achieved high detection rate and relatively moderate amount of false alarm rate. With the HLLH subband only the vertical features was used to design a classifier. With LL subband both vertical and horizontal and vertical features were used to design two classifiers which when combined provided sufficient discriminatory power to detect humans. This is supported by large deviations for the y-coordinates (use horizontal edges) of the predictions made by the classifier compared to the x-coordinates (use vertical edges) of the predictions for human location in the case of the HLLH subband. An approximation of the y-coordinate is made based on the first moment along the Y axis (see sections 7.2.1, and 7.6). This is added as an offset to the top left corner of the start address of the block to determine the approximate location along the X and Y-axis. However, the positional error along Y-axis is sometimes quite high compared to the dimension of the histogram. Background saliency based human detection achieved high accuracy whenever the background scene did have large areas with uniform illumination, or when humans are the dominant objects moving in the scene based on size. The presence of large amount of clutter also affects the detection capabilities of the classifiers, for example a stationary train in the background of stc_t1_c_4.avi sequence. Other problems such as occlusion due to humans wearing hats or overcoats which resulted in high miss detections in shape based classifier compared to histogram classifier (check detection rate of stc_t1_c.4.avi in section 8.3).

A performance bottleneck noted at the detection stage is that most of the candidate humans examined by the classifier turned out to be non humans hence the need to improve the feature extraction and discriminating capability of the classifiers. Towards this end further investigation is required on feature rejection techniques in the wavelet domain. Other investigations include:

- Investigation into background modelling techniques to detect ground plane;
- modelling of large scene landmarks in the background.

The shape-outline based detector requires resizing of candidate human window, and the result could also be a source of error since the mismatch measure penalises for unmatched points on the input pattern. The joint probabilistic data association filter

(JPDAF) tracker is designed primarily to reduce false detections (false alarms) and provide trajectory information. The assumption is that by making decisions based on a group of frames defined as a track window better decision would result. Within a track processing window, tracks are associated to human windows based on measurement error confidence interval expressed as Mahalanobis distance assuming measurements are normally distributed. This approach enabled different confidence measurements to be associated with different measurement clusters, enabling fast pruning of unlikely measurement by just tightening the confidence interval. Assumptions made in track window processing also enabled both sequential and batch estimation modes achieve high track association. Sequential estimation mode requires fixing the motion model, and the Mahalanobis confidence interval with track decision made solely on the previous frame. In batch model different motion models are examined using different confidence interval measure and the best of the models selected after several iterations, and decisions are made based on track processing window. The accuracy of the tracker is predicted in batch mode by iterative tracking and varying the confidence interval in steps of 0.1. This enabled optimum tracking parameters to be achieved. The tracker achieved real-time performance on applying frame resizing as part of the pre processing step.

The need to reduce total execution time to provide real-time response for the combined detection and tracking is obvious since the total execution time of the combined detector and the tracker pipelines guarantee a maximum of ten frames per second of 120 X 320 frames being acquired at 30 frames per second assuming a single video bit stream, and running of 2.6 GHz Pentium PC. This is based on Matlab profiling tool. For real-time processing clearly code optimization, and optimal scheduling strategy is required. Further for upward scalability of frame size and number of video streams, parallel processing is suggested to improve real-time response and throughput requirements. Towards this end both algorithmic architecture and parallel processing accelerator is proposed.

9.11 Review of Research Progress

The research started with the literature review which highlighted the fact that given sufficient computational resources most existing algorithms would be able to improve

detection rate if additional techniques are incorporated as either part of the pre and post processing steps. In Gaussian mixture modelling performance depends on the dimension of humans compared with other moving background objects. If the background motion is dominant and the relative size of the human is small then detection rate tends to be low and vice versa. Also there is large computational load in modelling per pixel process. Additionally it requires a means of discriminating the human class from the non human class. The two approaches to human detection proposed are pattern recognition techniques based on patch classifier (used in the current investigation). Of the two approaches considered, shape-outline classifier technique requires less computational resources when deployed (after training). The histogram detector appears to be less sensitive to algorithmic parameter changes (the ROC curve tends to be flat). Furthermore it was noted that most algorithms are not able to maintain accuracy level when the underlying scene constraints are violated. The algorithm presented for adaptive monitoring and control of operating accuracy investigated how close the predictions are to the realised accuracy. Indeed, it provides a means of improving the accuracy irrespective of scene background complexity in the proposed pattern spaces. It indicates when parameters need to be adjusted. It could be useful in situation where the expected accuracy is high but the realised accuracy is low and has to be improved, hence signal for manual intervention. Counting in highly dense scene also requires a different approach since localization techniques might not be able to locate most humans in high density areas due to multiple feature occlusions. A major source of computational overhead in the current implementation is resizing of candidate humans to fit the dimension of the classifiers. The standard frame dimension used (240 x 320) probes more than ten thousand candidate windows to detect all humans assuming the maximum human count in a frame is more than five. This turned out to be an overhead in human detection and tracking especially. Another limitation is the high number of candidate humans which are typically examined most of which turns out to be spurious. It also increases the computational load. One possibility of reducing the number of candidates is to characterise the silhouette of humans in the window in order to reject most of the spurious candidates before classification. The outcome of the theoretical investigations on scheduling and parallel processing is summarised in chapter nine as part of the recommendations for future work.

CHAPTER TEN

CONCLUSIONS

10.1 Conclusions

The project has addressed the problem of improving the accuracy of human detection and tracking independent of scene complexity. A parameter driven online accuracy estimation algorithm linked to both the detection and the tracking stage has been presented. By optimizing the parameters the desired accuracy required can be met as close as possible. The detection part is based on two reduced complexity feature extraction and classifiers designs techniques. The classifiers operate in parallel to realise high detection rate. Together with the second part, the JPDAF tracker, it is able to realise high detection rate.

- The specification, implementation, and accuracy evaluation in software of the algorithms have also been detailed.
- The problem of scale changes due to changes in perspective projection is solved by multiscale wavelet domain decomposition of video frames and use of scale independent pattern classifier. The performance of the classifiers based on confusion matrix, and ROC curves have also been presented.
- Accuracy comparisons with Gaussian mixture modelling based detector, and mean shift tracking have also been presented which demonstrates higher detection for most of the test sequences. As shown from the comparative study the effect of scene background factors has less effect in the proposed shape-space. However more tests are required.
- Modular algorithmic structure has been synthesised for modular synthesis of human detection and tracking to improve processing scalability. Finally parallel processing technique has been recommended to improve response time.

The techniques presented could be built upon to provide additionally functionality such as anomalous behaviour analysis and detailed window analysis based on silhouettes. Operational efficiency has been demonstrated by the high accuracy level achieved through systematic algorithmic parameter setting using the test sequence, modular and scalable algorithmic architecture presented to cope with changes in frame size and number of channels. Classifier based approach to human detection provides a cost-effective means of achieving high accuracy using moderate amount of computing power. However to realise its full potential adequate training is required, and detection by part capability.

The proposed JPDAF tracker achieved high detection rate consistent with the initial puts from the detection stage. Despite achieving high detection rates the high false alarm rate is still a problem. This has implications on computational load, and limits its suitability as generic human detection and tracking. One solution is to design a second classifier in the spatial domain to reject spurious candidates. To reduce tracking errors it is proposed to combine the proposed tracker with mean shift tracking algorithm

10.2 Future Work

To extend the system to include anomalous behaviour analysis and detection the following algorithmic investigations are proposed:

10.2.1 Algorithmic investigations

- Investigation into wavelet based histogram classifier for detection of humans in groups of two, three and four, and view independent. The inadequacy of using classifiers trained on single humans for detecting groups of humans has been highlighted earlier on.
- Evaluate the performance of human detection and tracking with moving background and camera motion using the proposed approach.
- Background modelling schemes for handling non uniform illuminations changes,

and modelling schemes for motion detection in the presence of moving large background objects.

- Silhouette-based analysis of human windows to identify behaviour such as identification of moved object, abandoned object, and unauthorised entry or intrusion. It is proposed that behaviour is represented as hidden Markov states stored in a behaviour database.
- Comparative study of contour based tracking with JPDAF for data association, versus the proposed method.

Sections 10.2.2 to 10.2.5 details out performance and architectural issues related to real-time processing and application scalability.

10.2.2 Performance Enhancements: Parallel Processing for Optimum Execution Time and Throughput

It is clear from the profiling times shown in tables 7.4, 7.5, 7.6, 8.4 and 8.5 that the total processing time fails to meet real time performance of 30 frames per second assuming input frame of size 320W X 240H. Additionally, more processing power is required since at the high performance end up to nine video streams may be processed. Thus there is a need to investigate parallel processing techniques to reduce execution time and at the same time increase throughput. One option is an accelerator based approach to speed up the application. The remaining sections discuss possible investigations into this aspect of processing.

10.2.3 Proposed Macro Architecture of Multiprocessor Accelerator

A programmable coprocessor based on commercial off-the-shelf (COTS) components consisting of multiple SMT (simultaneous multithreading) processors (Pentium IV, IBM POWER5, Xeon, RISC processor, etc), dual ported RAM, and FPGA as shown in figure 10.1 is proposed. The bus interconnection network may be tightly coupled to a daughter board or loosely coupled as in network of work stations. The complete system could be realised on a server or network of personal computers. The FPGA is normally attached to the host processor. Memory could be shared or partitioned

between processors. The proposed architecture has two processing modes, namely, multithreading and SIMD extension modes. Different tasks would be running in different processing modes depending on performance gain achievable. How the optimal mapping is to be achieved is one focus for further study. For a generic micro architecture description of an SMT, the reader is referred to Turandot [Moudgill et al 1999] for a description of speculative out-of-order superscalar processor model. The main pipeline stages of an SMT are: instruction fetch, instruction decode, register renaming, queue, instruction issue within instruction window, register transfer, execution, register reorder, and retirement.

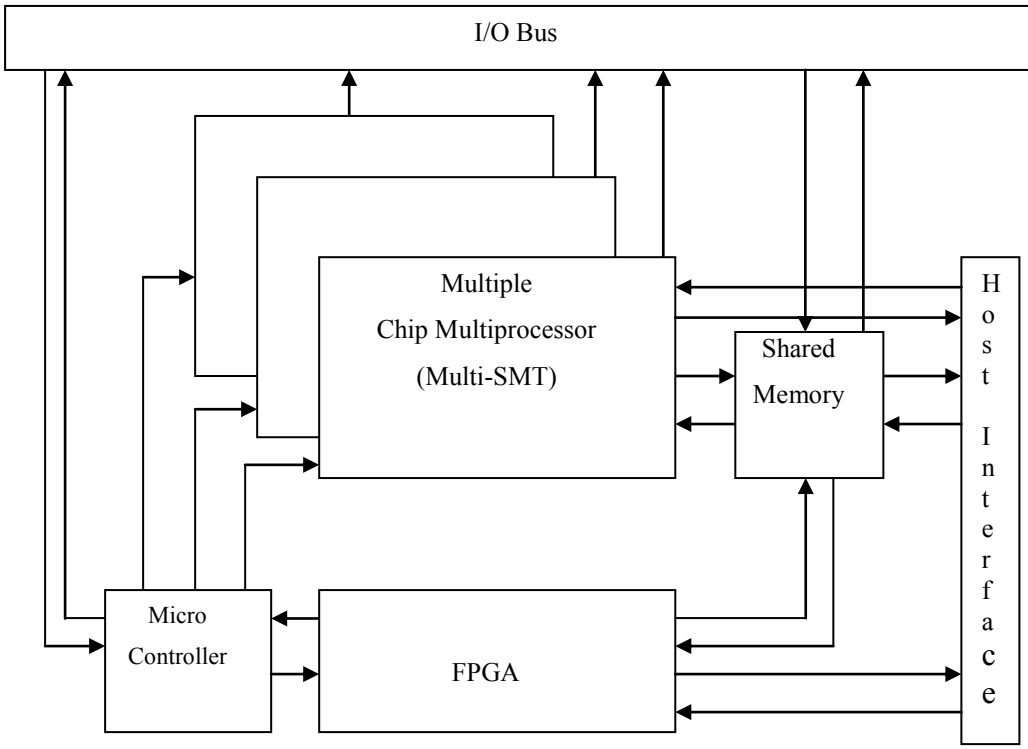

Figure 10.1 Block diagram of proposed accelerator

Different processor implementation would have sub stages further increasing the depth of the pipeline. For example Xeon, a Pentium IV processor realised in 90nm technology has 31-stage instruction pipeline, whilst Pentium III has ten (10). The memory subs system relies on the buffers provided by Pentium IV processors, namely, L1 and L2 caches, and DMA transfers. It relies on hardware and software pre fetch policies on page fault request. The shared memory provides temporary storage of

intermediate results and buffer for loading or dumping of results. Since each SMT features on-chip program and data memories, patches (object windows) are passed asynchronously to each processor. There are two I/O buses, one for input and the other for output. The controller is responsible for scheduling that task on the SMP processors, the FPGA and DMA transfers between the host CPU and shared memory, shared memory and SMTs and FPGA. The communication network could be a bus network, optical network of network of workstations with multicore processors. The controller is responsible for DMA transfers and task scheduling. Table 10.1 and 10.2 provide the main system parameters to be used in evaluating the performance of the accelerator based on Intel Pentium IV dual core multiprocessor.

Table 10.1 System architectural parameters for the proposed accelerator

System Parameters[1]	**Value**
L1 cache latency	0.794 ns
L2 cache latency	7.296 ns
Main memory latency	143.9 ns
Main memory bandwidth	1.24 GB/s
System Bus interface bandwidth	6.4 GB/s
Bus speed	400MHz
Processor	Intel 2.66GHz; 2 Threads per processor
DRAM	2GB

10.2.4 Task Mapping and Scheduling on Multiprocessor Accelerator

The sequential code is initially optimized by reducing unused variables, redundant operations, and reducing the complexity of conditional branches. Then algorithmic

task partitioning based on the execution time profiling of the different task modules is analyzed.

Table 10.2 Marcro architectural parameters of Pentium IV

Pipeline Stage	**Bandwidth**	**Latency**
Fetch	3	4
Dispatch	3	4
Issue	6	1
Execute	7	Variable
Memory Read/Write	3	Variable
Retire	3	1

Critical sub tasks which determines overall execution time are initially used in identifying the best case and the worst case execution times. Sub tasks are statically scheduled to reduce the execution time. Next data level parallelism is exploited using SIMD extensions to further reduce execution time. Finally SMT mode is exploited to optimize the execution time and throughput. Tasks are initially scheduled in multi programmed mode which assigns critical tasks to threads on the multicore processors in baseline execution mode. Top down optimization is recommended. It is supported by several studies on SMT which exploit concurrency to optimized instruction level parallelism and improve hardware resource utilization, i.e, reduce the number of unused slots in an instruction cycle (horizontal waste), and the reduce the number of unused cycles (vertical waste), [Tullsen et. al 1995]. Data input and output is handled by direct memory access (DMA) transfer between the host processor and the accelerator and is overlapped with processing. The DRAM is implemented as shared memory bank.

The following strategy is recommended for optimizing performance: Initially code optimization using Streaming SIMD Extension (SSE3) instruction set is undertaken. The static schedule for the human detection and tracking at the task level is shown in figure 10.3 with five threads labelled as 1,2,3,4, and 5. Labels A to D

denote regions of overlap during processing. Between the I/O thread, the shape based detector, histogram based detector, and combined shape and histogram detector are the regions of overlap enabling I/O and processing can take place in parallel. Similarly at the tracking phase there are regions of overlap between the detection phase and the tracking phase since the output from the detector phase is written unto the database of found humans and is also input to the tracking phase. Frame based processing can be schedule simultaneously with window-based processing since a given frame would be associated with several windows. Thus whilst the current frame is being processed the part of the previous windows could be in process in parallel. There are two sub tasks pipeline options in the wavelet-based classifier, namely, levels one and two wavelet decompositions.

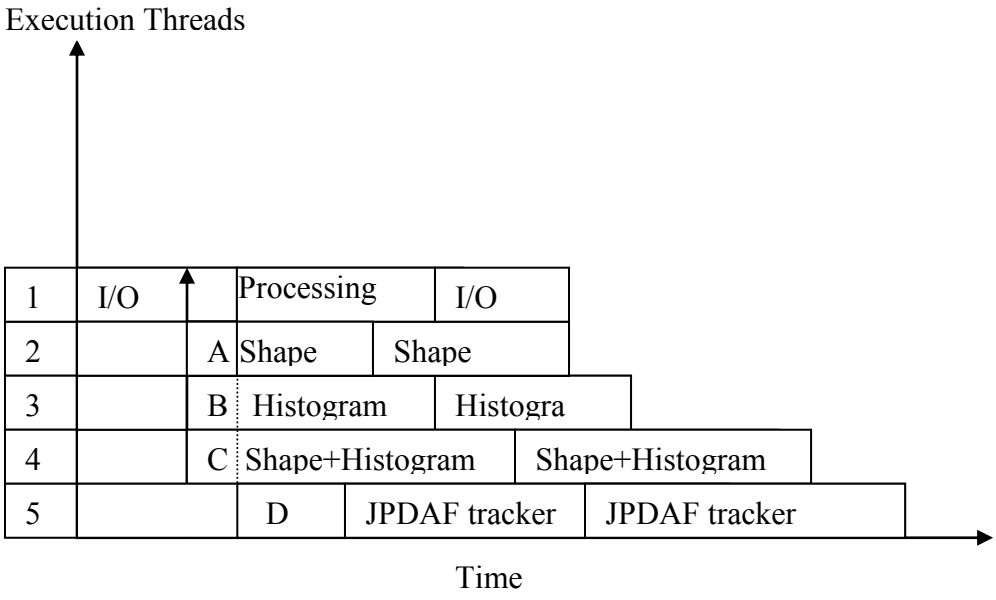

Figure 10.2 Execution threads for the main human detection and tracking tasks

Three different configuration modes are available namely, shape only mode, shape and level one wavelet decomposition, and shape and level two wavelet decomposition modes for human detection, corresponding to the three tables. Two tracking processing modes are also available, namely, intensity template mode only, and multiple templates mode (involving some combination of intensity, directional gradient, chromatic red and chromatic green template) JPDAF tracking. Thus there are six different processing modes. The detection functions are classified as frame based if

the function operates on whole frames, and window-based if function operates on windows (frame patches). For the purpose of determining the optimal schedule, functions are classified under the following categories, input-output, overheads, main, pre processing and post processing tasks. To ease the analysis of a thread task pipeline, sub tasks are classified in input-output, pre processing, main overheads ,and post processing For the purpose of intra task scheduling, a task pipeline consist of three main parts, namely, initialization, load, main process and dump. Figure 10.3 shows the baseline static intra task schedule which defines the sub task pipeline for subsequent optimization. To meet multiple video streams requirements (scalability), replication of this basic pipeline is recommended to allow different architecture configuration which would meet real-time processing requirement. This schedule is applicable to both the detection and the tracking stage.

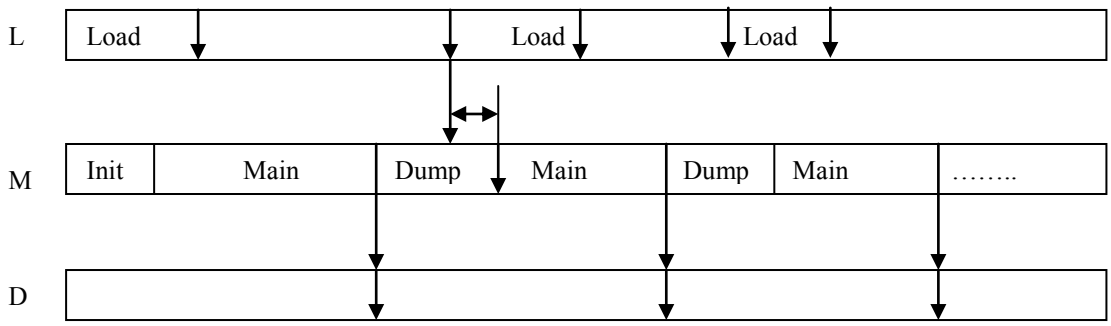

Figure 10.3 Static schedule showing main processing sub tasks overlapped with frame access

To achieve real-time processing of thirty frames per second using 240 X 320 frames would require a processing window of 33 milliseconds, thus the sum of the load and dump operations must run within this time limit. The pipeline labels L, M, and D denote the load, main and dump execution threads respectively. Since the edge saliency task in level one wavelet classifier takes about twenty-milliseconds to execute on a 32X64 window and a standard frame (240X320) requires about 70 calls per frame, the execution time of this sub task can be reduced by SIMD processing. With this approach either through MMX extension of Pentium IV CMP it is possible to have multiple SIMD parallelize code version of this task reducing effectively the main task pipeline by about 72% (1-0.73/1.91) from 1.91 second level to 0.73 seconds.

Wavelet analysis could also be reduced using a hardware accelerator (as discussed earlier on to achieve higher throughput. Thus a standard frame could be split into fifty-five sub windows (5X11 patches) for processing achieving an execution time of 2.5 milliseconds. Similar scheme could be applied to frame resizing. Thus by converting the whole task from frame based processing to mixed mode (frame-based and window-based processing [processing spatial neighbourhood windows]), execution time could be reduced significantly. This applies to all the three human detection pipelines. In the case of the JPDAF tracker (see tables 8.4 and 8.5) the main bottleneck lies with motion estimation sub task. Since the current implementation is block-based it would also benefit from chip level solution. The same analysis could be extended to cover multiple video streams.

10.2.5 Implementation of 9/7 Biorthogonal Wavelet Transform on Field Programmable Gate Array (FPGA)

Direct implementation of wavelet transform based on the filter bank approach is inefficient due to the following: the large amount of intermediate points computation required during an octave subband decomposition. More than half the computed samples are not used, large memory is required to store all the computations of the subband. Thus systems with limited memory would be constrained. There is also high latency since all computations for a subband is completed before the next level is computation is initiated. These factors limits real-time performance since it takes a large amount of the execution time. This prompted the investigation into programmable processor as an accelerator for this task, and hence the use of FPGA which allows optimal scheduling with minimum storage requirement. For example, an algorithm implemented in [Benkrid et al 2001] for a 256*256 image achieves real-time performance at 75MHz. For a J-stage wavelet transform of N by M frame it has a period of NM cycles. The algorithm implements row (column) wavelet transform using RPA [Mallat 1989], and then implement the column (row) transform using parallel filter, and line buffer, frame buffer, and specialised hardware units (1-K line delay converter, shift register logic, and address generators) to accelerate computations.

References

[Agga94] Aggarwal J. K. Q. Cai, W. Liao and B. Sabata. Articulated and Elastic Non-Rigid Motion: A Review. Workshop on Motion of Non-Rigid and Articulated Objects. Austin, TX, pp. 2 -14, 1994.

[Agga99] Aggarwal J. K, and Cai Q. Human Motion Analysis: A Review. Computer Vision and Image Understanding, vol. 73, no. 3, pp. 428-440, 1999.

[Agui05] Aguilera J, Wildenauer H, Kampel M, Borg M, Thirde D, and Ferryman J. Evaluation of Motion Segmentation Quality for Aircraft Activity Surveillance. In Joint IEEE International Workshop on Visual Surveillance and Performance Evaluation of Tracking and Surveillance (VS-PETS), 2005.

[Akan92] Akansu A. N., and Haddad, R. A. Multiresolution Signal Decomposition. Academic Press, Boston, 1992.

[Alba02] Albanesi M. G., Ferratti M, Dell'Olio. Effectiveness of VLIW Architecture in a Data Parallel Image Application. 2002 IEEE International Workshop on Computer Architectures for Machine Perception (CAMP), pp. 172–183, April 2002.

[Ali01] Ali A., and Aggarwal J. Segmentation and Recognition of Continuous Human Activity. In Proceedings of IEEE Workshop on Detection and Recognition of Events In Video, pp. 28-35, 2001.

[Amda67] Amdahl G. M. Validity of the Single-Processor Approach to Achieving Large Scale Computing Capabilities. In AFIPS Conference Proceedings, vol. 30, Atlantic City, N. J, pp. 483 -485, 18-20th April 1967.

[Amoo88] Amoozegar Farid. Neural-Network-Based Target Tracking State-of-the-Art-Survey. In Optical Engineer, vol. 37, issue 3, March 1988.

[Andr02] Andreopoulos Y, Munteanu A, Van Der Auwere G, Schelkens P, and Cornelis J. Scalable Wavelet Video-Coding with In-Band Prediction-Implementation and Experimental Results. In Proceedings of IEEE International Conference on Image Processing, vol. 3, Rochester, NY, pp.729-732, September 2002.

[Anto04] Antoine J-P, Murenzi R., Vandergheynst P., and Syed T. A. Two Dimensional Wavelets and Their Relatives, Cambridge University, Cambridge Press, 2004.

[Bao05] Bao P., Lei Zhang, and Xiaolin Wu. Canny Edge Detection Enhancement by Scale Multiplication. In IEEE Transactions on Pattern Analysis and Machine Intelligence, vol. 27, no.9, pp. 1485-1490, 2005.

[Belo01] Belongie S., Malik J., and Puzicha J., Matching Shapes. In Proceedings of Eighth International Conference on Computer Vision, pp. 454-461, 2001.

[Blac99] Blackman S., and R. Popoli. Design and Analysis of Modern Tracking Systems. Artech House, Norwell, MA, 1999.

[Bar72] Bar-Shalom Y., and Jaffer A. G. Adaptive Nonlinear Filtering for Tracking with Measurements of Uncertain Origin. In Proc. of 11th IEEE Conference on Decision and Control, pp. 243-247, 1972.

[Bar88] Bar-Shalom Y., and Fortmann T. Tracking and Data Association, volume 179 of Mathematics in Science and Engineering. Academic Press, 1988.

[Bar92] Bar-Shalom Yaakov. Multitarget/Multisensor Tracking: Applications and Advances: Volume II. Artech House, 1992.

[Bash06] Bashir F., and Porikli F. Performance Evaluation of Object Detection and Tracking Systems. In Proceedings of 9th IEEE International Workshop on PETS, New York, pp. 7 -14, June 2006.

[Bast80] Bastiaan M. Gabor Expansion of a Signal into Gaussian Elementary Signals. In Proceedings of IEEE, vol. 68, pp. 538-539, 1980.

[Benk01] Benkrid A., Crookes D., and Benkrid K. Design and Implementation of 2-D Biorthogonal Discrete Wavelet Transform on FPGA. In Proceedings of the 9th Annual IEEE Symposium on Field-Programmable Custom Computing Machines (FCCM'01), 2001.

[Benn88] Benner R. E., Gustafson J. L., and Montry G. R. Development and Analysis of Scientific Application Programs on a 1024-Processor Hypercube. Report no. SAND 88-0317, Sandia National Laboratories, Feb. 1988.

[Bere02] Berekovic M., Hans-Joachim Stolberg, and Peter Pirsch. Multi-core System-On-Chip Architecture for MPEG-4 Streaming Video. In IEEE Transactions on Circuits and Systems for Video Technology, vol. 12, no.

8, pp. 688-699, 2002.

[Berg05] Berg Alexander C., Tamara L. Berg, and Jitendra Malik. Shape Matching and Object Recognition using Low Distortion Correspondences. In Proc. IEEE Computer Society Conference on Computer Vision and Pattern Recognition (CVPR'05), 2005.

[Bhan86] Bhanu B. Automatic Target Recognition: State of the Art Survey. In IEEE Trans. Aerospace and Electronic systems, AES-22(4): 364 -379, 1986.

[Bile05] Bileschi Stanley and Lior Wolf. A Unified System for Object Detection, Texture Recognition, and Context Analysis Based on the Standard model Feature Set. In Proc. British Machine Vision Conference, 2005.

[Bing02] Bing X., and C. Charoensak. Rapid FPGA Prototyping of Gabor-Wavelet Transform for Applications in Motion Detection. In Proc. of 7th Intl. Conference on Control, Automation, Robotics and Vision, pp. 1653–1657, 2002.

[Birc98] Birchfield S. Elliptical Head Tracking Using Intensity Gradients and Colour Histograms. In Proc. IEEE Conf. Computer Vision and Pattern Recognition, pp. 232-237, 1998.

[Blac96] Black M, and Jepson, A. Eigentracking: Robust Matching and Tracking of Articulated Objects Using a View-Based Representation. In European Conference on Computer Vision, ECCV' 96, Cambridge, 1996.

[Blum07] Blum, A. L., and Langley, P. Selection of Relevant Features and Examples in Machine Learning. In Artificial Intelligence, vol. 97, no. 1-2, pp. 245-271, 1997.

[Bobi96a] Bobick Aaron and James Davis.Real-Time Recognition of Activity Using Temporal Templates. In IEEE Workshop on Applications of Computer Vision, pp.39-42, December 1996.

[Bobi96b] Bobick Aaron and Davis, James. An Appearance-Based Representation of Action. In Proceedings of IEEE International Conference on Pattern Recognition and Machine Intelligence (ICPR'96), pp.307-312, 1996.

[Bogh05] Boghossian B., and J. Black. The Challenges of Robust 24/7 Video Surveillance Systems. In IEE International Symposium on Imaging for Crime Detection and Prevention, pp. 33-38, 2005,

[Bose92] Boser B. E., I. M. Guyon, and V. N. Vapnik. A Training Algorithm for Optimal Margin Classifier. In Proceedings of 5th ACM Workshop on Computational Learning Theory, Pittsburgh, PA, July 1992.

[Bou05] Bouaynaya N., and Schonfeld D. A Complete System for Head Tracking using Motion-Based Particle Filter and Randomly Perturbed Active Contour. Proceedings of SPIE Conference on Image and Video Communications and Processing, vol. 5685, March 2005.

[Bregl97] Bregler C. Learning and Recognizing Human Dynamics in Video Sequences. In Proc. IEEE Conference on Computer Vision and Pattern Recognition, Puerto Rico, pp. 568-574, 1997.

[Brog00] Broggi A., Bertozzi M., Fascioli A., and Sechi, M. Shape-Based Pedestrian Detection. In Proceedings of the IEEE Intelligent Vehicles Symposium, pp. 215- 220, 2000.

[Brow05] Brown Lisa M., Senior Andrew W., Ying-li Tian, Jonathan Connell, Arun Hampapur, Chiao-Fe Shu, Hans Merkl, Max Lu. Performance Evaluation of Surveillance Systems Under Varying Conditions. In proceedings of IEEE International Conference on Performance Evaluation of Tracking and Surveillance, January 2005.

[Broo03] Brooks R. Model-Based Three-Dimensional Interpretations of Two-Dimensional Images. In IEEE Transactions on Pattern Analysis and Machine Intelligence, vol. 5, pp. 140-149, 2003.

[Burg96] Burges C. J. C. Simplified Support Decision Rules, 1996.

[Burt83] Burt, P. J., and Adelson E. H. The Laplacian Pyramid as a Compact Image Code. In IEEE Transactions on Communications, vol. 31, no. 4, pp. 532-540, 1983.

[Byrt88] Byrt Ted, Janet Bishop and John B. Carlin. Bias, Prevalence, and Kappa. Journal of Clinical Epidemiology, Vol. 46, no. 5, pp. 423-429, 1988.

[Cann86] Canny J. A Computational Approach to Edge Detection. In IEEE Transactions on Pattern Analysis and Machine Intelligence, vol. 8, pp. 79- 698, 1986.

[Cent85] Centor R. M, and Schwartz J. S. S. An Evaluation of Methods for Estimating the Area Under the Receiver Operating Characteristics (ROC) Curve. Medical Decision Making, vol. 5, no. 2, pp. 149-156, 1985.

[Cedr95] Cedras Claudette and Mubarak Shah. Motion-Based Recognition: A Survey. In Image and Vision Computing, vol. 13, no. 2, pp. 129–155, March 1995.

[Chen01] Chen Yunqiang, Yong Rui, and Thomas S. Huang. JPDAF Based HMM for Real-Time Contour Tracking. In Proceedings of IEEE Computer Society Conference on Computer Vision and Pattern Recognition, vol. 1, pp. I543-I550, 2001.

[Chen06] Cheng Fang-Hsuan, Yu-Liang Chen. Real-Time Multiple Objects Tracking and Identification Based On Discrete Wavelet Transform. In Pattern Recognition, vol. 39, pp. 1126–1139, 2006.

[Chi04] Chi-Man Pun and Moon-Chen Lee. Extraction of Shift Invariant Wavelet Features for Classifcation of Images with Different Sizes. In IEEE Transactions on Pattern Analysis and Machine Intelligence, vol. 26, no. 9, pp. 1228- 1233, September 2004.

[Cody04] Cody Kwok, Dieter Fox, and Marian Meila. Real-Time Particle Filters. In Proceedings of the IEEE, pp. 469-484, 2004.

[Coll00] Collins R. T., Lipton A. J., Kanade T. Fujiyoshi H, Duggins H, Tsin Y, Tolliver T, Enomoto N, Hasegawa O, Burt P, Wixson L. A System for Video Surveillance and Monitoring. Carnegie Mellon University, Pittsburgh, PA, Tech Report, CMU-RI-TR-00-12, 2000.

[Coll01] Collins Robert T., Alan J. Lipton, Hironobu Fujiyoshi, Takeo Kanade. Algorithms for Cooperative Multisensor Surveillance. In Proceedings of the IEEE, vol. 89, no. 10, October 2001.

[Comm00] Commaniciu Dorin, Visvanathan Ramesh, and Peter Meer. Real-Time Tracking of non-Rigid Objects using Mean Shift. In Proceedings of IEEE Conference on Computer Vision and Pattern Recognition, vol. 2, pp. 13-15, 2000.

[Comm02] Comanciu D., and Meer, P. Mean Shift: A Robust Approach Toward Feature Space Analysis. In IEEE Transactions on Pattern Analysis and Machine Intelligence, vol. 24, no. 5, pp. 603-619, 2002.

[Comm03] Commaniciu D., Ramesh V., and Meer, P. 2003. Kernel-Based Object Tracking. IEEE Trans. on Pattern Analysis and Machine Intelligence, vol. 25, pp. 564-575, 2003.

[Conx07] Conxia Dai, Yunfei Zheng, and Xin Li. Pedestrian Detection and Tracking in Infrared Imagery using Shape and Appearance. In Computer Vision and Image Understanding, vol. 106, Issue 2-3, pp. 288-299, May 2007.

[Cox93] Cox. I. J. A Review of Statistical Data Association Techniques for Motion Correspondence. International Journal on Computer Vision, vol. 10, no.1, pp. 53-66, 1993.

[Cox96] Cox I. J., and Hingorani Sunita L. An Efficient Implementation of Reid's Multiple Hypothesis Tracking Algorithm and Its Evaluation for the Purpose of Visual Tracking . In IEEE Transactions on Pattern Analysis and Machine Intelligence, vol. 18, no. 2, pp. 138 -150, 1996.

[Curt05] Curtis-Maury Mathew, Tanping Wang, Christos Antonopoulos and Dimitrios Nikolopoulos. Integrating Multiple Forms of Multithreaded Execution on Multi-SMT Systems: A Study with Scientific Applications. In Proceedings of the Second IEEE International Conference on Quantitative Evaluation of Systems (QEST'05).

[Dala05] Dalal N., and Triggs B. Histogram of Oriented Gradients for Human Detection. In Proceedings of IEEE Conference on Computer Vision and Pattern Recognition, vol. 2, pp. 886-893, June 2005.

[Dani08] Danielsson Oscar, Steffan Carlsson, and Josephine Sullivan. Object Detection Using Multi-Local Feature Manifolds. In Proceedings of Digital Image Computing: Techniques and Applications (DICTA08), pp. 612-618, dec. 2008.

[Daub90] Daubechies I. The Wavelet Transform: Time-Frequency Localization and Signal Analysis. In IEEE Transactions on Information Theory, vol. 36, no. 6, pp.961-1005, 1990.

[Daub91] Daubechies I. Ten lectures on Wavelets (CBMS-NSF Series Appl. Math), SIAM, 1991.

[Daub88] Daubechies I. Orthonormal Bases of Compactly Supported Wavelets. In Communication on Pure and Applied Mathematics, vol. XLI, pp. 909-996, 1988.

[Dee08] Dee H. M., and Velastin S. A. How Close are We to Solving the Problem of Automated Visual Surveillance? A Review of Real-World Surveillance, Scientific Progress and Evaluative Mechanisms. Springer, In Special Issue on Video Surveillance Research in Industry and Academic (Machine Visions and Applications), No. 19 (5-6), pp. 329-343, 2008.

[Dela99] Delamarre Quentin and Faugeras Olivier. 3D Articulated Models and Multi-view Tracking With Silhouettes. In Proceedings of IEEE International Conference on Computer Vision, vol. 2, pp. 716-721, 1999.

[Dela01] Delamarre Quentin, and Faugeras Olivier. 3D Articulated Models and Multiview Tracking With Physical Forces. In Computer Vision and Image Understanding, vol. 81, pp.328-357, 2001.

[Den01] Dengsheng Zhang and Guojun Lu. A Comparative Study on Shape Retrieval Using Fourier Descriptors with Different Shape Signatures. In International Conference onIntelligent Multimedia and Distance Education (ICIMADE ’01), ND, 1-3 June 2001.

[Devi82] Devijver P.A and J. Kittler. Pattern Recognition. A Statistical Approach. Prentice-Hall Inc, London, 1982.

[Dona06] Donatello Conte, Pasquale Foggia, Jean-Michell Jolion, Mario Vento. A Graph-Based Multiresolution Algorithm for Tracking Objects in Presence of Occlusion. In Pattern Recognition 39, pp. 562 -572, 2006.

[Dyan99] Dyan Peter. Unsupervised Learning. In MIT Encyclopedia of the Cognitive Sciences, Edited by Wilson R. A, Keil, and Keil, F. 1999.

[Elga90] Elgammal A, Duraiswami R., Harwood D., and Davis L. Background and Foreground Modelling Using Nonparametric Kernel Density Estimation for Visual Surveillance. In Proceedings of IEEE, vol. 7, pp. 1151-1163, 1990.

[Ever10] Everingham Mark and Gool Luc Van. The PASCAL Visual Object Classes (VOC) Challenge. International Journal on Computer Vision, vol. 88, pp.303-338, 2010.

[Edwa98] Edwards G., Taylor C., and Cootes T. Interpreting Face Images Using Active Appearance Model. In International Conference on Face and gesture Recognition, pp. 300-305, 1998.

[Erk98] Erkel A. R., Van P. M., and T. Pattynama. Receiver Operating Characteristics (ROC) analysis: Basic Principles and Applications in Radiology. European Journal of Radiology, vol. 27, pp. 88-94, 1998.

[Enzw09] Enzweiler M and Gavrila M. Monocular Pedestrian Detection: Survey and Experiments. IEEE Transaction on Pattern Analysis and Machine Intelligence, vol. 31, no. 12, Dec. pp. 2179-2195, 2009.

[Fabb08] Fabbri R., Da F. Costa L., and Torreli Julio C. 2D Euclidean Distance Transform Algorithms: A Comparative Survey. ACM Computing Surveys, vol. 40, no. 1, article 2, 2008.

[Farr09] Farrugia Nicolas, Franck Mamalet, Sebastian Toux, Fan Yan and Michel Paindavoine. Fast and Robust Face Detection on Parallel Optimized Architecture on FPGA. In IEEE Transactions on Circuits and Systems for Video Technology, vol. 19, no. 4, April 2009.

[Fazl09] Fazli S., Hamed Moradi Pour, and Hamed Bouzari. Multiple Object Tracking Using improved GMM-Based Motion Segmentation. In Proceedings of the 6th International Conference on Electrical Engineering/Electronics, Computer Engineering, Telecommunications and Information Technology (ECTI-CON 2009), Thailand, vol. 2, pp.1130-1133, 2009.

[Fei04] Fei-Fei L., Fergus R., and Perona P. Learning Generative Visual Models from Few Training Examples: An Incremental Bayesian Approach Tested on 101 Object Categories. Proceedings of Computer Vision and Pattern Recognition Workshop on Generative-Model Based on Vision, 2004.

[Fieg97] Fieguth P., and Terzopoulos D. Colour-Based Tracking of Heads and Other Mobile Objects at Video Frame Rates. In Proceedings IEEE Conference on Computer Vision and Pattern Recognition (CVPR), pp. 21-27, 1997.

[Flee92] Fleet D. J. Measurement of Image Velocity. Norwell, Massachusetts, Kluwer, 1992.

[Flee91] Fleet D. J., and Adelson E. H. Design and Use of Steerable Filters. In IEEE Transactions on Pattern Analysis and Machine Intelligence, vol.13, pp. 891- 906, 1991.

[Flor02] Florian Radu. Named Entity Recognition as a House of Cards: Classifier Stacking. In Proceedings of the 6th Conference on Natural Language Learning, vol. 20, pp. 1-4, 2002.

[Food96] Foody G. M., and M. K. Arora. Incorporating Mixed Pixels in the Training, Allocation, and Testing Stages of Supervised Classifications. In Pattern Recognition Letters, vol. 17, pp. 1389-1398, 1996.

[Franc99] Francos A., and Porat M. Analysis and Synthesis of Multicomponent Signals Using Positive Time-Frequency Distributions. In IEEE Transactions on Signal Processing, vol. 47, no. 2, pp. 493- 504, 1999.

[Free91] Freeman William T., and Adelson Edward H. The Design and Use of Steerable filters. In IEEE Transactions on Pattern Analysis and Machine Intelligence, vol. 13, no. 9, pp. 891-906, 1991.

[Freu95] Freund Y., and Schapire R. A Decision-Theoretic Generalization of On-Line Learning and Application to Boosting. Computational Learning Theory, pp. 23-37, 1995.

[Frey00] Frey B. Filling in Scenes by Propagating Probabilities through layers into Appearance Models. In Proc. IEEE Conference on Computer Vision and Pattern Recognition, vol. 1, pp. 185-192, 2000.

[Gabr04] Gabriella Csurka, Christopher R. Dance, Lixin Fan, Jutta Williamsowski, Cedric Bray. Visual Categorization with Bags of Keypoints. In the 8th European Conference on Computer Vision-ECCV, 2004.

[Gavr96] Gavrila D. M., and Davis L. A. 3-D model-based Tracking of Humans in Action: A Multi-view Approach. In Proc. IEEE Conference on Computer Vision and Pattern Recognition, pp. 73-80, 1996.

[Gere98] Gerek, O., and E. Cetin. Linear/NonLinear Adaptive Polyphase Subband Decomposition Structures for Compression. In IEEE International Conference on Acoustic, Speech, and Signal Processing, vol. 3, pp.1345-1348, 1998.

[Geve04] Gevers Theo and Harro Stokman. Robust Histogram Construction from Color Invariants for Object Recognition. In IEEE Transactions on Pattern Analysis and Machine Intelligence, vol. 26, no.1, pp.113- 118, January 2004.

[Give99] Givers T and A. W. M. Smeulders. Color Based Object Recognition. In Pattern Recognition, vol. 32, no. 3, pp. 453-464, 1999.

[Gree94] Greenspan H., Belongie S., Goodman R., Perona P., Rakshit S., and Anderson C. Over Complete Steerable Pyramid Filters and Rotation Invariance. In IEEE Conference on Computer Vision and Pattern Recognition (CVPR), pp. 222-228, 1994.

[Gunt00] Gunther Jager and Ursula Benz. “Measures of Classification Accuracy Based on Fuzzy Similarity,” IEEE Transactions on Geoscience and

Remote Sensing, vol. 38, no.3, May 2000.

[Gunt00] Gunther Jager and Ursula Benz. Measures of Classification Accuracy Based on Fuzzy Similarity. In IEEE Transactions on Geoscience and Remote Sensing, vol. 38, no. 3, pp. 1462-1467, May 2000.

[Guoq00] Guoqiang Peter Zhang. Neural Networks for Classification: A Survey. In IEEE Transactions on Systems, Man, and Cybernetics-Part C; Applications and Reviews, vol. 30, no. 4, pp. 451- 462, November 2000.

[Hann01] Hanna M. T., and S. A. Mansoori. The Discrete Time Wavelet Transform: Its Discrete Time Fourier Transform and its Filter Bank Implementation. In IEEE Trans. Circuits Systems II: Analog and Digital Signal Process. vol. 48 (2) pp. 180 -183, 2001.

[Harr88] Harris C., and Stephens M. A. Combined Corner and Edge Detector. In 4th Alvery Vision Conference, pp. 147-151, 1988.

[Hari00a] Haritaoglu I., David Harwood and Larry S. Davis. An Appearance-Based Body Model for Multiple People Tracking. In Proceeding of International Conference on Pattern Recognition, vol. 4, pp. 184 -187, 3-7 Sept. 2000.

[Hari00b] Haritaoglu I., Harwood D., and Davis L. W4: Real-Time Surveillance of People and Their Activities. In IEEE Transaction on Pattern Analysis and Machine Intelligence, vol. 22, no. 8, pp. 809-830, 2000.

[Hast01] Hastie T., Robert Tibshirani, and Jerome Friedman. The Elements of Statistical Learning (Springer Series in Statistics) pp. xvi+533. 2001.

[Hay99] Haykins S. Neural Networks: A Comprehensive Foundation. Prentice-Hall International, 2nd Edition, 1999.

[Horn89] Hornik K. Multilayer Feedforward Networks are Universal operators. In Neural Networks, vol. 2, 1989.

[Horp03] Horprasert T., Kim K., and Harwood D. Codebook-based Adaptive Background Subtraction for Raw Compressed Videos and a Performance Evaluation Methodology for Detection Algorithms. To be submitted in European Conference on Computer Vision 2003.

[Huan08] Huang K., Liangsheng Wang, Tienniu Tan, and Steve Maybank. A Real-Time Object Detecting and Tracking System for Outdoor Night Surveillance. In Pattern Recognition vol .41,pp. 432-444, 2008.

[Hutt93] Huttenlocher D., Noh J., and Rucklidge W. Tracking Non rigid Objects In Complex Scenes. In IEEE International Conference on Computer Vision (ICCV), pp. 93-101, 1993.

[Huwe98] Huwer S. and Niemann H. 2-D Object Tracking Based on Projection-Histograms. In Proceedings of the 5th European Conference on Computer Vision, vol. 1, pp. 861-876, 1998.

[Isar98] Isard M., and Blake A. Condensation-Conditional Density Propagation for Visual Tracking. In International Journal on Computer Vision, vol. 29, no. 1, pp. 5-28, 1998.

[Ferr06] IEEE Computer Society. Proceedings of the Ninth IEEE International Workshop on Performance Evaluation of Tracking and Surveillance

(PETS 2006) Edited by J. M. Ferryman, 2006.

[Jav02] Javed O., and M. Shah. Tracking and Object Classification for Automated Surveillance. In Proceedings European Conference on Computer Vision, vol. 4, 2002.

[Jaggi95] Jaggi Seema, Willsky Allan, Karl W. Clem, Mallat Stephane. Multiscale Geometric Feature Extraction and Object Recognition with Wavelets and Morphology. In Proceedings of IEEE International Conference on Image Processing, vol. 3, pp. 372-375, 1995.

[Jang00] Jang D. S., and H.-I. Choi. Active Models for Tracking of Moving Objects. In Pattern Recognition, vol. 33, no. 7, pp.1135-1146, 2000.

[Jens95] Jensen K., and D. Anastassiou. Subpixles Edge Localization and Their Interpolation of Still Images. In IEEE Transactions on Image Processing, vol. 4, pp. 285-295, March 1995.

[Jeps03] Jepson Allan D., David J. Fleet, and Thomas F. El-Maraghi. Robust Online Appearance Models for Visual Tracking. In IEEE Transactions on Pattern Analysis and Machine Intelligence, vol. 25, no. 10, 2003.

[Jian06] Jian C., Jie Yang, YUE Zhou, Yingying Cui. Flexible Background Mixture Models for Foreground Segmentation. In image and Vision Computing, vol. 20, pp. 1-10, 2006.

[Jord04] Jordan R. A Survey of Techniques For Object Detection, Final project Report), Department of computer Sciences, University of British Columbia. 2004.

[Juri01] Jurie Frederic and Dhome Michael. A Simple and Efficient Template Matching Algorithm. In Proceedings of 8th IEEE International Conference on Computer Vision, 2001.

[Ju96] Ju S, M. Black, and Y. Yacob. Cardboard People: A Parameterized Model of Articulated Motion. In Proc. IEEE Conference on Automatic Face and Gesture Recognition, pp. 38-44, 1996.

[Kang04] Kang J, Cohen, I. and Medioni, G. Object Reacquisition using Geometric Invariant Appearance Model. In International Conference on Pattern Recognition (ICPR), pp. 759-762, 2004.

[Kara00] Karaulova I, A. P. M. Hall, and A. D. Marshall. A Hierarchical Model of Dynamics for Tracking People with Single Video Camera. In Proc. British Machine Vision Conference, pp. 262-352, 2000.

[Karl01] Karlson R., and F. Gustafsson. Monte Carlo Data Association for Multiple Target Tracking. In IEEE Target Tracking: Algorithms and Applications, Netherland, October 2001.

[Khot90] Khotanzad A., and J.–H. Lu. Classification of Invariant Image Representation Using a Neural Network. In IEEE Transactions on Acoustics, Speech, and Signal Processing, vol. 38, no. 6, pp.1028-1038, June 1990.

[Kots07] Kotsiatis S. B. "Supervised Machine Learning: A Review of Classification Techniques, Informatica vol. 31, 2007, pages 249-268.

[Kulk94] Kulkarni A. D. Artificial Neural Networks for Image Understanding. VNR, New York, 1994.

[Kuhn55] Kuhn H. The Hungarian Method of Solving The Assignment Problem. In Naval Research Logistics Quarterly, vol. 2, pp. 83-97, 1955.

[Lain95] Laine A. F., H. Fan, and W. Yang. Wavelets for Contrast Enhancement of Digital Mammography. In IEEE Engineering in Medicine and Biology Magazine, vol. 14, pp. 536-550, September 1995.

[Laks00] Lakshmi Aparna Ratan, W. Eric L. Grimson, and William M. Welle III. Object Detection and Localization by Dynamic Template Warping. In International Journal of Computer Vision, vol. 36, no. 2, pp. 131-147, 2000.

[Law03] Law N.F., and Siu. A Fast and Efficient Computational Structure for the 2D-Over-Complete Wavelet Transform. In IEEE International Conference on Acoustic, Speech, and Signal Processing (ICASSP'03), vol. 3, pp. II-309-II312, 2003.

[Lowe04] Lowe D. G. Distinctive Image Features from Scale Invariant Key Points. In International Journal in Computer Vision, vol. 60, no. 2, November 2004.

[Lowe99] Lowe D. G. Object Recognition from Local Scale-Invariant Features. In Proc. of the International Conference on Computer Vision, Corfu, 1999.

[Lee04] Lee D. J, P. Zhan, A. Thomas, R. Schoenberger. Shape-Based Human Intrusion Detection. SPIE International Symposium on Defence and Security, Visual Information Process XIII, vol. 5438, pp.81-91, Orlando, Florida, USA, April 12-16, 2004.

[Lee02] Lee L., and W. Grimson. Gait Analysis for Recognition and Classification. In Proceedings of International Conference on Automatic Face and Gesture Recognition, pp. 155-162, 2002.

[Liew92] A. W. C. Liew, and N. F. Law. Reconstruction from 2D Wavelet Transform Modulus Maxima using Projections. In IEE Proceedings on

Vision, Image and Signal Processing, vol. 147, pp. 710-732, 1992.

[Lin94] Lin Weisi. Parallel Realization of A Computer Vision System. IEEE Region 10's Ninth Annual International Conference. Theme: Frontiers of Computer Technology (TENCON '94), 1994.

[Lipt98] Lipton A. J, Fujiyoshi H, and Patil R. S. Moving Target Classification and Tracking from Real-Time Video. In Proceedings of IEEE Workshop on Applications of Computer Vision, pp. 8-14, 1998.

[Lipt99] Lipton A. J. Local Application of Optic flow to Analyze Rigid Versus Non Rigid Motion. In Proc. International Conference on Computer Vision Workshop Frame-Rate Vision, Corfu, Greece, 1999.

[Lowe91] Lowe D. G. Fitting Parameterized 3-D models to Images. In IEEE Transactions on Pattern Analysis and Machine Intelligence, vol. 13, pp. 441-450, 1991.

[Mall89] Mallat S. G. Multifrequency Channel Decomposition of Images and Wavelet Models. In IEEE Transactions on Acoustic, Speech, and Signal Processing, vol. 37, pp. 2091-2110, 1989.

[Mall92] Mallet S., and S. Zhong. Characterization of Signals from Multiscale Edges. In IEEE Transactions on Pattern Analysis and Machine Intelligence, vol. 14, pp. 710-732, 1992.

[Mand99] Mandal M. K., and Aboulnasr T. Fast Wavelet Histogram Techniques for Image Indexing. In Proceedings of IEEE Workshop on Content-Based Access of image and Video Libraries, 1999.

[Mano06] Manohar Vassant, Boonstra Mathew, Korzhova Valentina, Padmanabhan Soundarajan, Goldgof Dmitry and Kasturi Rangarchar. PETS vs. VACE Evaluation Programs: A Comparative Study. Proceedings of the 9th IEEE International Workshops on PETS. Edited by James M. Ferryman, New York, June 18, 2006.

[Marc02] Marcenaro L, M. Ferrari, L. Marchesotti, and C. S. Regazzoni. Multiple Object Tracking Under Heavy Occlusion using Kalman Filters Based on Shape Matching. In Proceedings of IEEE International Conference on Image Processing, vol. 3, pp. 341-344, 2002.

[Mar99] Marchand Eric, Bouthemy Patrick, Chaumette Francois, and Moreau Valerie. Robust Real-Time Visual Tracking using a 2-D-3-D Model-Based Approach. In Proceedings of the 7th IEEE International Conference on Computer Vision. Vol. 1, pp. 262-268, 1999.

[Marr80] Marr D., and E. Hildreth. Theory of Edge Detection. Proceedings of the Royal Society, London, vol. 207, pp. 187-217, 1980.

[Marr82] Marr D. Vision, San Francisco: W. H. Freeman, 1982.

[Mayb00] Maybank S. J., and T. N. Tan. Special Section on Visual Surveillance-Introduction. In International Journal on Computer Vision, vol. 37, no. 2, pp. 173-174, 2000.

[Mcke00] Mckenna S., Jabri Z. Duric., A. Rosenfeld, and H. Wechsler. Tracking Groups of People. In Computer Vision and Image Understanding, vol. 80, no. 1, pp. 42- 56, 2000.

[Meye95] Y. Meyer. Ondelettes et Operateurs, Tome I. Paris, Herrmann, 1990.

[Meye99] Meyer D, J. Psl, and H. Niemann. Gait Classification with Hidden Markov Models for Trajectories of Body Parts Extracted by Mixture Densities. In Proceedings British Machine Vision Conference, pp. 459-

468, 1999.

[Miko03] Mikolajczyk K., and Schmid, C. A Performance Evaluation of Local Descriptors. In IEEE Conference on Computer Vision and Pattern Recognition (CVPR), pp. 1615-1630, 2003.

[Mitt05] Mittelman Roni and Moshe Porat. A New Approach to Feature Extraction for Wavelet-Based Texture Classification. In IEEE

International Conference on Image Processing (ICIP 2005), vol. 3, pp.

1128-1131, Sept. 2005.

[Moe01] Moeslund Thomas B., & Erik Granum. A Survey of Computer Vision-

Based Human Motion Capture. In Computer Vision and Image Understanding vol. 81, pp. 231-268, 2001.

[Mog97] Moghadam B., and Pentland, A. Probabilistic Visual Learning for Object Representation. In IEEE Transactions on Pattern Analysis and Machine Intelligence, vol. 19, no. 7, pp. 696-710, 1997.

[More77] Morefield C. L. Application of 0-1 Integer programming to Multitarget

Tracking Problems. In IEEE Transactions on Automation Control (AC-

22(6), June 1977.

[Moud99] Moudgill Mayan, Pradip Bose and Jaime H. Moreno. Validation of Turandot, a Fast Processor model for Microarchitecture Exploration. In Proceedings of IEEE International Conference on Performance, Computing and Communications Conference, February 1999.

[Mund06] Munder S., and D. M. Gavrila. An Experimental Study on Pedestrian Classification. IEEE Transactions on Pattern Analysis and Machine Intelligence, vol. 28, no. 11, pp. 1863 -1868, November 2006.

[Niyo94] Niyogi S. A., and E. H. Adelson. Analyzing and Recognizing Walking Figures in XYT. In Proceedings of IEEE Conference on Computer Vision and Pattern Recognition, pp. 469-474, 1994.

[Niyo99] Niyogi S. E., and E. H. Adelson. Analyzing and Recognizing Walking Figures in XYT. In Proceedings of IEEE Conference on Computer Vision and Pattern Recognition, pp, 469-474, 1999.

[Ober01] Oberti F., Elena Stringa, and Gianni Vernazza. Performance Evaluation Criterion for Characterizing Video-Surveillance Systems. In Real-Time Imaging, No. 7, pp. 457-471, 2001.

[Olso00] Olson C. Maximum-Likelihood Template Tracking. In Proc. IEEE Conference on Computer Vision and Pattern Recognition , vol. 2, pp. 52-57, 2000.

[Open02] The OpenMP Architecture Review Board. OpenMP C and C++ Application Program Interface,Second Edition,March 2002.

[Oren97] Oren M. C. Papageorgiou, P. Sinha, E. Osuna, and T. Poggio. Pedestrian Detection using Wavelet Templates. In Proceedings of Computer Vision and Pattern Recognition, pp. 193–99, 1997.

[Owec04] Owechko Yuri, Swarup Medasani, and Narayan Srinivass. Classifier Swarms for Human Detection in Infrared Imagery. In Proceedings of Conference on Computer Vision and Pattern Recognition Workshop (CVPRW'04), vol. 8, pp. 125- 135, June 2004.

[Pain05] Painkras E., Charoensak Charayaphan. A VLSI Architecture for Gabor Filtering in Face Processing Applications. In Proc. 2005 International Symposium on Intelligent Signal Processing and Communication Systems, pp. 437-440, 2005.

[Pais08] Paisitkriangkrai S., Shen S., Zhang J. Performance Evaluation of Local Features in Human Classification and Detection. IET Computer Vision, 2008, vol. 2, no. 4, pp. 236-246.

[Papa99] Papageorgiou C., and Tomaso Pogio. A Pattern Classification Approach to Dynamical Object Detection. In Proceedings of International Conference on Computer Vision, Greece, pp. 1223 -1228, 1999.

[Papa98] Papageorgiou C., P. Michael Oren, and Tomaso Poggio. A General Framework for Object Detection. In Sixth International Conference on Computer Vision, vol. 2, pp. 1223 -228, 1999.

[Pete99] Peterfreund N. The PDAF Based Active Contour. In Proceedings of the 7th IEEE International Conference on Computer Vision,vol.1, pp. 227-233, 1999.

[Plan01] Plankers R., and Pascal Fua. Articulated Soft Objects For Video-Based Body Modeling. In Proceedings of the 8th IEEE International Conference on Computer Vision, vol. 1, pp. 394-401, July 2001.

[Pogg89] Poggio T., and F. Girosi. Networks for Approximation and Learning. In Proceedings of IEEE, vol. 78, no. 9, Sept. 1990.

[Pola94] Polana R., and Nelson R. Low Level Recognition of Human Motion. In Proc. IEEE Workshop on Motion of Non Rigid and Articulated Objects. Austin, TX, pp. 77-82, 1994.

[Pori05] Porikli F., and Tuzel Oncel. Multi-Kernel Object Tracking. In Proceedings of IEEE International Conference on Multimedia and Expo, Amsterdam, 2005.

[Poul96] Poularikas Alexander (Chief Editor). The Transforms and Applications Handbook, CRC Press, and IEEE Press, (Electrical Engineering Handbook Series), pp. 747-828, 1996.

[Pun03] Pun C. –M., and M. –C. Lee. Log-Polar Wavelet Energy Signatures for Rotation and Scale Invariant Texture Classification. In IEEE Transactions on Pattern Analysis and Machine Intelligence, vol. 25, no. 5, pp. 590-603, May 2003.

[Quan97] Quanq Minh Tieng, and W. W. Boles. Recognition of 2D Object Contours using the Wavelet Transform Zero-Crossing Representation. In IEEE Transactions on Pattern Analysis and Machine Intelligence, vol.

19, pp. 910-916, 1997.

[Rasm01] Rasmussen C., and Hager G. Probabilistic Data Association Methods for Tracking Complex Visual Objects. In IEEE Transactions on Pattern Analysis and Machine Intelligence, vol, 23, no. 6, pp.560-576, 2001,

1979.

[Reid79] Reid D. B. An Algorithm for Tracking Multiple Targets. In IEEE Transaction on Automation and Control, vol. 24, no. 6, pp. 843-854, 1979.

[Ren03] Ren J., Astheimer P., and Feng D. Real-Time Moving Object Detection under Complex Background. In Proceedings of 3rd IEEE International Symposium on Image and Signal Processing and Analysis, pp. 662-667, 2003.

[Riou91] Rioul O., and M. Vetterli. Wavelets and Signal Processing. IEEE Signal Processing Magazine, pp. 14-38, October 1991.

[Rohr94] Rohr K. Towards Model-Based Recognition of Human Movements In Image Sequences. In Computer Vision, Graphics, and Image Processing: Image Understanding, vol. 59, no. 1, pp. 94-115, 1994.

[Roge03] Roger L. Claypoole, Geoffrey M. Davis, Wim Sweldens, Richard G. Baraniuk. Nonlinear Wavelet Transforms for Image Coding Via Lifting. In IEEE Transactions on Image Processing, vol. 12, no. 12, December

2003.

[Rose05] Rosenberg C,, Herbert Martial, and Schneiderman Henry. Semi-Supervised Self-Training of Object Detection Models. In 17th IEEE Workshop on Computer Vision (WACV/MOTIONS '05), vol. 1, 2005.

[Sang96] Sang-II Park, M. J. T. Smith and R. Murenzi. Multidimensional Wavelets for Target Detection and Recognition. In SPIE International Symposium on Aerospace/Defense Sensing and Controls, Orlando, Florida, April 8-12, 1996.

[Sang04] Sang Min Yoon and Hyunwoo Kim. Real-Time Multiple People Detection Using Skin Color, Motion and Appearance Information. In International Workshop on Robot and Human Interactive Communication, pages 331-334, 2004.

[Said96] Said A., and W. A. Pearlman. An image Multiresolution Representation for Lossless Image Compression. In IEEE Transactions on Image Processing, vol. 5, no. 9, pp. 1303-1310, 1996.

[Sar93] Sar-Sarraf H. Multiscale Wavelet Representation and Its Application to Signal Classification. PhD Dissertation, University of Tennessee, Knoxville, May 1993.

[Seni06] Senior Andrew, Hampapur Arun, Tian Ying_Li, Brown Lisa, Pankanti, and Bole Ruud. Appearance Models for Occlusion Handling. In Image and Vision Computing, vol. 20, pp. 1 -11, 2006.

[Scha02] Scharr M. Van Der, J. Ye, Y. Andreopoulos, and A. Munteanu. Fully Scalable 3-D Overcomplete Wavelet Coding Using Adaptive Motion Compensated Temporal Filtering. In ISO/IEC/JTC1/SC29/WG11, M9037, MPEG, Shanghai, China, October 2002.

[Schn00] Schneiderman H., and Takeo Kanade. A Histogram-Based Method for Detection of Faces and Cars. In Proceedings on International Conference on Image Processing, vol. 3, pp. 504 -507, 2000.

[Schn04a] Schneiderman H. Learning a Restricted Bayesian Network for Object Detection. In IEEE Conference on Computer Vision and Pattern Recognition, IEEE June 2004.

[Schn04b] Schneiderman H. Feature-Centric Evaluation for Efficient Cascaded Object Detection. In IEEE Conference on Computer Vision and Pattern Recognition (CVPR), IEEE June, 2004.

[Serb04] Serby D., Kollier_Meier S., and Gool, L.V. Probabilistic Object Tracking Using Multiple Features. In IEEE International Conference on Pattern Recognition (ICPR), pp. 84-187, 2004.

[Seth87] Sethi I., and Jain, R. Finding Trajectories of Feature Points in a Monocular Image Sequence. In IEEE Transactions on Pattern Analysis and Machine Intelligence, vol. 9, no. 1, pp.56-73, 1987.

[Shaf98] Shafarenko I., Petrou M, and Kittler J. Histogram-Based Segmentation in Perceptually Uniform Color Space. IEEE Transaction on Image Processing, vol. 7, no. 9, pp.1354-1358, 1998.

[Shen99] Shen, D., and Ip H. H. S. Discriminative Wavelet Shape Descriptors for Invariant Recognition of 2-D Pattern. In Pattern Recognition, vol. 32, pp. 151-165, 1999.

[Shin01] Shin M.C., D. B. Goldgof, K. W. Bowyer, and S. Nikiforou. Comparison of Edge Detection Algorithms Using Structure from Motion Task. In IEEE Transactions on Systems, Man, and Cybernetics-Part B: Cybernetics, vol. 31, pp. 589-601, August 2001.

[Side00] Sidenbladh H., and M. Black. Stochastic Tracking of 3D Human Figures using 2D Image Motion. In Proceedings of European Conference on Computer Vision, Ireland, pp. 702-718, 2000.

[Sita94] Sitaraman, K. A. Ejnioui, N. Ranganathan. A Parallel Algorithm for Object Recognition in Images. In Proc. IEEE International Workshop on Computer Architectures for Machine Perception (CAMP), 2003.

[Smit05] Smith Kevin, Daniel Gatica-Perez, Jean-Marc Odobez, and Sileye Ba. Evaluating MultiObject Tracking. Proceedings of the IEEE Computer Society Conference on Computer Vision and Pattern Recognition (CVPR'05) IEEE Press, 2005.

[Song 06] Song Bi, Amit K. Roy-Chowdhury, and N. Vaswani. Integrated Tracking

and Recognition of Human Activities in Shape Space. International Journal in Computer Vision, Graphics and Image Processing, pp. 468–

479, 2006.

[Stau98] Stauffer Chris and Grimson W. E.L. Adaptive Background Mixture Models for Real-Time Tracking. Proceedings of the IEEE Computer Society Conference on Computer Vision and Pattern Recognition '98. IEEE Press, 1998.

[Steff98] Steffens J, E. Elagin, and H. Neven. Person Spotter-Fast and Robust System for Human Detection, Tracking and Recognition. In Proceedings of IEEE International Conference on Automatic Face and Gesture Recognition, pp. 516- 521, 1998.

[Stra96] Strang G., and T. Nguyen. Wavelets and Filter Banks. Wellesley-Cambridge Press, 1996.

[Stri97] Strickland Robin N, and Hee Il Hahn. Transform Methods For Object Detection and Recovery. In IEEE Transactions on Image Processing, vol. 6, no. 5, pp. 724-735, May 1997.

[Stri00] Stringa E. Morphological Change Detection Algorithms for Surveillance Applications. In Proceedings of British Machine Vision Conference, pp.402- 412, 2000.

[Subr99] Subramanian K, S. S. Dlay and Rind F.C. Wavelet Transform for use in Motion Detection and Tracking Application. In Proceedings of IEE Conference on Image Processing and Its Applications. 1999.

[Swai91] Michael J. Swain and Ballard Dana H. Color Indexing. In International

Journal of Computer Vision, vol. 7, no. 1, pp. 11-32, 1991.

[Swel96] Sweldens W. The Lifting Scheme: A Custom-Design Construction of Biorthogonal Wavelets. In Applied and Computational Harmonic Analysis, vol. 3, no. 2, pp.186-200, 1996.

[Swel97] Sweldens W. The Lifting Scheme: A Construction of Second-Generation Wavelets. In SIAM Journal of Mathematical Analysis, vol. 29, no. 2, pp. 511-546, 1997.

[Taka88] Takas Barnabas and Lev Sadovnik. Three-Dimensional Target Recognition and Tracking using Neural Networks Trained on Optimal Views. Optical Eng. vol.37, no.3, March pp. 819-828, 1988.

[Tang00] Tang Y.Y., Yang I. H., Liu J., and Ma H. Wavelet Theory and Its Application to Pattern Recognition (Series in Machine Perception and Artificial Intelligence, vol. 36). World Scientific, Singapore, 2000.

[Tan98] Tan T. N., G. D. Sullivan, and K. D. Baker. Model-Based Localization and Recognition of Road vehicles. In International Journal in Computer Vision vol. 29, no. 1, pp. 22–25, 1998.

[Tani87] Tanizaki H. Non Gaussian State Space Modelling of Non Stationary Time Series. In Journal of American Statistical Association, vol. 82, pp. 1032-1063, 1987.

[Tax00] Tax David M. J., Breukelen Martin Van, Duin Robert P. W, and Kittler Josef. Combining Multiple Classifiers by Averaging or by Multiplying. In Pattern Recognition, vol. 33, pp. 1475-1485, 2000.

[Terz92] Terzopoulos D., and Szeliski R. Tracking with Kalman Snakes. In Active Vision. Blake A and Yuille A (Editors). MIT press, 1992.

[Teol98] Teolis Anthony. Computational Signal Processing with Wavelets Applied and Numerical Harmonic Analysis Series), Birkhauser Verlag AV, 1998.

[Tian96] Tian T., and C. Tomasi. Comparison of Approaches to Egomotion Computation. In Proc. IEEE Conf. Computer Vision and Pattern Recognition, 1996.

[Tieu03] Tieu K., and Viola P. Boosting image Retrieval. International Journal of Computer Vision, vol. 56, no. 1, pp17-36, 2003.

[Toma99] Tomaso Pogio and Papageorgiou Constantine. Trainable Pedestrian Detection System. In Proceedings of IEEE Intelligent Vehicles Symposium, Stuttgart, pp. 241 -246, 1999.

[Tou74] Tou J. T., and Gonzalez R. C. Pattern Recognition Principles. Addison-Wesley, London, 1974.

[Tree68] Trees Van H. Classical Detection and Estimation Theory-Detection, Estimation, and Modulation Theory. John Wiley & Sons, Inc, pp. 1946, 1968.

[Tull95] Tullsen Dean M., Susan J. Eggers, and Henry M. Levy. Simultaneous Multithreading: Maximizing On-Chip Parallelism. In Proceedings of the 22nd Symposium on Computer Architecture, pp. 392-403, 1995.

[Unse95] Unser M. Texture Classification and Segmentation using Wavelet Frames. In IEEE Transactions in Image Processing, vol. 4, no. 11, pp. 1549 –1560, 1995.

[Vapn82] Vapnik V. Estimation of Dependencies Based on Empirical Data. Springer-Verlag, 1982.

[Veen01] Veenam C., Reinders M., and Backer E. Resolving Motion Correspondence for Densely Moving Points. In IEEE Transaction on Pattern Analysis and Machine Intelligence, vol. 23, pp. no.1, pp. 54-72, 2001.

[Viol01] Viola P., and Jones Michael. Robust Real-time Object Detection. In International Workshop on Statistical and Computational Theories of Vision-Modeling, Learning, Computing and Sampling, Vancouver, Canada, July 13, 2001.

[Viol03] Viola P., Jones Michael, and D. Snow. Detecting Pedestrians Using Patterns of Motion and Appearance. Proceedings of International Conference on Computer Vision, pp. 734 -741, 2003.

[Viol03] Viola P., and Tieu K. Boosting image Retrieval. International Journal on Computer Vision, vol. 56, 1, 17-36, 2003.

[Vish94] Vishwanath M. The Recursive Pyramid Algorithm for The Discrete

Wavelet Transform. In IEEE Transactions on signal Processing, vol. 42, no. 3, pp. 673- 676, March 1994.

[Wact97] Wachter S., and H. H. Nagel. Tracking Persons in Monocular Image

Sequences. In Proceedings of IEEE Workshop on Non rigid and Articulated Motion, pp. 2- 9, 1997.

[Wang95] Wang Yuping and Cai Yuanlong. Construction and Properties of B-Spline Wavelet Filters for Multiscale Edge Detection. In Proceedings of the IEEE International Conference on Image Processing, vol. 2, pp. 2145-2148, 1995.

[Wata85] Watanabe S. Pattern Recognition: Human and Mechanical. Wiley, New York, 1985.

[Webb99] Webb Andrew (Defence Evaluation and Research Agency, UK). Statistical Pattern Recognition, Arnold, London, 1999.

[Weim04] Weiming Hu, Tienu Tan, Liang Wang, and Steve Maybank. A Survey on

Visual Surveillance of Object Motion and Behaviors. In IEEE Transactions on Systems, Man, and Cybernetics-Part C: Applications and Reviews, vol. 34, no. 3, August 2004.

[Wei06] Wei Qui Bouaynaya, and Schofeld D. Automatic Multi-Head Detection and Tracking Systems Using a Novel Detection-Based on Particle Filter and Data Fusion. Proceedings of IEEE International Conference on Acoustic Speech, and Signal Processing, vol. 2, 2005, pp.661-664.

[Wein06] Weinman Jerod J., Allen Hanson, and Erik Learned-Miller. Joint Feature Selection for Object Detection and Recognition. University of Massachusetts-Arhmerst Technical Report, 06-45, pp. 12, 2006.

[Wohl99] Wohler C., and Anlauf Joachim K. A Time Delay Neural Network Algorithm for Estimating Image-Pattern Shape and Motion. In Image and Vision Computing, vol. 17, pp. 281-294, 1999.

[Wre97] Wren, C. R., A. Azarbayejani, T. Darell, and A. P. Pentland. Pfinder: Real-Time Tracking of the Human Body. In IEEE Transactions on Pattern Analysis and Machine Intelligence vol. 19, pp. 780 -785, July 1997.

[Wu93] Wu Z., and Leahy R. An Optimal Graph Theoretic Approach to Data Clustering: Theory and Applications to Image Segmentation. In IEEE Transactions on Pattern Analysis and Machine Intelligence, vol. 11, pp. 101-1113, 1993.

[Wu05] Wu B., and Nevatia R. Detection of Multiple, Partially Occluded Humans in Single Image by Bayesian Combination of Edgelet Part

Detectors. Proceedings on International Conference on Computer Vision vol. I, pp. 90-97, 2005.

[Wu06] Wu Bo and Ram Nevatia. Tracking of Multiple, Partially Occluded Humans based on Static Body Part Detection. In Proceedings of the IEEE computer Society Conference on Computer Vision and Pattern Recognition, Vol. 1, pp. 951- 958, 2006.

[Wu07] Wu Bo and Nevatia Ram. Detection and Tracking of Multiple Partially Occluded Humans by Bayesian Combination of Edgelet Based Part Detectors. In International Journal of Computer Vision, Springer Science, USA, 2007.

[Wuns95] Wunsch P., and Laine A. F. Wavelet Descriptors for Multiresolution Recognition of Handprinted Characters. In Pattern Recognition, vol. 28,

no. 8, pp.1237-1247, 1995.

[Xu92] Xu L., Kryzak A., and Suen C. V. Methods of Combining Multiple Classifiers and their Applications in Handwriting Recognition. In IEEE Transactions on Man and Cybernetics, vol. 22, no. 3, pp. 418-435, 1992.

[Yasu94] Yasun Xu, J. Weaver, Healy D, and Lu J. Wavelet Domain Transform Filters: A Spatially Selective Noise Filtering Technique. In IEEE Transaction on Image Processing, vol. 3, no. 6, pp. 747-758, Nov. 1994.

[Yeas04] Yeasin Mohammed, Ediz Polat, and Rajeev Sharma. A MultiObject Tracking Framework for Interactive Multimedia Applications. In IEEE Transactions on Multimedia, vol. 6, no. 3, June 2004.

[Yilm04] Yilmaz A., Li X., and Shah M. Contour-Based Object Tracking With Occlusion Handling in Video Acquired Using Mobile Cameras. IEEE Trans. Pattern Analysis and Machine Intelligence, vol. 26, no. 11, pp.

1531-1536, 2004.

[Yilm06] Yilmaz A., Javed Omar, and Shah Mubarak. Object Tracking: A Survey. In ACM Computing Surveys, vol. 38, no. 4, Article 13, December 2006.

[Zeha04] Zehang Sun, George Bebis, Ronald Miller. Object Detection using Feature Subset Selection. In Pattern Recognition, no. 37, pp. 165-2176, 2004.

[Zett90] Zettler W. R., Huffman J, and D. C. P. Linden. Application of Compactly Supported Wavelets to Image Compression. In SPIE/SPSE Symposium on Electronic Imaging Science, no. 1244, pp. 150-160, February 1990.

[Zhan89] Zhang J. D. Wang, and Q. N. Tran. A Wavelet-Based Multiresolution Statistical Model of Texture. In IEEE Transactions on Image Processing, vol. 7, no. 11, pp. 1621-1627, 1989.

[Zhan97] Zhang J. D. Wang, and Q. N. Tran. Wavelet-Based Multiresolution Image Models. Technical Report, Department of Electrical Engineering and Computer Sciences, University of Wisconsin-Milwaukee, February 1997.

[Zhou04] Zhou Shaohua, Rama Chellappa, Moghaddam Baback. Visual Tracking and Recognition Using Appearance-adaptive Models in Particle Filters. IEEE Transactions on Image Processing, vol. 13, November 2004.

Appendix A

Commercial Video Analytics Software Features

Company: CIEFFE, Location United Kingdom

Area of specialisation: video analytics software

Generic features:

Windows-based GUI

PTZ camera control through software

Multiview screen display

Site map overlaid with camera location

Live video acquisition and synchronised multi camera playback

Visualization of alarms and alarm management

Remote control and configuration

Parameter driven configuration of software (time, speed, size, etc)

Zone selection

Directional virtual tripwire

Text annotation of videos

End user features:

Motion detection

Motion-based recognition

Motion detection and tracking

Abnormal behaviour detection

Abandoned object detection

Removed object detection

Multiple object tracking

Image processing functions

Gamma correction, saturation, sharpening, blurring, contrast enhancement, Equalization reversing, masking, negative and mosaic, and compression/decompression

Configurability

Supports 1 to 30 cameras

Supports analogues cameras

Internet protocol based (IP)

Alarms

Camera occlusion alarms

Security

Embedded hardware architecture

Embedded operating systems

Integrated firewall for direct internet connection

Real-time processing

25 -30 frames per second

Company: Aimetis, Canada

Area of specialisation: video analytic software and Network video vendor

Generic features

Client server-based

Windows-based GUI

Video management

Remote live video recordings and playback

Automated control of PTZ camera

End user functionality

Motion tracking

Object classification

Object counting (humans/ cars)

Alarms

Sirens

Text to speech

Configurability

Supports up to 16 cameras

Array of storage device

Local hard disk, RAID, storage area network (SAN)

Company Name: Videoalert, Software vendor. Integrates with third party platform and software sub system

End user functionality

Alerts

Event detection

Directional virtual tripwire

Object tracking/Counting

Abandoned objects

Monitoring traffic rule violation

Data statistics

Company Name: Vis-a-pix, Video analytics software vendor

Location: Germany

Generic functions

Zone definitions

Virtual tripwire

Camera locations overlaid with site map

Live video record/playback

Interactive monitoring of camera operations

Runs on windows environment

End user functionality

Alarms implemented as coloured events

People counting

Vehicle detection

Intrusion detection

Behaviour analysis

Anomalous behaviour detection

Works in indoor and outdoor environment

Configuration

Integrate with analogue and digital cameras;

Supports up to 8 cameras per personal computer

Accuracy

Detection rate of 90% in zone areas

APPENDIX B

Proposed Structure of Human Detection and Tracking Algorithm

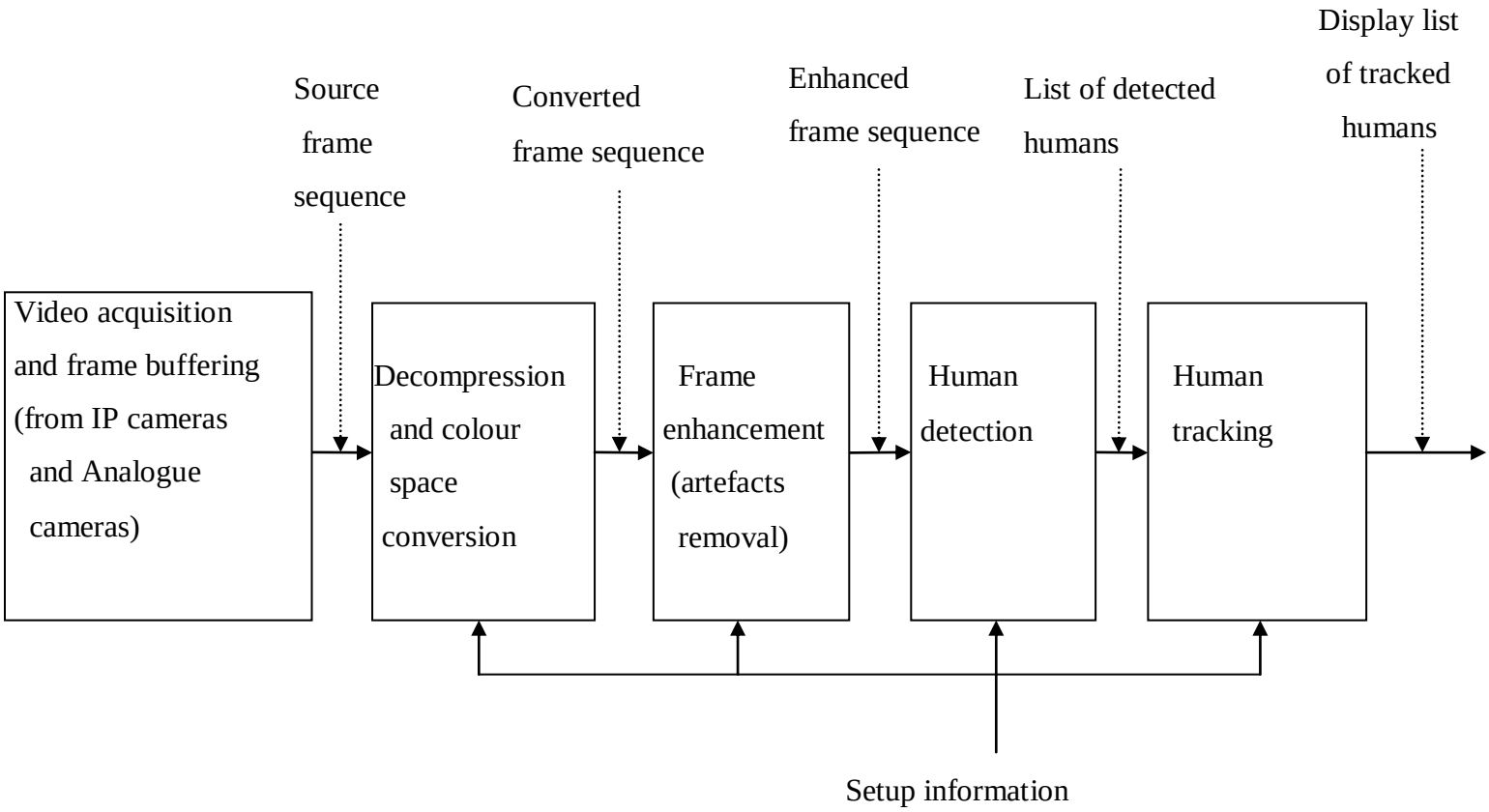

Video acquisition and buffering

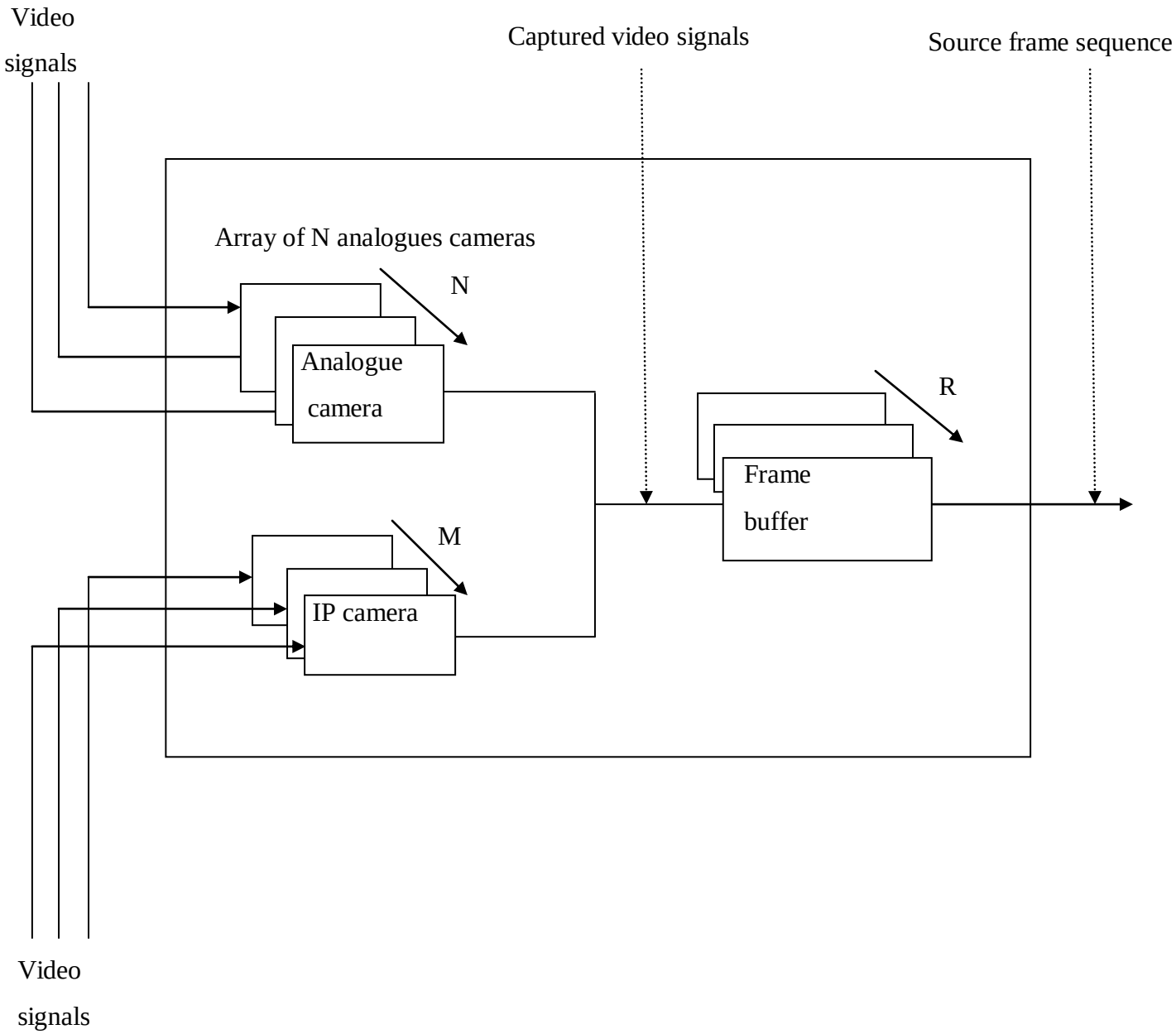

Decompression and colour space conversion

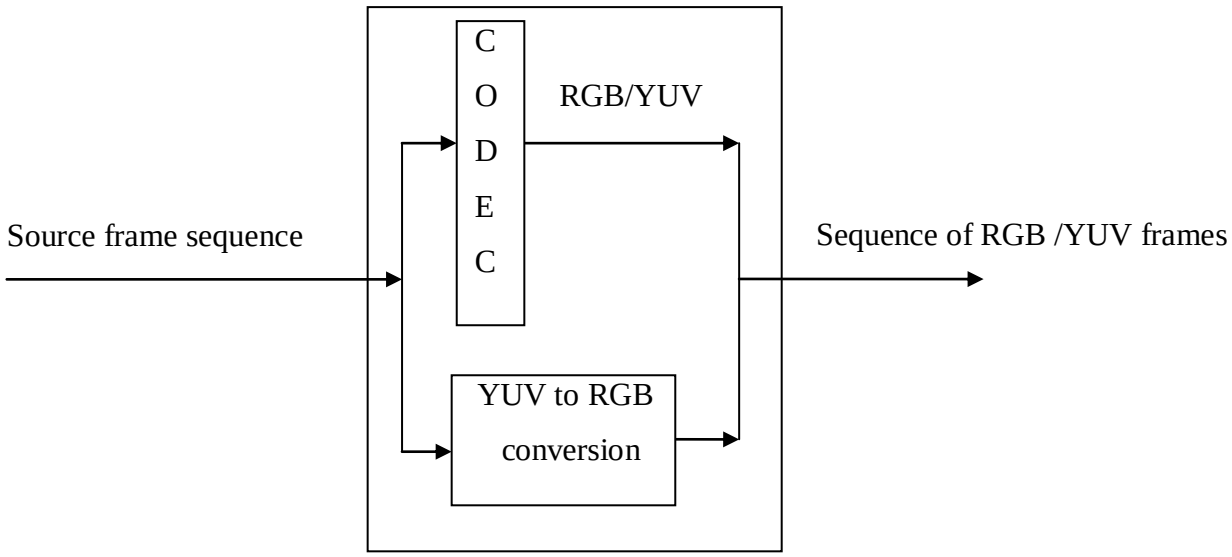

Frame enhancement

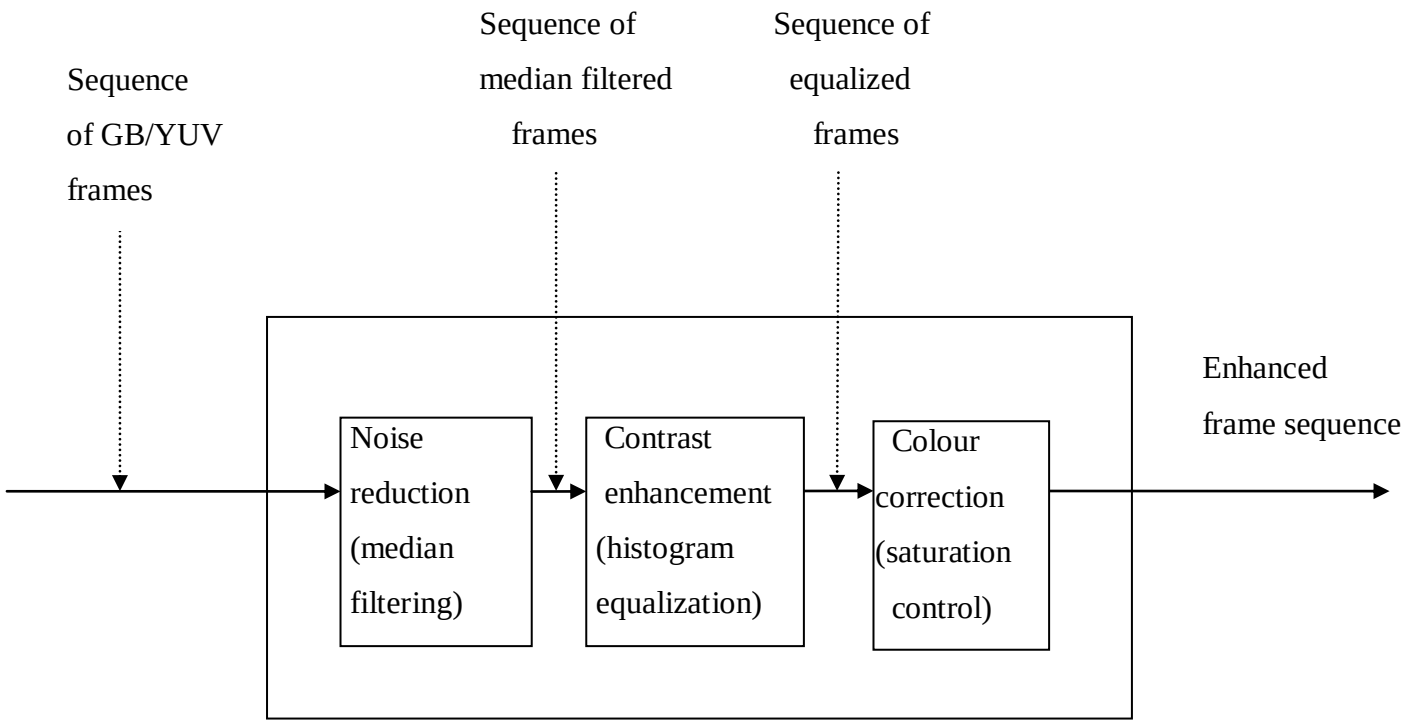

Human detection

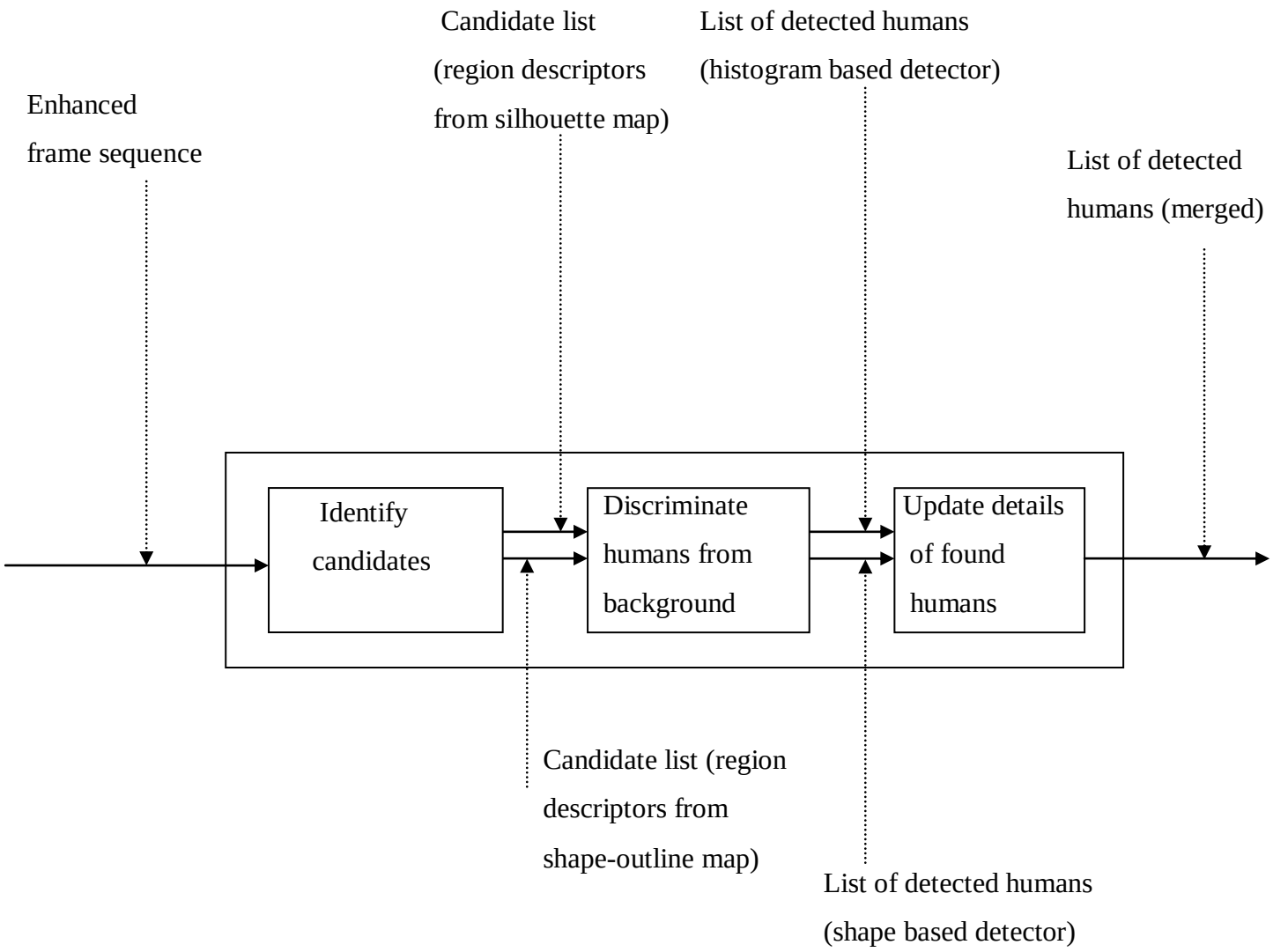

Identify candidates

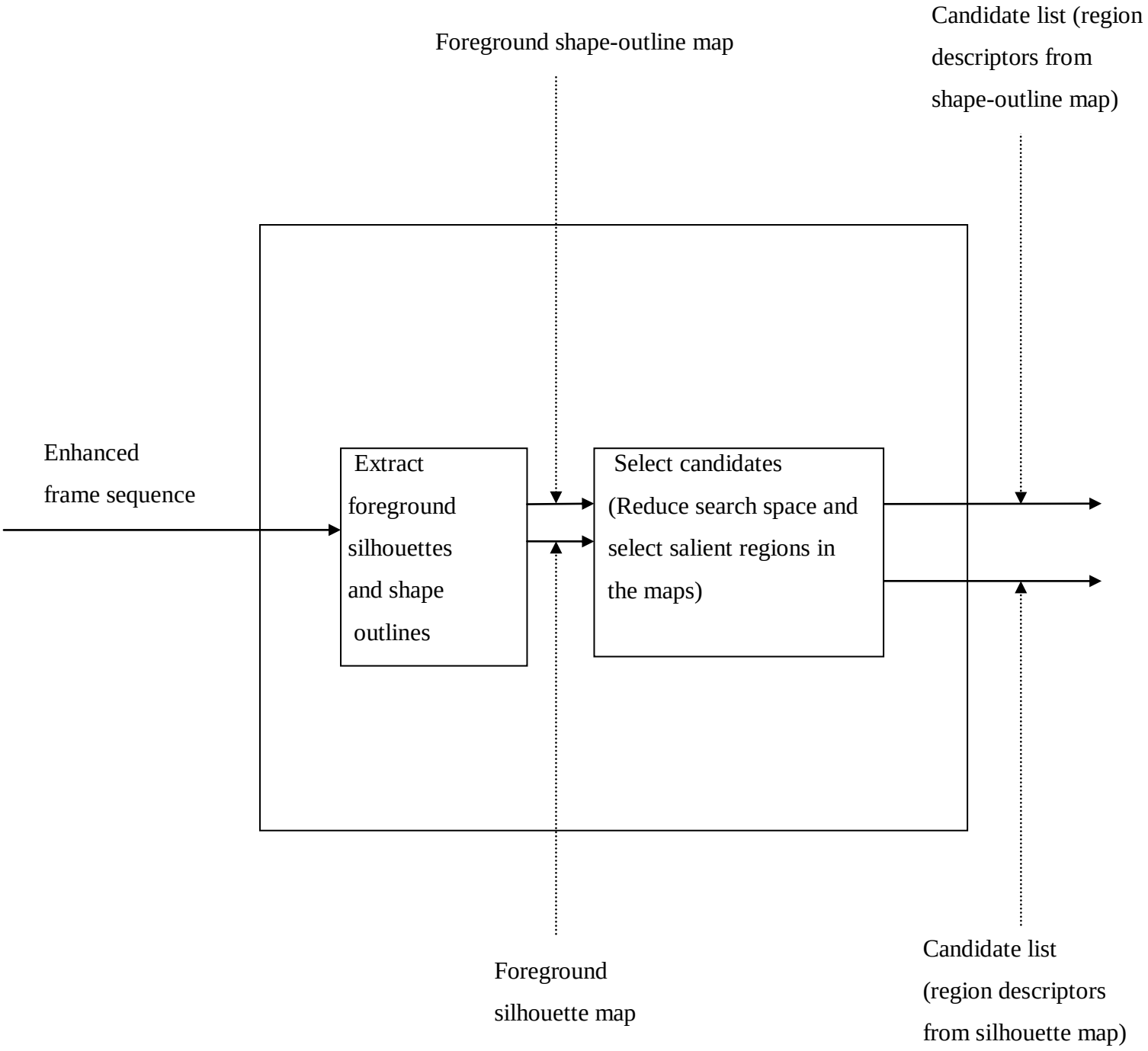

Human discrimination

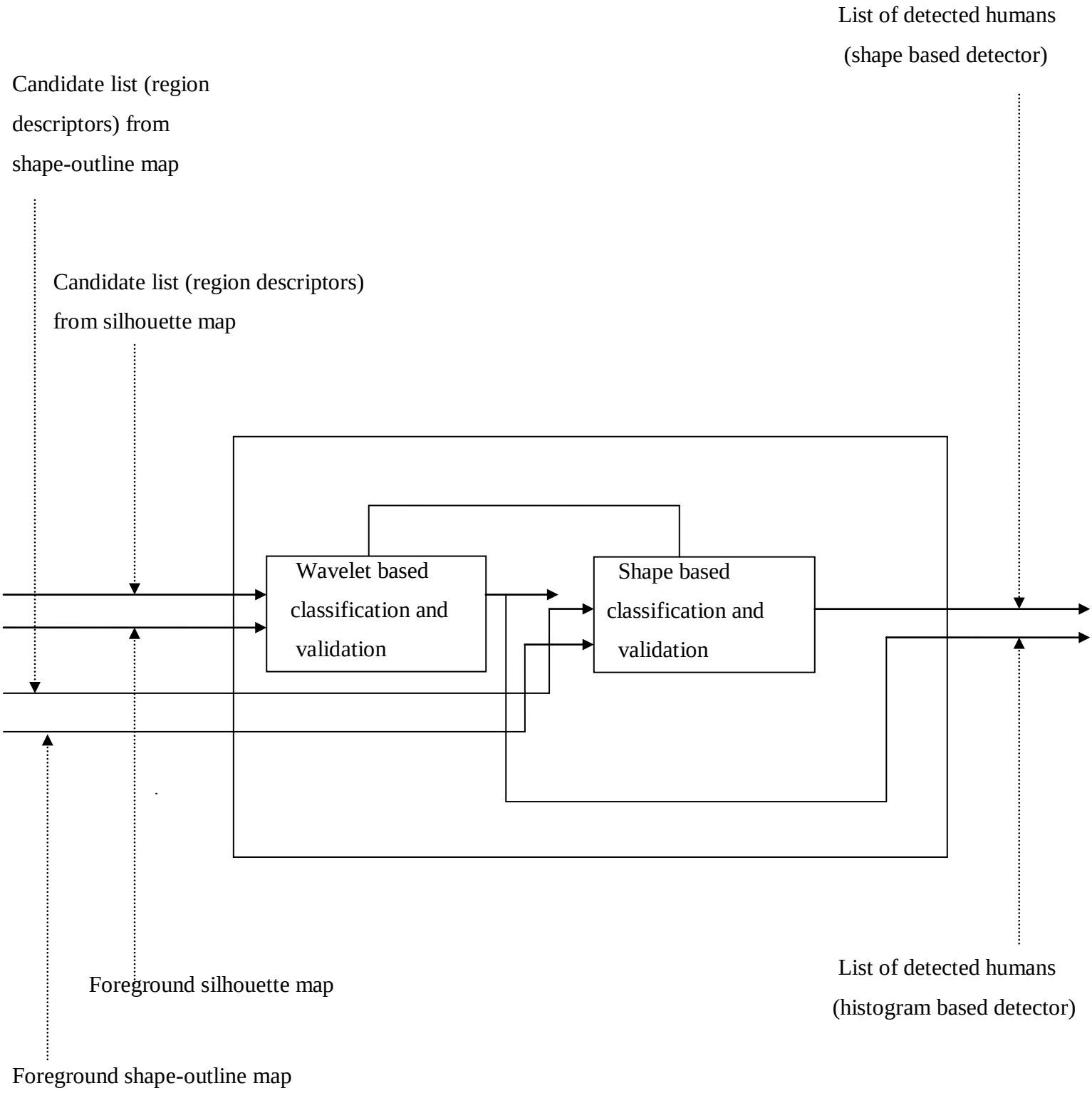

Update details of found humans

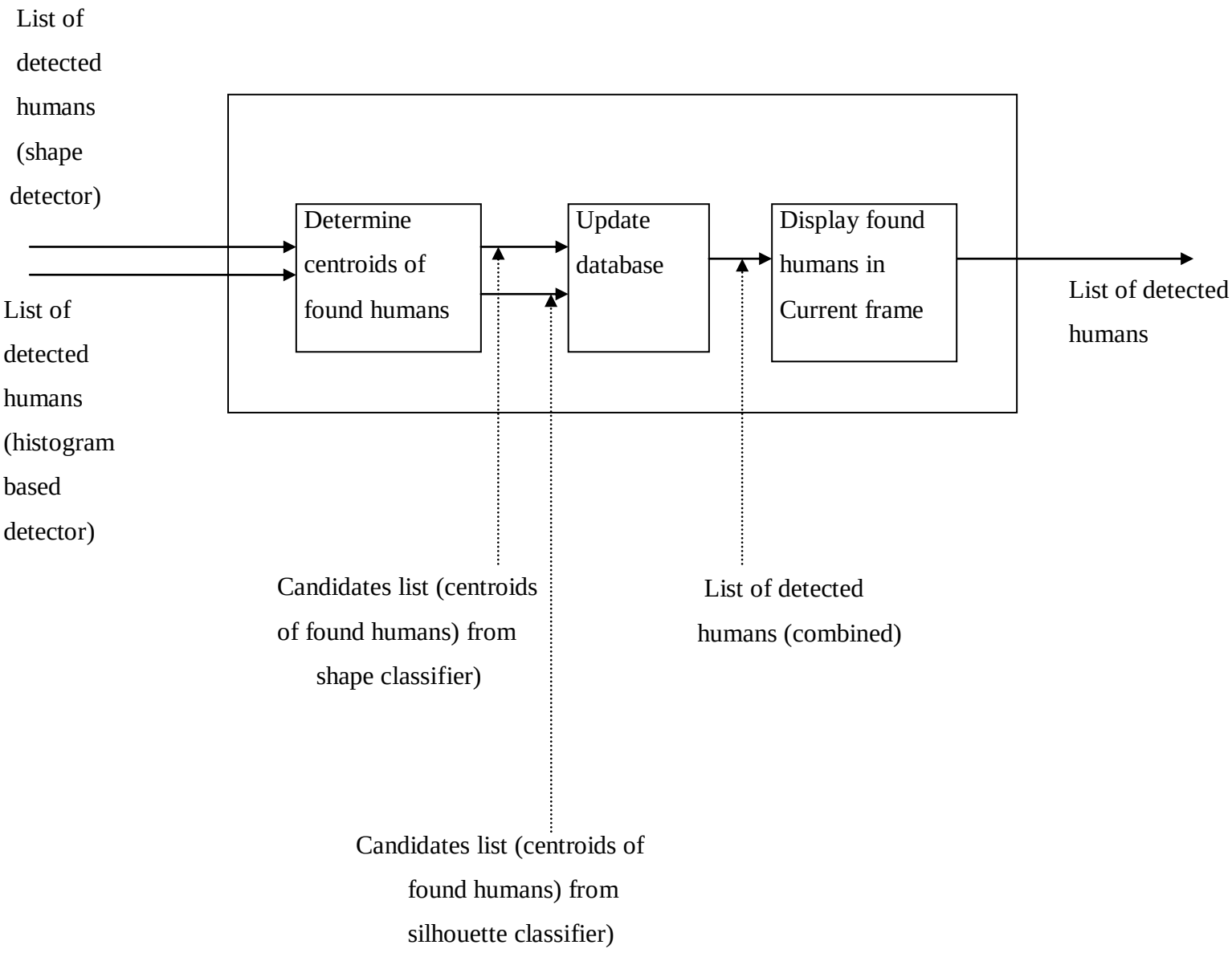

Extract foreground silhouettes and shape outlines

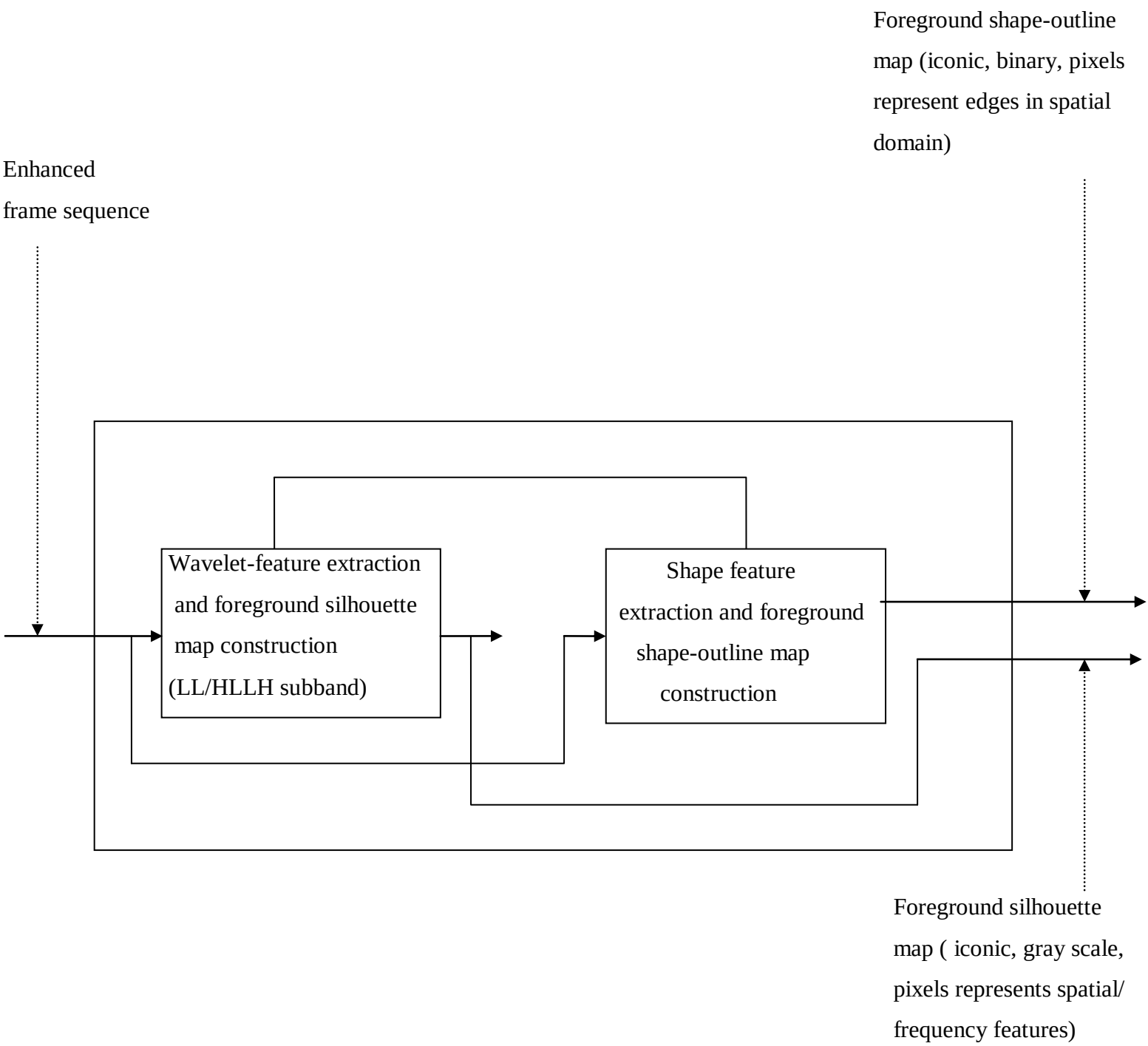

Wavelet-feature extraction and foreground silhouette map construction (LL/HLLH subband)

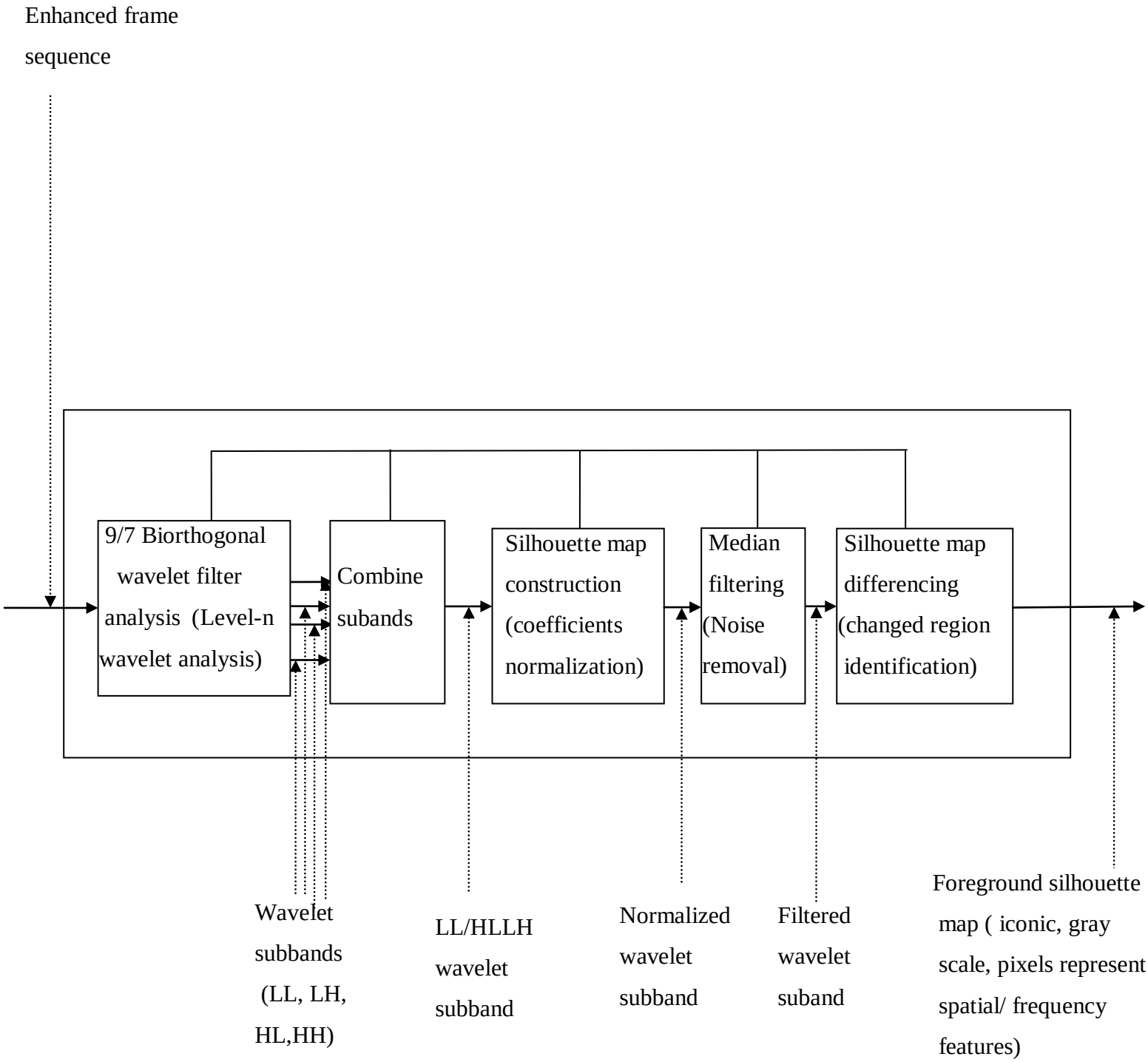

Shape feature extraction and foreground shape-outline map

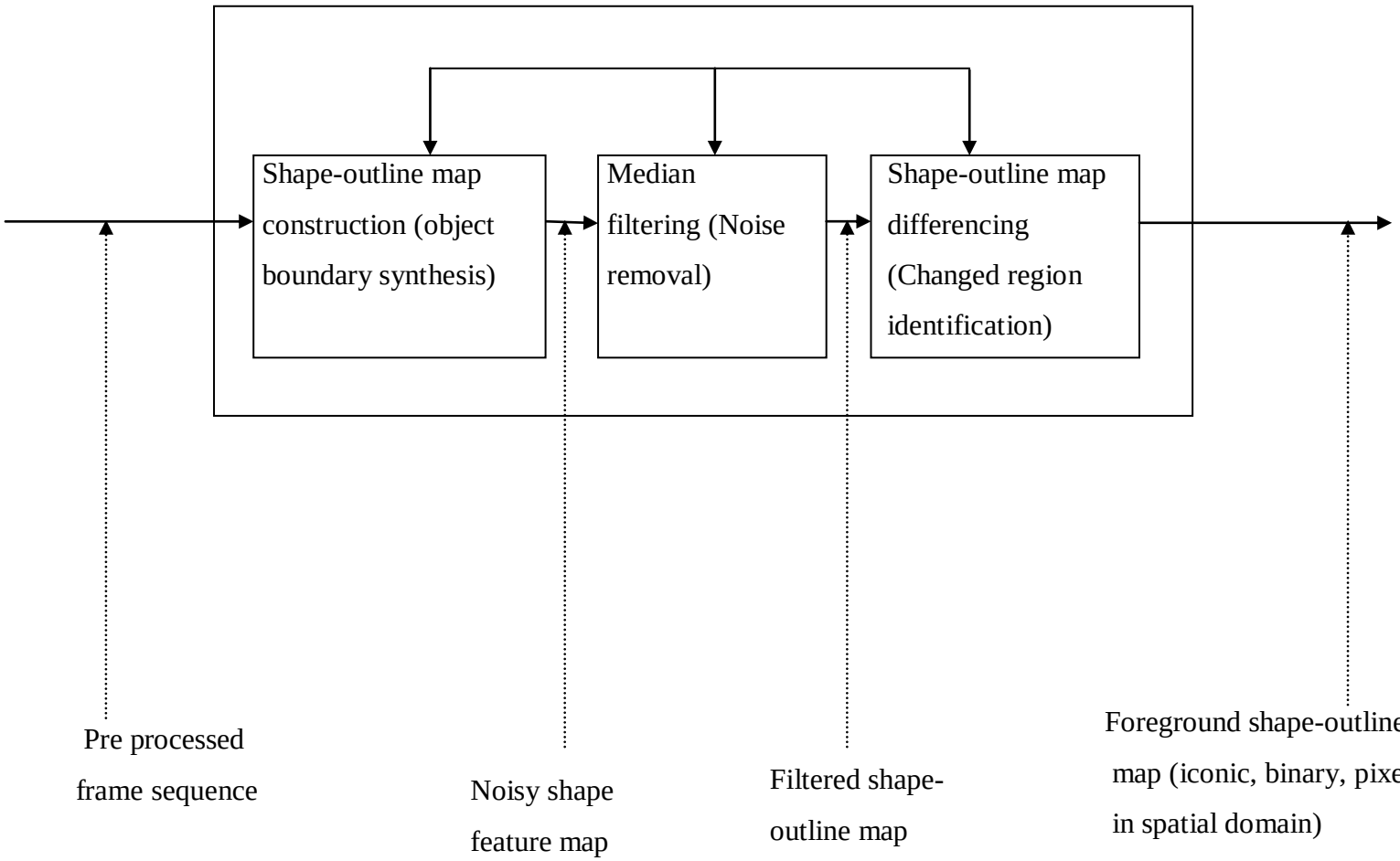

Level 3 wavelet analysis

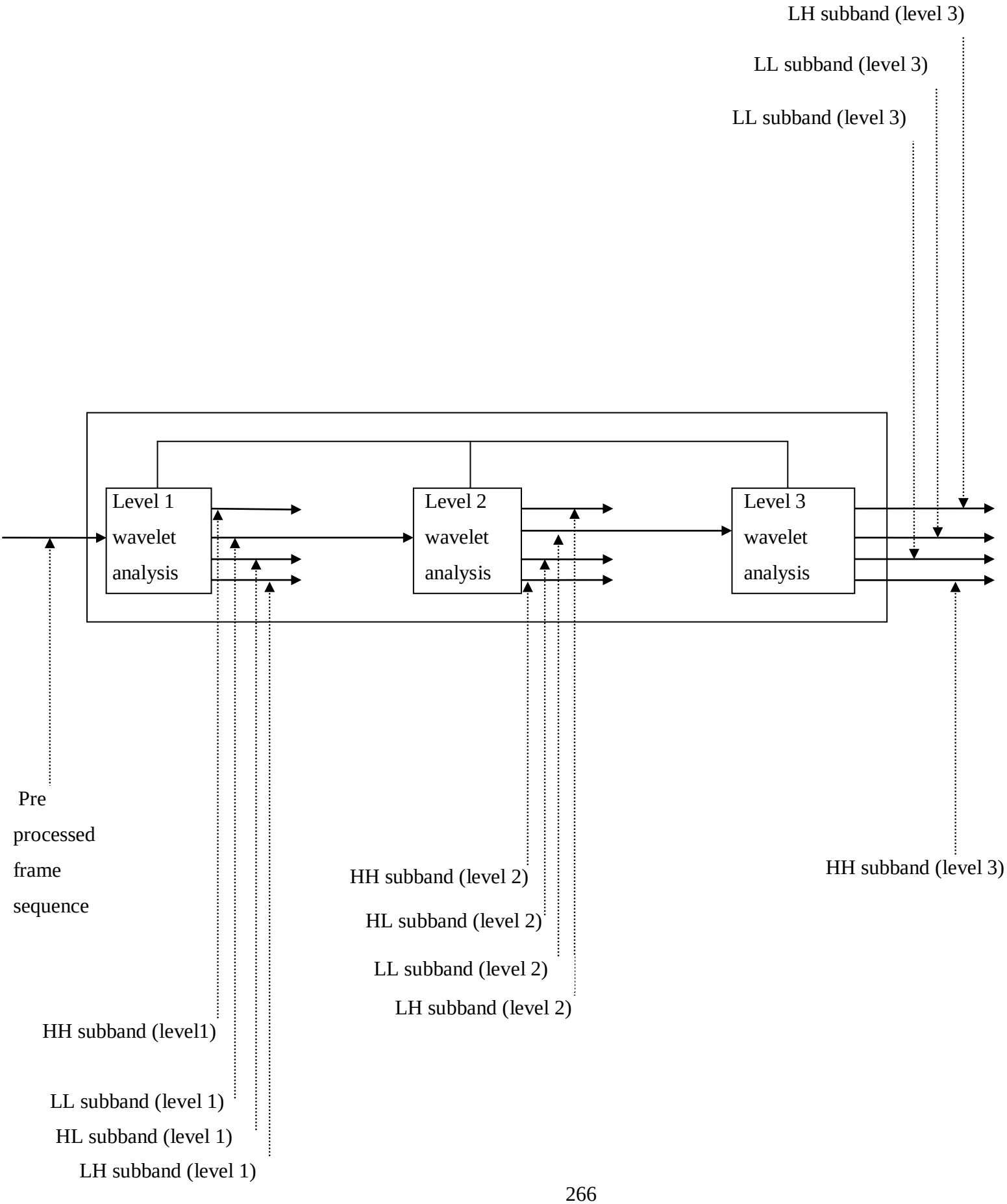

Level 2 wavelet analysis

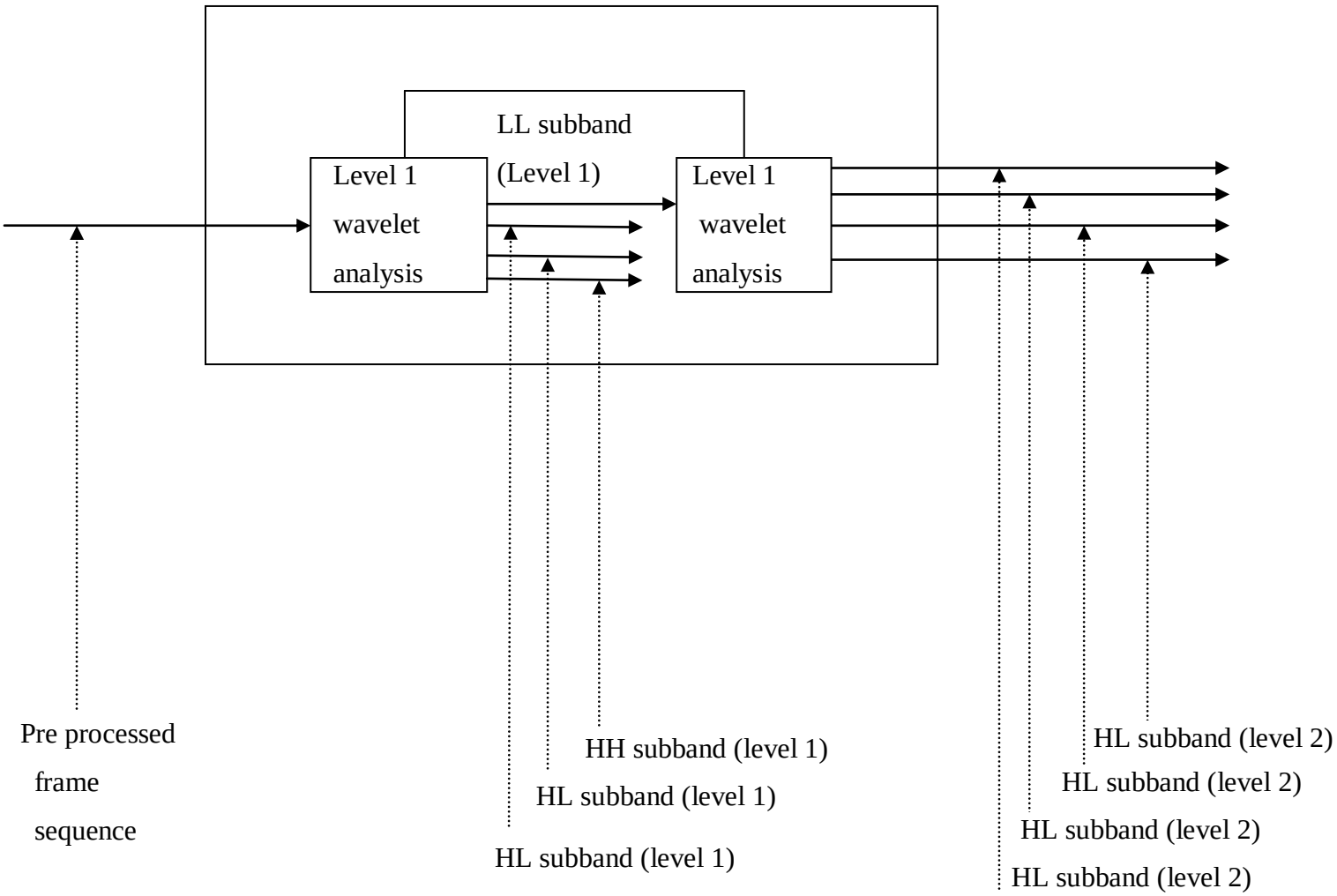

Level 1 wavelet analysis

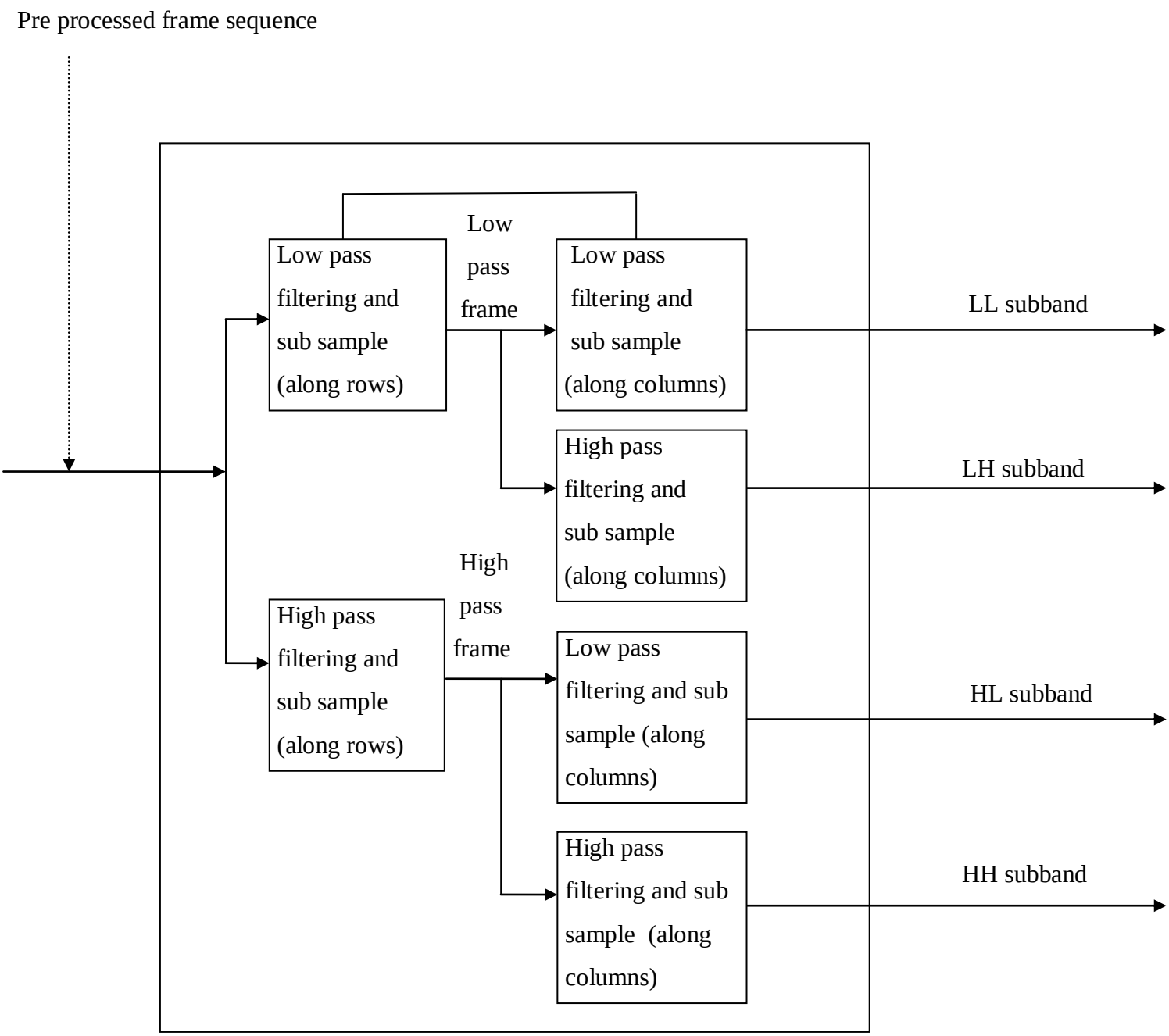

Select candidate regions

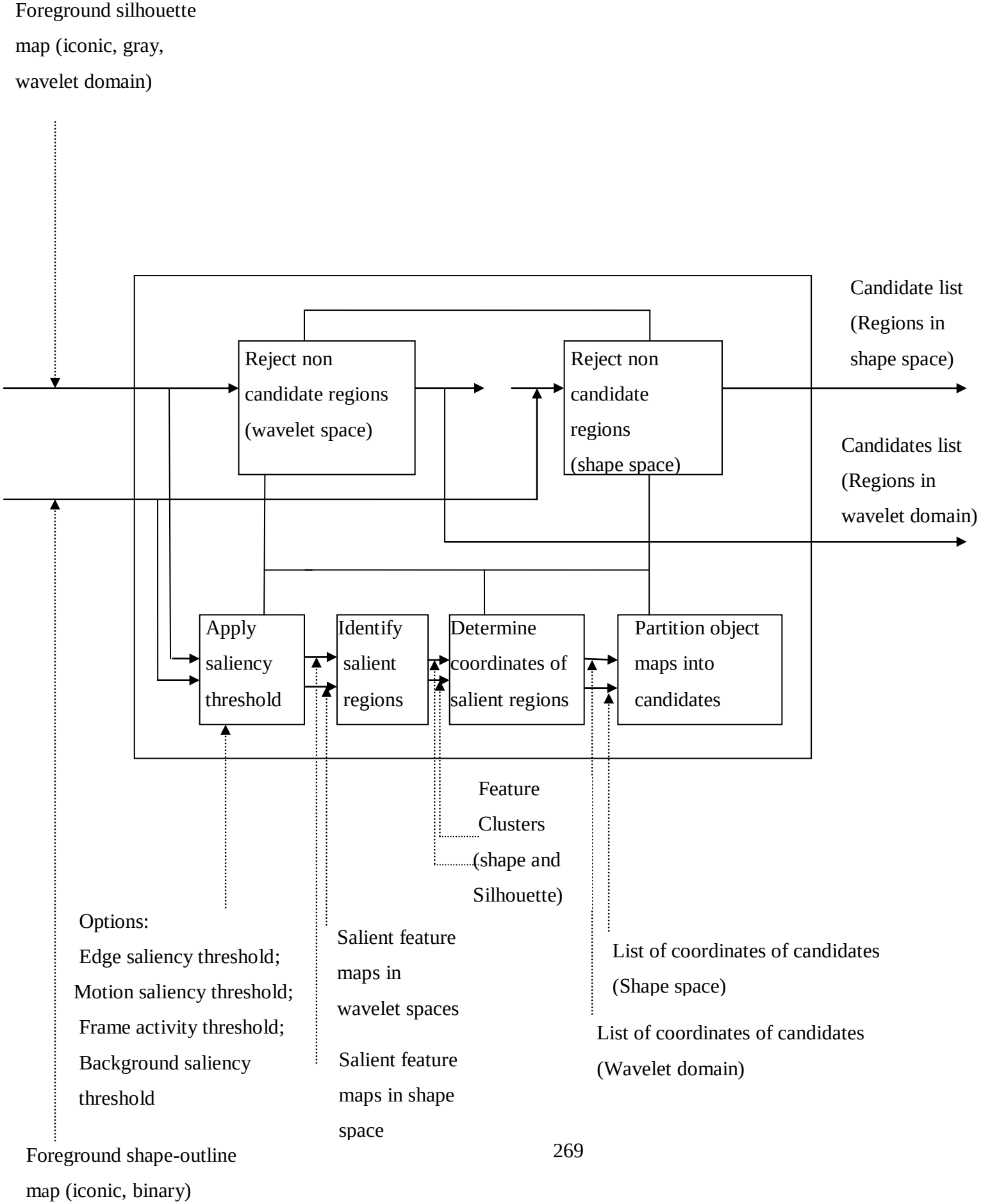

Wavelet based classification and validation

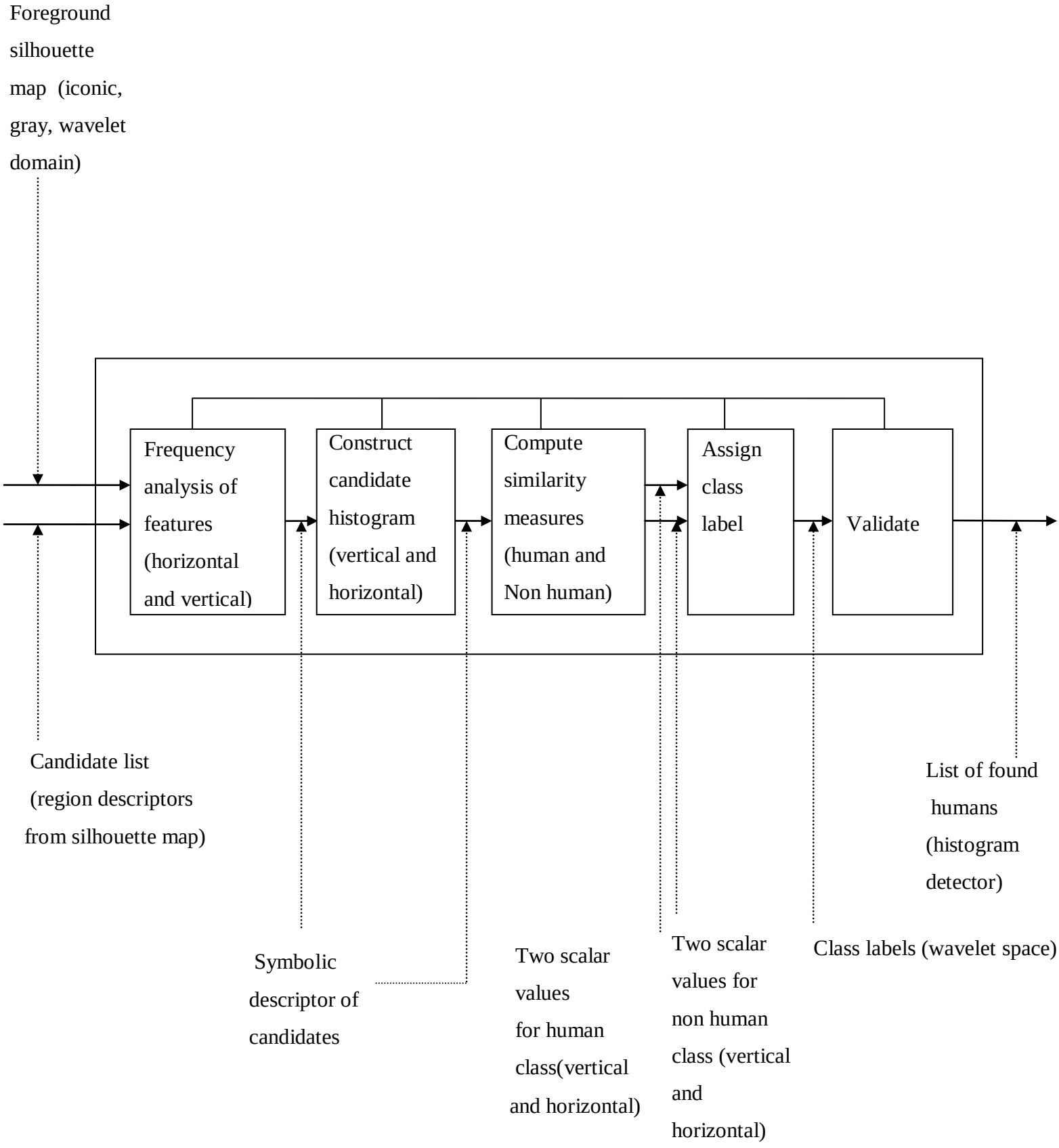

Shape based classification and validation

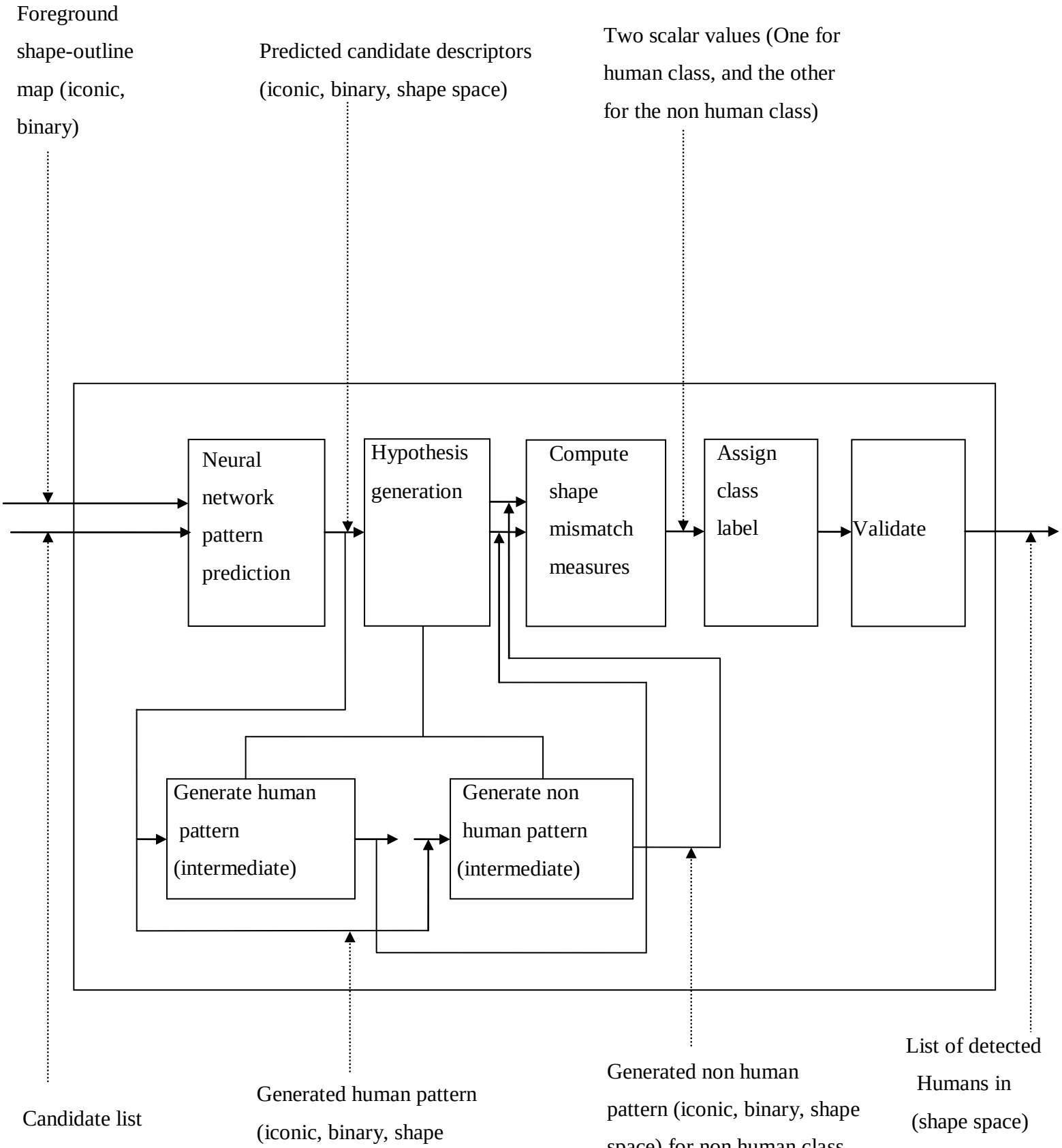

Human tracking

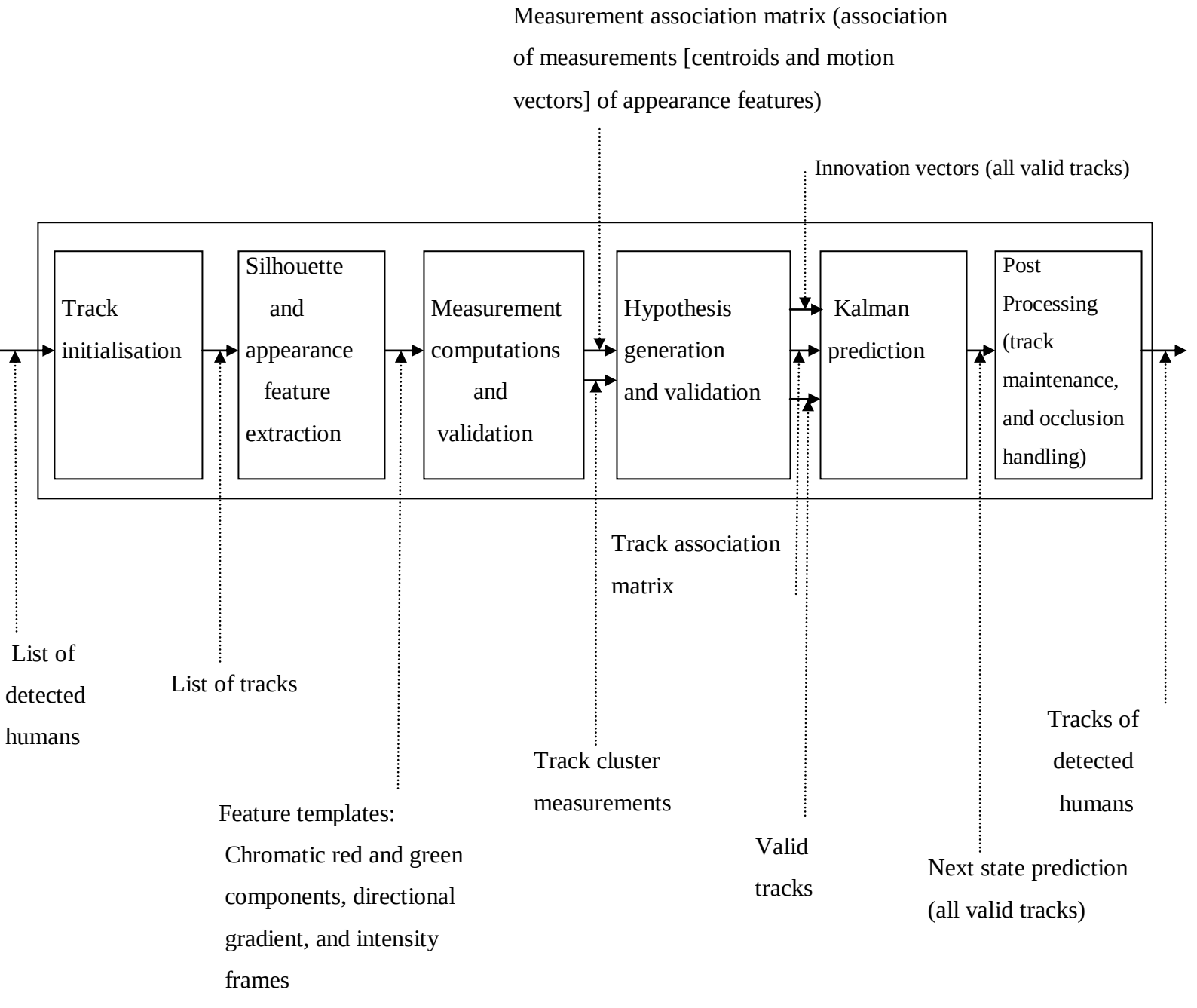

Legend

Sequence

Label

Decomposition

Appendix C

Characteristics of Human Detection and Tracking:

- Detection
  - Provides location and boundary information
  - Optionally may provide pose information
- Tracking
  - Location, direction, and trajectory information (tracks)
  - Requires motion model, search strategy, and matching criteria
    - By optimization of a cost function
    - Taylor approximation
    - Kalman prediction
    - Stochastic sampling (Monte Carlo based Sampling, Particle filter)
    - Based on behaviour analysis
      - Hidden Markov Model (HMM)
      - Hierarchical principal component analysis (HPCA)
- Space-time domain detection and tracking of humans
  - Human detection
    - Feature-based
      - Point-based feature
      - Scale invariant feature transform (SIFT feature)
    - Appearance-based features
      - Shape/silhouette/contour + appearance characteristics;
      - Density based representations
      - Dependence graph
      - View-based
        - Supervised classifier
          - Support vector machine
          - Feed forward neural network
      - Sub space methods

- Principal Component Analysis classifier
- Eigen space decomposition classifiers

- Non Segmented
  - Classifier based
    - Boosting
    - Feed forward neural network
    - Support vector classifier
    - Self organizing feature map
  - Segmented
    - Foreground/background modelling
      - Frame differencing
      - Background subtraction
      - Gaussian mixture modelling
      - Mean shift clustering
      - Density estimation based on colour, texture, intensity, gradient
      - Optical flow
      - Spatio-temporal entropy+ morphological operations
    - Model-based recognition
      - 2-D human model + motion model+ search strategy
      - 3-D human model + motion model + search strategy
    - Motion-based recognition
      - Spatial-temporal motion analysis
      - Gait-based recognition

- Human Tracking
  - Tracker types
    - Feature-based
      - Point-based Feature
        - Centroids + Kalman prediction
    - Kernel/Region-based
      - Geometric shape (rectangular, ellipse, circle)
      - Appearance-based (probability distribution based)
      - Multiview appearance

- Support vector classifier
- Feedforward classifier
- Template based (Intensity, gradient, colour)

- Silhouette-based
  - Contour-based
  - Shape-based+ interior representation

- Wavelet Domain Detection and Tracking of Humans
  - Wavelet domain detection
    - Candidate features
      - Multiscale edge and motion
      - Multiscale phase information
      - Multiscale wavelets coefficients
  - Multiscale feature classification
    - Feedforward neural network
    - Self organizing feature maps
  - Wavelet-domain tracking
    - Template matching + motion model + search strategy
- Model-based Detection and Tracking of Humans
- Appearance-Based Detection and Tracking of Humans
- Shape-Based Detection and Tracking of Humans
  - Edgelet based representation
  - Fourier based representation
  - Spline based representation
  - View based
    - Part based representation
    - Full human representation
- Motion-Based Recognition and Tracking of Humans
  - 2-D models
  - 3-D model

- Motion correspondence
  - Affine-based transform
  - Kernel or template based matching

APPENDIX D 1.1

Edge Saliency

Sequence: Hamilton2b.avi
Rows: 240
Columns: 320
Frames: 1000

A: Dbase_spacingX
B: Dbase_SpacingY
C:Object width
D:Object height
FactorY:Scale factorY
FactorX:Scale factorX
F:Fixed background flag
Theshold1: Object Outline threshold
E:Median filtering
HE: Histogram equalization

SHAPE-BASED DETECTOR

TPR	FPR	FNR	A	B	C	D	E	Threshold	HE	F	FactorX	FactorY	MaxNoObjects
61.4	3.06	38.6	24	32	48	64	1	5	0	1	2	2	8
54.52	3.66	45.48	24	32	48	64	1	5	0	1	1.5	1.5	8
48.13	3.77	51.87	24	64	48	128	1	5	0	1	1	1	8
60.07	4.53	39.93	16	50	32	100	1	5	0	1	2	2	8
56.09	5.74	43.91	16	40	32	80	1	5	0	1	0.2	0.2	8
56.09	6.45	43.91	16	32	32	64	1	5	0	1	2	2	8
52.47	8.14	47.53	17	50	32	100	1	5	0	1	1.5	1.5	8
25.33	8.37	74.67	24	64	48	128	1	5	0	1	0.5	0.5	8
63.33	8.75	36.67	12	50	24	100	1	5	0	1	2	2	8
49.82	9.19	50.18	16	40	32	80	1	5	0	1	0.2	0.2	8
39.19	10.62	63.81	16	32	32	64	1	5	0	1	1	1	8
39.45	11.33	60.55	16	50	32	100	1	5	0	1	1	1	8
45.36	12.11	54.64	12	50	24	100	1	5	0	1	1.5	1.5	8
59.11	13.54	40.89	16	40	32	80	1	5	0	1	0.2	0.2	8
32.45	15.62	67.55	12	50	24	100	1	5	0	1	1	1	8
51.26	16.72	48.73	16	40	32	80	1	5	0	1	0.2	0.2	8
50.78	22.06	49.22	16	40	32	80	1	5	0	1	0.2	0.2	8
45.82	24.49	54.16	16	40	32	80	1	5	0	1	0.2	0.2	8

HISTOGRAM-BASED DETECTOR (Edge saliency only)

HE: Histogram equalization
ThreshA:Feature detection threshold
ThreshB:Motion detection threshold
C:Object width
D:Object height
E:Wavelet coefficient threshold
LEVEL:Wavelet decomposition level
F:Background memory
H:Detection by part flag
N:Normalize_Flag
MD:MedianFilter_Flag
S: Saturation control flag
S0:Scale factor
SUB:Subsample flag
OT:Object Outline Threshold

LEVEL	TPR	FPR	FNR	ThreshA	ThreshB	C	D	E	DBX	DBX	F	HE	S0	MD	SUB	OT
1	0	0														
1	1.45	0.41	98.55	0.5	0.2	32	120	0.25	16	60	0	0	0.5	1	1	1
1	4.46	1.84	95.54	0.5	0.2	32	120	0.25	16	60	0	0	1	1	1	1
1	10.86	3.15	89.14	0.6	0.1	32	100	0.25	16	50	1	0	0.5	1	1	1
1	6.03	3.76	93.97	0.5	0.2	32	120	0	16	60	0	0	1	0	1	1
1	12.79	4.09	87.21	0.6	0.1	32	100	0.25	16	50	1	0	0.5	1	1	1
1	7.6	4.47	92.4	0.5	0.2	32	120	0.25	16	60	0	0	0.5	0	1	1
1	7.6	4.47	92.4	0.5	0.2	32	120	0.25	16	60	1	0	0.5	0	1	1
1	10.49	4.48	89.51	0.6	0.1	24	100	0.25	12	50	1	0	1	1	1	1
1	17.37	8.09	82.63	0.3	0.2	32	120	0.25	16	60	1	0	0.5	1	1	1
1	13.75	8.38	86.25	0.1	0.1	48	128	0.25	24	64	1	0	0.5	1	1	1
1	23.76	8.97	76.24	0.6	0.1	32	64	0.25	16	32	1	0	1	1	1	1
1	17.85	9.9	82.15	0.2	0.1	32	120	0.25	16	60	1	0	0.5	1	1	1
1	17.85	9.9	82.15	0.2	0.5	32	120	0.25	16	60	1	0	0.5	1	1	1
1	36.43	19.93	63.57	0.1	0.1	48	128	0.25	24	64	1	0	1	1	1	1
1	79.01	56.18	20.99	0.1	0.1	24	100	0.25	12	50	1	0	1	1	1	1

LEVEL	TPR	FPR	FNR	ThreshA	ThreshB	C	D	E	F	HE	F	H	S0	N	S	SUB	OT
2	20.51	7.98	79.49	0.4	0.2	32	80	0.25	0	0	0	1	1	0	0	1	1
2	18.21	8.49	81.79	0.3	0.7	32	80	0.25	0	0	0	1	1	0	0	1	1
2	16.65	9.1	83.35	0.1	0.2	32	100	0.25	0	0	0	1	1	0	0	1	1
2	26.54	13.52	73.46	0.5	0.8	32	80	0.25	1	0	0	1	1.5	1	0	1	1
2	24.73	13.61	75.27	0.2	0.7	32	80	0.25	0	0	0	1	1	0	0	1	1
2	31.85	22.15	68.15	0.1	0.1	32	80	0.25	1	0	0	1	1.5	1	0	1	1
2	43.43	32.37	56.57	0.1	0.1	32	64	0.25	1	0	0	1	1.5	1	0	1	1

HISTOGRAM-BASED DETECTOR (Combined)

LEVEL	TPR	FPR	FNR	ThreshA	ThreshB	C	D	E	DBX	DBX	F	HE	S0	H	MD	SUB	OT
1	0	0															
1	61.16	24.61	33.84	0.3	0.2	48	128	0.25	24	64	1	0	0.5	0	1	1	1
1	60.92	25.57	39.08	0.5	0.2	48	128	0.25	24	64	1	0	0.5	0	1	1	1
1	62.12	25.57	37.88	0.2	0.2	48	128	0.25	24	64	1	0	0.5	0	1	1	1
1	54.28	25.85	45.72	0.1	0.2	24	100	0.25	24	100	1	0	0.5	0	1	1	1
1	63.69	27.5	36.31	0.5	0.2	48	128	0.25	24	64	1	0	0.25	0	1	1	1
1	62	28.95	38	0.3	0.2	32	120	0.25	16	64	1	0	0.5	0	1	1	1
1	62.61	32.81	37.39	0.5	0.2	32	120	0.25	16	60	1	0	0.5	0	1	1	1
1	66.95	37.39	33.05	0.3	0.2	32	100	0.25	16	50	1	0	0.5	0	1	1	1
1	65.14	41.74	34.86	0.3	0.2	24	100	0.25	12	50	1	0	0.5	0	1	1	1
1	70.69	51.63	29.31	0.5	0.2	32	100	0.25	16	50	1	0	0.5	0	1	1	1
1	67.43	55.73	32.57	0.5	0.2	24	100	0.25	12	50	1	0	0.5	0	1	1	1
1	73.22	56.21	26.78	0.3	0.2	32	64	0.25	16	32	1	0	0.5	0	1	1	1
1	80.7	78.17	19.3	0.5	0.2	32	64	0.25	16	32	1	0	0.5	0	1	1	1

Level	TPR	FPR	FNR	ThreshA	ThreshB	C	D	E	DBX	DBX	F	HE	S0	H	MD	SUB	OT
2	0	0															
2	63.93	27.76	36.07	0.3	0.2	48	128	0.25	24	64	1	0	1	0	1	1	1
2	64.66	29.83	35.34	0.5	0.2	48	128	0.25	24	64	1	0	1	0	1	1	1
2	66.71	30.75	33.29	0.5	0.2	48	128	0.25	24	64	1	0	0.5	0	1	1	1
2	62.12	34.53	37.88	0.1	0.2	24	100	0.25	12	50	1	0	0.5	0	1	1	1
2	68.52	35.81	31.48	0.5	0.4	32	120	0.25	16	60	1	0	0.5	0	1	1	1
2	68.52	35.81	31.48	0.5	0.2	32	120	0.25	16	60	1	0	0.5	0	1	1	1
2	67.79	39.81	32.21	0.5	0.2	24	100	0.25	12	50	1	0	1	0	1	1	1
2	72.01	40.1	27.99	0.5	0.2	32	64	0.25	16	32	1	0	1	0	1	1	1
2	72.5	40.24	27.5	0.5	0.2	32	100	0.25	16	50	1	0	1	0	0	1	1
2	78.17	40.27	21.83	0.3	0.2	48	128	0.25	24	64	1	0	0.5	0	1	1	1
2	70.93	40.32	29.07	0.5	0.2	32	120	0.25	16	60	1	0	0.5	0	0	1	1
2	74.07	41.51	25.93	0.5	0.4	32	80	0.25	16	40	1	0	0	0	1	1	1
2	73.7	42.63	26.3	0.5	0.2	32	64	0.25	16	32	1	0	0.5	0	1	1	1
2	69.12	42.91	30.64	0.5	0.2	24	100	0.25	12	50	1	0	0.5	0	1	1	1
2	76.72	43.26	23.28	0.5	0.2	32	100	0.25	16	50	1	0	0.5	0	0	1	1
2	76.6	45.17	23.4	0.5	0.2	32	64	0.25	16	32	1	0	1	0	0	1	1
2	74.07	45.51	25.93	0.5	0.7	32	80	0.25	16	40	1	0	1	0	1	1	1
2	80.1	48.13	19.9	0.5	0.2	32	64	0.25	16	32	1	0	0.5	0	0	1	1
2	86.01	49.57	13.99	0.3	0.2	48	128	0.25	48	128	1	0	0.25	0	1	1	1

APPENDIX D 1.2

MOTION SALIENCY

Sequence: Hamilton2b.avi
Rows: 240
Columns: 320
Frames: 1000

A: Dbase_spacingX
B: Dbase_SpacingY
C:Object width
D:Objectheight
S0: Scale factor
F:Fixed background flag
MaxNoObjects=8
Theshold1: Object Outline threshold

SHAPE BASED DETECTOR

TPR	FPR	FNR	A	B	C	D	E	Threshold1	HE	F	S0
53.56	4.51	46.44	16	32	32	64	1	5	0	1	2
61.88	3.65	38.12	16	50	32	100	1	5	0	1	2

HISTOGRAM-BASED DETECTOR

A:Feature detection threshold
B:Motion detection threshold
C:Objectwidth
D:Objectheight
E:Wavelet coefficient threshold
LEVEL:Wavelet decomposition level
F:Background memory
H:Detection by part flag
N:Normalize_Flag
MD:MedianFilter_Flag
S: Saturation control flag
S0:Scale factor
SUB:Subsample flag
OT:Object Outline Threshold
DBX: Object window spacing along X direction
DBY: Object window spacing along y direction

LEVEL	TPR	FPR	FNR	ThreshA	ThreshB	C	D	E	DBX	DBY	F	HE	S0	MD	SUB	OT	S
1	22.8	13.42	77.2	0.5	0.2	32	64	0.25	16	32	1	0	0.5	0	1	1	0
1	22.07	15.91	77.93	0.7	0.1	32	64	0.25	16	32	1	0	0.5	0	1	1	0
1	11.58	5.1	88.42	0.7	0.1	32	100	0.25	16	50	1	0	0.5	0	1	1	0
1	10.37	1.44	89.63	0.5	0.2	48	100	0.25	24	50	1	0	0.5	0	1	1	0
1	9.53	5.73	90.47	0.5	0.2	32	100	0.25	16	50	1	0	0.5	0	1	1	0
1	9.53	5.75	90.47	0.5	0.2	32	100	0.25	16	50	1	0	0.5	0	1	1	0
1	3.38	4.32	96.62	0.1	0.7	32	64	0.25	16	32	1	0	0.5	0	1	1	0
1	1.21	0.61	98.78	0.5	0.2	48	128	0.25	24	64	1	0	0.5	0	1	1	0
1	0.97	1.68	99.03	0.1	0.7	32	100	0.25	16	50	1	0	0.5	0	1	1	0

LEVEL	TPR	FPR	FNR	ThreshA	ThreshB	C	D	E	DBX	DBX	F	HE	S0	MD	SUB	OT	S
2	25.93	19.15	74.07	0.2	0.5	32	64	0.25	16	32	1	0	0.5	0	1	1	0
2	21.53	16.77	76.65	0.2	0.5	32	100	0.25	16	50	1	0	0.5	0	1	1	0
2	22.56	23.53	77.44	0.1	0.7	32	64	0.25	16	32	1	0	0.5	0	1	1	0
2	21.47	18.59	78.53	0.1	0.7	32	100	0.25	16	50	1	0	0.5	0	1	1	0
2	19.42	13.7	80.58	0.5	0.2	32	64	0.25	16	32	1	0	0.5	0	1	1	0
2	12.55	6.29	87.45	0.2	0.5	48	100	0.25	24	50	1	0	0.5	0	1	1	0
2	7.72	6.61	92.28	0.1	0.7	48	100	0.25	24	50	1	0	0.5	0	1	1	0
2	6.63	2.73	93.37	0.2	0.5	48	128	0.25	24	64	1	0	0.5	0	1	1	0
2	1.93	1.56	98.07	0.1	0.7	48	128	0.25	24	64	1	0	0.5	0	1	1	0

HISTOGRAM-BASED DETECTOR(Combined)

LEVEL	TPR	FPR	FNR	ThreshA	ThreshB	C	D	E	DBX	DBY	F	HE	S0	MD	SUB	OT	S
1	69.6	44.79	30.4	0.5	0.2	32	64	0.25	16	32	1	0	0.5	0	1	1	0
1	69.6	44.79	30.4	0.7	0.1	32	64	0.25	16	32	1	0	0.5	0	1	1	0
1	64.66	38.5	35.34	0.5	0.2	32	100	0.25	16	50	1	0	0.5	0	1	1	0
1	64.66	33.37	35.34	0.5	0.2	48	100	0.25	24	50	1	0	0.5	0	1	1	0
1	64.66	38.5	35.34	0.7	0.1	32	100	0.25	16	50	1	0	0.5	0	1	1	0
1	64.17	33.69	35.83	0.7	0.1	48	100	0.25	25	50	1	0	0.5	0	1	1	0
1	62	25.04	38	0.5	0.2	48	128	0.25	24	64	1	0	0.5	0	1	1	0

LEVEL	TPR	FPR	FNR	ThreshA	ThreshB	C	D	E	DBX	DBY	F	HE	S0	MD	SUB	OT	S
2	61.22	41.93	32.81	0.5	0.2	32	100	0.25	16	50	1	0	0.5	0	1	1	0
2	67.19	40.79	32.81	0.2	0.5	32	100	0.25	16	50	1	0	0.5	0	1	1	0
2	67.19	40.67	32.81	0.7	0.2	32	64	0.25	16	32	1	0	0.5	0	1	1	0
2	67.19	40.67	32.81	0.7	0.1	32	64	0.25	16	32	1	0	0.5	0	1	1	0
2	67.19	42.38	32.81	0.3	0.5	32	64	0.25	16	32	1	0	0.5	0	1	1	0
2	66.22	42.36	33.78	0.5	0.2	32	64	0.25	16	32	1	0	0.5	0	1	1	0
2	65.38	35.63	34.62	0.5	0.2	48	100	0.25	24	50	1	0	0.5	0	1	1	0
2	64.78	39.48	35.22	0.1	0.7	32	64	0.25	16	32	1	0	0.5	0	1	1	0
2	64.05	30.94	35.95	0.5	0.2	48	128	0.25	24	64	1	0	0.5	0	1	1	0

APPENDIX D 2.1

(EDGE SALIENCY)

Sequence: Stc_t1_c_3.avi
Nrows: 420
Ncols: 560
Nslice: 3021

A: Dbase_spacingX
B: Dbase_SpacingY
C:Object width
D:Object height
E:MedianFlag
TPR:True positive rate
FPR:False positive rate
FNR:False negative rate
HE:Histogram equalization
FactorY: Scale factorY
FactorX: Scale factorX
F:Fixed background flag
Theshold1: Object Outline threshold
HE:Histogram equalization

SHAPE-BASED DETECTOR

TPR	FPR	FNR	A	B	C	D	E	THRESHOLD1	HE	F	FactorX	FactorY	MaxNoObject
67.04	1.41	32.96	16	50	32	100	1	15	0	1	0.2	8	8
64.15	2.11	38.85	24	50	48	100	1	15	0	1	2	2	8
74.66	2.63	25.34	16	50	32	100	1	15	0	1	0.2	8	8
62.36	2.75	37.64	16	50	32	100	1	15	0	1	0.2	0.2	8
65.13	2.81	34.87	16	50	32	100	1	15	0	1	0.2	0.2	8
83.95	3.36	16.05	32	64	48	128	1	15	0	1	0.25	0.25	8
81.43	4.94	18.57	32	64	48	128	1	15	0	1	0.5	0.5	8
40.92	4.95	59.08	25	50	48	128	1	15	0	1	1	1	7
60.82	4.98	39.18	16	50	32	100	1	15	0	1	0.2	0.2	8
39.97	5.77	60.23	25	50	56	128	1	15	0	1	1	1	7
37.74	5.77	62.26	32	64	32	90	1	15	0	1	1	1	7
75.28	6.24	24.72	32	64	48	128	1	15	0	1	1	1	7
39	6.99	61	25	50	64	128	1	15	0	1	1	1	7
77.06	7.08	22.94	32	64	48	128	1	15	0	1	1	1	7
46.3	8.54	53.7	32	64	48	128	1	15	0	1	1	1	7
38.08	12.6	61.92	32	64	64	128	1	15	0	1	1	1	7
40.42	13.69	*59.58*	25	50	56	128	1	15	0	1	1	1	7
21.34	26.34	78.66	32	64	48	128	1	15	0	1	0.5	0.5	7

***, and **: Are used in combination with other parameters from histogram based classifier to generate combined classifier analysis**

HISTOGRAM-BASED DETECTOR (EDGE SALIENCY ONLY)

ThreshA:Feature detection threshold
ThreshB:Motion detection threshold
C:Object width
D:Object height
E:Wavelet coefficient threshold
LEVEL:Wavelet level decomposition
F:Background memory
H:Detection by part flag
N:Normalize_Flag
M:MedianFilter_Flag
S: Saturation control
S0:Second order flag
SUB:Subsample flag
OT:Object Outline Threshold
HE:Histogram equalization

	LEVEL	TPR	FPR	FNR	ThreshA	ThreshB	C	D	E	F	HE	M	S0	N	MaxNoObject	S
	1	66.97	7.22	33.03	0.4	0.3	48	128	0.35	1	0	0	0	0	8	0
	1	62.24	7.89	37.76	0.6	0.7	48	128	0.35	1	0	0	0	0	8	0
	1	68.82	8.99	31.18	0.4	0.7	32	64	0.35	1	0	0	0	0	8	0
	1	66.91	11.02	33.09	0.4	0.3	48	128	0.35	1	0	0	0	0	8	0
	1	66.79	11.07	33.21	0.4	0.7	48	128	0.35	1	0	0	0	0	8	0
	1	64.7	11.82	35.3	0.2	0.7	56	128	0.35	1	0	0	0	0	8	0
	1	69.8	14.88	30.2	0.2	0.7	48	128	0.35	1	0	0	0	0	8	0
	1	66.54	20.99	33.46	0.1	0.7	64	128	0.35	1	0	0	0	0	8	0
Average		**66.59625**	**11.735**													
Standard deviation		**2.3317862**	**4.459516**													
Baseline		**68.212066**	**14.82523**													

	LEVEL	TPR	FPR	FNR	ThreshA	ThreshB	C	D	E	F	HE	M	S0	N	MaxNoObject	S
	2	51.29	4.89	48.71	0.6	0.7	48	128	0.35	1	0	0	0	0	8	0
	2	58.24	5.33	41.76	0.4	0.7	48	128	0.35	1	0	0	0	0	8	0
	2	65.56	11.73	34.44	0.2	0.7	48	128	0.35	0	0	0	0	0	8	0
	2	66.36	13.01	33.64	0.2	0.7	56	128	0.35	0	0	0	0	0	8	0
	2	65.38	14.81	34.62	0.2	0.7	56	128	0.35	1	0	0	0	0	8	0
	2	65.44	15.66	34.56	0.1	0.7	64	128	0.35	1	0	0	0	0	8	0
	2	60.15	15.76	39.85	0.2	0.7	48	128	0.35	0	1	1	0	0	8	0
	2	59.41	18.19	40.59	0.2	0.7	48	128	0.35	1	0	0	0	0	8	0

HISTOGRAM-BASED DETECTOR (COMBINED)

	LEVEL	TPR	FPR	FNR	ThreshA	ThreshB	C	D	E	F	HE	M	S0	N	MaxNoObject	0
	1	92.87	1.66	7.13	0.6	0.7	48	128	0.35	1	0	0	0	0	8	0
	1	91.27	3.78	8.73	0.4	0.7	32	64	0.35	1	0	0	0	0	8	0
	1	91.51	4.28	8.49	0.4	0.3	48	128	0.35	1	0	0	0	0	8	0
	1	91.51	4.34	8.49	0.4	0.7	48	128	0.35	1	0	0	0	0	8	0
	1	89.79	5.84	10.21	0.2	0.7	56	128	0.35	1	0	0	0	0	8	0
	1	87	9.72	12.3	0.2	0.7	48	128	0.35	0	0	0	0	0	8	0
	1	86.47	14.52	13.53	0.1	0.7	64	128	0.35	1	0	0	0	0	8	0
	1	79.4	29.23	20.6	0.4	0.3	48	64	0.35	1	0	0	0	0	8	0
	1	24.42	32.06	75.58	0.2	0.7	48	128	0.35	1	0	0	0	0	8	0
	1	91.14	53.48	8.86	0.1	0.7	48	128	0.35	1	0	0	0.5	0	8	
Average		**82.538**	**15.891**													
Standard deviation		**20.799296**	**17.03174**													
Baseline		**95.429301**	**26.44719**													

	LEVEL	TPR	FPR	FNR	ThreshA	ThreshB	C	D	E	F	HE	M	S0	N	MaxNoObject	0
	2	90.9	0.66	9.1	0.6	0.7	48	128	0.35	1	0	0	0	0	8	0
	2	78.66	0.8	21.34	0.2	0.7	32	128	0.35	1	1	0	0	0	8	0
	2	83.27	2.36	16.73	0.2	0.7	32	128	0.35	1	0	1	0	0	8	0
	2	90.59	2.5	9.4	0.4	0.7	48	128	0.35	1	0	0	0	0	8	0
	2	89.61	7.19	10.39	0.2	0.7	56	128	0.35	0	0	0	0	0	8	0
	2	89.98	7.51	10.03	0.2	0.7	48	128	0.35	0	0	0	0	0	8	0
	2	89.67	9.41	10.33	0.1	0.7	64	128	0.35	1	0	0	0	0	8	0
	2	87.95	9.81	12.05	0.2	0.7	48	128	0.35	1	1	0	0	0	8	0
	2	88.03	10.65	11.87	0.2	0.7	56	128	0.35	1	0	0	0	0	8	0
	2	70.93	42.15	29.07	0.2	0.7	48	128	0.35	1	1	0	0	0	8	0
	2	94.51	79.3	5.49	0.2	0.7	48	128	0.35	1	0	0	0	0	8	0

UNDECIMATED WAVELET TRANSFORM (OVER COMPLETE WAVELET REPRESENTATION)

EDGE SALIENCY ONLY

LEVEL	TPR	FPR	FNR	ThreshA	ThreshB	C	D	E	F	HE	M	S0	N	MaxNoObject
1	60.33	14.98	39.67	0.6	0.7	48	128	0.35	1	0	0	0	0	8
2	16.54	8.9	83.46	0.6	0.7	48	128	0.35	1	0	0	0	0	8

UNDECIMATED WAVELET TRANSFORM WITH HISTOGRAM EQUALIZATION

LEVEL	TPR	FPR	FNR	ThreshA	ThreshB	C	D	E	F	HE	M	S0	N	MaxNoObject
EDGE SALIENCY ONLY														
1	58.6	36.17	41.39	0.6	0.7	48	128	0.35	1	0	0	0	0	8
1	41.64	16.26	58.36	0.6	0.7	48	128	0.35	1	1	0	0	0	8
2	13.16	6.6	86.84	0.6	0.7	48	128	0.35	0	1	0	0	0	8
COMBINED CLASSIFIER														
1	91.7	43.2	8.3	0.6	0.7	48	128	0.35	1	0	0	0	0	8
1	88.87	5.01	11.13	0.6	0.7	48	128	0.35	1	1	0	0	0	8
2	84.75	1.03	5.25	0.6	0.7	48	128	0.35	1	0	0	0	0	8
2	80.44	7.65	19.56	0.6	0.7	48	128	0.35	1	1	0	0	0	8

APPENDIX D 2.2

MOTION SALIENCY

Sequence: **Stc_t1_c_3.avi**
Rows: 420
Columns: 560
Frames: 3021

A: Dbase_spacingX
B: Dbase_SpacingY
C:Object width
D:Object height
E:MedianFlag
FPR:False positive rate
FNR:False negative rate
HE:Histogram equalization
S0: Scale factor
F:Fixed background flag
MaxNoObjects=8
Theshold1: Object Outline threshold

SHAPE BASED DETECTOR

	TPR	FPR	FNR	A	B	C	D	E	THRESHOLD1	HE	F	S0
	64.15	1.11	38.85	24	50	48	100	1	15	0	1	2
Average	**64.15**	**1.11**	**38.85**									
Standard deviation	**0**	**0**	**0**									
Baseline	**64.15**	**1.11**	**38.85**									

ThreshA:Feature detection threshold
ThreshB:Motion detection threshold
C:Object width
D:object height
E:Wavelet coefficient threshold
LEVEL:Wavelet decompostion level
F:Background memory flag
H:Detection by part
N:Normalize_Flag
M:MedianFilter_Flag
S: Saturation control flag
S0:Scale factor
SUB:Subsample flag
OT:Object Outline Threshold
HE: Equalization

HISTOGRAM-BASED DETECTOR

(Decimated wavelet transform)

LEVEL	TPR	FPR	FNR	ThreshA	ThreshB	C	D	E	F	HE	S0	M	SUB	OT	S
1	12.62	42.02	87.33	0.4	0.3	48	128	0.35	1	0	0.5	0	1	10	0
1	9.66	36.74	90.34	0.6	0.7	48	128	0.35	1	0	0.5	0	1	10	0
1	12.67	42.02	87.33	0.4	0.7	48	128	0.35	1	0	0.5	0	1	10	0
1	13.65	43.26	86.35	0.1	0.7	64	128	0.35	1	0	0.5	0	1	10	0
1	15.81	38.81	84.19	0.4	0.3	56	128	0.35	1	0	0.5	0	1	10	0
1	13.84	44.5	86.16	0.2	0.7	48	128	0.35	1	0	0.5	0	1	10	0
1	16.67	42.02	87.33	0.4	0.3	48	128	0.35	1	0	0.5	1	1	10	0

LEVEL	TPR	FPR	FNR	ThreshA	ThreshB	C	D	E	F	HE	S0	M	SUB	OT	S
2	2.64	16.72	97.36	0.4	0.3	48	128	0.35	1	0	0.5	**0**	1	10	**0**
2	1.29	12.36	98.71	0.6	0.7	48	128	0.35	1	0	0.5	**0**	1	10	**0**
2	2.64	16.72	97.36	0.4	0.7	48	128	0.35	1	0	0.5	**0**	1	10	**0**
2	6.89	30.06	93.11	0.1	0.7	64	128	0.35	1	0	0.5	**0**	1	10	**0**
2	5.23	24.85	94.77	0.2	0.7	56	128	0.35	1	0	0.5	**0**	1	10	**0**
2	2.64	16.72	97.36	0.4	0.3	48	128	0.35	1	0	0.5	**1**	1	10	**0**

(HISOTGRAM-BASED DETECTOR (COMBINED)

LEVEL	TPR	FPR	FNR	ThreshA	ThreshB	C	D	E	F	HE	S0	M	SUB	OT	S
1	77.59	66.56	22.41	0.2	0.7	56	128	0.35	1	0	0.5	0	1	10	0
1	79.84	63.33	20.16	0.2	0.7	64	128	0.35	1	0	0.5	0	1	10	0
1	76.97	69.99	23.03	0.4	0.7	48	128	0.35	1	0	0.5	0	1	10	0
1	76.22	68.79	23.78	0.6	0.7	48	128	0.35	1	0	0.5	0	1	10	0
1	76.97	69.99	23.03	0.4	0.3	48	128	0.35	1	0	0.5	0	1	10	0
1	73.1	79.72	26.9	0.4	0.3	32	64	0.35	1	0	0.5	0	1	10	0
1	72.97	75.47	27.03	0.4	0.3	48	128	0.35	1	0	0.5	**1**	1	10	0

LEVEL	TPR	FPR	FNR	ThreshA	ThreshB	C	D	E	F	HE	S0	MD	SUB	OT	S
2	80.84	44.93	19.16	0.4	0.3	48	128	0.35	1	0	0.5	0	1		
2	72.41	30.41	27.59	0.6	0.7	48	128	0.35	1	0	0.5	0	1	10	0
2	80.84	44.93	19.16	0.4	0.7	48	128	0.35	1	0	0.5	0	1	10	0
2	77.34	54.66	22.66	0.1	0.7	64	128	0.35	1	0	0.5	0	1	10	0
2	72.53	54.81	27.47	0.2	0.7	56	128	0.35	1	0	0.5	0	1	10	0
2	71.22	66.79	28.78	0.4	0.3	48	128	0.35	1	0	0.5	1	1	10	0

APPENDIX D 3.1

EDGE SALIENCY

Sequence : Stc_t1_c_4.avi

Rows: 420
Columns: 560
Frames: 3021

A: Dbase_spacingX
B: Dbase_SpacingY
C:Object width
D:Object height
E:MedianFlag
TPR:True Positive Rate
FPR:False Positive Rate
FNR:False Negative Rate
HE:Histogram equalization
S0: Scale factor
F:Fixed background flag
MaxNoObject: Maximum number of objects
Theshold1: Object Outline threshold

SHAPE-BASED CLASSIFIER

TPR	FPR	FNR	A	B	C	D	E	Threshold1	HE	F	S0
52.08	0.8	47.96	24	64	48	128	1	15	0	1	2
51.06	0.83	48.94	24	50	48	100	1	10	0	1	2
46.82	1.21	53.18	16	32	32	64	1	15	0	1	2
48.94	1.21	51.06	16	64	32	128	1	15	0	1	2
25.45	2.26	74.55	32	64	24	64	1	15	0	1	1
25.29	2.43	74.71	16	32	32	64	1	15	0	1	1
29.85	3.96	70.15	12	64	24	120	1	15	0	1	1
29.85	4.09	70.15	16	32	32	64	1	15	0	1	1
29.85	4.09	70.15	16	60	32	120	1	15	0	1	1
32.14	4.74	67.86	16	64	32	128	1	15	0	1	1
29.2	5.15	70.18	24	60	48	120	1	15	0	1	1
29.2	5.15	70.18	24	64	48	128	1	15	0	1	1
41.6	11.5	58.4	16	64	32	128	1	15	0	1	1
54.06	10.85	45.84	24	64	48	128	1	15	0	1	0.2
46.98	3.03	53.02	24	64	48	128	1	15	0	1	0.2
47.96	2.52	52.04	24	64	48	128	1	15	0	1	0.2
51.55	2.04	48.45	24	64	48	128	1	15	0	1	0.2
52.69	2.67	47.45	24	64	48	128	1	15	0	1	0.2

ThreshA:Feature detection threshold
ThreshB:Motion detection threshold
C:Obect width
D:Object height
E:Wavelet coefficient threshold
LEVEL: Wavelet decomposition level
F:Background memory
H:Detection by part
N:Normalize_Flag
M:MedianFilter_Flag
S: Saturation control
S0:Scale factor
SUB:Sub sample flag
OT:Object Outline Threshold

HISTOGRAM-BASED CLASSIFIER

LEVEL	TPR	FPR	FNR	ThreshA	ThreshB	C	D	E	F	HE	S0	M	SUB	OT	S
1	46.33	18.08	53.67	0.1	0.9	50	100	0.35	1	0	0.25	0	1	1	0
1	50.9	44.26	49.1	0.1	0.9	30	100	0.35	1	0	1	0	1	1	1
1	27.9	62.48	72.1	0.1	0.9	48	120	0.4	0	0	1	0	1	3	0
1	32.82	69.85	76.18	0.2	0.9	32	100	0.35	0	0	1	0	1	3	0
1	24.8	99.83	75.2	0.5	0.8	48	120	0.35	0	0	1	0	1	3	0
1	24.8	99.83	72.5	0.2	0.9	48	120	0.35	0	0	1	0	1	3	0
1	21.37	99.86	78.63	0.2	0.5	32	120	0.35	0	0	1	0	1	3	0
1	17.62	99.87	82.38	0.2	0.5	24	120	0.35	0	0	1	0	1	3	0

LEVEL	TPR	FPR	FNR	ThreshA	ThreshB	C	D	E	F	HE	S0	M	SUB	OT	S
2	4.89	30.91	95.11	0.1	0.9	48	120	0.4	0	0	1	0	1	3	0
2	56.77	35	43.23	0.5	0.8	48	120	0.35	0	0	1	0	1	3	0
2	55.63	35	44.37	0.2	0.5	32	120	0.35	0	0	1	0	1	3	0
2	43.56	35	56.44	0.2	0.5	24	120	0.35	0	0	1	0	1	3	0
2	67.75	37.03	32.46	0.1	0.9	64	128	0.35	1	0	0.25	0	1	1	0
2	55.63	42	44.37	0.1	0.6	32	120	0.35	0	0	1	0	1	3	0
2	58.4	42.92	41.6	0.2	0.7	48	120	0.35	0	0	1	0	1	3	0
2	58.4	60.42	41.6	0.1	0.9	48	120	0.4	0	0	1	0	1	3	0
2	46.82	69.66	53.18	0.2	0.8	32	100	0.35	0	0	1	0	1	3	0
2	34.42	77.24	65.58	0.3	0.8	32	64	0.35	0	0	1	0	1	3	0

HISTOGRAM-BASED CLASSIFIER (Combined)

LEVEL	TPR	FPR	FNR	ThreshA	ThreshB	C	D	E	F	HE	S0	M	SUB	OT	S
1	75.2	50.97	24.8	0.1	0.9	50	100	0.35	1	0	0.125	0	1	1	0
1	53.02	58.5	46.98	0.2	0.7	48	120	0.35	1	0	1	0	1	3	0
1	53.02	58.5	46.98	0.1	0.9	48	120	0.35	1	0	1	0	1	3	0
1	53.02	58.5	46.98	0.4	0.9	48	120	0.35	1	1	0.2	0	1	3	0
1	50.08	62.73	49.92	0.1	0.8	32	128	0.35	1	0	1	0	1	3	0
1	48.59	67.22	51.41	0.2	0.8	32	100	0.35	1	0	1	0	1	3	0
1	47.8	71.75	52.2	0.3	0.8	32	64	0.35	1	0	1	0	1	3	0
1	44.37	99.8	55.63	0.2	0.9	48	120	0.35	1	0	1	0	1	3	0
1	41.76	99.83	58.24	0.2	0.9	32	120	0.35	1	0	1	0	1	3	0
1	38.17	99.84	61.83	0.2	0.9	24	120	0.35	1	0	1	0	1	3	0
1	37.03	99.86	62.97	0.2	0.9	32	64	0.35	1	0	1	0	1	3	0
1	35.24	99.87	64.76	0.2	0.9	24	64	0.35	1	0	1	0	1	3	0

LEVEL	TPR	FPR	FNR	ThreshA	ThreshB	C	D	E	F	HE	S0	M	SUB	OT	S
2	74.06	57.69	25.94	0.2	0.7	48	120	0.35	1	0	1	0	1	3	0
2	71.45	58.24	28.55	0.1	0.9	48	120	0.35	1	0	1	0	1	3	0
2	71.45	67.1	28.55	0.2	0.8	32	100	0.35	1	0	1	0	1	3	0
2	56.93	73.19	43.07	0.1	0.9	48	120	0.35	1	1	0.2	0	1	3	0
2	66.23	75.36	33.77	0.3	0.7	32	64	0.35	1	0	1	0	1	3	0
2	69.33	99.86	59.87	0.2	0.9	48	120	0.35	1	0	1	0	1	3	0
2	36.54	99.88	63.46	0.2	0.9	32	120	0.35	1	0	1	0	1	3	0
2	71.8	99.88	29.2	0.1	0.9	48	120	0.35	1	0	1	0	1	3	0
2	53.67	99.89	76.18	0.2	0.9	24	120	0.35	1	0	1	0	1	3	0
2	60.69	99.93	64.6	0.2	0.9	32	64	0.35	1	0	1	0	1	3	0
2	23.16	99.94	76.84	0.2	0.9	24	32	0.35	1	0	1	0	1	3	0

APPENDIX D 3.2

MOTION SALIENCY

Sequence: Stc_t1_c_4.avi

NROWS: 420
NCOLS: 560
NSLICE: 3021
MaxNoObjects=8
A: Dbase_spacingX
B: Dbase_SpacingY
C:ObjectWidth1
D:ObjectHeight1
m:MedianFlag
TPR:True positive rate
FPR:False positive rate
FNR:False negative rate
HE:Histogram equalization
OT:Object outline threshold
F:Fixed background flag
S0:Scale factor

SHAPE-BASED DETECTOR

TPR	FPR	FNR	A	B	C	D	E	THRESHOLD1	HE	F	S0
48.94	1.24	51.55	16	64	32	128	1	15	0	1	2

ThreshA:Feature detection threshold
ThreshB:Motion detection threshold
C:Object width
D:Object height
E:Wavelet coefficient threshold
LEVEL:Wavelet decomposition level
F:fixed background memory flag
H:Detection by part flag
N:Normalize_Flag
M:MedianFilter_Flag
S: Saturation control
S0:Second order flag
SUB:Subsmaple flag

HISTOGRAM-BASED DETECTOR

LEVEL	TPR	FPR	FNR	ThreshA	ThreshB	C	D	E	F	HE	S0	M	SUB	OT	S
1	37.36	12.16	62.64	0.1	0.9	32	128	0.35	1	0	0.5	0	1	3	0
1	39.48	12.91	60.52	0.1	0.9	48	120	0.35	1	0	0.5	0	1	3	0
1	36.7	14.75	63.3	0.2	0.7	48	128	0.35	1	0	0.5	0	1	3	0
1	36.7	14.75	63.3	0.2	0.8	48	128	0.35	1	0	0.5	0	1	3	0
1	36.7	14.75	63.3	0.2	0.7	48	128	0.35	1	0	0.5	0	1	3	0
1	37.85	15.1	62.15	0.2	0.7	48	120	0.35	1	0	0.5	0	1	3	0

LEVEL	TPR	FPR	FNR	ThreshA	ThreshB	C	D	E	F	HE	S0	M	SUB	OT	S
2	8.65	4.86	91.35	0.7	0.2	32	128	0.35	1	0	0.5	0	1	3	0
2	25.45	7.33	74.55	0.2	0.7	48	128	0.35	1	0	0.5	0	1	3	0
2	25.45	7.33	74.55	0.2	0.8	48	128	0.35	1	0	0.5	0	1	3	0
2	25.45	7.33	74.55	0.2	0.7	48	128	0.35	1	0	0.5	0	1	3	0
2	25.45	7.33	74.55	0.2	0.7	48	128	0.35	1	0	0.5	1	1	3	0
2	24.63	7.55	75.37	0.2	0.7	48	120	0.35	1	0	0.5	0	1	3	0
2	36.22	9.13	63.17	0.1	0.9	48	128	0.35	1	0	0.5	0	1	3	0
2	20.55	16.96	79.45	0.3	0.7	32	128	0.35	1	0	0.5	0	1	3	0
2	23.65	19.17	76.35	0.2	0.9	32	128	0.35	1	0	0.5	0	1	3	0
2	10.93	19.5	89.07	0.3	0.7	32	64	0.35	1	0	0.5	0	1	3	0

HISTOGRAM-BASED CLASSIFIER (COMBINED)

LEVEL	TPR	FPR	FNR	ThreshA	ThreshB	C	D	E	F	HE	S0	M	SUB	OT	S
1	49.1	71.8	50.9	0.7	0.2	32	128	0.35	1	0	0.5	1	1	3	0
1	49.1	72.42	50.9	0.7	0.2	32	128	0.35	1	0	0.5	0	1	3	0
1	50.57	75.81	49.43	0.3	0.8	48	128	0.35	1	0	0.5	0	1	3	0
1	50.57	76.83	49.43	0.3	0.7	48	128	0.35	1	0	0.5	0	1	3	0
1	51.22	76.98	48.78	0.2	0.8	48	128	0.35	1	0	0.5	0	1	3	0
1	52.37	78.8	47.63	0.1	0.9	48	128	0.35	1	0	0.5	0	1	3	0
1	50.41	82.69	49.59	0.7	0.2	32	128	0.35	1	0	0.5	0	1	3	0
1	50.41	82.69	49.59	0.2	0.9	32	120	0.35	1	0	0.5	0	1	3	0
1	49.27	84.58	50.73	0.3	0.7	32	64	0.35	1	0	0.5	0	1	3	0

LEVEL	TPR	FPR	FNR	ThreshA	ThreshB	C	D	E	F	HE	S0	M	SUB	OT	S
2	49.1	61.72	50.19	0.7	0.2	32	128	0.35	1	0	0.5	0	1	3	0
2	50.9	67.83	49.1	0.3	0.8	48	120	0.35	1	0	0.5	0	1	3	0
2	53.67	70.24	46.33	0.2	0.7	48	128	0.35	1	0	0.5	1	1	3	0
2	52.69	72.73	47.31	0.2	0.7	48	128	0.35	1	0	0.5	0	1	3	0
2	52.69	72.73	47.31	0.2	0.8	48	120	0.35	1	0	0.5	0	1	3	0
2	57.76	75.64	42.25	0.1	0.9	48	120	0.35	1	0	0.5	0	1	3	0
2	55.14	80.2	44.86	0.2	0.9	32	128	0.35	1	0	0.5	0	1	3	0
2	50.41	82.44	49.59	0.3	0.7	32	64	0.35	1	0	0.5	0	1	3	0

APPENDIX E1

JPDAF TRACKER (HAMILTON2B.AVI)

SEQUENCE: HAMILTON2.AVI
NROWS: 240
NCOLS: 320
NSLICE: 3021 (USED 1000)
CLASSIFIER_SEARCH_WINDOW_WIDTH: 48
CLASSIFIER_SEARCH_WINDOW_HEIGHT: 128
A: MAXIMUM DISPLACEMENT FOR CENTROID MATCHING X
B: MAXIMUM DISPLACEMENT FOR CENTROID Y
C: TRACKER_WIDTH
D: TRACKER_HEIGHT
E: FRAME_ACTIVITY_CENTROID
MAG_FACT :MAGNIFICATION FACTOR
SAT_CONTROL: SATURATION CONTROL
S0: SCALE FACTOR
CLUST_FLAG: TRACK CLUSTER_FLAG

	NUMBER	TPR	FPR	FNR	A	B	C	D	E	MODEL	MAG_FACTOR	SAT_CONTROL	S0	CLUST_FLAG
CLUSTER_FLAG	1	69.84	42.36	30.16	0.5W	0.5H	0.5W	0.5H		1	0.5	0	1	0
	2	70.81	41.78	29.19	0.25W	0.25H	0.25W	0.25H		1	0.25	0	1	0
1	3	59.95	45.34	40.05	0.25W	0.25H	0.25W	0.25H		1	0.25	0	0.5	0
2	4	56.09	41.16	43.91	0.25W	0.25H	0.25W	0.25H		6	0.25	0	0.5	0
2	5	68.52	36.46	31.48	0.25W	0.25H	0.25W	0.25H		6	0.25	0	1	0
2	6	70.81	41.78	29.19	0.25W	0.25H	0.25W	0.25H		5	0.25	0	1	0
2	7	59.95	45.34	40.05	0.25W	0.25H	0.25W	0.25H		5	0.25	0	0.5	0
1	8	70.45	40	30	0.25W	0.25H	0.25W	0.25H		4	0.25	0	1	0
2	7	68.52	34.46	31.48	0.25W	0.25H	0.25W	0.25H		3	0.25	0	1	0
2	8	70.33	41.61	29.67	0.25W	0.25H	0.25W	0.25H		2	0.25	0	1	0

APPENDIX E2

JPDAF TRACKER (STC_T1_C_3.AVI)

SEQUENCE: STC_T1_C_3.AVI
NROWS: 420
NCOLS: 560
NSLICE: 3021 (USED 1944)
CLASSIFIER_SEARCH_WINDOW_WIDTH: 48
CLASSIFIER_SEARCH_WINDOW_HEIGHT: 128
A: MAXIMUM DISPLACEMENT FOR CENTROID MATCHINGX
B: MAXIMUM DISPLACEMENT FOR CENTROID MATCHINGY
C: TRACKER_WIDTH
D: TRACKER_HEIGHT
E: FRAME_ACTIVITY_CENTROID
E: FRAME_ACTIVITY_CENTROID
MAG_FACT :MAGNIFICATION FACTOR
SAT_CONTROL: SATURATION CONTROL
S0: SCALE FACTOR
CLUST_FLAG: TRACK CLUSTER_FLAG

CLUSTER_FLAG	NUMBER	TPR	FPR	FNR	A	B	C	D	E	MODEL	MAG_FACTOR	SAT_CONTROL	S0	CLUSTER_FLAG
0	1	77.68	44.99	22.32	0.25W	0.25H	0.25W	0.25H	1	1	0.25	0	1	0
0	2	77.68	44.99	22.32	0.25W	0.25H	0.25W	0.25H	1	2	0.25	0	1	0
0	3	61.62	54.96	38.38	0.25W	0.25H	0.25W	0.25H	1	3	0.25	0	1	0
0	4	60.89	50.52	39.11	0.25W	0.25H	0.25W	0.25H	1	4	0.25	0	1	0
0	5	61.62	54.96	38.38	0.25W	0.25H	0.25W	0.25H	1	5	0.25	0	1	0
0	6	75.77	43.12	24.12	0.25W	0.25H	0.25W	0.25W	1	6	0.25	0	1	1
0	7	64.21	57.93	35.79	0.25W	0.25H	0.25W	0.25W	1	1	0.25	1	1	1
0	8	69.07	59.75	30.93	0.25W	0.25H	0.25W	0.25W	1	1	0.25	1	1	2
0	9	68.27	54.88	31.73	0.25W	0.25H	0.25W	0.25W	1	1	0.25	0	1	2
0	10	71.4	52.53	28.6	0.25W	0.25H	0.25W	0.25W	1	1	0.25	1	1	2

APPENDIX E3

JPDAF TRACKER (STC_T1_C_4.AVI)

SEQUENCE: STC_T1_C_4.AVI
NROWS: 420
NCOLS: 560
NSLICE: 3021 (USED 150)
CLASSIFIER_SEARCH_WINDOW_WIDTH: 48
CLASSIFIER_SEARCH_WINDOW_HEIGHT: 128
A: MAXIMUM DISPLACEMENT FOR CENTROID MATCHINGX
B: MAXIMUM DISPLACEMENT FOR CENTROID MATCHINGY
C: TRACKER_WIDTH
D: TRACKER_HEIGHT
E: FRAME_ACTIVITY_CENTROID
E: FRAME_ACTIVITY_CENTROID
MAG_FACT :MAGNIFICATION FACTOR
SAT_CONTROL: SATURATION CONTROL
S0: SCALE FACTOR
CLUST_FLAG: TRACK CLUSTER_FLAG

CLUSTER_FLAG	NUMBER	TPR	FPR	FNR	A	B	C	D	E	MODEL	MAG_FACTOR	SAT_CONTROL	S0	CLUSTER_FLAG
0	1	66.86	24.32	3.12	0.5W	0.5H	0.25W	0.25H		1	0.5	1	1	0
0	2	70.64	45.29	29.36	0.5W	0.5H	0.125W	0.125H		1	0.25	1	1	0
0	3	72.59	43.67	27.41	0.5W	0.5H	0.125W	0.125H		1	0.25	0	1	0
0	4	56.12	20.57	43.88	0.5W	0.5H	0.25W	0.25H		1	0.5	0	1	0
0	5	71.29	44.29	28.71	0.5W	0.5H	0.5W	0.5H		1	1	0	1	0
0	6	72.27	46.03	27.73	0.5W	0.5H	0.5W	0.5H		1	1	1	1	0
0	7	51.71	51.66	48.29	0.5W	0.5H	0.5W	0.5H		1	1	1	0.5	0

APPENDIX F

Graphs of PETS 2006 metrics for stc_t1_c_3.avi sequence is shown below. One hundred and ninety-four track groups were used. Each track group consist of ten consecutives frames defined in overlapping fashion.

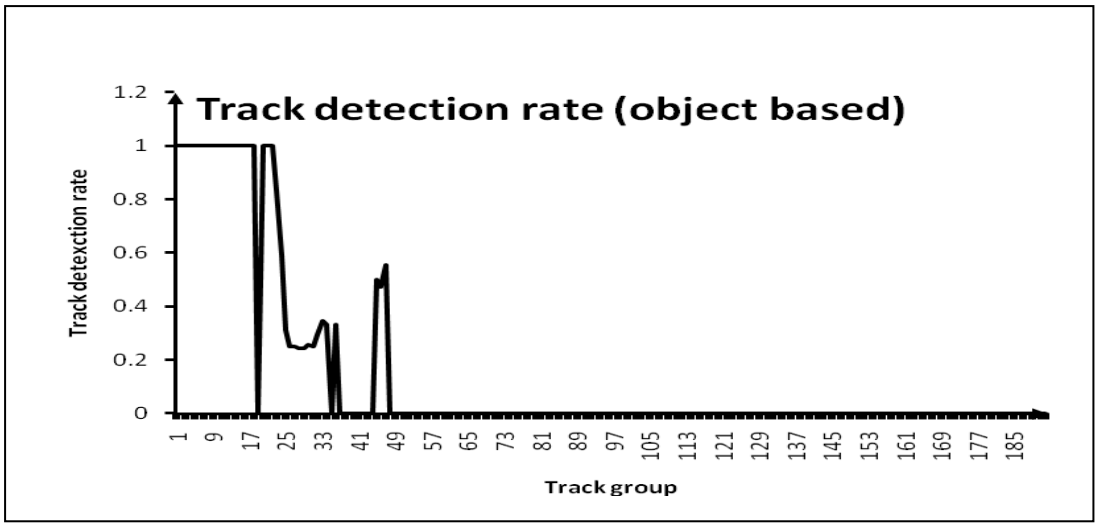

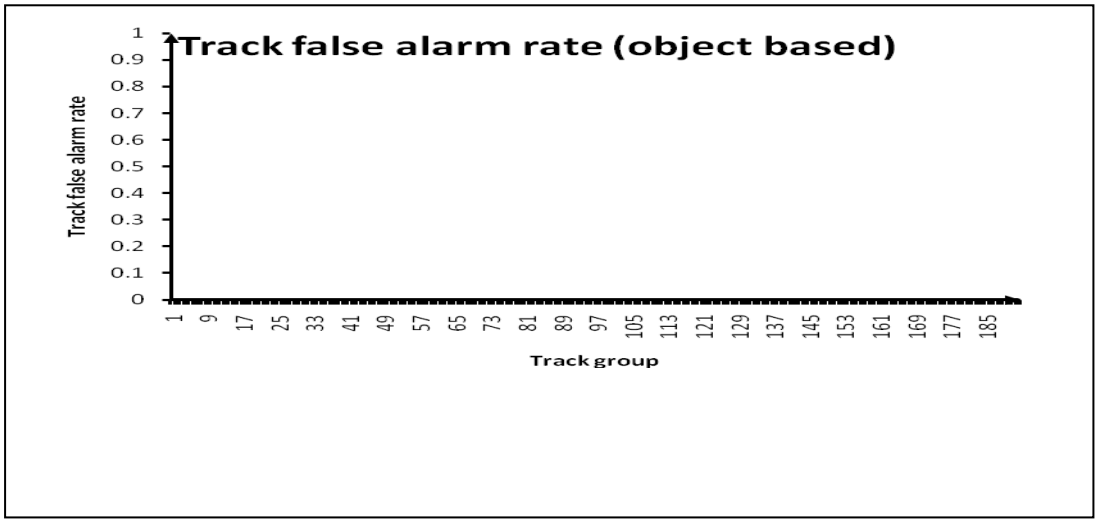

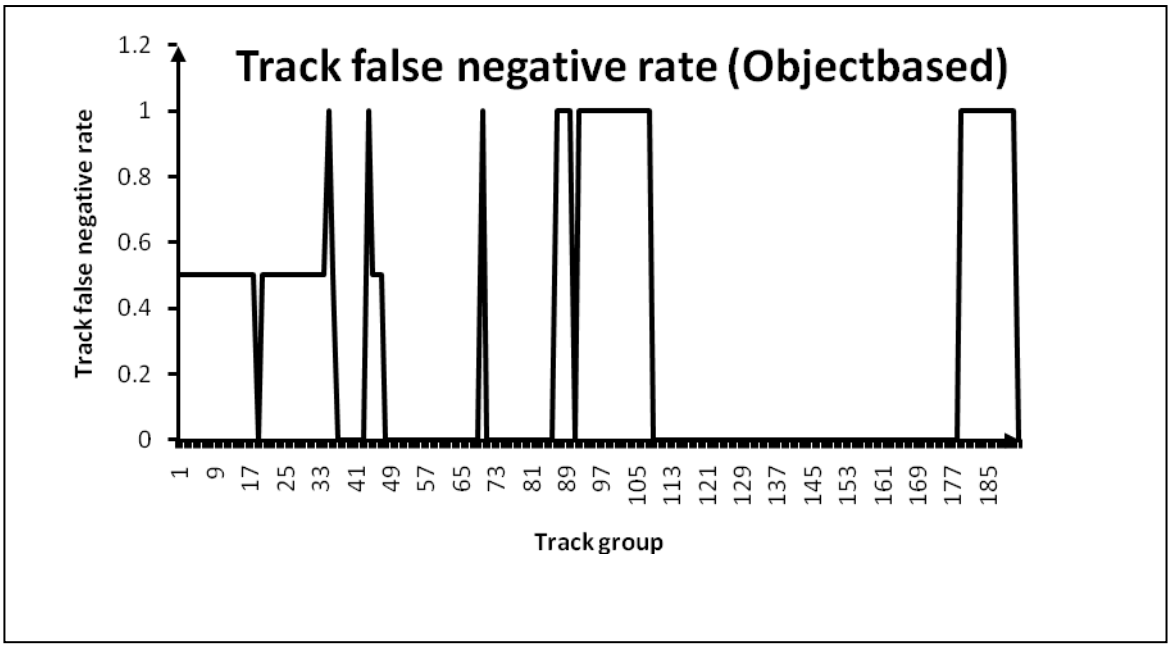
Track false negative rate (Objectbased)
Track false negative rate
1.2
1
0.8
0.6
0.4
0.2
0
1 9 17 25 33 41 49 57 65 73 81 89 97 105 113 121 129 137 145 153 161 169 177 185
Track group

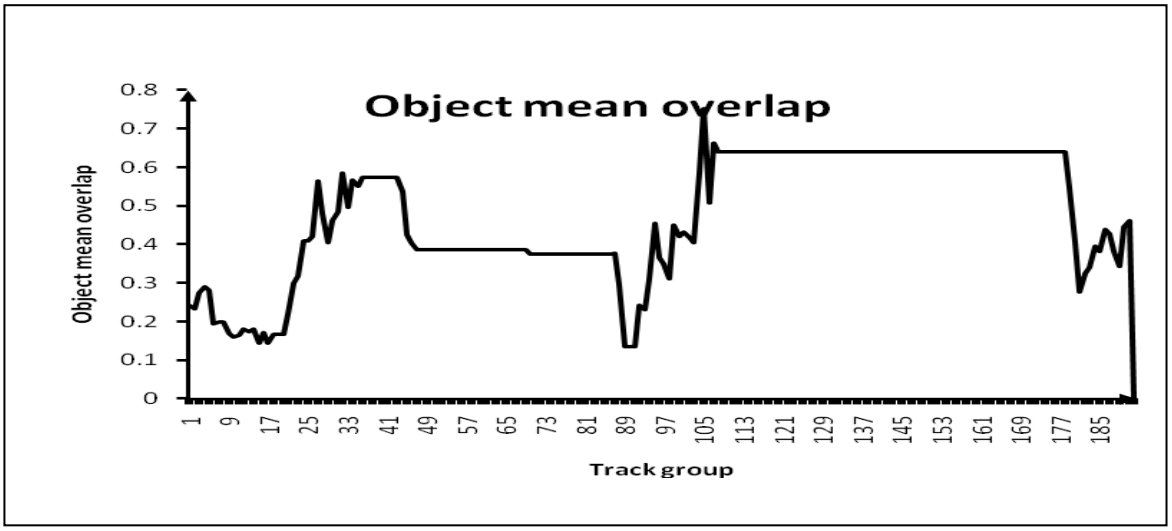
Object mean overlap
Object mean overlap
0.8
0.7
0.6
0.5
0.4
0.3
0.2
0.1
0
1 9 17 25 33 41 49 57 65 73 81 89 97 105 113 121 129 137 145 153 161 169 177 185
Track group

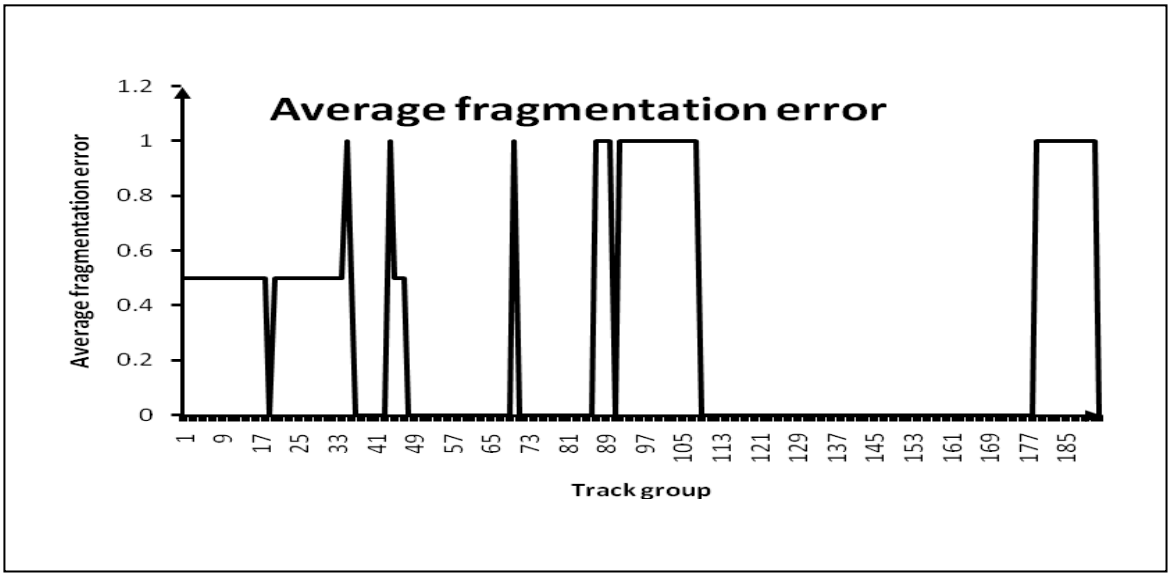
Average fragmentation error
Average fragmentation error
1.2
1
0.8
0.6
0.4
0.2
0
1 9 17 25 33 41 49 57 65 73 81 89 97 105 113 121 129 137 145 153 161 169 177 185
Track group

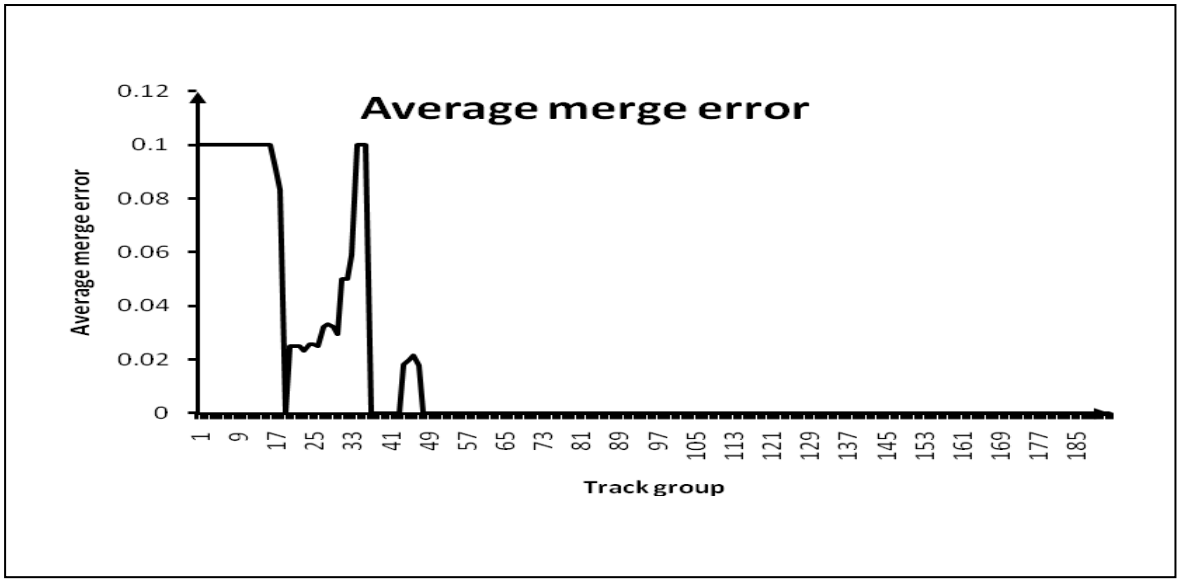
Average merge error
Average merge error
0.12
0.1
0.08
0.06
0.04
0.02
0
1 9 17 25 33 41 49 57 65 73 81 89 97 105 113 121 129 137 145 153 161 169 177 185
Track group

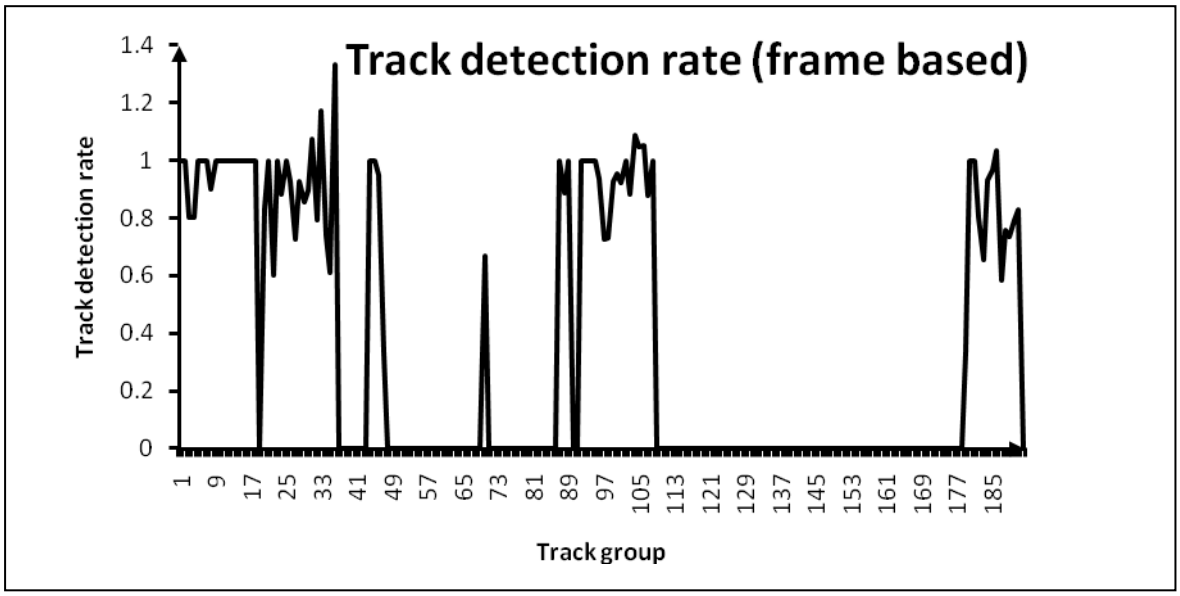
Track detection rate (frame based)
Track detection rate
1.4
1.2
1
0.8
0.6
0.4
0.2
0
1 9 17 25 33 41 49 57 65 73 81 89 97 105 113 121 129 137 145 153 161 169 177 185
Track group

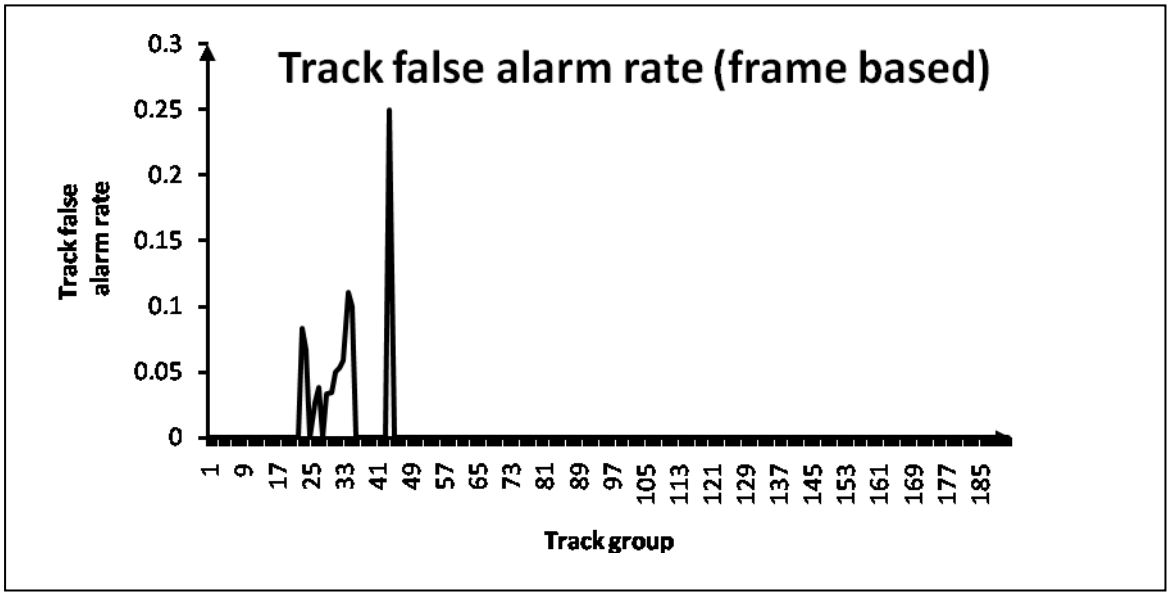
Track false alarm rate (frame based)
Track false alarm rate
0.3
0.25
0.2
0.15
0.1
0.05
0
1 9 17 25 33 41 49 57 65 73 81 89 97 105 113 121 129 137 145 153 161 169 177 185
Track group

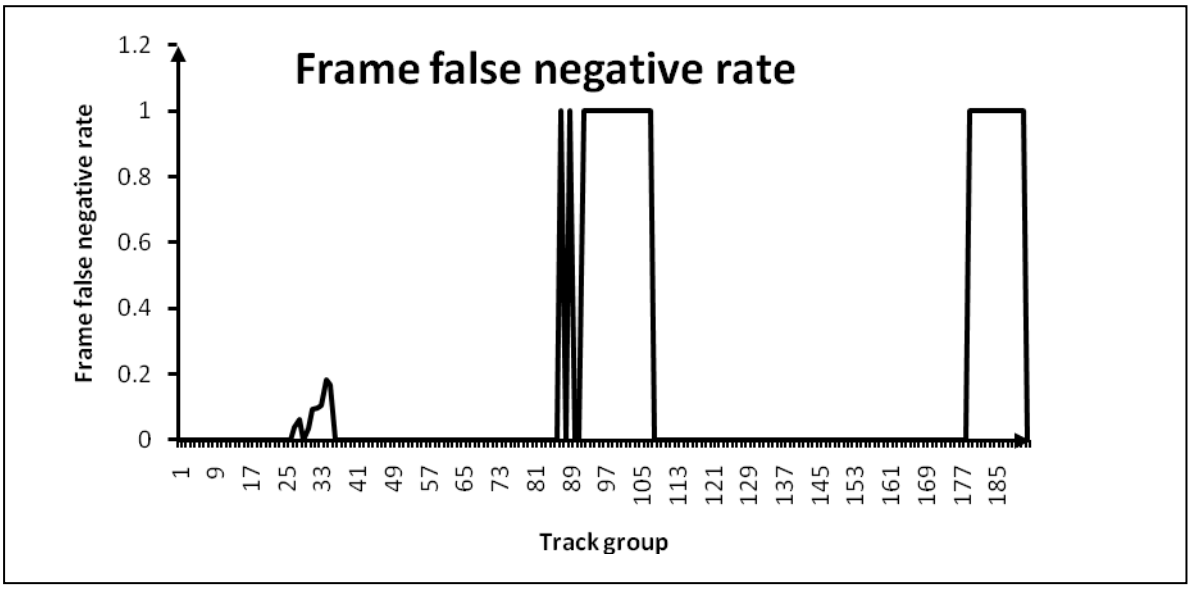
Frame false negative rate
Frame false negative rate
1.2
1
0.8
0.6
0.4
0.2
0
1 9 17 25 33 41 49 57 65 73 81 89 97 105 113 121 129 137 145 153 161 169 177 185
Track group

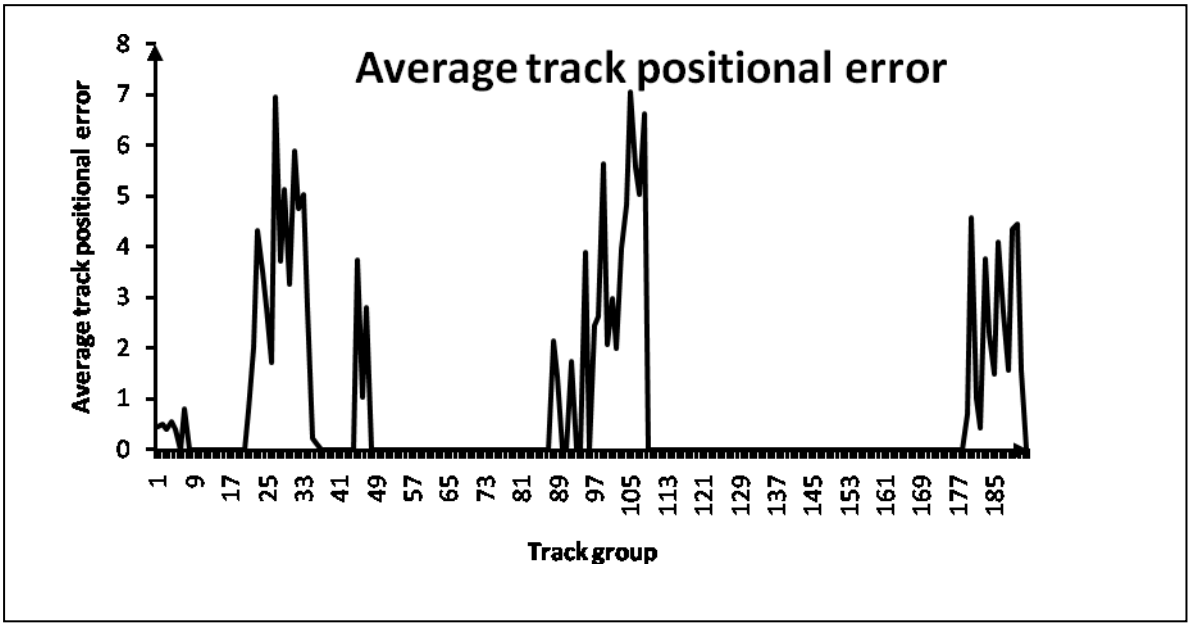
Average track positional error
Average track positional error
8
7
6
5
4
3
2
1
0
1 9 17 25 33 41 49 57 65 73 81 89 97 105 113 121 129 137 145 153 161 169 177 185
Track group